

University of Groningen

Biogas feedstock potentials and related water footprints from residues in China and the European Union

Yuan, Zili; Gerbens-Leenes, P W

Published in:
The Science of the Total Environment

DOI:
[10.1016/j.scitotenv.2021.148340](https://doi.org/10.1016/j.scitotenv.2021.148340)

IMPORTANT NOTE: You are advised to consult the publisher's version (publisher's PDF) if you wish to cite from it. Please check the document version below.

Document Version
Publisher's PDF, also known as Version of record

Publication date:
2021

[Link to publication in University of Groningen/UMCG research database](#)

Citation for published version (APA):

Yuan, Z., & Gerbens-Leenes, P. W. (2021). Biogas feedstock potentials and related water footprints from residues in China and the European Union. *The Science of the Total Environment*, 793, [148340]. <https://doi.org/10.1016/j.scitotenv.2021.148340>

Copyright

Other than for strictly personal use, it is not permitted to download or to forward/distribute the text or part of it without the consent of the author(s) and/or copyright holder(s), unless the work is under an open content license (like Creative Commons).

The publication may also be distributed here under the terms of Article 25fa of the Dutch Copyright Act, indicated by the "Taverne" license. More information can be found on the University of Groningen website: <https://www.rug.nl/library/open-access/self-archiving-pure/taverne-amendment>.

Take-down policy

If you believe that this document breaches copyright please contact us providing details, and we will remove access to the work immediately and investigate your claim.

Downloaded from the University of Groningen/UMCG research database (Pure): <http://www.rug.nl/research/portal>. For technical reasons the number of authors shown on this cover page is limited to 10 maximum.

Chemical Synthesis of Cell Wall Constituents of *Mycobacterium tuberculosis*

Mira Holzheimer, Jeffrey Buter,* and Adriaan J. Minnaard*



Cite This: <https://doi.org/10.1021/acs.chemrev.1c00043>



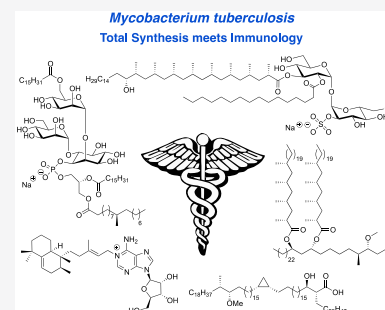
Read Online

ACCESS |

Metrics & More

Article Recommendations

ABSTRACT: The pathogen *Mycobacterium tuberculosis* (*Mtb*), causing tuberculosis disease, features an extraordinary thick cell envelope, rich in *Mtb*-specific lipids, glycolipids, and glycans. These cell wall components are often directly involved in host–pathogen interaction and recognition, intracellular survival, and virulence. For decades, these mycobacterial natural products have been of great interest for immunology and synthetic chemistry alike, due to their complex molecular structure and the biological functions arising from it. The synthesis of many of these constituents has been achieved and aided the elucidation of their function by utilizing the synthetic material to study *Mtb* immunology. This review summarizes the synthetic efforts of a quarter century of total synthesis and highlights how the synthesis laid the foundation for immunological studies as well as drove the field of organic synthesis and catalysis to efficiently access these complex natural products.



CONTENTS

1. Introduction	A
2. Mycolic Acids	D
2.1. α -Mycolic Acid	E
2.2. <i>cis</i> - and <i>trans</i> -Configured Keto- and Methoxy-mycolic Acids	F
2.3. Methoxy-mycolic Acid	J
3. β -D-Mannosyl Phosphomycoketide	L
4. 1,3-Methyl-Branched Lipids	P
4.1. Catalytic Asymmetric Deoxypropionate Synthesis	P
4.2. Phthiocerol Dimycocerosate A	P
4.3. Phenolic Glycolipid	S
4.4. Phthioceranic and Hydroxyphthioceranic Acid	V
5. Trehalose Glycolipids	AC
5.1. Ac ₂ SGL	AC
5.2. Sulfolipid-1	AD
5.3. Acyl Trehaloses	AF
6. Glycerolipids	AH
6.1. β -Gentiobiosyl Diacylglycerides	AH
6.2. Tuberculostearic Acid Containing Phosphoglycerolipids	AI
7. Terpene Nucleosides	AK
8. Mycobactins	AO
9. Cell Wall Oligo- and Polysaccharides	AT
9.1. Phosphatidylinositol Mannosides	AW
9.2. Higher Order Oligosaccharides	BO
10. Conclusion and Outlook	CA
Author Information	CB

Corresponding Authors	CB
Author	CB
Notes	CB
Biographies	CB
Acknowledgments	CB
References	CB

1. INTRODUCTION

The pathogen *Mycobacterium tuberculosis* (*Mtb*), causing the tuberculosis (Tb) disease, has been a scourge for mankind since ancient times. As a matter of fact, the oldest confirmed “case” of the disease can be dated back to a Neolithic settlement in the Eastern Mediterranean, 9000 years ago.¹ But also other civilizations, such as ancient Egypt, suffered deaths caused by Tb.² Detection of mycobacterial DNA in a number of Egyptian mummies is evidence for the early “success” of *Mtb* as a global pathogen.^{3–5} Throughout the millennia, the cause of this disease was a mystery to humankind until the pioneering, and Nobel Prize winning, work of Robert Koch, who in 1882 found that *Mtb* is the source of this pest that caused countless fatalities.⁶ To this day, *Mtb* continues to be a major global health threat.⁷ Contrary to any other pathogen, *Mtb* managed to infect an

Received: January 14, 2021

estimated 1.7 billion people worldwide, which is over 20% of the world population. Every year, approximately 10 million people fall ill from this infectious disease which is therefore classified as a pandemic. Moreover, Tb is the world's most deadly bacterial disease with a dead toll exceeding 1.5 million annually. Despite the fact that a large part of infected individuals might clear latent infection over time,⁸ Tb is listed in the World Health Organization top-10 causes of death.

Tb is primarily a lung pathogen (80–85% of the cases) and therefore an airborne disease which is transmittable by coughing; however, extrapulmonary Tb is also frequent.⁹ These forms of Tb are non-infectious, and most notably manifest themselves in the pleural cavities just outside the lung (tuberculous pleurisy), central nervous system (tuberculous meningitis), genitourinary system (in urogenital tuberculosis), lymphatic system (mycobacterial cervical lymphadenitis), and bones and joints (in Pott's disease). Extrapulmonary Tb is observed mostly in children and immunocompromised humans, in particular HIV patients.¹⁰ Other Tb risk factors are malnutrition, diabetes, and substance abuse (i.e., smoking and alcohol). An HIV/Tb coinfection is particularly worth highlighting since the HIV/Tb synergy dramatically impacts the progression of the Tb disease.⁷ Tb is an opportunistic infection meaning that the likelihood of HIV patients progressing into active Tb is 18 times(!) higher than those who are not HIV infected, even for those using antiretroviral treatment. In 2019, 8.2% of recorded Tb patients were also diagnosed with HIV, and in the same year 15% of the tuberculosis deaths were ascribed to HIV-infected persons. Therefore, HIV prevention alone can significantly impact attenuation of the Tb pandemic.

Taking into account the aforementioned risk factors, it is not surprising that Tb is mostly prevalent in developing countries, where 95% of the Tb deaths are situated, and thus disproportionately affects the poor. Due to the enormous efforts of raising Tb awareness, prevention, developments in point-of-care diagnostics, and the subsequent rapid treatment, the number of Tb deaths decreased significantly until the year 2000, although the incidence rate has been stable since.¹¹ Despite these encouraging developments in controlling the Tb disease, there is a dramatic rise in multidrug resistant tuberculosis (MDR Tb), meaning the bacilli are resistant to at least both of the first-line antibiotics isoniazid and rifampicin, two of the most powerful anti-Tb drugs.¹² From the clinical perspective the patient is practically incurable with a standard first-line treatment meaning the clinician has to resort to the second-line antibiotics (mostly weak in activity and toxic) including the aminoglycosides (e.g. capreomycin, amikacin, and kanamycin), fluoroquinolones (e.g. levofloxacin, moxifloxacin, and ciprofloxacin), and the most recently approved antibiotics bedaquiline (2012), delamanid (2014), and pretomanid (2019). An even worse development is the emergence of extensively drug resistant tuberculosis (XDR Tb) tuberculosis strains which, besides being resistant to isoniazid and rifampicin, are also resistant to fluoroquinolones and at least one of the three second-line injectable drugs (i.e., capreomycin, amikacin, and kanamycin).¹² Needless to say, both MDR Tb and XDR Tb complicate treatment and also reduce positive treatment outcomes.¹³ Surprisingly, in contrast to where tuberculosis causes the most disturbance, these drug-resistant forms of Tb are mostly prevalent in eastern European countries (i.e., Ukraine, Belarus, west Russia, Azerbaijan, Republic of Moldova) and gradually make their way into western Europe.^{14,15}

The “success” of *Mtb* as the world's leading pathogen can largely be attributed to its parasitic nature. *Mtb* is able to persist in its human host up to decades by evading host immune responses and surviving within macrophages (= immune cells). By creating this intracellular niche, the bacterium is largely protected from other immune responses while having access to host nutrients such as lipids and iron.^{16–22} Moreover, residence in the macrophage also provides partial cloaking from antibiotics.

Another physical protector of *Mtb* is its thick lipophilic cell wall that provides a fortress against the hostile, bactericidal environment within macrophages as well as against antibiotics, consequently complicating tuberculosis treatment.²³ The cell wall consists of a complex array of (glyco)lipids, polysaccharides, and peptidoglycans, which exhibits low permeability of drugs into the mycobacterial cell.^{24–27} As a result, a typical Tb drug regimen against drug susceptible Tb takes up to one year, whereas treatment of drug resistant forms of Tb can take several years. In both cases a cocktail of antibiotics is administered and patient compliance with the lengthy therapy is of utmost importance for successful treatment.²⁸

Figure 1 depicts a molecular representation of the cell envelope of *Mtb*, showing an exquisite, and highly complex, architecture buildup of many different layers.

On the inside of the cell envelope lays the so-called mycobacterial inner membrane or plasma membrane (PM). This lipid bilayer consists primarily of glycerol-based phospholipids, mainly phosphatidylethanolamines (cephalins). Here one also finds phosphatidylinositol mannosides (PIMs),^{29,30} the first of the many biologically active glycoconjugates in the *Mtb* cell wall.³¹ Connected to the plasma membrane is the periplasm, which consists of lipomannan (LM) and lipoarabinomannan (LAM), with the latter being a complex oligosaccharide which is a known virulence factor of tuberculosis.³² Noncovalently bound to the periplasm is the arabinogalactan peptidoglycan (AGP) complex of which the peptidoglycan (PG) provides shape and osmotic stability.^{33,34} PG is cross-linked with peptide bonds, which gives rigidity to the cell wall. Covalently connected to the PG sugar moieties is the arabinogalactan which is a polymeric saccharide that spans a large part of the overall cell wall and eventually branches out to connect with mycolic acids. The mycolic acids are the major constituent of the mycobacterial outer membrane (MOM), forming the thick lipophilic membrane that is characteristic for mycobacteria. The mycolic acid-based glycolipids form an interwoven network of the long aliphatic (C₇₀–C₉₀) mycolic acid chains that contribute to the fluidity of the cell wall.³⁵ The outer membrane also hosts another wide range of lipophilic molecules such as sulfoglycolipids (SGL), diacyltrehaloses (DAT), polyacyltrehaloses (PAT), phtiocerol dimycocerosates (PDIM), and others. The cell-wall is topped by an outermost compartment, a loosely bound structure called the capsule (not shown in Figure 1) which primarily consists of polysaccharides and peptides.³⁶

The cell wall morphology of *Mtb* is well understood, and a considerable number of constituents that make up the cell wall are known.^{24,37} However, it is surprising how little is known about the antigenic properties and other biological functions of the majority of these lipids. Since the mycobacterial cell envelope is at the interface with human host cells,³⁸ its constituents play a key role in *Mtb* pathogenicity but also in host immune responses.^{39–45} The identification of new lipids and their exact, molecular, function is therefore instrumental to understand *Mtb* survival and virulence mechanisms but also to

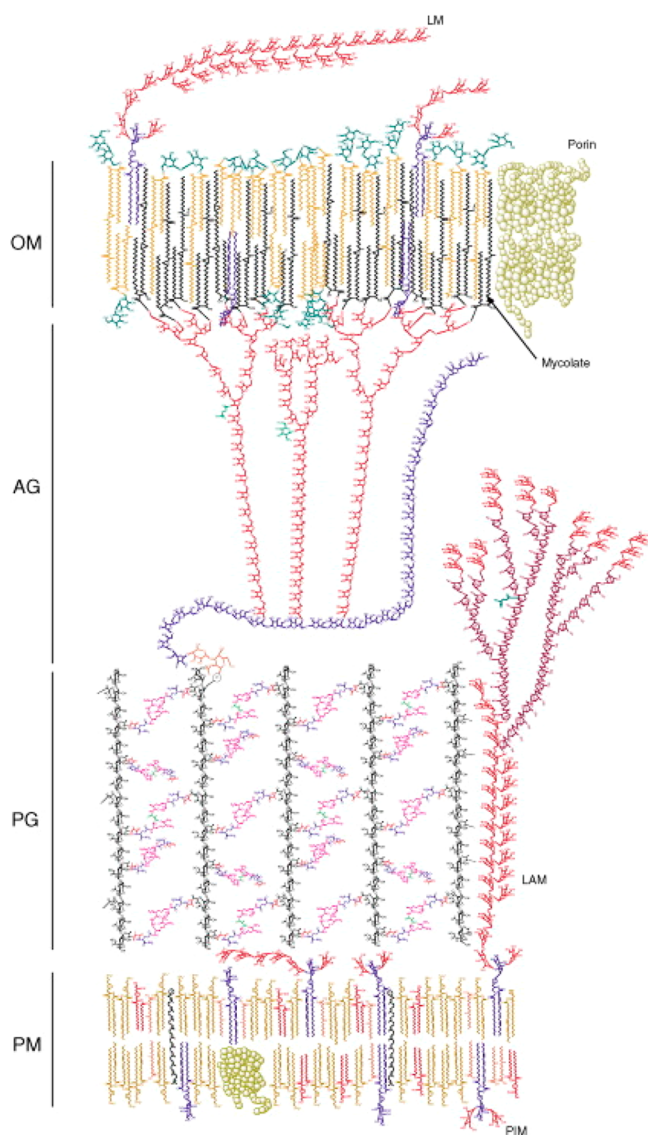


Figure 1. Schematic representation of the cell wall of *Mtb* (Reproduced with permission from ref 25. Copyright Elsevier 2009).

understand basic human immune responses. Moreover, studies on *Mtb* cell wall components can significantly aid the discovery of new antibiotic targets,⁴³ vaccine adjuvants,⁴⁶ and biomarkers^{47–50} for tuberculosis diagnosis.

Throughout evolution, humans acquired two sets of defense strategies against unwanted invaders of the body.^{51,52} The most primitive one is the innate immune system which is a nonspecific defense mechanism that acts within hours of invasion by the unwanted guest (e.g., pathogens such as bacteria, fungi, viruses).⁵³ Parts that make up the innate immune system are anatomical barriers such as skin and chemicals in the blood, gastrointestinal tract (gut bacteria), and eyes (tears) but also phagocytic cells such as macrophages, neutrophils, and dendritic cells that can devour and digest these foreign invaders.

The second defense mechanism is that of adaptive (i.e., acquired) immunity, which is more complex than the innate immune system.⁵⁴ The adaptive immune system is a cellular defense mechanism that first has to recognize the foreign invader and process it prior to defending against it. Once recognized, “an army of immune cells” is created that specifically attack the invader. The adaptive immune system is thus an antigen-specific

immune response and also includes “memory” that makes future response against the specific invader more efficient. Antibodies are an important part of adaptive immunity.

The adaptive immune response is regulated by a collection of cell surface glycoproteins which is called the major histocompatibility complex (MHC). These proteins are able to bind small peptides (*antigens*) from pathogens and present these on the cell surface for recognition by T-cells which either kill the foreign invader (killer T-cells) or orchestrate an immune response (helper T-cells).

One other class of cell surface proteins that is able to present antigens to T-cells are CD (cluster of differentiation) proteins. Instead of small peptides, the CD1 protein subclass is able to recognize and present lipids.^{55,56} This part of the acquired immunity significantly broadens the diversity of molecules recognized by the immune system creating a tighter defense network against foreign invaders. Recognition of lipids by CD1 proteins is particularly interesting in the context of *Mtb*, since the mycobacterial outer membrane is largely comprised of a wide array of lipids and thus creates a plethora of opportunities for CD1 mediated immunity against *Mtb*. Throughout the past 30 years a variety of *Mtb* lipids, of which many are presented in this review, have been shown to be recognized by CD1 proteins.⁵⁷

Besides recognition by CD1 proteins, mycobacterial cell wall components such as, and most notably, trehalose dimycolate are also recognized by the immune receptor Mincle (macrophage-inducible C-type lectin).^{58,59} This transmembrane protein is expressed on different immune cells such as macrophages, dendritic cells, and neutrophils. Mincle activation, by binding of extracellular lipids, leads to signaling through FcR- γ and finally activation of the transcription factor NF- κ B. Ultimately this signaling pathway induces expression of chemokines, cytokines, and growth factors resulting in an overall pro-inflammatory response. Consequently, as key part of the innate immune response, inflammatory cells move in to the site of activation. Mincle is a potent receptor and unique in its ability to recognize a wide array of low molecular weight (glyco)lipids derived from microorganisms (bacterial and fungal) as well as those from self-damage.^{60,61} Since its discovery, Mincle and its agonists have received great attention, and Mincle is suggested to be a promising target for the development of subunit vaccines and vaccine adjuvants.⁶² In particular for *Mtb*, such a development would mark a scientific breakthrough, as to this date the only used vaccine is the BCG vaccine which shows varying levels of efficacy.⁶³

The discovery of biologically active small molecules (such as lipids) from *Mtb* and the investigation of their biological, and more specific immunogenic, role is significantly hampered by tedious isolation procedures and, when successful, small isolated quantities. Also, one should not forget that *Mtb* is a slow growing bacterium, dividing only once every \sim 24 h, and also requires culturing in biosafety 3 level laboratories due to its pathogenicity. Synthetic organic chemistry has the great potential to circumvent these problems by total synthesis of sufficient and (stereochemically) pure material. Moreover, an often-underestimated aspect of synthetic efforts is that the chemically synthesized product is void of biological contaminants which might be part of the natural isolate below the limit of detection of (bio)analytical tools. Such impurities, how minute these might be, can be a source of data misinterpretation by causing hard to prove false positive (enhanced bioactivity) or false negative (toxicity) results. Therefore, the pure synthetic

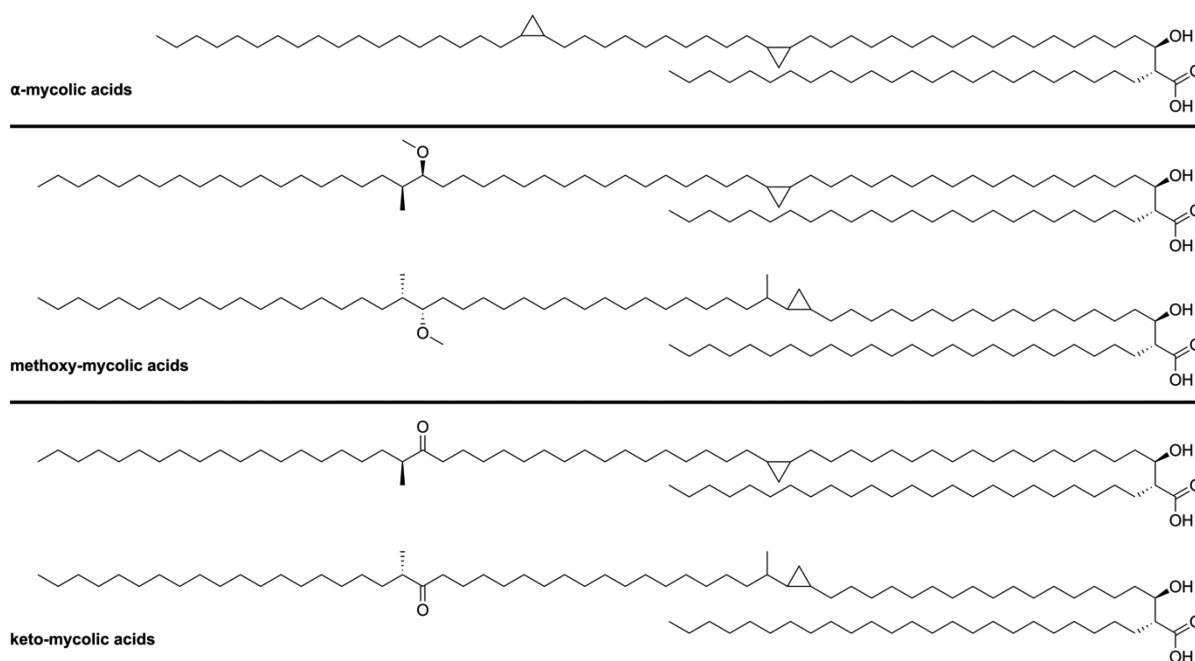


Figure 2. Classification of mycolic acids based on their functional groups.

material can be viewed as a 'gold standard' in biological evaluations.

Total synthesis of complex natural products can also be used to unequivocally confirm or revise the proposed chemical structure, by comparison of spectroscopic and chromatographic data of natural isolate and synthetic material. It is noteworthy that isolation of these mycobacterial membrane cell wall components only provides small amounts of purified natural product. Thus, researchers often have to rely on collisional HPLC-MS or GC-MS data since isolated quantities are not sufficient for extensive NMR structural analysis. Often this is sufficient to propose the structure, and sometimes also the stereochemistry, but it does not provide ultimate proof of the molecular structure of the isolated material.

Furthermore, development of synthetic routes to prepare natural products opens up possibilities to access various synthetic analogues and non-natural modifications. These can be used as chemical probes or to gain insight into structure–activity relationships which will serve to ultimately expand the fundamental molecular understanding of the biological and immunological processes in question.

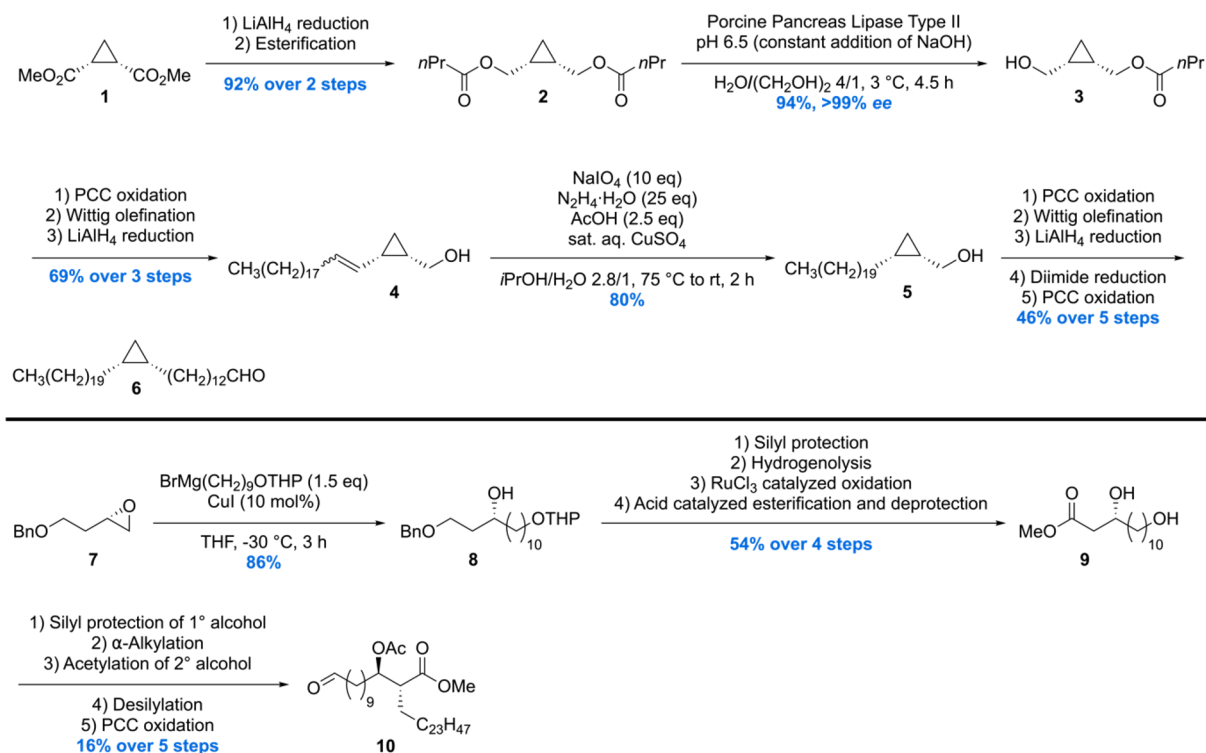
Besides aiding biological and immunological investigations, and as we will see, many *Mtb* cell wall components exhibit an exquisite molecular architecture which forms a playground for synthetic chemists to develop and showcase novel methodology. In this review, we discuss a quarter century of stereoselective total syntheses of natural products from *Mtb* (from 1995 up to June 2021) focusing on cell wall components and pathogen-shed lipids. The emphasis lies on the construction of complete natural products of *Mtb* and fragments thereof, not simplified analogues, highlighting the stereoinducing steps. We will also discuss the stereoselective synthesis of complex optically pure constituents, of lipidic nature, of the natural products. Additionally, where applicable, a brief description on how the synthetic material was used in biological or immunological studies to address fundamental questions on virulence mechanisms and *Mtb* immunology is provided. The membrane components discussed contain lipids, such as mycolic acids, phthiocerol-based lipids,

1,3-multimethyl-branched lipids and their trehalose glycolipids, lipopeptides, terpene nucleosides, as well as oligo- and polysaccharides.

2. MYCOLIC ACIDS

An important class of mycobacterial cell envelope lipids comprises the mycolic acids, which make up for a large part of the cell membrane of *Mtb*. Mycolic acids were isolated by Anderson⁶⁴ nearly 100 years ago, but it was in the 1960s that the overall structure of these fatty acids was elucidated.^{65–67} Mycolic acids are long-chain α -alkyl- β -hydroxy fatty acids, which show considerable structural diversity with respect to their functional groups and carbon chain length, depending on the mycobacterial species and strain.⁶⁸ Mycolic acids occur as free acids as well as esterified to the arabinogalactan layer of the cell envelope. Furthermore, mycolate esters of trehalose, trehalose mono- and dimycolate (TMM and TDM, respectively) and glycerol monomycolate (GroMM) are produced by *Mtb* as well.³⁵ A special case of mycolate esters is glucose monomycolate (GMM). Mycobacteria do not produce GMM by themselves; however, when *M. smegmatis*, *M. Phlei*, and *M. Avium* were cultured in the presence of glucose, their total lipid extracts exhibited a GMM-specific T cell response of LDN5.⁶⁹ Moreover, crude sonicates of *M. Leprae* (leprosy causing bacterium), isolated from infected armadillo liver, also showed stimulation of LDN5 indicating a mammalian source of glucose suffices in GMM biosynthesis. From these experiments it was concluded that exogenous glucose is needed to produce GMM. Thus, GMM is a 'biochimeric molecule'⁷⁰ in which mycobacteria-produced mycolate is coupled with host-produced glucose.⁶⁹

Depending on the functional groups present in their main chain, mycolic acids are divided into three categories (Figure 2).⁷¹ α -Mycolic acids are the most abundant group of mycolic acids and form around 60% of the total isolatable mycolic acids from *Mtb* depending on the bacterial strain.⁶⁸ They contain two strictly *cis*-configured cyclopropyl groups, of unknown absolute configuration, and their alkyl chains range from 74 to 80

Scheme 1. Synthesis of Methyl α -Mycolate Building Blocks 6 and 10

carbons. The other two classes of mycobacterial mycolic acids comprise methoxy- and keto-mycolic acids. These contain α -methyl-methoxy and α -methyl-keto moieties distal, and cyclopropyl groups proximal, to the carboxylic acid moiety. Contrary to the α -mycolic acids the cyclopropyl groups found in keto- and methoxy-mycolic acids can be both *cis*- or *trans*-configured. The *trans*-cyclopropyl mycolic acids additionally contain an α -methyl group.⁶⁶

The (*R,R*)-configuration of the α -alkyl- β -hydroxy carboxylic acid unit has been shown to be crucial for T-cell recognition of mycolic acids when presented by CD1b.⁶⁹ Furthermore, the stereochemistry of the distal α -methyl-methoxy unit is *S,S*, as proven by synthesis of both diastereomeric forms followed by comparison of their optical rotation with the natural product.^{67,72,73} The stereochemistry is relevant as it influences the binding of the mycolic acid to CD1b.⁷³ To date, the absolute stereochemistry of the *cis*-cyclopropyl group has not been indisputably elucidated, although evidence from CD1b binding studies points toward the (*R,S*)-configuration.⁷³

Mycolic acids have been found to exhibit various biological functions.⁷⁴ Mycolic acids form a tight hydrophobic barrier (called mycomembrane), which serves as physical protection and fortification against the harsh environment within macrophages as well as antibiotics due to its low permeability.^{75,76} Mycolic acids are essential for *Mtb* viability, a feature that is exploited in treatment of Tb. Enzymes involved in the biosynthesis of mycolic acids are targets of small molecule inhibitors⁷⁷ such as the well-established first-line drug isoniazid^{78–80} and the more recently developed drugs delamanid⁸¹ and pretomanid.⁸² Furthermore, mycolic acids are linked to *Mtb* virulence⁸³ and play a role in host–pathogen interactions. Free mycolic acids induce host innate immune responses such as alveolar macrophage activation and differentiation to foamy macrophages (=lipid-laden macrophages).^{84,85} Mycolic acids also act as antigens in serological

assays,⁸⁶ and mycolic acids and their carbohydrate esters are recognized by T-cells.^{69,87–89} Mycolates and synthetic analogues thereof are therefore of interest in the field of vaccine (adjuvant) development and have been identified as potent activators of the immune receptor Mincle.^{58,90}

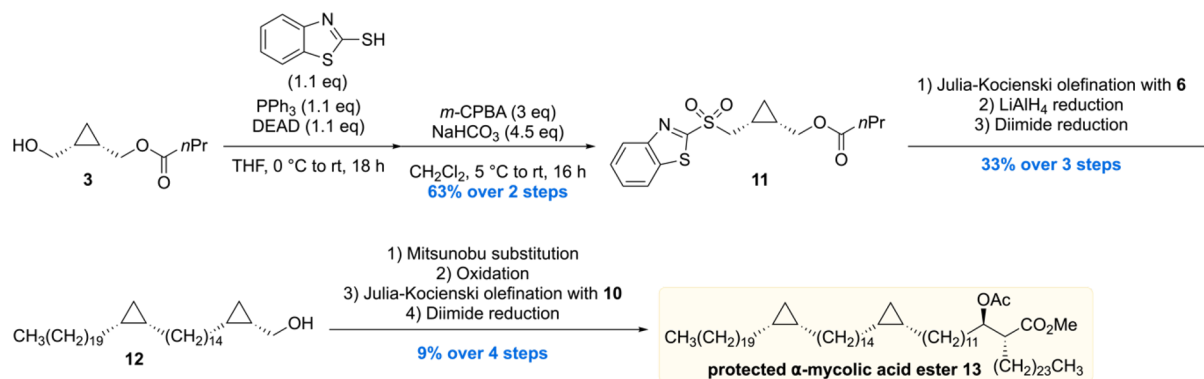
To aid such immunological studies, most notably, the Prandi laboratory developed efficient semisynthesis of glycerol and glucose monomycolates by connecting the glycerol and glucose precursors with mycolic acid isolates.^{90–92} Although the synthetic products, which are a mixture of mycolate esters, were of great importance in the immunological studies, in this review we focus on total syntheses of well-defined chemical structures.

2.1. α -Mycolic Acid

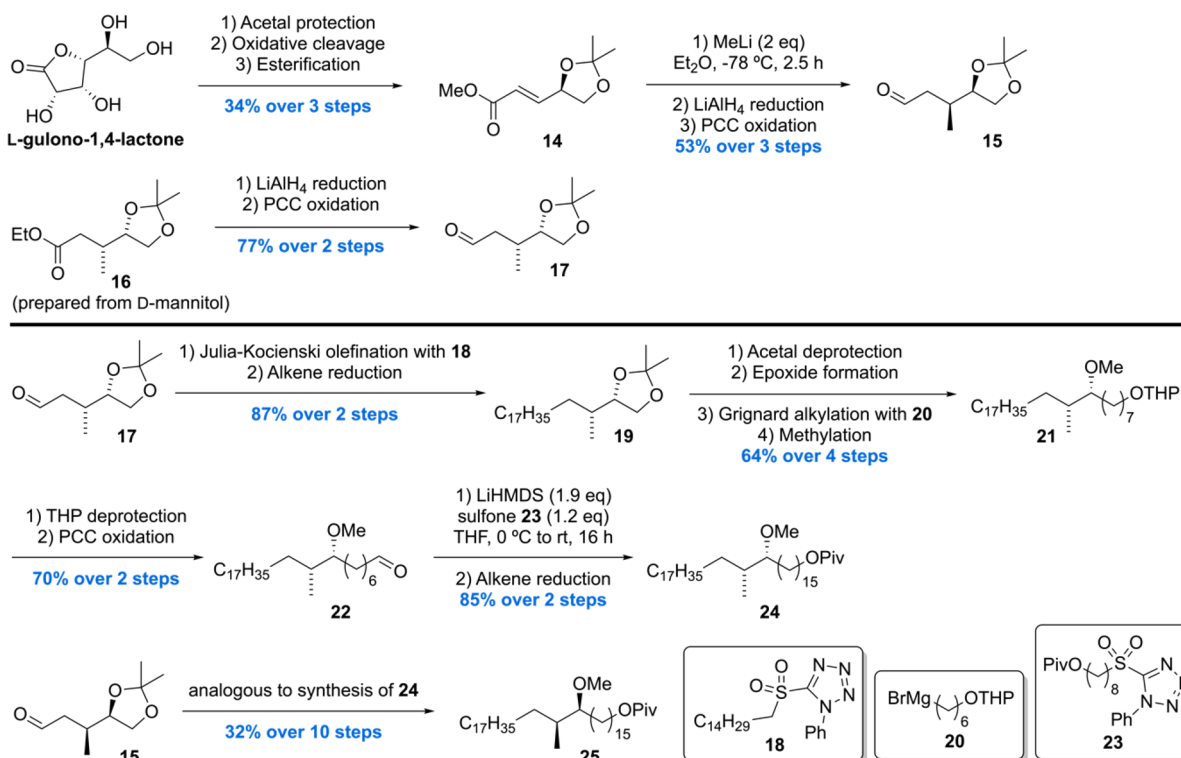
The first asymmetric synthesis of an α -mycolic acid as its methyl ester was reported by the group of Baird.^{93,94} The synthesis was initialized by the conversion of *meso*-methyl ester **1** into *meso*-diester **2** (Scheme 1). This molecule was subjected to enzymatic desymmetrization using porcine pancreas lipase type II providing alcohol **3** in 94% and >99 *ee*.⁹⁵ Further elaboration set the stage for a hydrogenation of the rather sensitive allyl cyclopropane **4**, which was carried out with diimide, to avoid ring opening, delivering **5**. A set of straightforward transformations to extend the carbon chain gave rise to building block **6**.

A second building block **10** was synthesized from enantiopure epoxide **7** by regioselective ring-opening to furnish chiral alcohol **8**. Silylation, hydrogenolysis followed by $\text{RuCl}_3 \cdot \text{H}_2\text{O}$ oxidation of the alcohol, and subsequent esterification/deprotection gave diol **9**, which was converted into **10** using a five steps sequence involving protection, α -alkylation, acetylation, deprotection, and oxidation.

To complete the synthesis of the protected α -mycolic acid, another cyclopropane fragment **11** had to be constructed which

Scheme 2. Completion of the Synthesis of Methyl α -Mycolate

Scheme 3. Baird's Methoxy-Mycolic Acid Building Block Synthesis Part 1



could then be joined with **6** and **10** (Scheme 2). A Mitsunobu/oxidation sequence initiated on enantiopure alcohol **3** gave sulfone **11**. Next, a Julia–Kocienski olefination of **11** with **6** and two subsequent reductions gave alcohol **12** in 33% over the three steps. **12** was then reacted to give the appropriate sulfone for another Julia–Kocienski olefination, but then with building block **10**. A diimide reduction provided the acetate protected α -mycolic acid methyl ester, the end-stage of the synthesis.

The synthetic material was compared to isolated α -mycolic acid (a mixture of homologues with **13** as the predominant compound) after esterification by means of ^1H and ^{13}C NMR. The spectra of natural and synthetic materials were found to be virtually identical, but it was also recognized that in this case NMR analysis does not provide ultimate proof of structure, in particular of the absolute and relative stereochemistry of the cyclopropane rings. The specific rotation of synthetic and natural protected α -mycolic acid was found to be very similar as well, but it has to be noted that the rotation is likely determined by the β -acetoxy ester part. Therefore, no conclusion on the

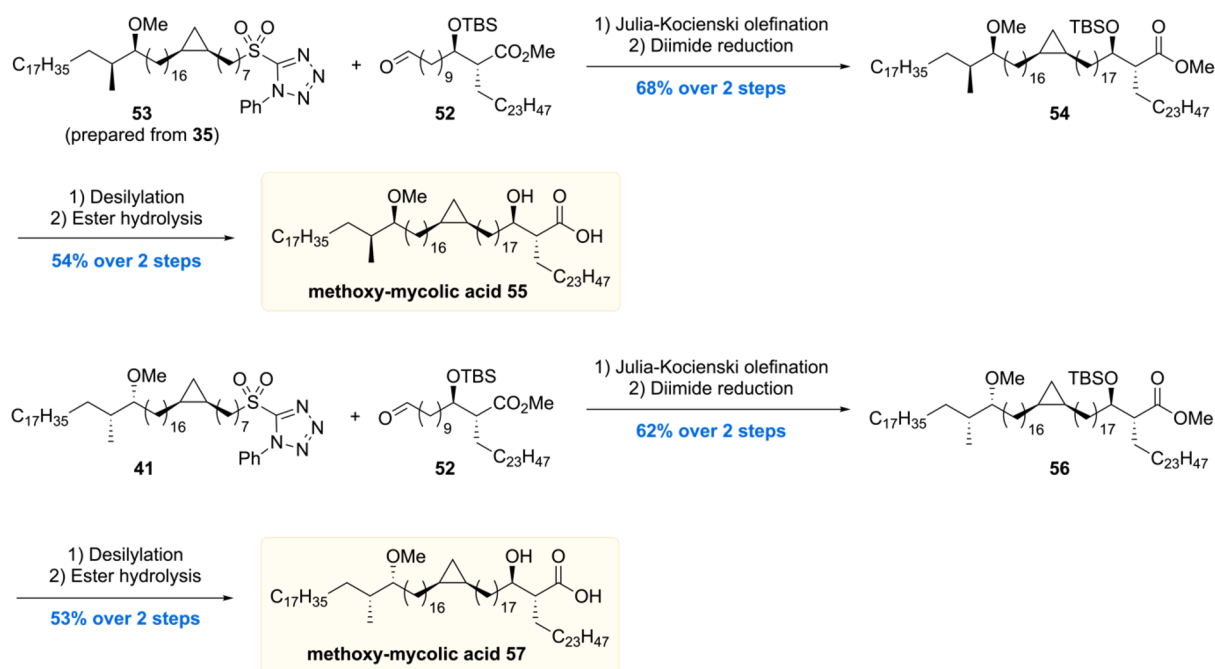
absolute stereochemistry of the cyclopropane moieties could be drawn. MALDI- and ESI-MS spectra of synthetic methyl α -mycolate corresponded to those of the natural isolate. Taken together, this total synthesis confirmed the overall, gross, molecular structure of naturally occurring α -mycolic acid.

2.2. *cis*- and *trans*-Configured Keto- and Methoxy-mycolic Acids

In 2007, the Baird laboratory reported the first total synthesis of two enantiomers **55** and **57** (with regard to the methoxy methyl motif) of methoxy-mycolic acid as well as two enantiomers **42** and **44** (with regard to the *cis*-cyclopropane motif) of methyl methoxy-mycolate.⁷² The synthesis strategy is based on the preparation of various aldehyde- and sulfone-equipped fragments and their subsequent connection through a Julia–Kocienski olefination/reduction sequence in analogy to their previous synthesis of α -mycolic acid.⁹⁴

The synthesis commenced with the preparation of two enantiomeric methoxy methyl building blocks **24** and **25**

Scheme 6. Baird's Methoxy-Mycolic Acid Assembly



(Scheme 3). Synthesis of **25** was initiated with the conversion of L-gulono-1,4-lactone to α,β -unsaturated ester **14** through an one-pot acetal protection, oxidative cleavage, and esterification sequence. Diastereoselective conjugate addition of methyl-lithium followed by LiAlH_4 reduction to the alcohol and subsequent oxidation gave aldehyde **15** in 53% over three steps. The enantiomeric aldehyde **17** was accessed in two steps from ethyl ester **16** (prepared from D-mannitol). Julia–Kocienski olefination of **17** with sulfone **18** followed by double bond reduction provided acetone **19** in 87% over two steps, which after four more synthetic steps led to THP ether **21**. Deprotection of the THP moiety followed by PCC oxidation furnished aldehyde **22**, which was subjected to another Julia–Kocienski olefination/reduction sequence with sulfone **23**, which completed the synthesis of the methoxy methyl intermediate **24**. The enantiomeric **25** was prepared from aldehyde **15** in analogy to **24**.

Next, the two methoxy methyl building blocks **24** and **25** were used to prepare three stereoisomeric *cis*-cyclopropyl building blocks **33**, **35**, and **40** (Scheme 4).

Cyclopropanecarboxaldehyde **26** was subjected to a Julia–Kocienski olefination with sulfone **27** giving alkene **28** in 78% yield. Further synthetic steps provided cyclopropanecarboxaldehyde **29**, which underwent Julia–Kocienski olefination with sulfone **30** (generated from **24**) followed by alkene reduction to give bromide **31**. Subsequent treatment of **31** with thiol **32** under basic conditions furnished thioether **33**. The diastereomeric thiol **35** was prepared in analogy using aldehyde **29** and sulfone **34** (prepared from **25**) in 63% yield over three steps. The synthesis of the (*S,S*)-cyclopropyl intermediate **40** was initiated by the synthesis of sulfone **37** in two steps from alcohol **36**. Julia–Kocienski olefination of **37** with 6-bromohexanal and subsequent double bond reduction with trisyl hydrazide provided bromide **38** in 59% over two steps. A series of synthetic transformations then delivered bromide **39**, which was subjected to nucleophilic substitution with thiol **32** to yield thioether intermediate **40**.

Next, sulfones **41** and **43** (prepared from **33** and **40**) were subjected to another sequence of Julia–Kocienski olefination with aldehyde **10** and diimide double bond reduction to give the diastereomeric protected methoxy-mycolic acid methyl esters **42** and **44** in 56% and 54% yield, respectively (Scheme 5). In order to also access the free mycolic acids, aldehyde building block **52** carrying a silyl protected β -hydroxy ester moiety was prepared (Scheme 5). Starting from iodide **45**, a series of steps provided aldehyde **46**, which was subjected to a Wittig reaction followed by Sharpless asymmetric dihydroxylation to give diol **47** in 82% over two steps. The α -hydroxyl of **47** was removed by preparing a cyclic sulfate followed by its regioselective reduction to give alcohol **48** in 63% yield over two steps. Stereoselective alkylation of allyl iodide with the enolate generated from **48** and subsequent silyl protection furnished alkene **49** in 50% yield over two steps. Further synthetic steps then provided pivaloyl ester **51**, which was hydrolyzed and oxidized to the desired aldehyde building block **52**.

In the final assembly (Scheme 6), Julia–Kocienski olefination of sulfone **53** or **41** with aldehyde **52** followed by diimide reduction provided **54** and **56** in 68% and 62% yield over two steps, respectively. Lastly, **54** and **56** were both subjected to desilylation and ester hydrolysis to give the two diastereomeric methoxy-mycolic acids **55** and **57**.

Four mycolic acid methyl esters **42**, **44**, **54**, and **56** were used to assess the proposed stereochemistry of the methoxy methyl motif by comparison of the optical rotation with the methyl ester of the natural sample ($[\alpha]_D^{22} -0.1$). Acetyl protected mycolic acid methyl esters **42** and **44** showed $[\alpha]_D^{22} +7.2$ and $+7.7$, respectively, indicating that in these cases the methoxy methyl motif is opposite to that in the natural mycolic acid. Methyl esters **56** and **54** exhibited $[\alpha]_D^{22}$ values of $+6.0$ and -1.0 , respectively. This led to the conclusion that **54** has the same stereochemistry in the methoxy methyl motif as natural mycolic acid, which is in agreement with the stereochemistry inferred by Asselineau in 1970.⁶⁷

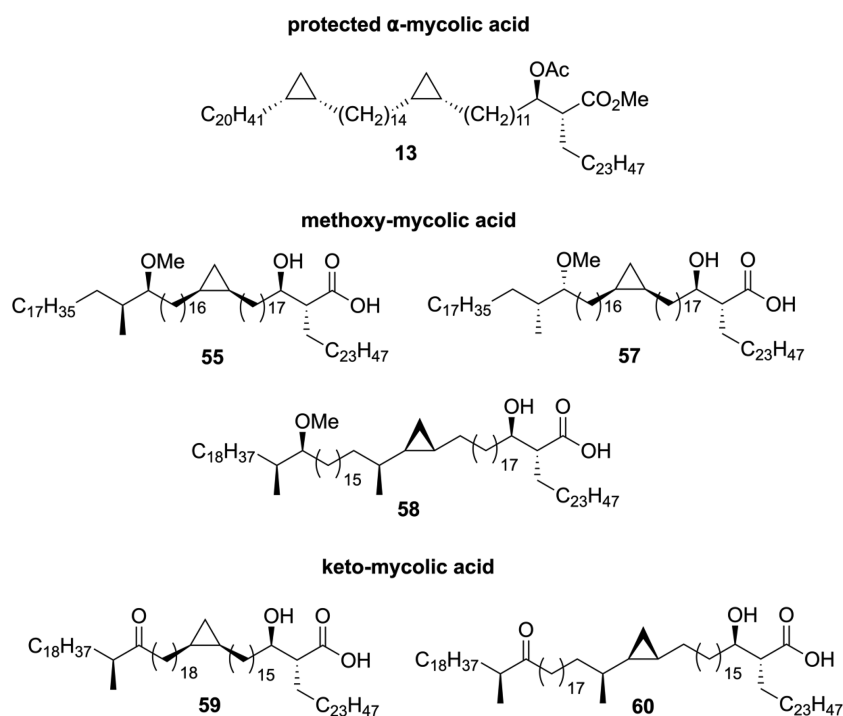


Figure 3. Mycolic acid representatives synthesized by the Baird laboratory.

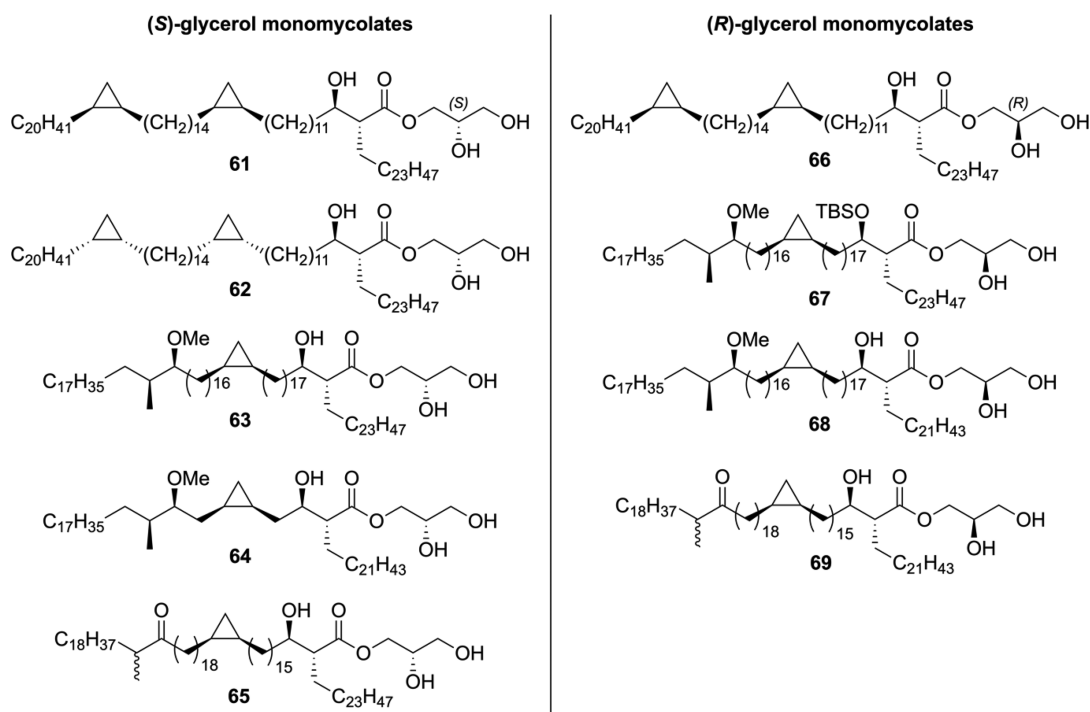
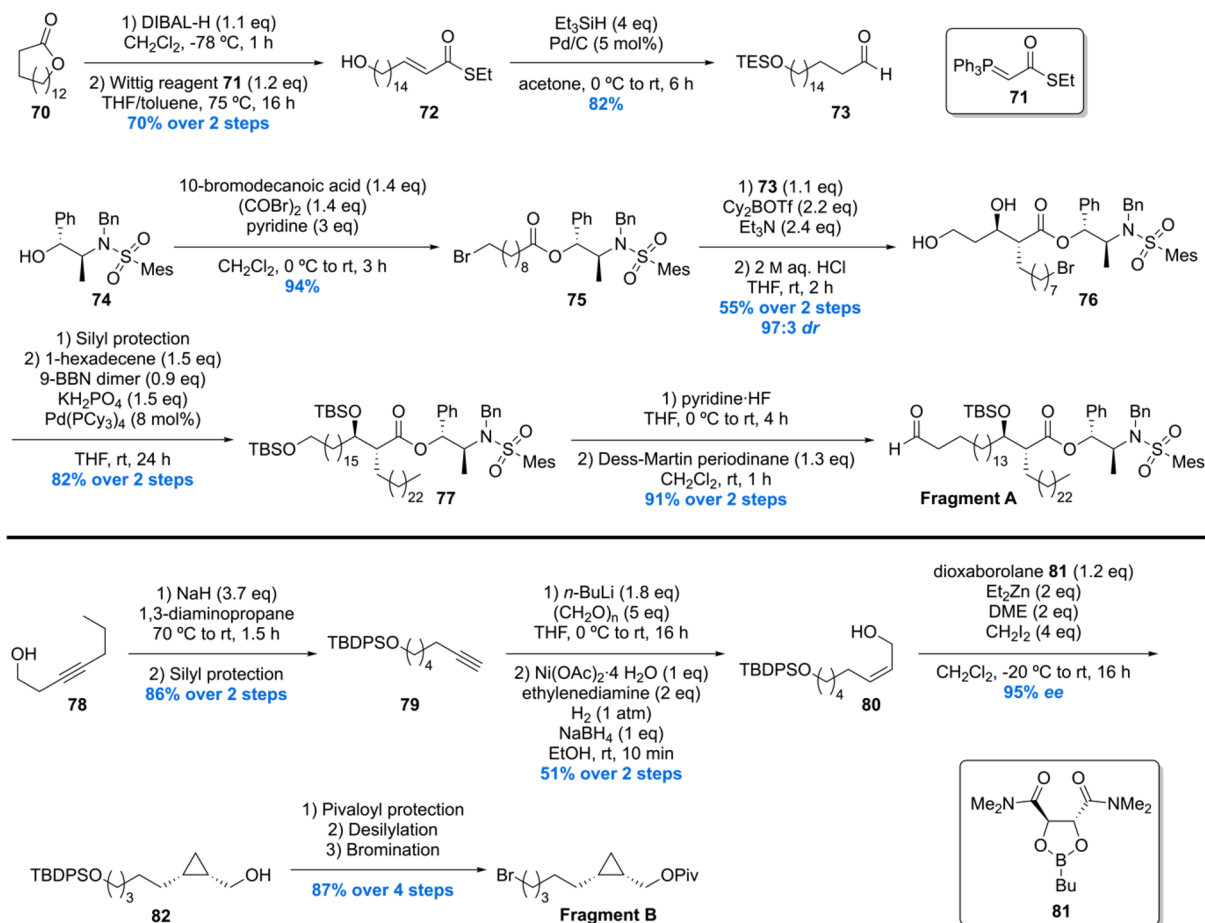


Figure 4. Synthetic (R)- and (S)-GroMM prepared by the Baird group.

Following the total synthesis of α - and methoxy-mycolic acid, the Baird laboratory communicated the synthesis of a *cis*-cyclopropyl containing keto mycolic acid⁹⁶ as well as keto- and methoxy-mycolic acids bearing *trans*-cyclopropyl units.⁹⁷ In the total syntheses of these mycolic acids (Figure 3), the same synthetic strategy was followed as in their previous synthesis of methoxy-mycolic acid,⁷² involving various Julia–Kocienski olefination/reduction sequences for the coupling of the fragments.

The preparation of various stereoisomers of α -, keto-, and methoxy-mycolic acids^{72,94,96,97} containing *cis*- or *trans*-cyclopropyl motifs aided the understanding of the structure–activity relationship of antibody binding to mycolic acids.⁸⁶ Antibody binding using ELISA (enzyme-linked immunosorbent assay) showed that the methyl esters of the tested synthetic mycolic acids possess no antigenicity, whereas the free mycolic acids show different levels of antibody binding depending on the type of functional groups. It was found that synthetic methoxy-

Scheme 7. Minnaard's Methoxy-Mycolic Acid Fragment A and B Synthesis



mycolic acid binds the strongest followed by hydroxy-, keto-, and α -mycolic acids. Furthermore, the stereochemistry of the methoxy methyl fragment was shown to significantly influence the binding ability of the synthetic mycolic acids. The tested natural and synthetic mycolic acids were found to bind to antibodies in sera from Tb positive and negative patients. Yet surprisingly, no mycolic acid was capable of reliably discriminating between Tb positive or negative sera. It remains unknown as to why the tested synthetic mycolic acids showed cross-reactivity, yet the lipophilic (or amphiphilic) nature of the tested lipids could be a source for these results.

Furthermore, the synthetic mycolic acids prepared in the Baird laboratory have been assessed for their role in airway immune responses in mouse pulmonary inflammation models.⁹⁸ Methoxy-mycolic acids were found to be inflammatory and to activate alveolar macrophages. Keto-mycolic acid exerted opposite effects, being anti-inflammatory and suppressing inflammatory response. In contrast, α -mycolic acids exhibited no inflammatory effects, indicating that they are not involved in promoting or suppressing the innate immune responses of the host. On the other hand, the oxygenated mycolic acid species (keto and methoxy) seem to possess different regulatory roles in the inflammatory responses of the host. These results hint toward the fact that *Mtb* is able to balance host immune responses by altering the expression levels of different oxygenated mycolic acid structures, as suggested previously.⁹⁹

The Baird laboratory also synthesized a range of different glycerol monomycolates (GroMM) from *Mtb*,¹⁰⁰ with both (*R*- and (*S*-) configuration on the glycerol unit (Figure 4). Starting

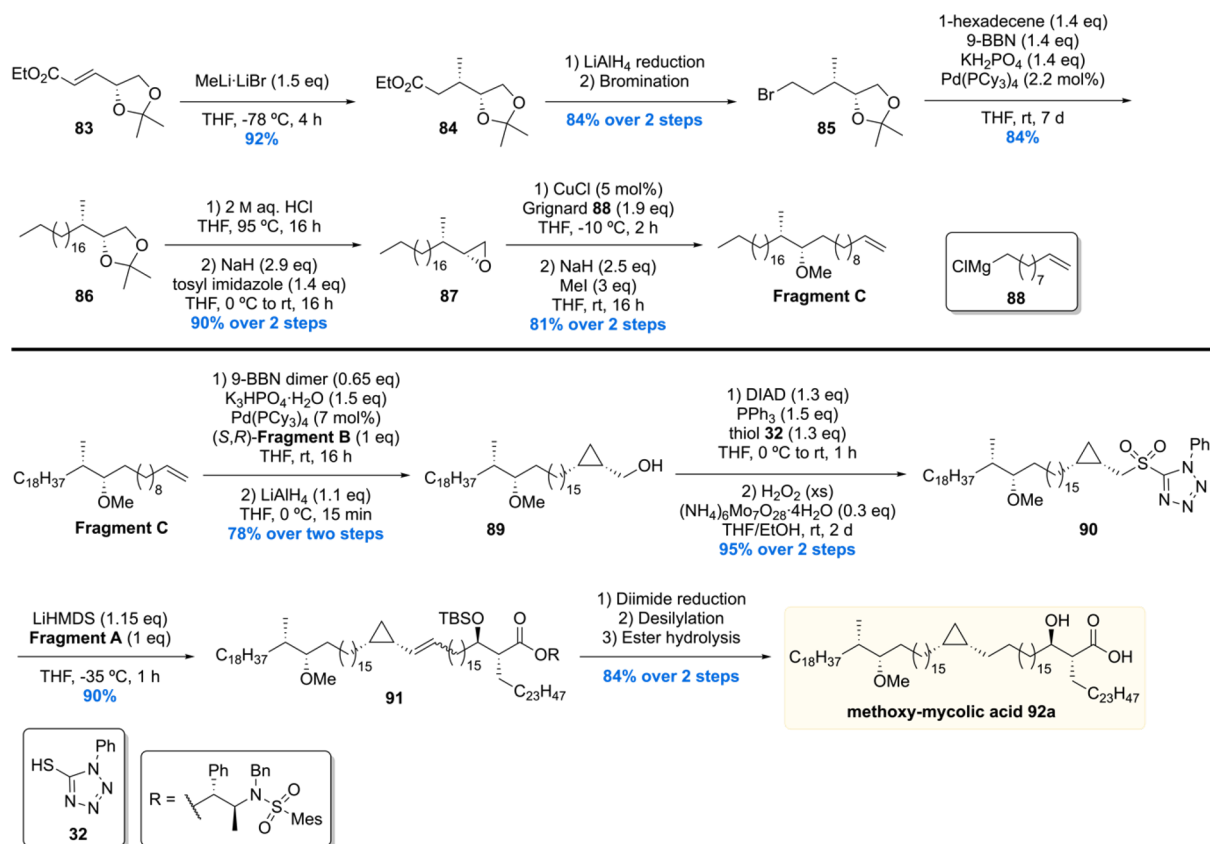
from commercially available (*R*- or (*S*-) solketal, a total of nine different GroMMs **61**–**69** were prepared. These were then evaluated for their ability to induce cytokine production in bone marrow-derived dendritic cells, yet none of the synthetic GroMMs displayed any effect. Besides that, in a follow-up report the GroMMs were shown to selectively induce CD11b-restricted germline-encoded mycolyl lipid-reactive (GEM) T-cell responses, similar to the response caused by free mycolic acids.¹⁰¹

2.3. Methoxy-mycolic Acid

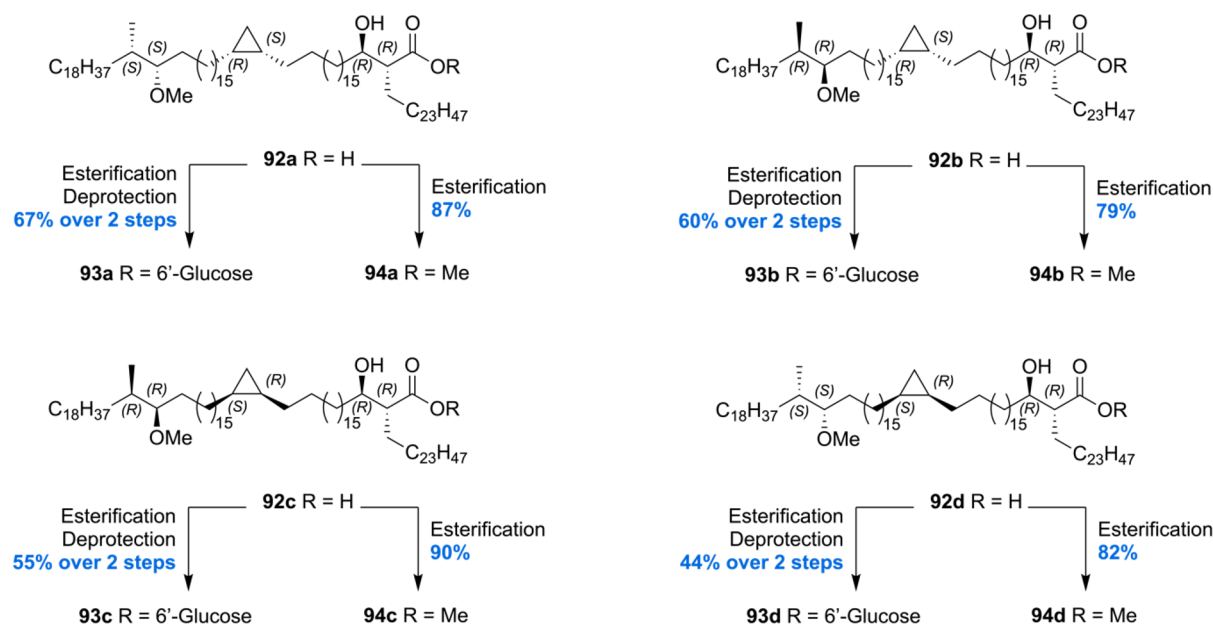
The most recent total synthesis of four diastereoisomers **92a**–**d** of methoxy-mycolic acid was communicated by our laboratory.⁷³ In order to access the target mycolic acids, a new synthetic strategy was developed involving the synthesis of three main fragments (A–C). For the assembly of the fragments to the desired mycolic acids, a Suzuki–Fu cross-coupling was incorporated in the synthesis to increase yield and to reduce the step count of the total synthesis. Two enantiomers of fragment B and C and the natural enantiomer of fragment A were prepared to access the four diastereomeric mycolic acids **92a**–**d**.

The synthesis of fragment A was initiated by the DIBAL-H reduction of lactone **70** followed by Wittig reaction providing α,β -unsaturated thioester **72** (Scheme 7). Subjecting **72** to a Fukuyama reduction produced saturated aldehyde **73** in 82% yield, notably with *in situ* protection of the free hydroxyl as its TES silyl ether. Next, chiral auxiliary **74** was esterified with the acyl bromide derived from 10-bromodecanoic acid delivering

Scheme 8. Minnaard's Methoxy-mycolic Acid Fragment C Synthesis and Fragment Unification

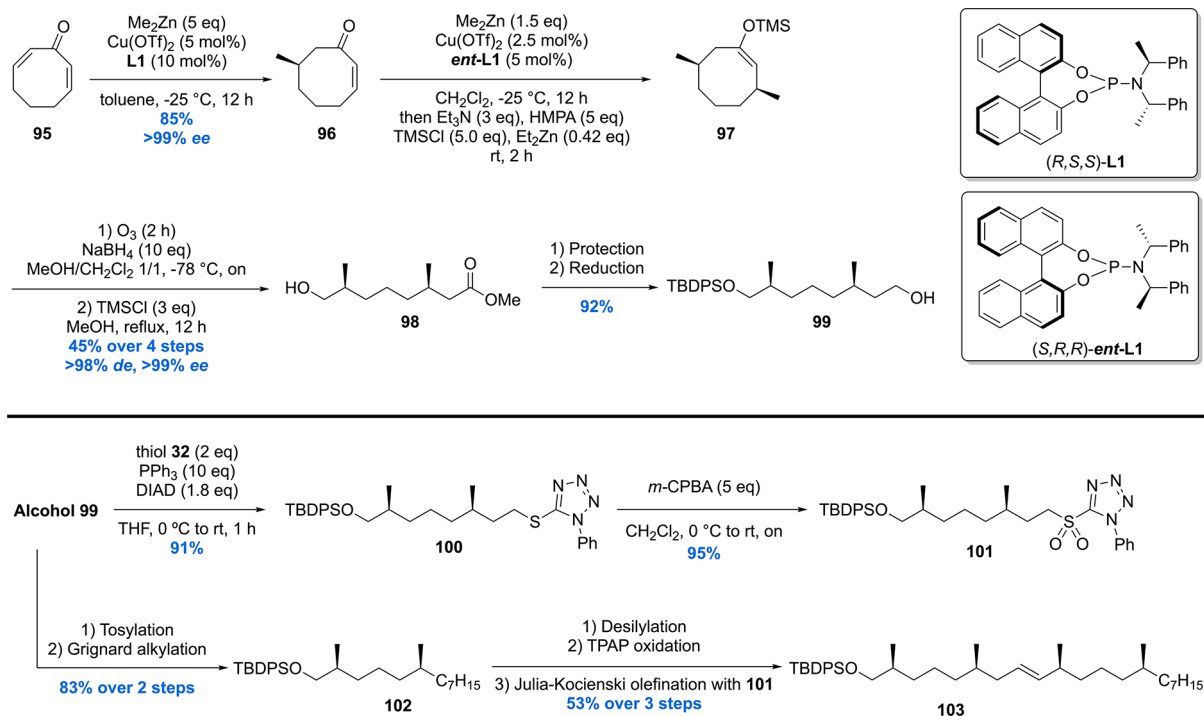


Scheme 9. Minnaard's Methoxy-mycolic Acid Derivatization



ester **75** in 94% yield. With **73** and **75** in hand, an Abiko–Masamune aldol reaction was performed, constructing the desired α -alkyl β -hydroxy-ester **76** in 55% yield with a *dr* of 97:3. Silyl protection of **76** followed by a Pd-catalyzed Suzuki–Fu cross-coupling with 1-hexadecene provided **77**. Selective silyl deprotection of the primary TBS ether followed by Dess–Martin oxidation concluded the synthesis of fragment **A** in 91% yield over two steps.

The synthesis of fragment **B** started with an alkyne–zipper reaction of **78** and subsequent silyl protection of the primary hydroxyl giving terminal alkyne **79** (Scheme 7). Next, **79** was deprotonated and treated with paraformaldehyde, and the product was subjected to a P-2 nickel reduction providing the desired *cis* allylic alcohol **80** in 51% yield over two steps. Charette asymmetric cyclopropanation of **80** yielded the desired cyclopropane **82** in 95% *ee*, which was protected as pivaloyl

Scheme 10. β -Mannosyl Phosphomycoketide Building Block Synthesis

ester, desilylated, and brominated giving fragment B in 87% yield over four steps. The other enantiomer of fragment B was synthesized in analogy.

The synthesis of fragment C was initiated with a diastereoselective conjugate addition of methyl lithium to **83** producing ester **84** (Scheme 8). Reduction of the ester moiety with LiAlH₄ to the corresponding alcohol followed by Appel bromination provided bromide **85**. Next, Suzuki–Fu cross-coupling between bromide **85** and 1-hexadecene furnished **86** in good yield. Acetonide deprotection of **86** and subsequent tosylation of the primary alcohol under basic conditions gave epoxide **87**. The epoxide moiety of **87** was then opened by reaction with Grignard reagent **88** in the presence of copper(I) followed by methylation of the alcohol providing fragment C in 81% yield over two steps. The enantiomer of fragment C was synthesized in the same manner. Notably all fragments were synthesized on (multi)gram scale, highlighting the efficiency and scalability of the synthetic route.

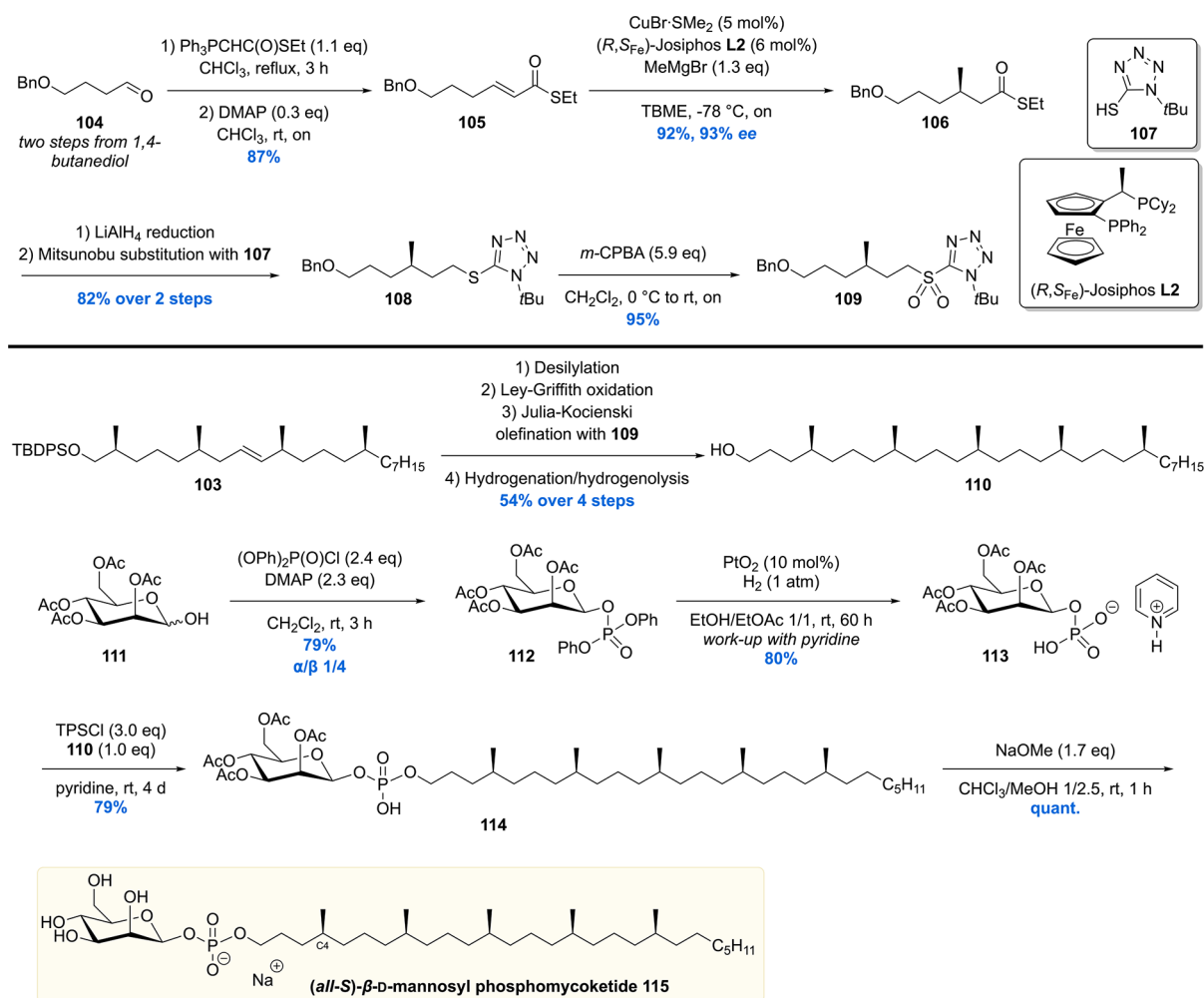
With all required fragments in hand, the final assembly was initiated by Suzuki–Fu cross-coupling of fragment C with fragment B (Scheme 8). After pivaloyl deprotection, the desired coupling product **89** was obtained in 78% yield over two steps. Next, the hydroxyl group of **89** was converted into the corresponding sulfone **90** by Misunobu reaction with **32** and oxidation. Sulfone **90** was then subjected to a Julia–Kocienski olefination with fragment A furnishing alkene **91** in 90% yield. The desired methoxy-mycolic acid **92a** was accessed from **91** by a three-step sequence. This strategy enabled the preparation of four methoxy-mycolic acid diastereomers **92a–d** (Scheme 9). In addition to the free mycolic acids, four diastereomers of the corresponding 6'-glucose- and methyl esters **93a–d** and **94a–d** were prepared for biological evaluation and comparison of optical rotations (Scheme 9).

The four synthetic mycolic acid diastereomers enabled confirmation of the stereochemical assignment of the methoxy methyl moiety. This was achieved by comparison of the specific

molar rotation, and the stereochemistry of the methoxy methyl unit was confirmed to be (S,S), as inferred by Asselineau and Baird (*vide supra*).^{67,94} The synthetic glucose monomycolates **93a–d** were tested for their T-cell antigenicity. It was found that all four diastereomers were able to activate LDNS T-cell lines in the presence of CD1b-expressing antigen presenting cells in a dose dependent manner. Furthermore, the free mycolic acids showed the ability to activate T-cells. Differences in T-cell response dependent on the stereochemistry of the methoxy methyl unit were observed, with the (S,S)-isomer **93a** and **93d** being the most potent over the natural and remaining synthetic mycolic acids. CD1b-tetramer staining experiments performed with synthetic glucose monomycolates **93a–d** showed minor differences dependent on the stereochemistry of the methoxy methyl moiety. Mycolates **93b** and **93c** with the natural (S,S)-configuration showed the strongest interaction between T-cell receptor and CD1b-mycolate, but no difference in interaction was observed regarding the cyclopropyl stereochemistry. However, in the case of free mycolic acids, significant differences based on the methoxy methyl stereochemistry were observed. Furthermore, mycolic acids **92a** and **92d** with the (R,S)-configuration on the cyclopropane ring show stronger interaction than the corresponding (S,R)-configured mycolic acids **92b** and **92c**. Assuming that the mycolic acids with the natural cyclopropane stereochemistry exert the highest T-cell receptor affinity, these results allowed the authors to propose that the naturally occurring stereochemistry of the *cis*-cyclopropane is (R,S).

3. β -D-MANNOSYL PHOSPHOMYCOKETIDE

Mannosyl phosphomycoketide (MPM) is a glycolipid antigen from *Mtb* that was found to be presented by CD1c. In 2000 Moody and co-workers reported the isolation of this molecule from *Mtb* and *M. avium*.¹⁰² MPM was postulated to be presented by CD1c by binding the alkyl chain within a hydrophobic groove. The moiety presented and recognized by the T-cell

Scheme 11. Completion of β -Mannosyl Phosphomycoketide

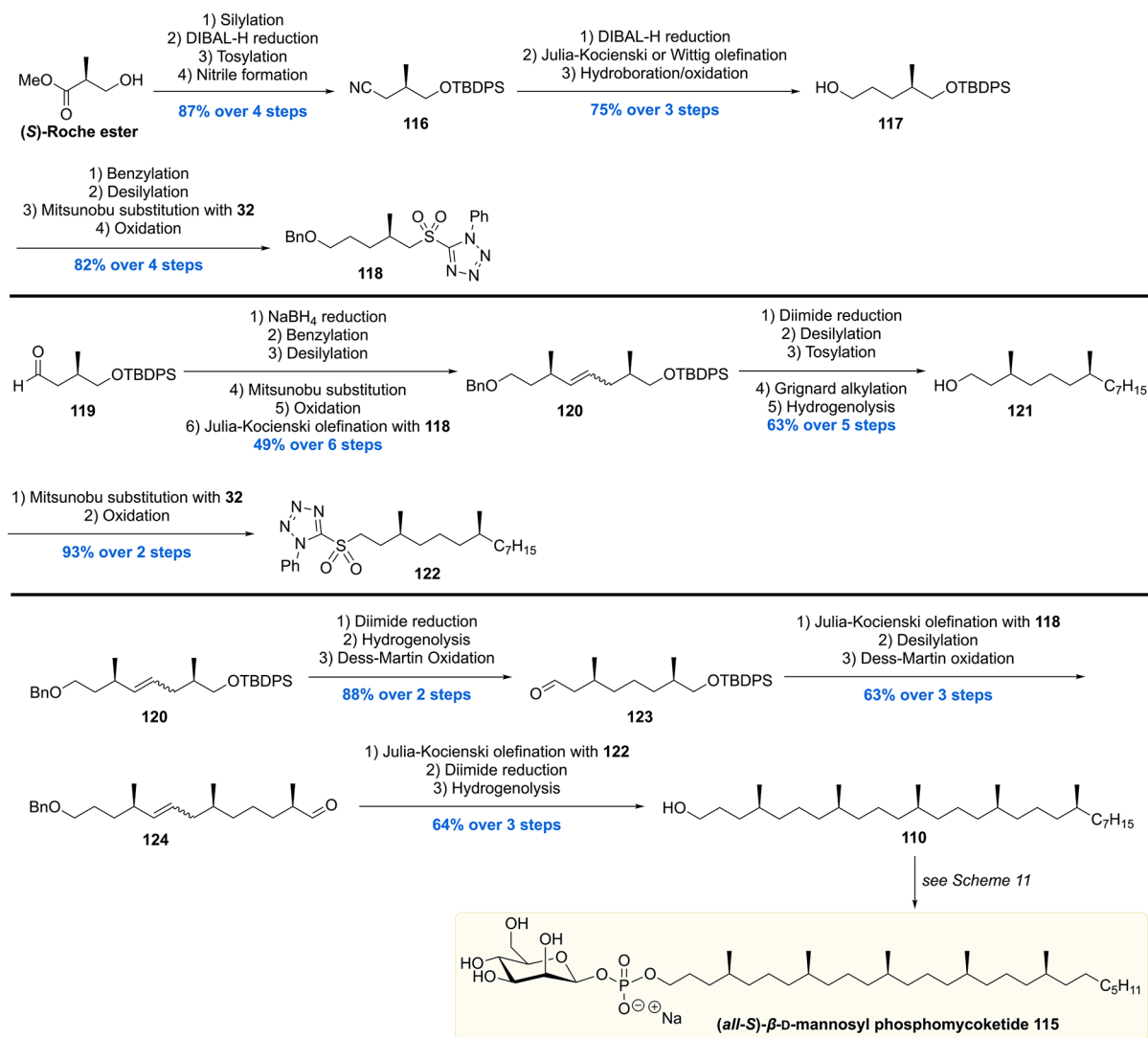
receptor is the hydrophilic mannosyl phosphate functionality. Interestingly, it was shown that the T-cell response was dependent on the chain length of the aliphatic moiety in MPM, with an optimum around C35. Also, the hydrophilic headgroup was shown to be crucial for the T-cell response as glucose, instead of mannose, was not recognized.

The structure of MPM was elucidated by mass spectrometry since only minute quantities of MPM were isolated. As a consequence, the assignment of the stereochemical elements present in the MPM chain and anomeric center remained unsolved. To elucidate the stereochemistry of MPM, a total synthesis was required followed by biological assays. In 2002, Crich and Dudkin set out to unravel the stereochemistry of the anomeric center of MPM by performing a stereorandom total synthesis of the mycoketide chain but stereoselectively synthesizing the glycosidic bond with both α - and β -stereochemistry.¹⁰³ The anomeric stereocenter was found to be a β -glycosidic bond by comparison of the MS fragmentation pattern with that in the original report. Despite these efforts, however, the stereochemistry of the methyl branches in the alkyl chain remained unknown.

In 2006, Minnaard and Feringa communicated the first asymmetric total synthesis of MPM (Schemes 10 and 11).^{104,105} At the start of the synthesis it was hypothesized that the biosynthesis of the mycoketide proceeds through an iterative sequence in which the methyl groups are introduced *all-syn* by

polyketide synthase pks12.¹⁰⁶ Arbitrarily, *all*-(*S*)-MPM **115** was chosen as the target.

The total synthesis started with dienone **95** which was prepared by means of a double IBX oxidation of cyclooctanone (Scheme 10).¹⁰⁷ Dienone **95** was used for the introduction of the first two stereogenic centers via sequential conjugate addition reactions of dimethylzinc. The first conjugate addition, in which a relatively high catalyst loading of 5 mol% of $\text{Cu}(\text{OTf})_2/10$ mol% of phosphoramidite **L1** was used to avoid Michael addition of the resulting zinc enolate, proceeded in an excellent *ee* of >99%, yielding compound **96** in 85% yield. The second asymmetric conjugate addition was performed using half the catalyst loading and using *ent*-**L1**. The enolate produced after conjugate addition was trapped *in situ* as its TMS enol ether **97** and subsequently converted into alcohol **98** using an ozonolysis-esterification protocol. The four-step sequence from **96** to **98** was performed with an overall yield of 45% and an excellent *de* of 98% and *ee* exceeding 99%. Alcohol **98** was subjected to silyl protection and ester reduction to provide building block **99**. Alcohol **99** was converted to the corresponding sulfone **90** by Mitsunobu reaction with tetrazole **32** followed by oxidation with *m*-CPBA in excellent yield. Furthermore, alcohol **99** was tosylated and then used in a Grignard alkylation in the presence of copper(I) to give silyl ether **102** in 83% over two steps. After desilylation of **91** and Ley-Griffith oxidation, the corresponding aldehyde was

Scheme 12. Piccirilli's Synthesis of β -Mannosyl Phosphomycoketide

coupled to sulfone **101** by means of Julia–Kocienski olefination. Alkene **103** was obtained in 53% over three steps.

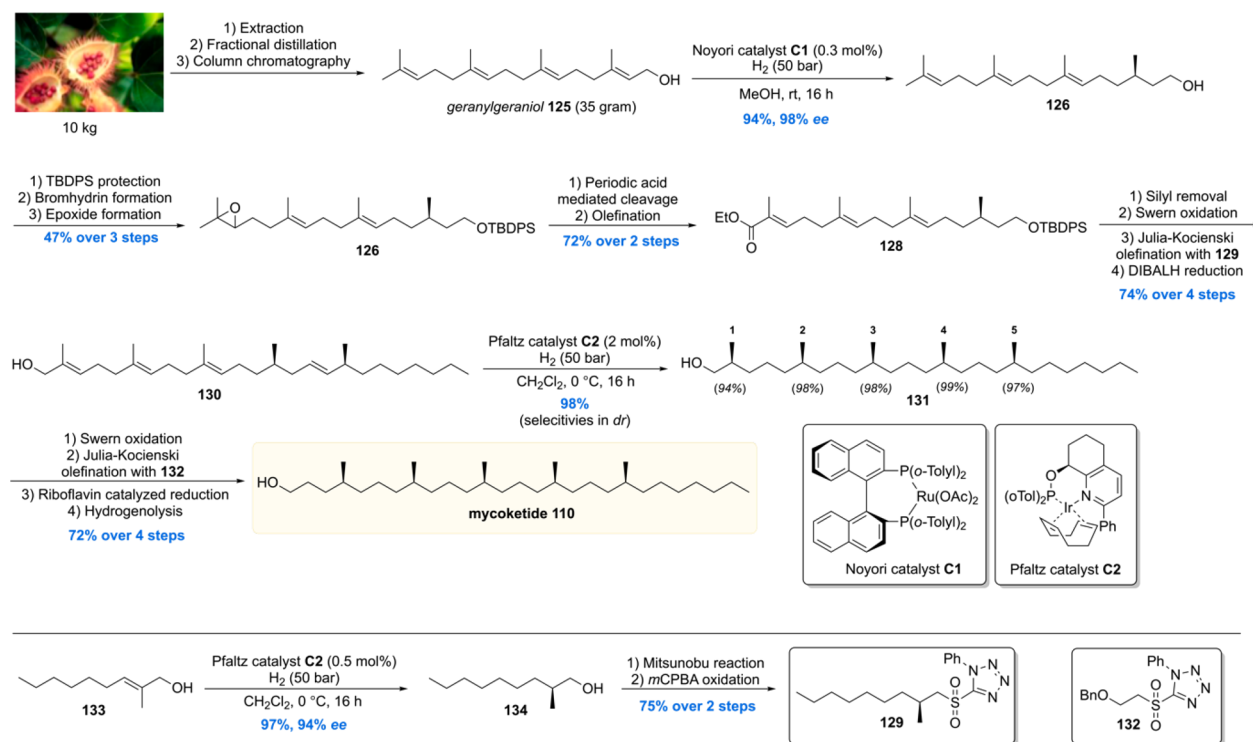
To complete the mycoketide chain, a fifth methyl-branched stereocenter had to be introduced (Scheme 11). This was realized by constructing sulfone building block **109** from 1,4-butanediol derived aldehyde **104**. This molecule was converted into pure (*E*)- α,β -unsaturated thioester **105** by performing a Wittig olefination (*E/Z* = 9:1) and subsequent DMAP-catalyzed isomerization. The fifth, and final, stereocenter of the MPM chain was introduced by means of an asymmetric copper-catalyzed conjugate addition with methylmagnesium bromide. The combination of 5 mol % of CuBr·SMe₂ with Josiphos ligand **L2** provided **106** in 92% yield with 93% *ee*. The thioester of **106** was fully reduced by LiAlH₄ and further functionalized to the sulfone **109**. A Julia–Kocienski olefination of the aldehyde generated from **103** and **109** was performed which produced, after orthogonal benzyl group hydrogenolysis and alkene hydrogenation, mycoketide **110** in a respectable 54% over the four steps.

The total synthesis of MPM was completed by connecting the mycoketide chain to the mannose headgroup (Scheme 11). This was realized by reacting **111** with diphenyl chlorophosphate to give predominantly the β -anomer of mannosyl phosphate **112** in

79% yield. The phenyl substituents were removed using Adams' catalyst which, after quenching with pyridine, afforded pyridinium mannosyl phosphate **113**. This fragment was reacted with mycoketide **110** to install the glycosidic bond with β -selectivity giving **114**. Removal of the acetate groups of the mannose concluded the first asymmetric total synthesis of *all*-(*S*)- β -MPM **115**.

Having achieved synthesis of milligram quantities of *all*-(*S*)-MPM **115**, the relative and absolute stereochemistry could be scrutinized in biological assays. Together with MPM, a set of analogues (*not shown*) were synthesized to perform a structure–activity relationship in order to find out what determines antigen binding by the T-cells. The synthetic compounds were tested and compared to natural isolate in an IL-2 release assay by subjecting CD1c-presenting cells to the MPMs.¹⁰⁸ It was found that *all*-(*S*)-MPM **115** exhibited a similar level of IL-2 release upon T-cell activation compared to the natural isolate. Notably, the stereorandom mixture of MPMs was significantly less potent. Also, when subjecting simplified MPM analogs with only a stereogenic C4-methyl (Scheme 11) to the T-cell activation assay, the molecule with (*S*)-stereochemistry showed much stronger activity than the (*R*)-isomer. These results thus showed that T-cell activation is highly sensitive to the stereochemistry of

Scheme 13. Minnaard's Second Synthesis of Mycoketide



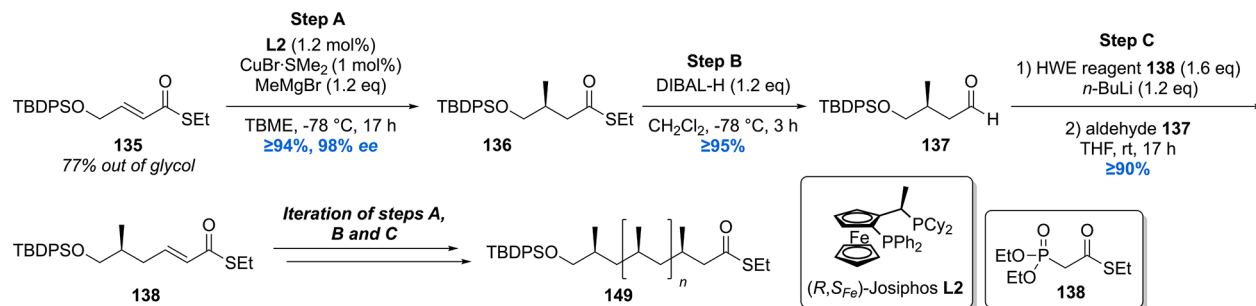
the MPM chain. In addition, synthetic α -MPM, phosphomycoketide (i.e., MPM without mannose), and mycoketide **110** were investigated, all showing no IL-2 release. All in all, as a result of the synthetic efforts and following biological evaluation, the overall structure of MPM was determined to have *all*-(*S*) stereochemistry for the methyl groups. The synthetic material was used to investigate the antigenicity of β -mannosyl phosphomycoketide. It was demonstrated that **115** is recognized by CD1c and that the lipid-branching pattern and (*S*)-stereochemistry were crucial for recognition.¹⁰⁹

The second total synthesis of *all*-(*S*)- β -mannosyl phosphomycoketide **115** was reported by the Piccirilli group (Scheme 12).¹¹⁰ Whereas in our synthesis asymmetric catalysis stood central, the Piccirilli laboratory mined from the chiral pool. Commercial (*S*)-Roche ester was used to construct sulfone **118** (11 steps) and sulfone **122** (13 steps from **119**). The sulfone building blocks came together in the assembly, by means of Julia–Kocienski olefinations, furnishing eventually MPM **115** with very high stereopurity (>96%). One other difference to our approach was the multiple reductions of the formed double bonds. Three diimide mediated reductions were employed as an alternative to our final Pd-catalyzed hydrogenation/debenzylation reaction. This methodology excludes potential epimerization of the nearby stereocenters, whereas the Pd-catalyst can cause this phenomenon by an isomerization/hydrogenation mechanism.

The MPM, as well as phosphomycoketide, synthesized was shared with immunologists who used it to establish the molecular basis of presentation by CD1c and its recognition by $\alpha\beta$ T cells.¹¹¹ A cocrystal structure of phosphomycoketide in CD1c was obtained and provided molecular insight in antigen binding and presenting to $\alpha\beta$ T cells.

Very recently the Minnaard lab executed a more streamlined and efficient total synthesis of the mycoketide lipid (Scheme 13).¹¹² When carefully examining the mycoketide structure, one

can envision the potential of geranylgeraniol **125** as a retrosynthetic precursor. Although geranylgeraniol is commercially available, its price (85 EUR/100 mg) limited its use for the development of a new total synthesis. This problem was overcome by isolation of geranylgeraniol from commercially available annatto seeds (*Bixa orellana*). Ten kilogram (~200 euro) of seeds was extracted with heptane followed by fractional distillation and column chromatography, affording 35 g of pure geranylgeraniol **125**. Initial investigations into a one-step *syn*-selective asymmetric reduction of the double bonds of **125** using Pfaltz catalyst **C2** showed that the reduction of the alkene proximal to the hydroxyl functionality had an inferior diastereoselectivity. To obtain maximum selectivity, albeit at the cost of the number of steps, the first stereocenter was introduced using a Noyori asymmetric hydrogenation with 0.3 mol % of catalyst **C1**, providing alcohol **126** in an excellent 94% yield with 98% *ee*. The alcohol was protected whereafter the terminal alkene was epoxidized, affording **127** in 47% over the three steps. The epoxide was then hydrolyzed to the vicinal diol as well as cleaved with periodic acid, with the resulting aldehyde subjected to a Horner–Wadworth–Emmons olefination to afford ester **128**. After removal of the protecting group and oxidation to the aldehyde, an additional stereocenter was introduced by means of a Julia–Kocienski olefination with stereochemical pure sulfone **129**, leaving the ester untouched. The ester was reduced, and compound **130** was subjected to an asymmetric hydrogenation with 2 mol% of Pfaltz catalyst **C2**. The stereocenters were introduced with excellent diastereoselectivities, producing *all*-*syn* alcohol **131** in 98% yield. Mycoketide **110** was then crafted out of this building block by a four-step sequence. This mycoketide total synthesis was completed with a longest linear sequence of 15 steps in 16% overall yield, which is a doubling of the overall yield compared to the previous 17 step synthesis which proceeded with 8% overall yield.

Scheme 14. General Iterative Deoxypropionate Synthesis Strategy Used in the Construction of *Mtb* Lipids¹¹⁸

4. 1,3-METHYL-BRANCHED LIPIDS

The mycobacterial cell envelope accommodates a variety of complex lipids and in particular a large number of 1,3-methyl-branched lipids and glycolipids in the outer membrane.^{44,113} These methyl-branched lipids form a tight, hydrophobic barrier by interaction with the covalently attached mycolic acid layer ultimately resulting in very low permeability of toxic molecules such as antibiotics.^{75,114,115} Apart from forming a thick physical barrier, these lipids are involved in receptor-mediated uptake by macrophages as well as modulation of the host immune response.^{17,40,116} Consequently, the 1,3-methyl-branched mycobacterial (glyco)lipids are of great interest to gain further insight into the immunology and pathophysiology of *Mtb*. Besides that, there has been growing interest by the organic chemistry community in constructing these chiral 1,3-methyl units with a high degree of stereocontrol and synthetic efficiency. The following section describes the synthesis of various 1,3-methyl-branched mycobacterial cell wall components and their use in biological studies. Furthermore, the accomplishments in synthetic method development are highlighted.

4.1. Catalytic Asymmetric Deoxypropionate Synthesis

After the synthesis of MPM, bearing a chiral 1,5-methyl array, our group gained interest in other *Mtb* lipids with repeating chiral 1,3-methyl units.¹¹³ Of particular interest are the complex glycolipids diacylated sulfoglycolipid (Ac₂SGL) and its “big brother” sulfolipid-1 (SL-1) (*vide infra*). These natural products contain lipid chains with up to eight repeating methyl groups, which is challenging to construct in an enantio- and diastereoselective fashion. Also, somewhat smaller molecules with shorter 1,3-methyl arrays were of synthetic and biological interest, which among others included PDIM-A, mycoside B, and diacyl trehaloses.

Since the deoxypropionate functionality is a repeating 1,3-methyl unit, at the time, an iterative synthesis seemed especially appealing. One iterative asymmetric synthesis of deoxypropionates that was used in several syntheses of *Mtb* lipids is based on the copper-catalyzed asymmetric conjugate addition (Cu-cat. ACA) of methylmagnesium bromide to α,β -unsaturated thioesters, by Feringa and Minnaard in 2005.¹¹⁷ The synthetic precursor for the iterative sequence is α,β -unsaturated thioester 135 (Scheme 14). A Cu-cat. ACA with methyl Grignard, using Josiphos L2 as the chiral ligand, proceeded in 94% yield and an excellent 98% ee. Thioester 136 was reduced to aldehyde 137 by DIBAL-H (or initially Fukuyama reduction), which was subjected to a Horner–Wadsworth–Emmons (HWE) olefination to provide α,β -unsaturated thioester 139 in high yields over the two steps. This sequence can be repeated until the desired number of methyl groups is installed. An attractive feature of this strategy is that the synthetic steps are easy to execute and high

yielding, and the sequence proved to be highly stereoselective as each consecutive methyl introduction led to increased diastereoselectivity. An obvious downside is the lack of convergence.

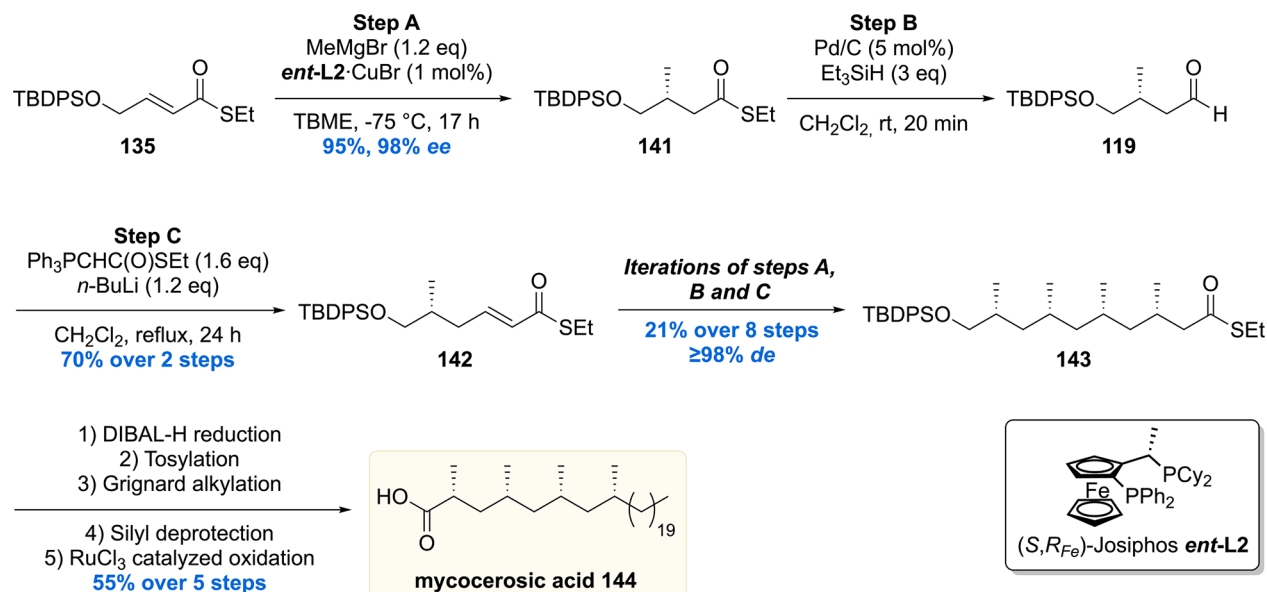
4.2. Phthiocerol Dimycocerosate A

The first *Mtb* lipid synthesized using the aforementioned iterative asymmetric conjugate addition protocol was phthiocerol dimycocerosate A (PDIM A).¹¹⁹ In 1999 two independent studies found that PDIM A is only present in virulent mycobacteria and that mutant strains deficient in PDIM A showed attenuated virulence.^{120,121} This finding thus suggested an important role for PDIM A as a virulence factor although its exact biological role remained elusive. In a study by Jackson and co-workers in 2004, it was found that PDIM production protects *Mtb* in its initial *in vivo* growth phase by protecting it from nitric oxide dependent killing mechanisms by macrophages and modulating the early immune response to infection.¹²² 10 years later, in connection to this finding, the Ramakrishnan laboratory reported that PDIM acts as a protective cloak for pathogen-associated molecular patterns (PAMPs).¹²³ These PAMPs can signal a Toll-like receptor dependent recruitment of microbicidal macrophages that produces reactive nitrogen species. This helps *Mtb* to evade these microbicidal macrophages but infect the permissive ones. PDIM has thus been linked to an immune-evasion mechanism.

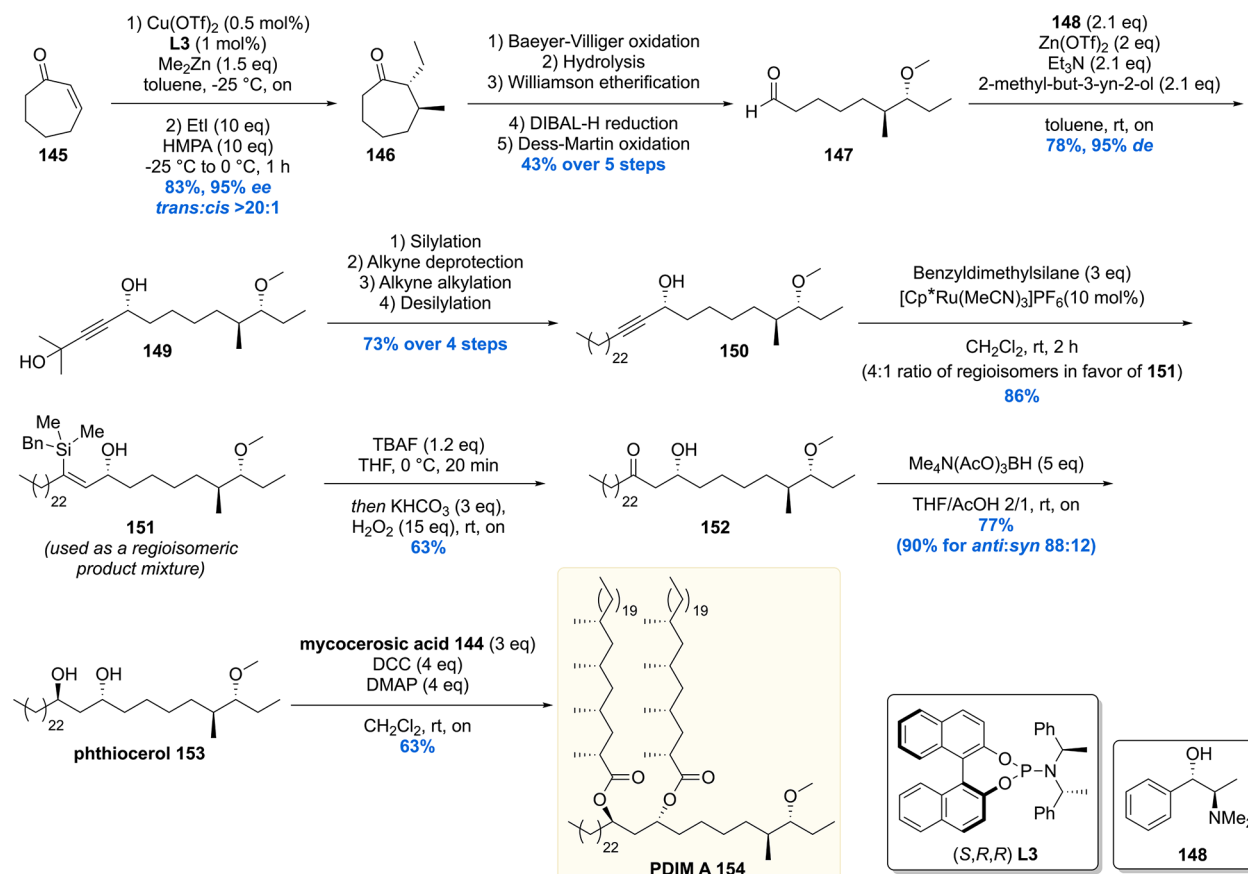
In 2001 the Guilhot laboratory showed that transposon mutants unable to synthesize or translocate PDIM A exhibit higher cell wall permeability and thus play a role in cell wall envelope architecture.¹²⁴ In further work from Guilhot and co-workers, it was demonstrated that PDIM is transferred from the *Mtb* cell wall into macrophage membranes to confer a lipid organization to modulate phagocytosis and infect macrophages.¹²⁵ Interestingly this biological function was attributed to a specific molecular conformation in which PDIM adopts a conical shape that inserts itself in the two opposing lipid bilayers of macrophage membranes.¹²⁶ This work, thus, shows that molecular shape confers biological activity and potentially explains previous work from the Briken lab, who revealed that the levels of PDIM A are in direct correlation with the ability of *Mtb* to escape the host phagosome and induce host cell necrosis.¹²⁷ Ramakrishnan and co-workers showed that this is likely caused by enhancing phagosomal permeabilization and that PDIM causes membrane damage,¹²⁸ which might be attributed to the conformation of PDIM.

Preceding the discovery of this intriguing biology, the structure and absolute configuration of the phthiocerol and mycocerosic acid chains were meticulously determined by the Polgar laboratory, by means of chemical degradation, in a series of publications ranging from 1954 to 1973.^{129–133} Confirmation

Scheme 15. Asymmetric Synthesis of Mycocerosic Acid by Cu-cat. ACA



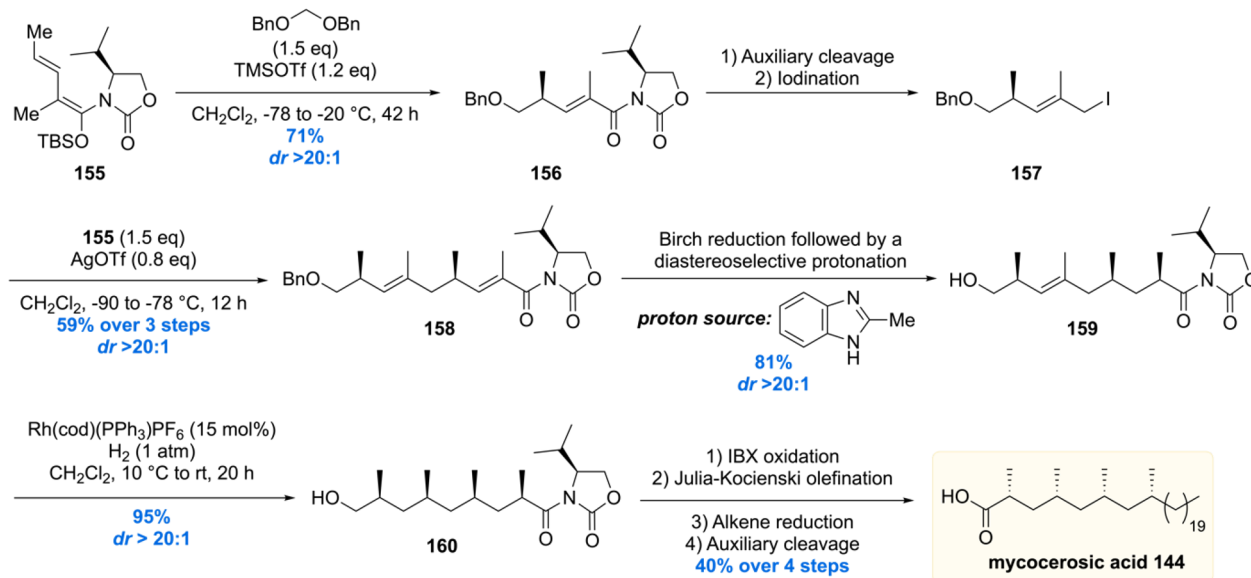
Scheme 16. Asymmetric Total Synthesis of PDIM A



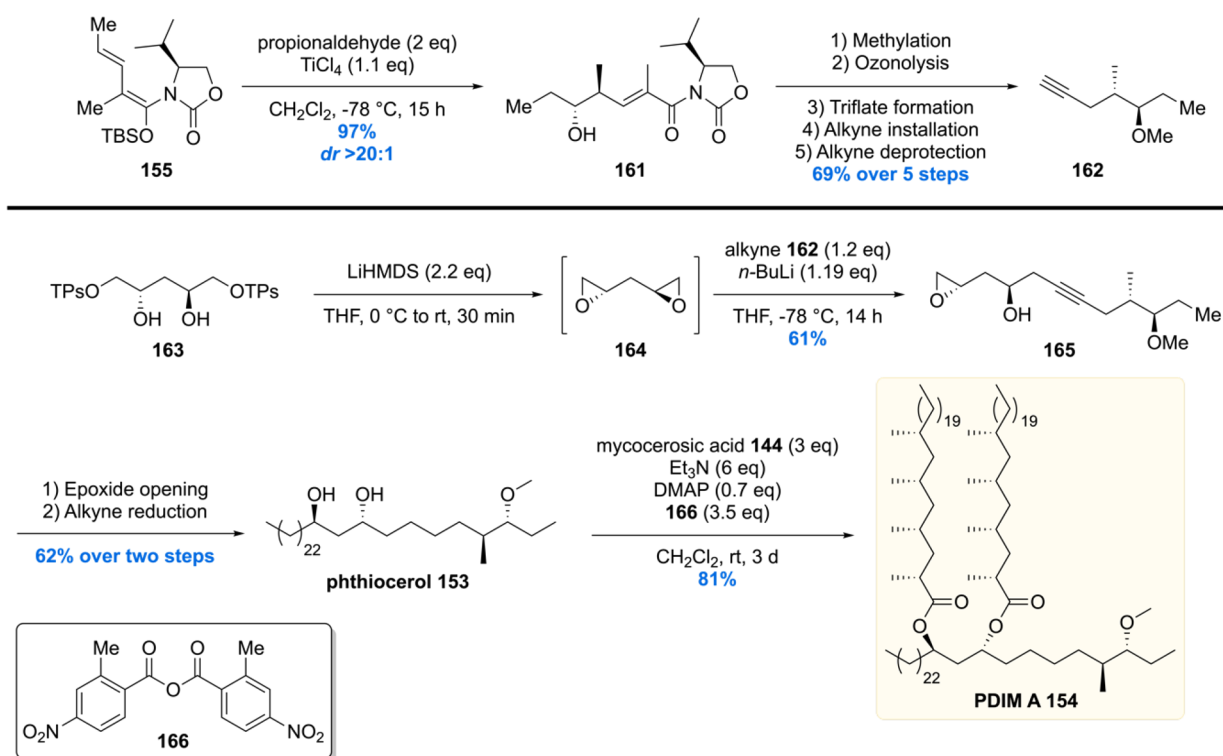
of the structure was provided by Guilhot and co-workers using MALDI and ¹H NMR analysis.¹²⁴ Despite the fact that these analyses were performed with care and did not contain any obvious flaws, misinterpretation of NMR data of complex lipids is easily made. The best way to confirm molecular structure is by means of chemical synthesis of a well-defined structure, which our group embarked upon by performing an asymmetric total synthesis of PDIM A (Schemes 15 and 16).

PDIM A consists of two parts: phthiocerol 153 which contains four stereogenic centers and mycocerosic acid 144 being the deoxypropionate moiety with four *all-syn* stereogenic methyl groups. Mycocerosic acid 144 was synthesized by the copper-catalyzed iterative conjugate addition sequence (*vide supra*).¹³⁴ The synthesis started from α,β -unsaturated thioester 135, and the four stereogenic methyl groups were installed providing thioester 143 in 15% yield over 11 steps and in

Scheme 17. Hosokawa Total Synthesis of Mycocerosic Acid



Scheme 18. Stereoselective Total Synthesis of PDIM A by the Hosokawa Laboratory

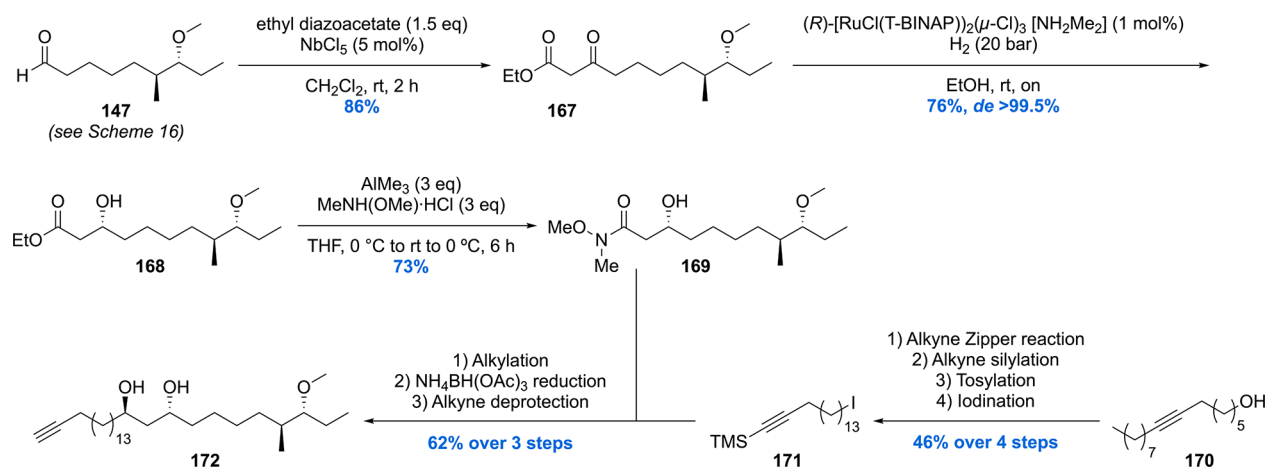


excellent $de > 98\%$ (Scheme 15). The thioester moiety of **143** was then reduced to the alcohol, followed by tosylation, Grignard alkylation, deprotection, and oxidation gave mycocerosic acid **144** in 55% yield over five steps.

Synthesis of the stereogenic methyl branch with a vicinal methoxy stereocenter of the phthiocerol moiety started with an asymmetric conjugate addition of Me_2Zn to cycloheptenone **145** in the presence of $\text{Cu}(\text{OTf})_2$ and phosphoramidite **L3** (Scheme 16). The enolate intermediate was trapped *in situ* with ethyl iodide to provide **146** with 95% *ee* and $> 20:1$ *de*. The functionalized cycloheptanone **146** was ring-opened through a Baeyer–Villiger oxidation/hydrolysis sequence, which after

three subsequent transformations provided aldehyde **147** in 43% over the five steps. The first stereogenic secondary alcohol was introduced by means of an asymmetric 1,2-addition of 2-methyl-3-butyn-2-ol to aldehyde **147**, employing (+)-*N,N*-dimethylphenidine **148** as the chiral ligand, to produce propargylic alcohol **149** with an excellent selectivity of 95% *de*. A four-step sequence converted **149** into alkyne **150**, which was hydrosilylated to yield vinyl silane **151** in 86%. The vinyl silane was oxidized to ketone **152** by means of a Tamao–Fleming oxidation which was diastereoselectively reduced with tetramethylammonium triacetoxyborohydride to yield phthiocerol **153**.

Scheme 19. Asymmetric Synthesis of the Phthiocerol Backbone in PGL-tb1



Ultimately, the hydroxy groups of the anti-1,3-diol **153** were esterified with mycocerosic acid **144** to produce the target molecule, PDIM A **154**. The NMR data and MALDI spectrum of the synthetic material were compared with the natural isolate and matched perfectly, thereby providing absolute confirmation of its proposed chemical structure. The synthetic material also aided in the development of an analytical procedure to detect PDIM A in *Mtb* samples.¹³⁵

In 2016 the Hosokawa laboratory reported the second stereoselective total synthesis of PDIM A.¹³⁶ The synthesis of mycocerosic acid **144** started with a vinylogous Mukaiyama alkylation of TBS enolate **155** and bisbenzyloxymethane (Scheme 17).¹³⁶ Stereinduction was efficiently achieved producing acyloxazolidinone **156** in 71% yield with an excellent *dr* > 20:1. Reductive auxiliary cleavage followed by iodination provided alkylating agent **157**. This reagent was used in another vinylogous alkylation with vinylogous TBS enol ether **155**, providing **158** in 59% over three steps, again with a diastereomeric ratio exceeding 20:1. The benzyl protecting group in **158** was removed by a Birch reduction, which also reduced the α,β -unsaturation to form the corresponding enolate. A diastereoselective protonation was performed with methylbenzimidazole as the proton source. More conventional proton sources (e.g., NH₄Cl and BHT) were shown to provide product **159** with poor diastereoselectivities (*dr* ~ 2:1), but methylbenzimidazole proved to be the reagent of choice, yielding **159** in 81% with a *dr* > 20:1. The last methyl-branched stereocenter was installed by means of a diastereoselective hydrogenation with 15 mol% Schrock–Osbourne catalyst, again providing an excellent diastereoselectivity (*dr* > 20:1), to furnish *all-syn* compound **160**. The synthesis of mycocerosic acid **144** was completed in four additional steps.

For the synthesis of PDIM A **154**, phthiocerol **153** had to be constructed (Scheme 18).¹³⁷ This time a vinylogous Mukaiyama aldol reaction was performed by reaction of propionaldehyde with vinylogous TBS enol ether **155**. The desired vinylogous aldol product **161** was isolated in near quantitative yield with a *dr* > 20:1. After methylation of the free alcohol, the chiral auxiliary was removed by means of ozonolysis, followed by a reductive workup. The intermediary alcohol was then converted into a good leaving group and substituted with an acetylene group providing **162** in 69% yield over five steps. The alkyne functionality of **162** was coupled with C₂-symmetric bis-epoxide **164** (prepared from diol **163**, TPPO = triisopropylbenzenesulfonate) to provide compound **165**. The epoxide was opened

with an alkyl nucleophile, and the triple bond was completely reduced to produce the desired phthiocerol **153**. As for the final step of the total synthesis, phthiocerol was esterified with mycocerosic acid **144** to give PDIM A **154** in its second total synthesis to date.

4.3. Phenolic Glycolipid

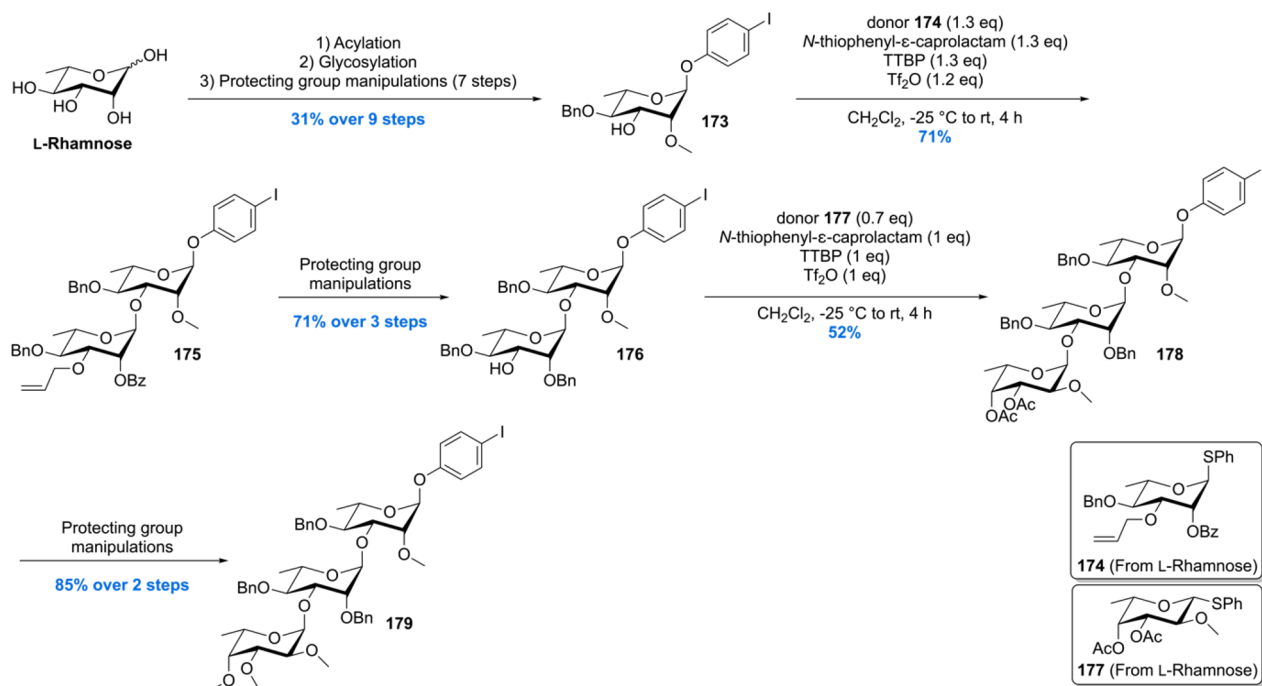
A molecule bearing structural similarities to PDIM A is phenolic glycolipid, PGL-tb1. Whereas PDIM A is purely lipidic, PGL-tb1 is essentially PDIM A linked to a phenol bearing a trisaccharide on the *para*-position. The first report about a PGL-tb1 came from the hands of Hunter and Brennan in 1981 in which they reported the isolation of PGL-tb1 from an *M. leprae* infected armadillo liver.¹³⁸ The structure was elucidated in following reports,^{139,140} but more importantly, PGL-tb1 was shown to be an antigen binding antibodies in both rabbit and human blood sera.¹³⁹

Although phenol-phthiocerol monosaccharides were known to be present in *M. bovis* since 1963,¹⁴¹ and later found to be present in *M. marinum*¹⁴² and *M. kansasii*,¹⁴³ no phthiocerol-based phenolic glycolipids were reported for *Mtb*. In 1989 this changed as the Daffé laboratory managed to show the existence of PGL-tb1 in the outer layer of the cell envelope in the Canetti strain of *Mtb*. A beautiful combination of chemical degradation with mass spectrometry and NMR analysis showed that PGL-tb1 from *Mtb* deviated in the trisaccharide part of the molecule from that of *M. leprae*,^{144,145} making the molecule somewhat species-specific and therefore a potential *Mtb* antigen.

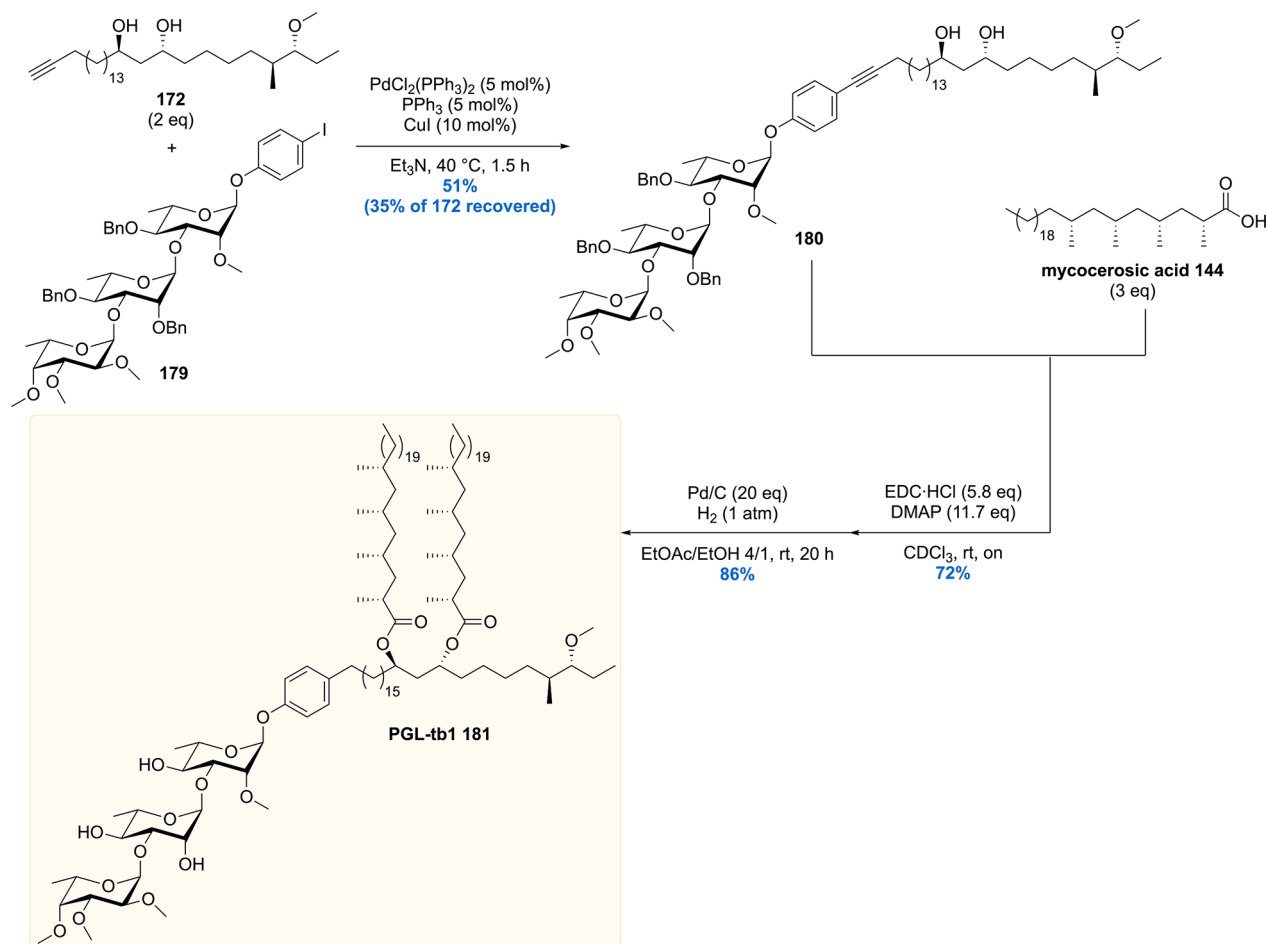
Despite having isolated PGL-tb1 for the first time from *Mtb*, Daffé and co-workers did not investigate the biological role of PGL-tb1. Yet, in 2004 it was shown that PGL-tb1 plays a major role in infection by conferring a “hyper lethal” phenotype, in murine disease models, in *Mtb* isolates belonging to the W-Beijing family.¹⁴⁶ This phenotype was shown to be the result of inhibiting the release of key inflammatory effector molecules (i.e., pro-inflammatory cytokines, tumor-necrosis factor- α , and interleukins 6 and 12) by cells of the host’s innate immune response. Knockout of the *pks1-15* gene, which is responsible for PGL-tb1 biosynthesis, resulted in loss of this hypervirulent phenotype.

The hypervirulent phenotype was further investigated by Sinsimer et al., and they showed the biological activity of PGL-tb1 is not caused by the molecule itself.¹⁴⁷ *Mtb* H37Rv (lab adapted strain), which does not produce PGL-tb1, was transformed to produce PGL-tb1 and subjected to *in vitro*

Scheme 20. Construction of the Trisaccharide Building Block for the Total Synthesis of PGL-tb1



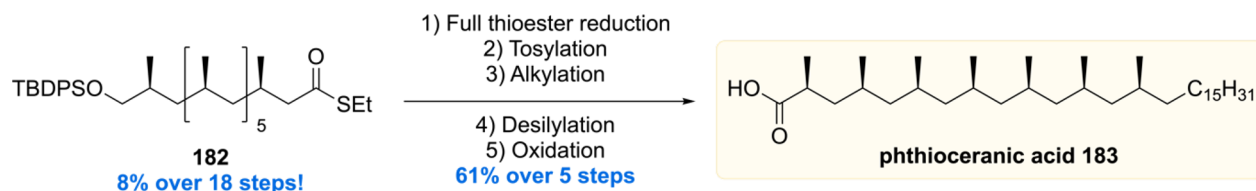
Scheme 21. Completion of the Total Synthesis of PGL-tb1



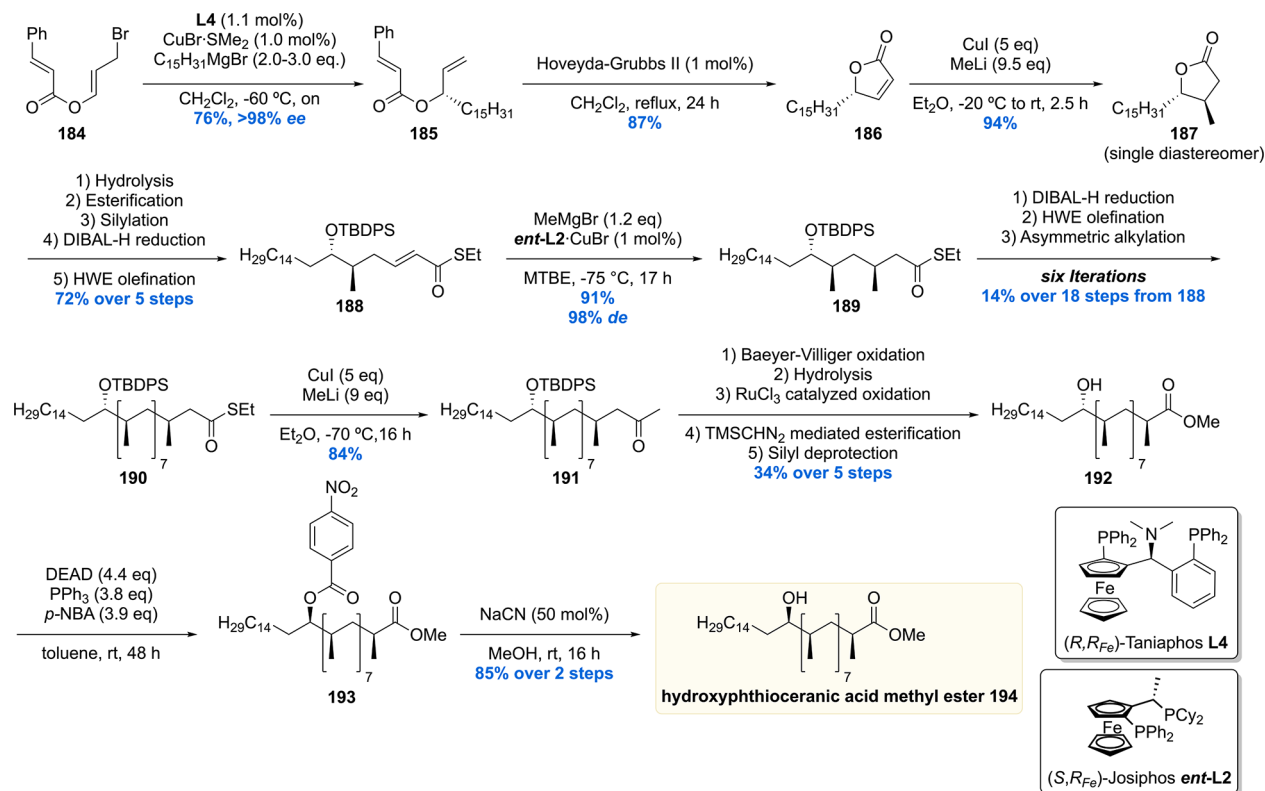
immunoassays. Also, here, suppressed induction of several pro- and anti-inflammatory cytokines in human monocytes was

observed; however, the production of PGL-tb1 did lead to increased virulence in mice and rabbits compared to the wild-

Scheme 22. Asymmetric Total Synthesis of Phthioceranic Acid



Scheme 23. First Generation Asymmetric Synthesis of Hydroxyphthioceranic Acid Methyl Ester



type H37Rv strain. It was therefore concluded that PGL-tb1 probably acts in synergy with other strain dependent factors. Still, PGL-tb1 is regarded as a virulence factor of *Mtb*.¹⁴⁸

A recent study in zebrafish addressed the role of PGL-tb1 in *Mtb* macrophage escapement. It was uncovered that the STING cytosolic sensing pathway in macrophages is activated by PGL-tb1, leading to chemokine production and recruitment of monocytes toward the site of infection. The resulting fusion of infected macrophages with monocytes enables transfer and further spreading of the bacterium. Thus, interruption of this PGL-tb1 dependent process could prove beneficial for clearing of *Mtb* infection.¹⁴⁹

The fact that PGL-tb1 can act as a target antigen for tuberculosis diagnosis was shown by the development of an ELISA based on PGL-tb1.¹⁵⁰ Since PGL-tb1 is produced in specific strains, in relatively small quantities, its isolation is tedious. Chemically synthesized PGL-tb1 can replace isolation procedures and assist the development of diagnostic tests and other biological assays.

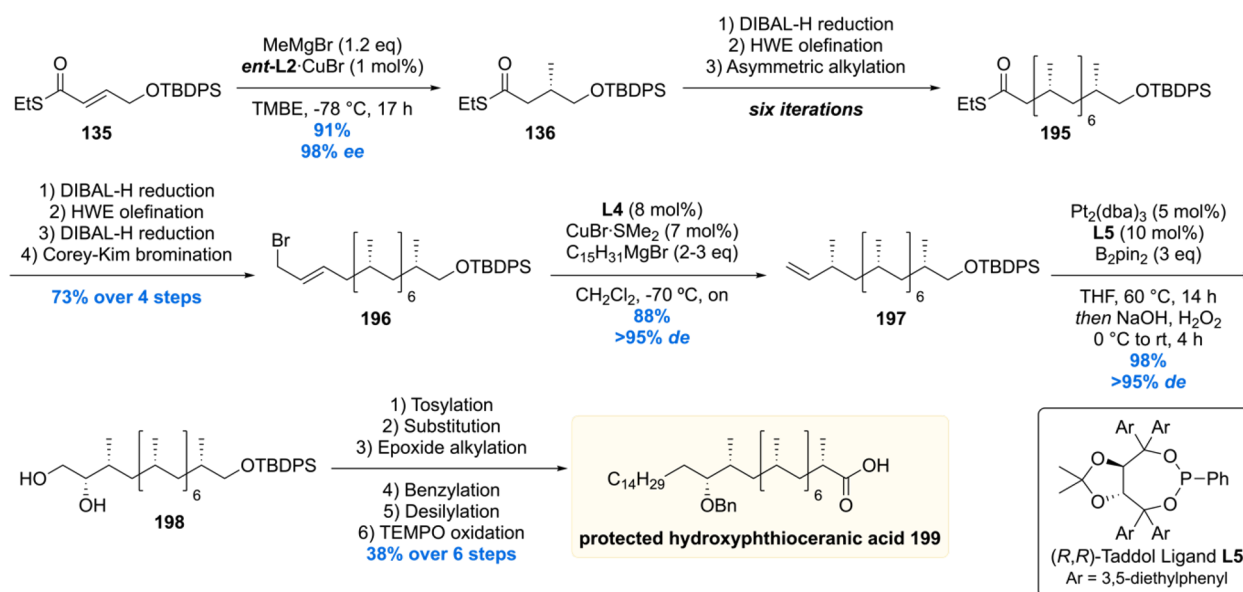
In 2012 our group reported the first, and up to date only, asymmetric synthesis of PGL-tb1 (Schemes 19–21).¹⁵¹ The synthesis started with the preparation of aldehyde 147 which was also used in the synthesis of PDIM A (Scheme 16).¹¹⁹ The aldehyde was converted into keto-ester 167 which was

stereoselectively hydrogenated using Noyori's catalyst with an excellent diastereoselectivity of >99% in 76% yield providing 168 (Scheme 19). After installation of this third stereocenter, the ester functionality in 147 was transformed into Weinreb amide 169. Compound 169 was alkylated with the alkyl lithium reagent generated from compound 171. The β -hydroxy ketone functionality formed by alkylation was then reduced to the 1,3-*anti* diol using the diastereoselective Saksena–Evans reduction using NH₄BH(OAc)₃. Deprotection of the alkyne provided key phthiocerol building block 172.

The trisaccharide building block 179 was constructed by conversion of L-rhamnose into glycoside acceptor 173 (Scheme 20). Glycosylation of 173 with glycosyl donor 174, using *N*-thiophenyl- ϵ -caprolactam and Tf₂O in a tri-*tert*-butyl pyrimidine (TTBP) buffered solution, provided the α -linked dirhamnoside 175 with full stereocontrol in 71% yield. After a three-step deprotection–protection sequence, the fucose functionality (177) was introduced to yield trisaccharide 179 after two subsequent steps (deacetylation and methylation).

Unification of the phthiocerol backbone 172 with trisaccharide 179 was achieved using a carefully optimized Sonagashira coupling, providing the desired cross-coupled product 180 in 51% yield, recovering 35% of precious phthiocerol building block 172 (Scheme 21). The mycocerosic acid esters were

Scheme 24. Second Generation Asymmetric Synthesis of Protected Hydroxyphthioceranic Acid



introduced followed by a benzylether hydrogenolysis to deprotect the trisaccharide and reduce the alkyne functionality. This concluded the first asymmetric total synthesis of PGL-tb1 **181**.

4.4. Phthioceranic and Hydroxyphthioceranic Acid

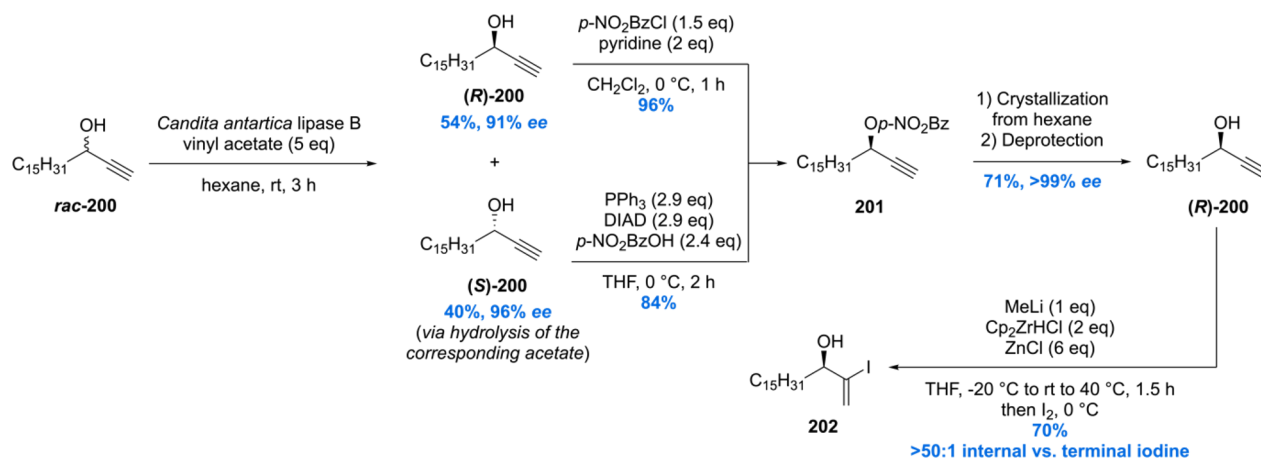
After the successful synthesis of mycocerosic acid and PGL-tb1, our group became interested in the synthesis of the even more complex lipids phthioceranic and hydroxyphthioceranic acid, which carry a total of seven to eight methyl branches as 1,3-*syn* arrays and an additional hydroxyl stereocenter. These two mycobacterial lipids are found as trehalose esters in the cell wall glycolipids Ac₂SGL and SL-1. By utilizing the in house developed Cu-cat. ACA strategy, phthioceranic acid Phthioceranic acid **183** was first synthesized in 2007 by ter Horst et al.¹¹⁸ The seven methyl units were installed in a linear fashion giving **182** in 8% yield over 18 steps (Scheme 22). With thioester **182** in hand, a five-step sequence gave phthioceranic acid in 61% yield over these steps.

The hydroxyphthioceranic acid lipid was synthesized using two different approaches as part of the total synthesis of Ac₂SGL (*vide infra*).¹⁵² In the first-generation synthesis (Scheme 23) the chiral hydroxyl moiety was constructed first using a copper/taniaphos L4-catalyzed allylic alkylation of ester **184** with C₁₅H₃₁MgBr producing desired olefin **185** in 76% yield with an excellent *ee* of >98%. Cyclization, by means of a ring-closing metathesis reaction, provided lactone **186** which was diastereoselectively methylated using a Gillman reaction to produce **187** in 94% yield. The α,β -unsaturated thioester **188** was synthesized in five steps from **187**, which set the stage for the iterative introduction of the remaining seven methyl groups. The stereogenic TBDPS protected alcohol in **188** proved not to be of influence on the asymmetric conjugate addition outcome as the methyl group was installed successfully providing **189** in 91% yield with *de* of 98%. Six iterations were performed to eventually provide deoxypropionate **190** in an 14% overall yield over the 18 steps from α,β -unsaturated thioester **188**. The thioester moiety in **190** was reacted with methyl lithium cuprate to yield the corresponding methyl ketone **191**, which in five steps was converted into hydroxyphthioceranic acid methyl ester **192**. Since the relative stereochemistry of the hydroxy functionality,

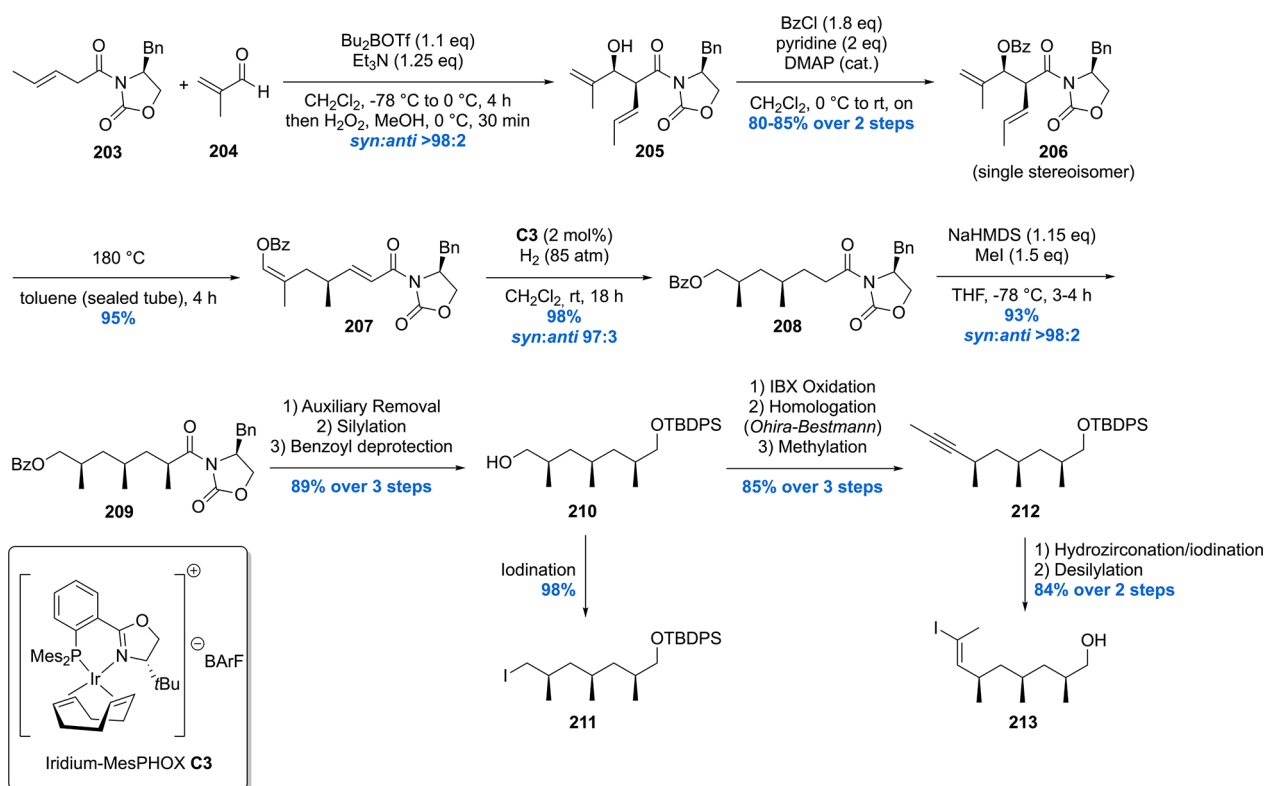
compared to the chiral methyl ramification, was unknown, an NMR comparison with natural hydroxyphthioceranic acid was performed which showed the hydroxyl function had opposite stereochemistry. This inconvenience was readily corrected by inversion of stereochemistry using a Mitsunobu reaction. The obtained *p*-nitrobenzoyl ester **193** was transesterified using MeOH and catalytic NaCN, affording hydroxyphthioceranic acid methyl ester **194** with the naturally occurring stereochemistry in place.

Critically reviewing our synthetic efforts, it was realized that the first-generation synthesis lacks the flexibility to also access phthioceranic acid from this route, which is required for the total synthesis of SL-1, the “big brother” of Ac₂SGL (*vide infra*). This is caused by first introducing the stereogenic hydroxyl functionality, which preferably is introduced in a late stage so that one route can provide both lipids. In addition, as the stereochemistry of this hydroxy group had been elucidated, the steps required for stereoinversion should be avoided. We achieved these goals (Scheme 24)¹⁵² by synthesis of compound **195**, the synthetic precursor to phthioceranic acid (Scheme 22), which was converted into allylic bromide **196** in four steps. Subjecting **196** to an asymmetric allylic alkylation with 7 mol% of CuBr·SMe₂ and 8 mol% of (*R,R*)-taniaphos L4 in the presence of MeMgBr, octamethyl alkene **197** was obtained in 88% yield with an excellent diastereomeric excess of >95%. The alkene functionality served as an excellent scaffold for the introduction of the stereogenic hydroxyl group. The most obvious reaction to do so, meanwhile also creating a functional group on the terminal carbon for introduction of the alkyl chain, is a Sharpless asymmetric dihydroxylation. Despite producing the desired product **198**, this reaction unfortunately provided a moderate diastereomeric excess of 70%.¹⁵³ This problem was eventually solved by performing an asymmetric diborylation reaction, which after oxidation provided the desired diol **198**. So, alkene **197** was reacted with bis(pinacolato)diboron (B₂pin₂) catalyzed by Pt₂(dba)₃ and taddol-based ligand L5. The diborylated product was oxidized to provide the desired diol **198** in 98% yield with a diastereomeric excess >95%. Having all stereocenters set, the aliphatic side chain and carboxylic acid

Scheme 25. Schneider's Hydroxyphthioceranic Acid Synthesis Part 1



Scheme 26. Schneider's Hydroxyphthioceranic Acid Synthesis Part 2



functionality were installed to yield protected hydroxyphthioceranic acid **199** in 38% over six steps.

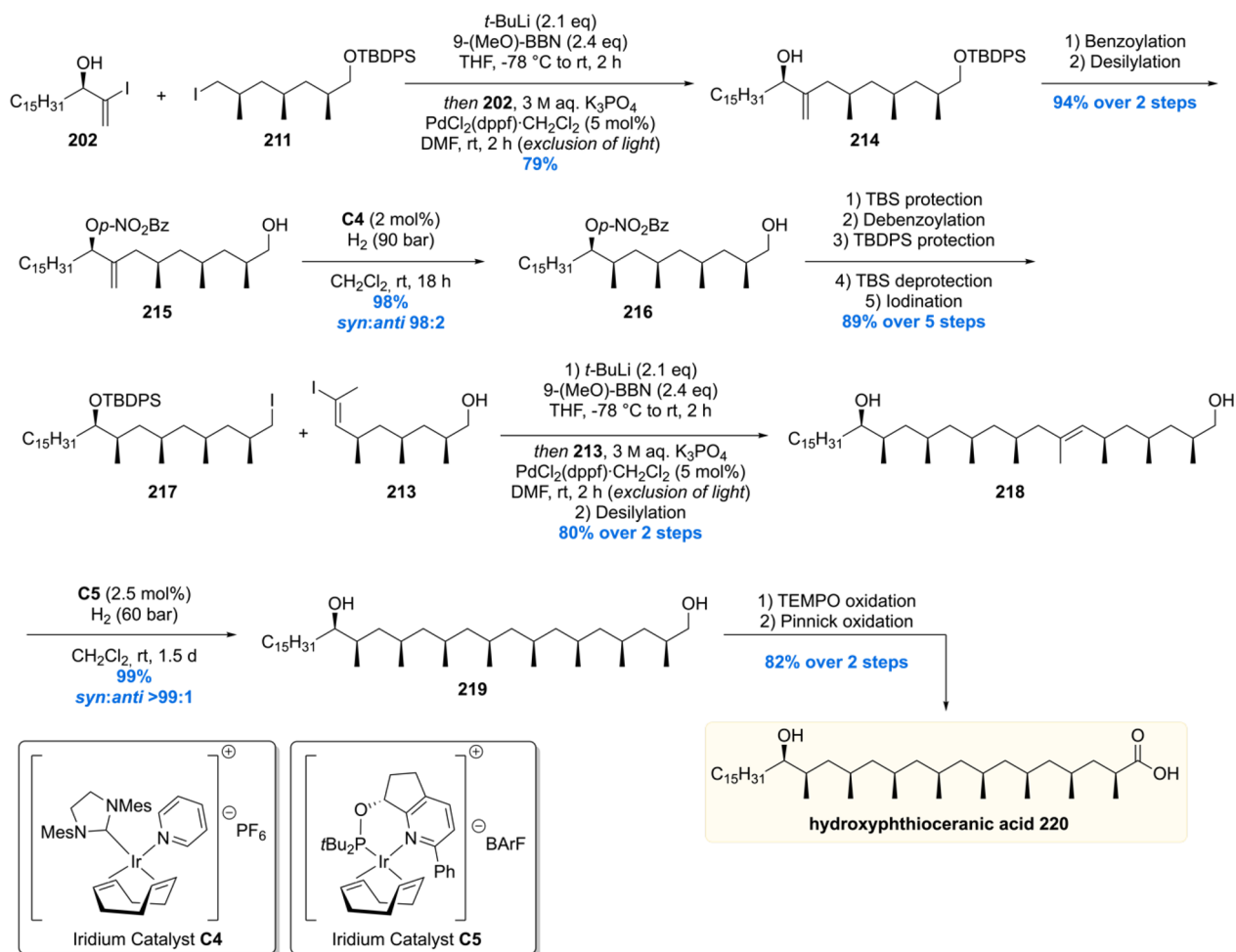
Since their first reported total syntheses^{118,152} phthioceranic and hydroxyphthioceranic acids have attracted a lot of attention. Over the past years, due to their exquisite and synthetically challenging 1,3-methyl ramification, five more stereoselective syntheses were reported by four different groups.^{154–158} This intriguing target motif has sparked the creativity of the chemical community to develop highly efficient and elegant solutions to the synthesis of the 1,3-methyl array.

In 2013, Schneider communicated a total synthesis in which the methyl branches were largely installed via iridium-catalyzed substrate controlled asymmetric hydrogenation (Scheme 25–27).¹⁵⁴ In contrast to ours, the Schneider synthesis is based on a more convergent approach in which three building blocks are unified. The synthesis started with the preparation of

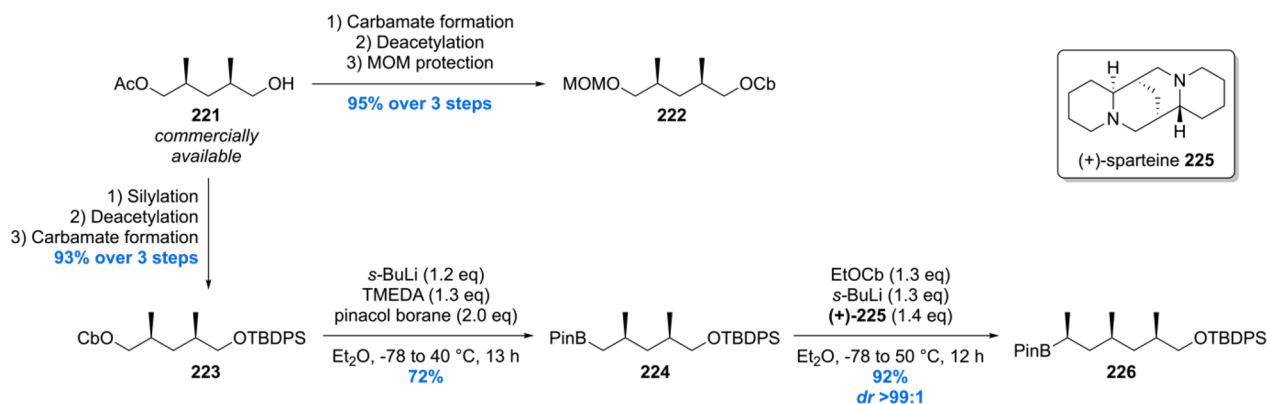
enantiopure (*R*)-**200** by an enzymatic kinetic resolution of propargylic alcohol *rac*-**200** employing commercially available Novozym 435 (Scheme 25). Both enantiomers were obtained in good yields with very high stereoselectivity (96% *ee* for (*S*)-**200** and 91% *ee* for (*R*)-**200**). Both of these products could be converted into benzoylated alcohol **201** which after multiple crystallizations from hexane, and subsequent deprotection, afforded (*R*)-**200** (>99% *ee*). Regioselective and substrate-controlled hydrozirconation employing a [Cp₂ZrHCl]/ZnCl₂ complex, followed by iodination, gave vinyl iodide **202** in 70% yield with no observable terminal iodide.

The other two building blocks to be crafted before assembly were alkyl iodide **211** and vinyl iodide **213**, which were reckoned to be available from common precursor **210** (Scheme 26).^{154,159,160} Starting with an Evans' radical reaction using **203** and methacrolein **204**, aldol product **205** was obtained with an

Scheme 27. Completion of the Total Synthesis of Hydroxyphthioceranic Acid by the Schneider Laboratory



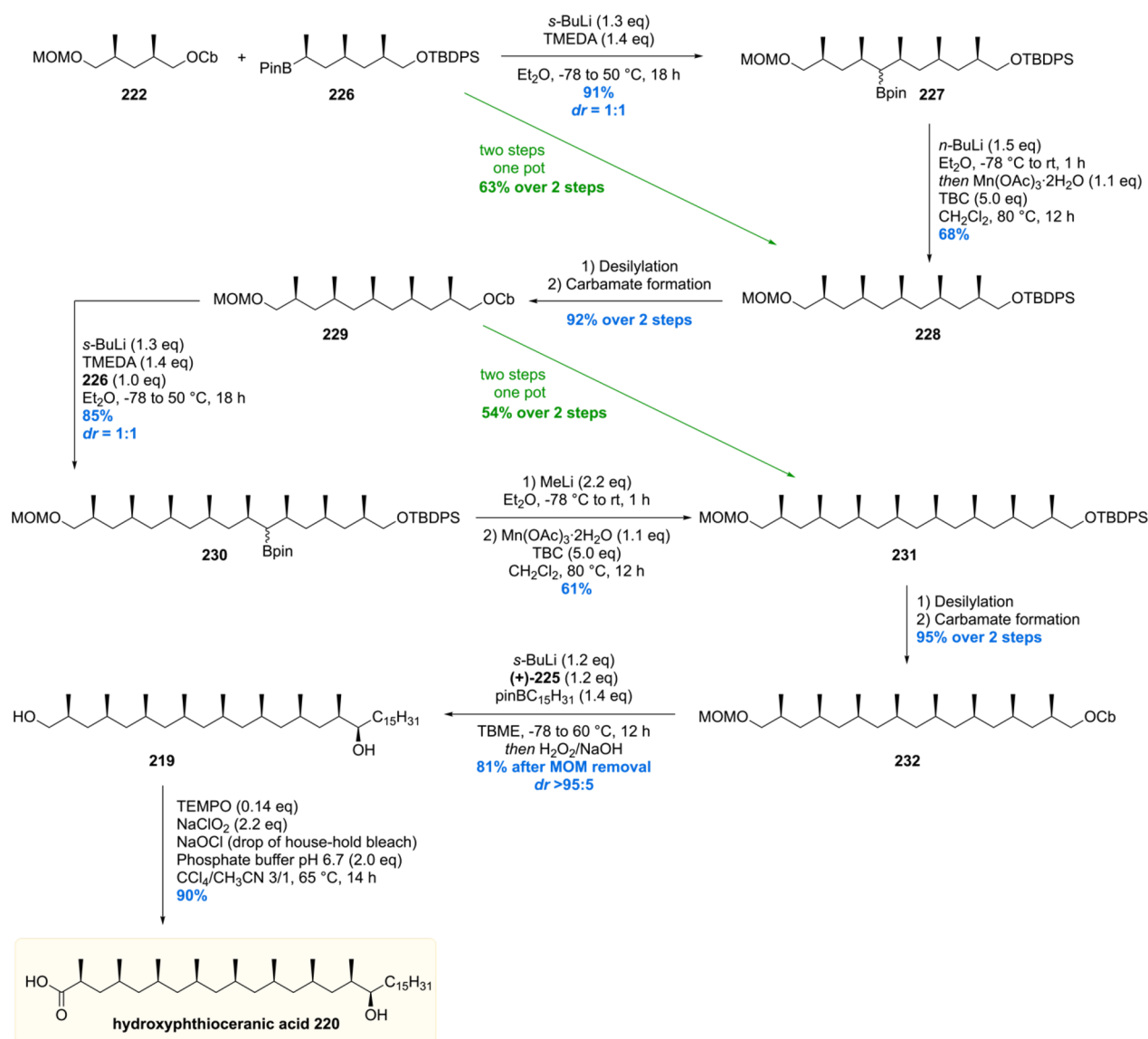
Scheme 28. Synthesis of Hydroxyphthioceranic Acid Building Blocks



excellent *syn:anti* ratio of >98:2. Benzoylation of **205** was followed by an oxy-Cope rearrangement yielding **207**. With the first chiral methyl branch set, the second methyl branch was installed by means of an asymmetric hydrogenation using 2 mol % of iridium catalyst **C3** delivering **208** in 98% yield and an excellent *dr* of 97:3. Further elaboration, by means of a stereoselective enolate alkylation, gave rise to trideoxypropionate **209** in 93% yield with a *syn:anti* ratio of >98:2. Auxiliary removal, silylation, and benzyl removal gave common intermediate **210** which could be easily converted into the building blocks **211** and **213**.

With the three desired building blocks in hand, the assembly of hydroxyphthioceranic acid commenced with a Suzuki cross-coupling of vinyl iodide **202** and trideoxypropionate **211**, yielding allylic alcohol **214** in 79% (Scheme 27). Diastereoselective hydrogenation of this substrate however failed due to accompanied alkene isomerization to the corresponding ketone. Therefore, **214** was benzoylated and desilylated in 94% yield over four steps before the diastereoselective hydrogenation with modified Crabtree's catalyst **C4**. Obtained in 98% yield and a 98:2 *syn:anti* ratio, **216** was easily converted to **217** in five steps. A Suzuki cross-coupling with building block **213** was performed

Scheme 29. Aggarwal's Hydroxyphthioceranic Acid Synthesis

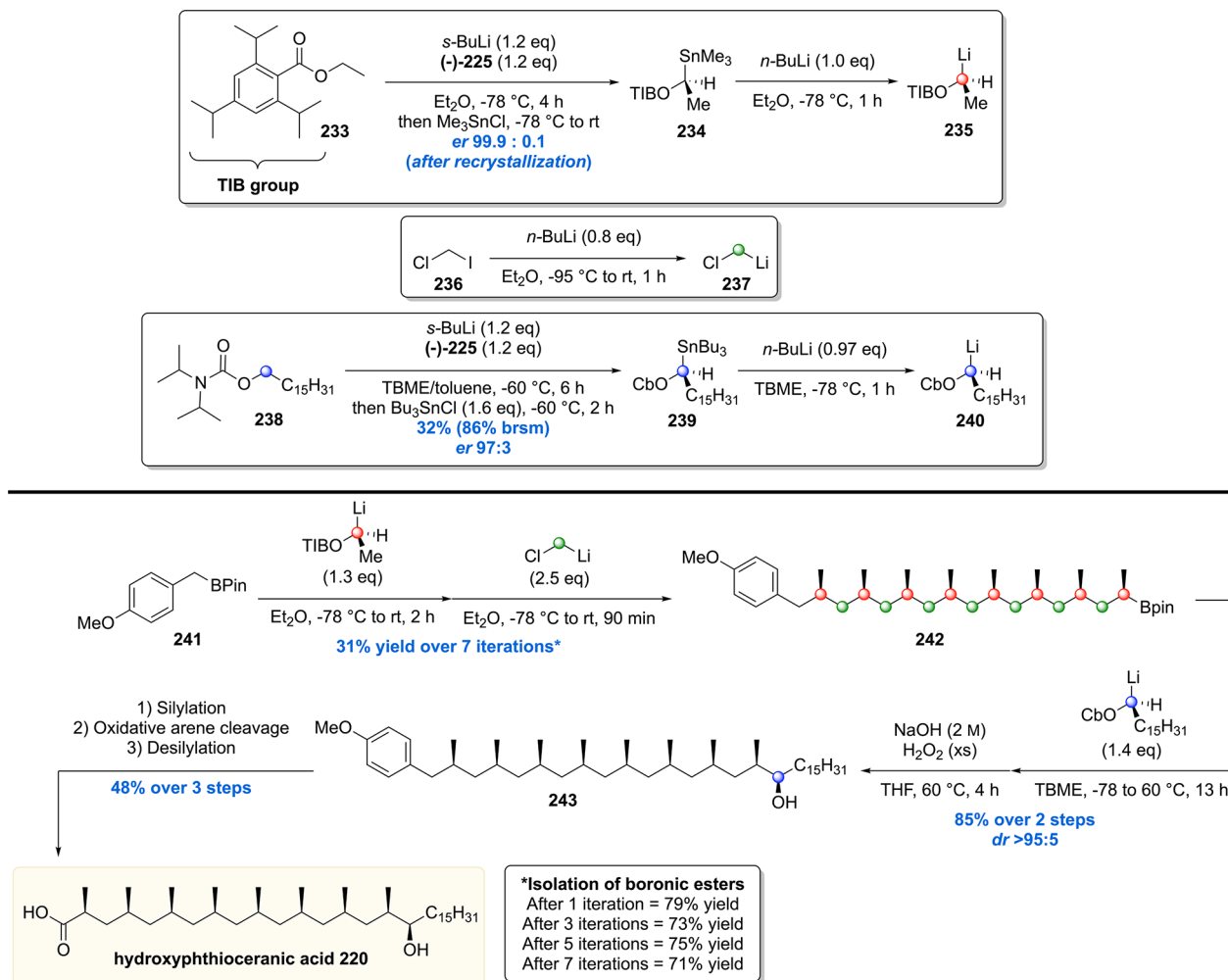


to give rise to alkene **218** after desilylation. To complete the construction of the deoxypropionate unit, another asymmetric iridium-catalyzed hydrogenation was performed affording diol **219** in 98% yield with an excellent *syn:anti* selectivity of >99:1. The synthesis of hydroxyphthioceranic acid **220** was finalized by a TEMPO oxidation of **219** followed by a Pinnick oxidation. Using this strategy, phthioceranic acid was also constructed (not shown).

The Aggarwal laboratory reported their hydroxyphthioceranic acid total synthesis in 2014, which was based on their in-house developed stereoselective lithiation–borylation–protodeboration strategy.¹⁵⁵ At first, two main building blocks were crafted from commercially available acetate **221** (Scheme 28). Standard protecting group manipulations furnished the 1,3-dimethyl carbamates **222** and **223**, of which the latter was borylated using standard conditions giving **224**. In order to obtain homologated product **226** with the correct stereochemistry, ethyl carbamate was deprotonated using *s*-BuLi/(+)-sparteine **225** followed by the addition of boronic ester **224**. Trimethylated boronic ester **226** was accessed in an excellent yield of 92% with a diastereomeric ratio of 99:1.

With sufficient quantities of the two key building blocks **222** and **226** synthesized, both were united by treatment of carbamate **222** with *s*-BuLi/TMEDA followed by addition of the boronic ester with **226** (Scheme 29). Pentamethylated product **227** was obtained smoothly in 91% yield with a diastereomeric ratio of 1:1 of the secondary boronic ester functionality. Protodeborylation of **227** was achieved by first treatment with *n*-BuLi (boronate formation) and subsequently Mn(OAc)₃·2H₂O (oxidant) and 4-*tert*-butylcatechol (TBC, H-donor) to provide **228** in a good yield of 68%. The two-step sequence described was also demonstrated to be feasible using a one-pot procedure providing the desired product **228** in effectively the same yield. Straightforward protecting group manipulations gave carbamate **229** which was subjected to the described lithiation/borylation/protodeboration strategy to give **231** in 51% yield over the two steps. Again, this sequence could be executed in one-pot as well, giving the product **231** in virtually the same yield. With the deoxypropionate functionality set, the final stereogenic center could be installed. After a two-step procedure, carbamate **232** was obtained, which by stereoselective deprotonation with *s*-BuLi/(+)-sparteine was borylated and subsequently oxidized to

Scheme 30. Aggarwal's "Assembly-Line" Synthesis of Hydroxyphthioceranic Acid



furnish alcohol **219** in 85% yield and an excellent diastereomeric ratio >95:5. Deprotection of the MOM group followed by chemoselective primary alcohol oxidation then gave hydroxyphthioceranic acid **220** in just 14 steps, an impressively small number and a considerable improvement compared to the Minnaard and Schneider routes (*vide supra*).

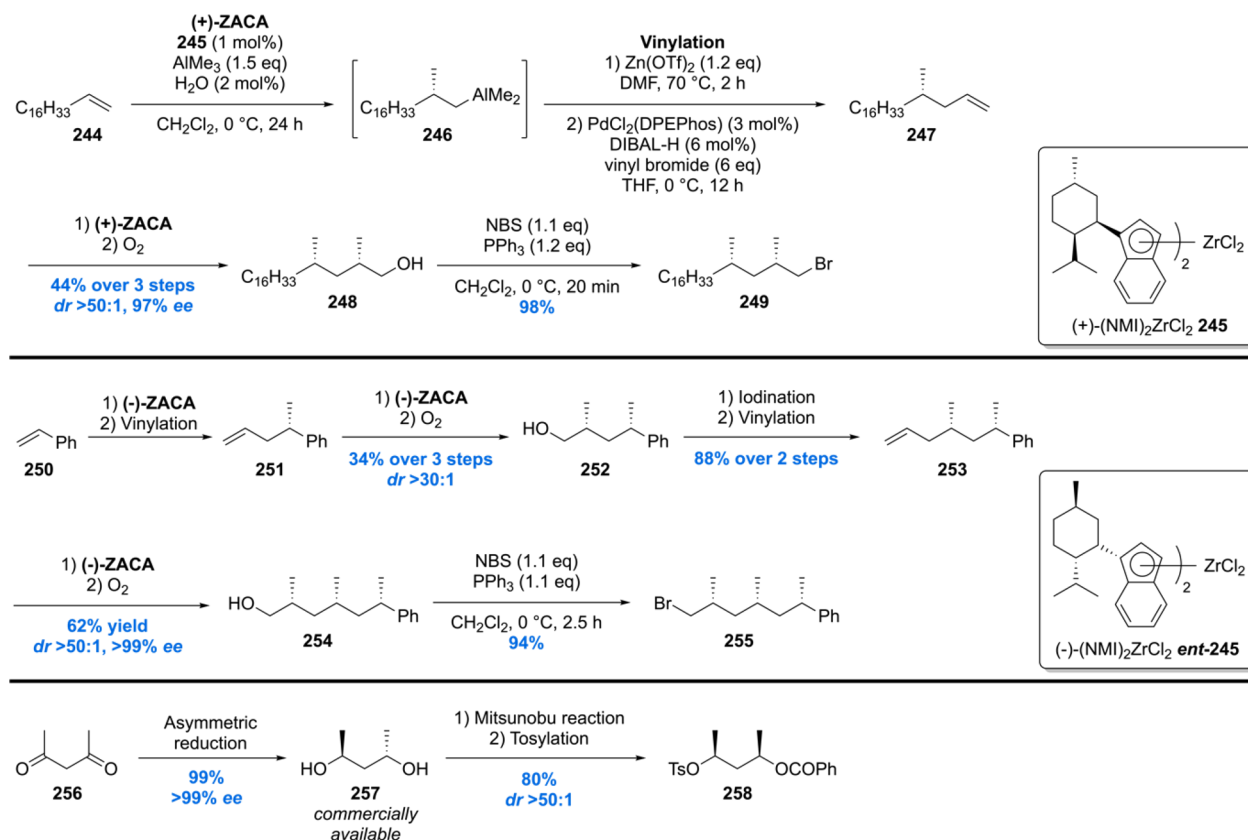
More recently the Aggarwal group reported the use of this methodology in an iterative fashion by an, even more efficient, "assembly-line synthesis" of hydroxyphthioceranic acid (Scheme 30).¹⁵⁶ This second-generation strategy improved on their previous synthesis in terms of step count (from 14 to 8, based on purification steps). To achieve this, the deoxypropionate motif was introduced by reaction of 4-methoxy aryl boronic ester **241** with lithium reagent **235**, followed by coupling with (chloromethyl)lithium **237**. After every two methyl installations, the corresponding boronic ester product was purified, which was realized in an average of 75% yield for two methyl group incorporations. After a total of seven iterations (31% overall yield), all desired stereogenic methyl groups were installed. Boronic ester **242** was then subjected to a reaction with lithium reagent **240**, which after hydrolysis of the intermediate boronate furnished alcohol **243**, in 85% yield and a diastereomeric ratio >95:5. Silyl protection, oxidative arene cleavage, and silyl deprotection then concluded the synthesis of hydroxyphthioceranic acid **220**.

In 2015 Negishi and co-workers reported the iterative synthesis of phthioceranic acid based on the Zr-catalyzed asymmetric carboalumination (ZACA) of alkenes to install the chiral methyl-branched groups.¹⁵⁷ The synthesis also proved to be convergent, requiring the synthesis of three optically pure building blocks (Scheme 31). Two of these building blocks were crafted by means of the ZACA reaction. To construct building block **249**, octadec-1-ene **244** was subjected to the asymmetric carboalumination reaction to produce the corresponding aluminate **246**. This intermediate was transmetalated to the organozinc reagent, a substrate used in the Negishi cross-coupling with vinyl bromide. The terminal alkene **247** obtained was once more subjected to the ZACA reaction and subsequently oxidized with molecular oxygen to provide alcohol **248** in 44% over the three steps with excellent stereoselectivities (*dr* > 50:1, 97% *ee*). Bromination completed the synthesis of building block **249**.

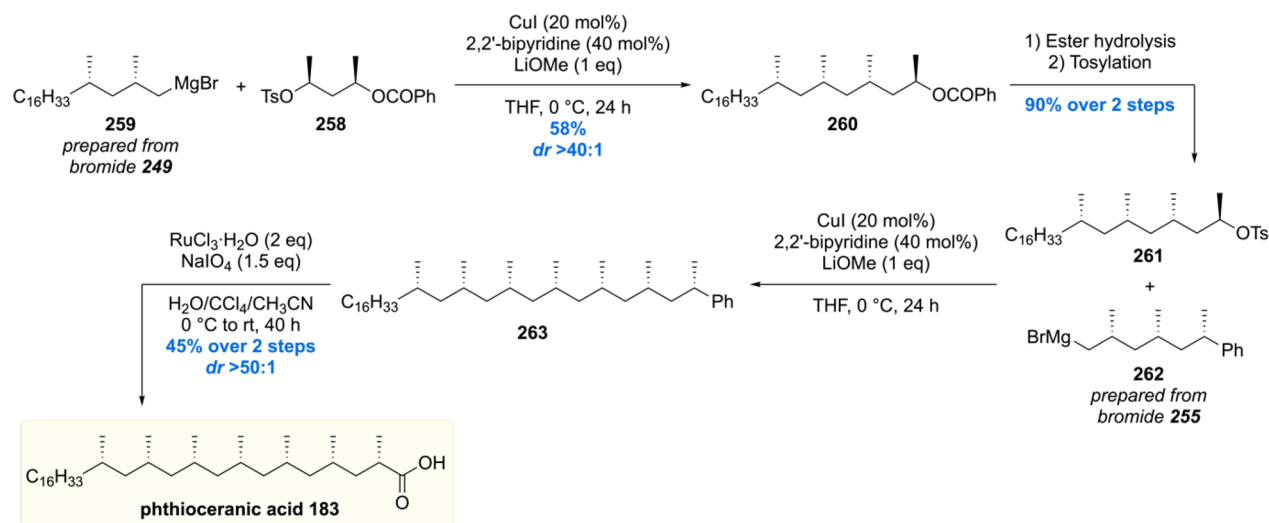
Building block **255** was crafted out of styrene which also efficiently reacted under the ZACA conditions to provide the desired stereogenic center. After vinylation of the intermediary aluminate, two subsequent ZACA reactions were performed to install the remaining two stereogenic centers, affording, after bromination, bromide **255** with a diastereomeric ratio of >50:1 with an enantiomeric excess >99%.

The third building block **258** was created out of enantiomerically enriched, commercially available, diol **257**. A Mitsunobu

Scheme 31. Synthesis of Phthioceranic Acid Building Blocks



Scheme 32. Completion of the Synthesis of Phthioceranic Acid



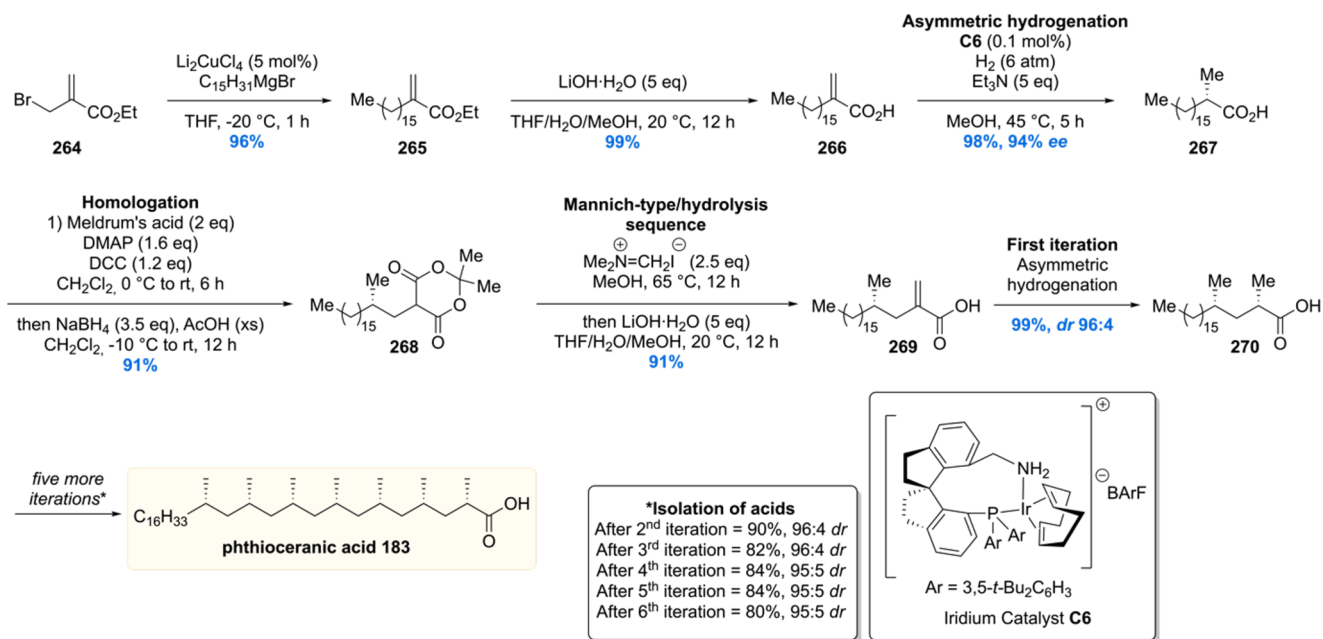
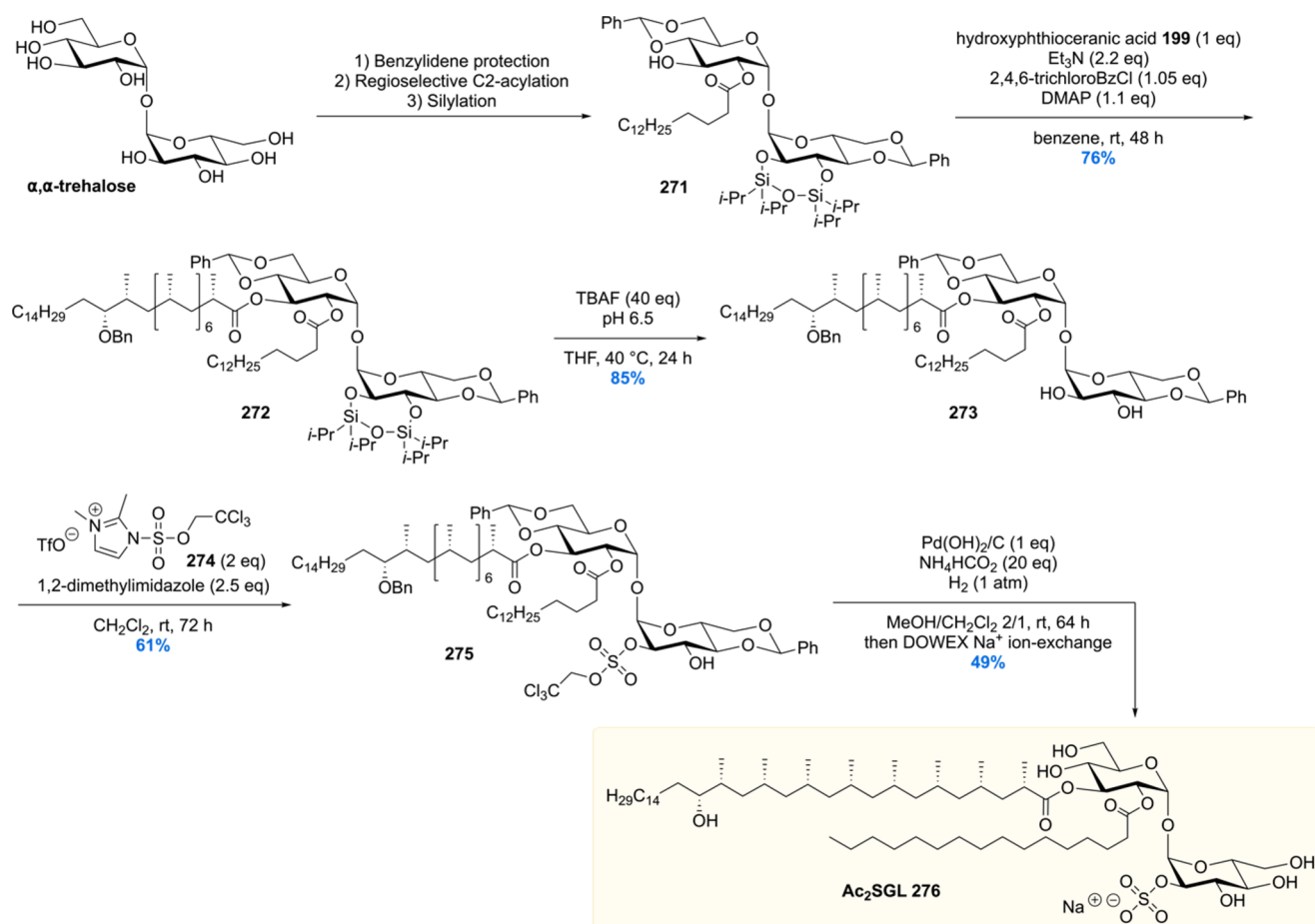
reaction and subsequent tosylation produced building block **258** in 80% yield with a *dr* of >50:1.

The building blocks were unified in only five steps to furnish phthioceranic acid (Scheme 32). Building block **249** was converted into the corresponding Grignard reagent and coupled with tosylate **258** in a S_N2 reaction by using cuprate chemistry. The diastereoselectivity proved to be excellent (*dr* > 40:1) providing the desired compound in 58% yield. The ester functionality in **260** was hydrolyzed, and the obtained alcohol was tosylated, in 90% over the two steps, to form **261**. Again, a Grignard reagent was formed, this time from building block **255**,

and coupled under similar conditions as previously mentioned to provide, after oxidative cleavage of the arene group, phthioceranic acid **183** with a diastereomeric ratio of >50:1.

The most recent dissemination of an iterative synthesis of phthioceranic acid was published by the groups of Zhu and Zhou in 2018 (Scheme 33).¹⁵⁸ Their total synthesis started with the nucleophilic displacement of the bromide in ethyl 2-(bromomethyl)acrylate **264** with a, from pentadecyl Grignard prepared, Gillman reagent, followed by hydrolysis of the ethyl ester. With the free carboxylic acid **266** in hand, the first stereogenic methyl group was installed by means of an

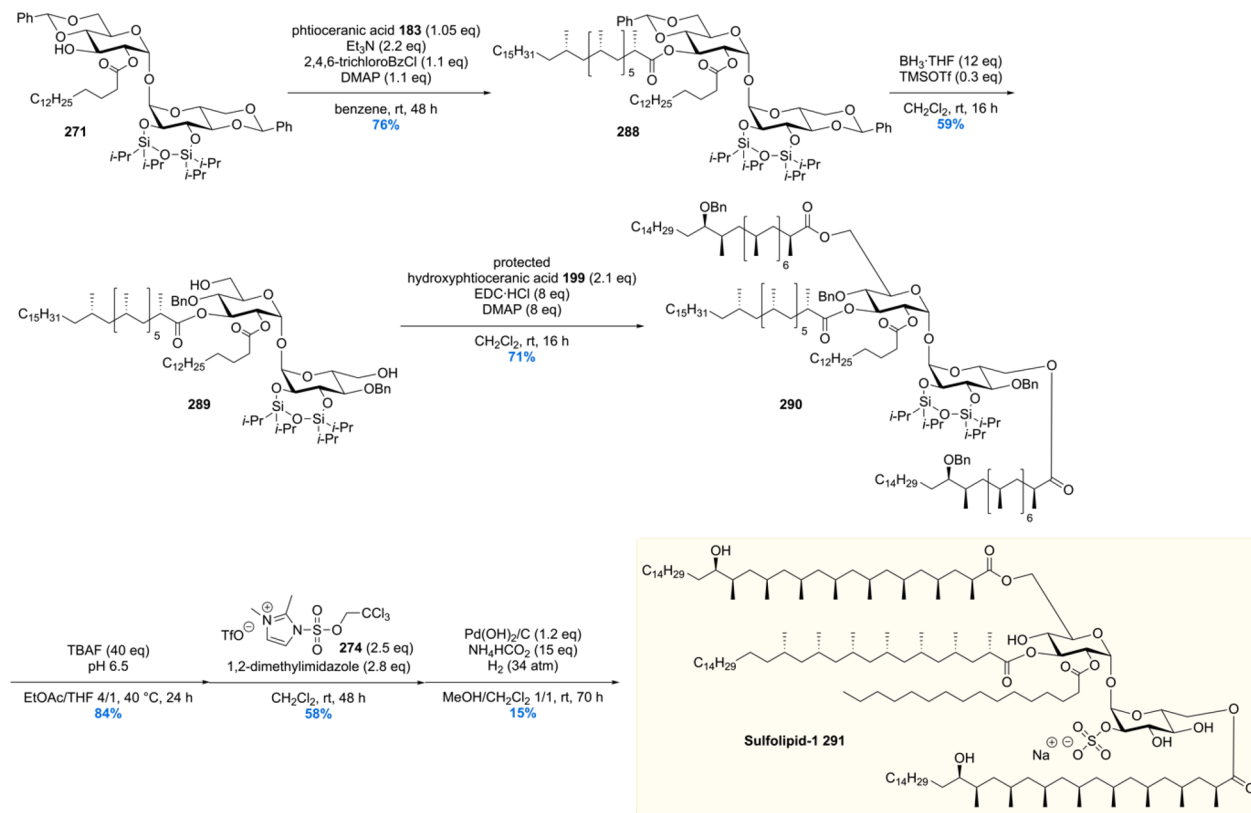
Scheme 33. Zhu and Zhou's 19-Step Phthioceranic Acid Synthesis

Scheme 34. Completion of the Total Synthesis of Naturally Occurring Ac₂SGL

asymmetric hydrogenation using only 0.1 mol% of chiral spiro *P,N*-ligand-based iridium catalyst **C6**, which proceeded in 94% *ee* and gave **267** near quantitative yield. The carboxylic acid was homologated by means of a carboxymethylation with Meldrum's

acid, followed by alkenylation with Eschenmoser's salt, and subsequent *in situ* hydrolysis to yield acrylic acid **269**. This two-step sequence proceeded in a yield of 81%, setting the stage for the first iteration in which the second stereogenic methyl branch

Scheme 36. Total Synthesis of SL-1



bacterial culture), however, makes chemical synthesis a viable tool for producing sufficient quantities for vaccine development studies. Our group set out to achieve the first complete total synthesis of naturally occurring Ac_2SGL ,¹⁵² which started with the synthesis of the deoxypropionates phthioceranic acid¹¹⁸ and hydroxyphthioceranic acid (see Schemes 22–24).

The synthesis of Ac_2SGL was achieved by coupling these to the trehalose core (Scheme 34). After protection and acylation of trehalose, protected hydroxyphthioceranic acid 199 (Scheme 24) was introduced by means of a Yamaguchi esterification, which proceeded in 76% yield to generate 272. The bis-silyl ether 272 was deprotected under buffered conditions and thereafter regioselectively sulfated at the C2'-position using 2,2,2-trichloroethyl sulfuryl imidazolium salt 274 providing protected sulfate 275. Hydrogenolysis of the 2,2,2-trichloroethyl protecting group and the benzylidene acetals of 275 yielded the target molecule, Ac_2SGL 276. All analytic data were in agreement with those of the natural isolate, and cytokine release assays showed that the synthetic material was equally potent as natural Ac_2SGL , thereby concluding the first asymmetric total synthesis of Ac_2SGL and allowing the confirmation of its proposed chemical structure.

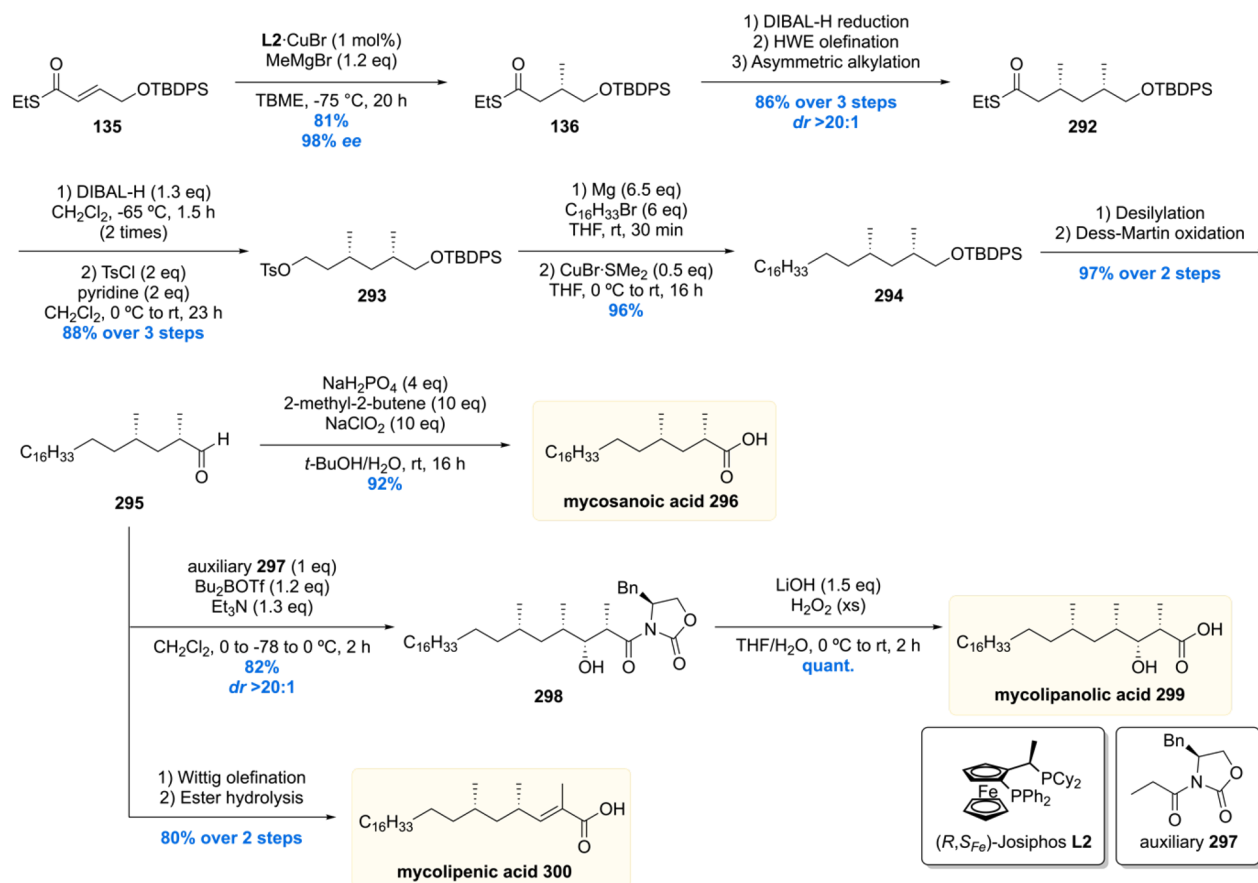
In 2018, another total synthesis of Ac_2SGL was reported (Scheme 35).¹⁶⁴ Here, the synthesis of the hydroxyphthioceranic acid was shortened by merging the asymmetric conjugate addition strategy used in Minnaard's total synthesis of Ac_2SGL with the stereoselective lithiation–borylation–protodeboronation strategy developed by Aggarwal (*vide supra*). Starting from thioester 135, the first three chiral methyl units were installed by three iterations of Cu-cat. ACA, DIBAL-H reduction, and Horner–Wadsworth–Emmons olefination, providing ketone 277.¹⁶⁵ A sequence of steps gave boronic ester 280, which set the stage for the installation of the last chiral methyl branch of

281 by stereoselective lithiation–borylation. A second building block 284 was synthesized by first introducing four chiral methyl units by means of Cu-cat. asymmetric alkylation producing ketone 282.¹⁶⁵ A series of functional group manipulations and protection/deprotection steps gave carbamate 284. Building blocks 281 and 284 were then coupled by Aggarwal's lithiation–borylation–protodeborylation approach providing, after protodeborylation of compound 285, MOM ether 231. Deprotection of the MOM ether followed by carbamoylation provided 286. The hydroxyl stereocenter was introduced by subjecting carbamate 286 to another lithiation–borylation reaction with linear alkyl boronic ester. The synthesis of hydroxyphthioceranic acid 220 was completed by deprotection and oxidation of silyl ether 287. The efficiency of the total synthesis was further improved by omitting hydroxyl protection in the hydroxyphthioceranic acid side chain prior to esterification, and thus, Ac_2SGL 276 was accessed in fewer steps and higher overall yield analogous to the previous total synthesis reported by Geerdink and Minnaard.¹⁵² Synthetic and natural Ac_2SGL as well as various saturated and unsaturated analogues lacking the hydroxyl in the lipid chain were used to generate Ac_2SGL -loaded CD1b tetramers providing a tool for the *ex vivo* study of T-cell function and reactivity in the future. This was anticipated to be useful for the design and evaluation of synthetic Ac_2SGL analogues as *Mtb* vaccine subunits.

5.2. Sulfolipid-1

After the first successful total synthesis of Ac_2SGL , our laboratory set out to synthesize SL-1, arguably *Mtb*'s most complex glycolipid to date.¹⁶⁶ SL-1 was first isolated by the Goren laboratory, who in 1970 managed to elucidate its molecular architecture by meticulous degradation studies.^{167–169} In contrast to Ac_2SGL containing two acyl chains,

Scheme 37. Asymmetric Synthesis of Mycosanoic, Mycolipanolic, and Mycolipenic Acids



sulfolipid-1 contains four acyl chains on the sulfated trehalose core, two times hydroxyphthioceranic acid, one phthioceranic acid, and one palmitic acid. Being a prominent cell wall constituent, sulfolipid-1 was postulated to be a virulence factor that mediates host–pathogen interaction. Early studies, before its structure elucidation, did show that levels of sulfolipid-1 correlated positively with virulence.¹⁷⁰ In the late 80s and early 90s it was demonstrated that sulfolipid-1 inhibits several key host responses to mycobacterial infection such as phagosome acidification and phagosome–lysosome fusion in cultured macrophages, activation of human neutrophil and macrophages, and cytokine production in human monocytes and neutrophils.^{170–174}

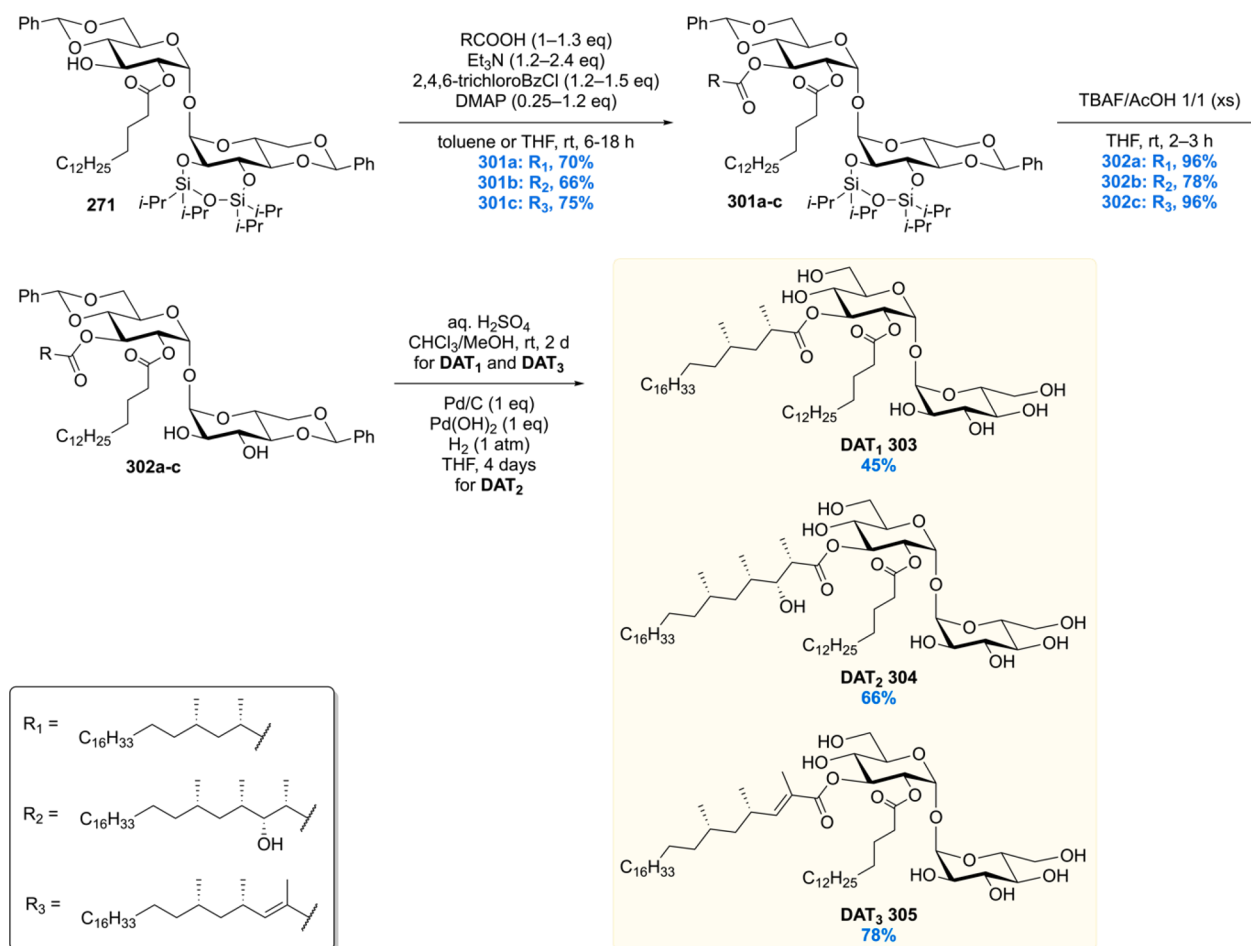
In contrast to these findings, the Bertozzi group, however, showed that knockout mutants of sulfotransferase *stf0*, therefore unable to produce sulfolipid-1, exhibit augmented survival in human macrophages.¹⁷⁵ Moreover, *in vitro* studies showed that the knockout mutants also proved to be more resistant against killing by the antimicrobial peptide LL-37, showing increased survival for Δstf0 in human macrophages. These contradictory findings show there is still a lot unknown about the exact role of sulfolipid-1 in *Mtb* pathogenesis and virulence.

Recently, however, a landmark publication reported a biological role for sulfolipid-1 that has profound influence on *Mtb* as the world's leading pathogen. The Shiloh lab discovered that SL-1 activates nociceptive neurons, present in the lung, and induces cough. Not only is cough a primary tuberculosis symptom, but more importantly, it is the primary mechanism of transmission of infection.¹⁷⁶ So, 50 years after its initial isolation,

a major role of virulence of *Mtb* has been attributed to this impressive glycolipid.

The total synthesis of SL-1 borrowed largely from the expertise gained during the total synthesis of Ac₂SGL.¹⁵² To prepare SL-1, protected and acylated trehalose 271 was reacted with phthioceranic acid 183 in a Yamaguchi esterification to provide 288 in 76% yield (Scheme 36). The benzylidene acetals were regioselectivity ring-opened to liberate the free 6-OH and 6'-OH groups. To achieve this, several reductive ring-opening conditions were scrutinized, among them the Lewis acids CoCl₂, Cu(OTf)₂, and TMSOTf in combination with BH₃·THF. The latter reaction conditions proved to be the best providing 289 in a still moderate but satisfactory yield of 59%.

The liberated alcohol functionalities were both acylated with benzyl protected hydroxyphthioceranic acid 199 using EDC as the coupling agent rather than a Yamaguchi esterification which only provided monoacylated product. Compound 290 was desilylated and then attempted to be sulfated as in the Ac₂SGL synthesis (Scheme 34). Unfortunately, the sulfation did not only take place at the desired C2' position, as in the Ac₂SGL synthesis, but also at the C3' position. This result was hypothesized to be caused by the reduced rigidity in compound 290 compared to that of compound 273 (Scheme 34) used in the Ac₂SGL synthesis. Whereas compound 273 had an intact benzylidene acetal, compound 290 is free of this conformational strain which might lead to exposing the C3' position to sulfation. The desired C2' sulfated product could be isolated in pure form which was then subjected to the final hydrogenolysis conditions described for the Ac₂SGL synthesis. Using atmospheric H₂ pressure, no conversion was observed. Increasing the hydrogen

Scheme 38. Completion of the Total Synthesis of DAT₁, DAT₂, and DAT₃

pressure to 17 bar did not lead to any product formation either. Further increase to 34 bar ultimately cleaved the benzyl protecting groups; however, the relatively labile sulfate group was partly cleaved as well, as confirmed by isolation of “desulfated SL-1”. The problematic hydrogenolysis was attributed to the long-tailed lipids that create a “coat of armor” around the trehalose core, impeding the reagents from accessing the benzyl reaction site. All in all, SL-1 **291** was synthesized, in a total of 46 steps, for the first time after its isolation 40 years ago, confirming the chemical structure of this impressive molecule.

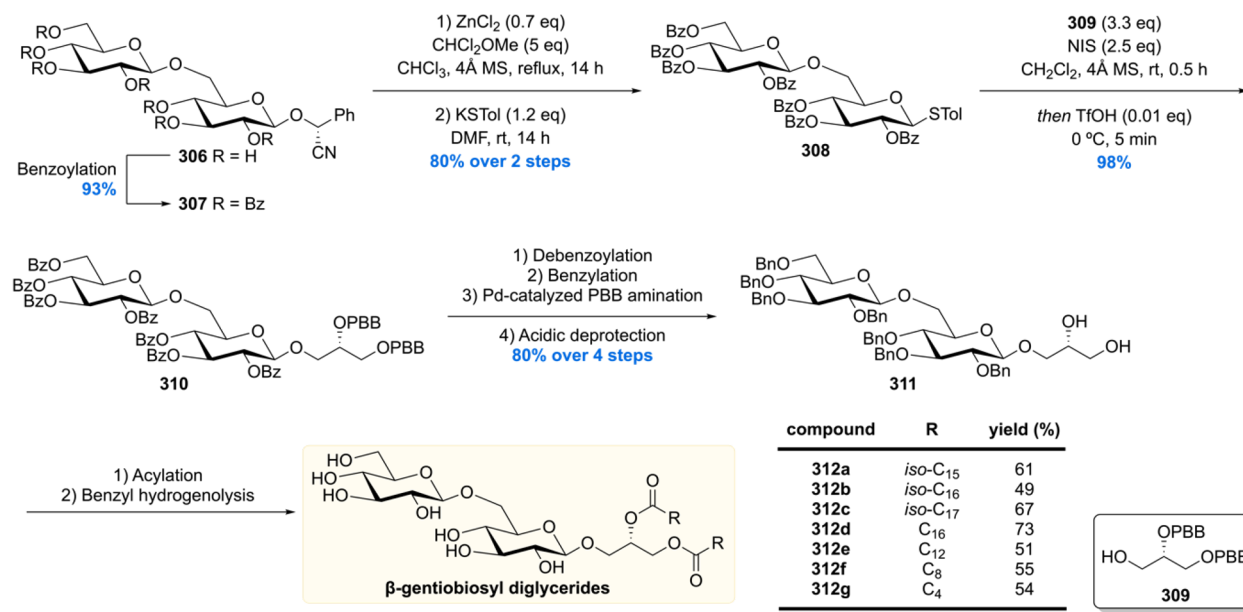
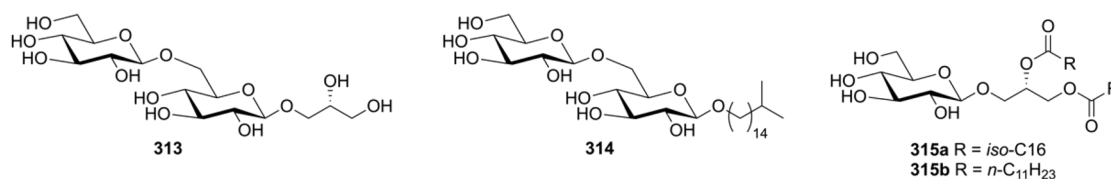
5.3. Acyl Trehaloses

The family of acyl trehaloses forms another class of mycobacterial cell wall glycolipids and is composed of di-, tri-, and poly acyl (or penta-acyl) trehaloses (DAT, TAT, and PAT, respectively) bearing linear fatty acid residues and the methyl-branched acyl residues mycosanoic, mycolipenic, and mycolipanic acids.^{177–180} Mycobacterial acyl trehaloses have been the subject of various studies since their first isolation in the 1980s and 90s, but to this date, their role in *Mtb* pathogenesis remains largely unknown. *Mtb* mutants deficient of DAT, TAT, and PAT show no changes in survival and replication, yet possess an altered cell surface composition and enhanced phagocytosis efficiency in mouse models.¹⁸¹ Thus, it was hypothesized that the function of these acyl trehaloses lies in the regulation of the cell envelope architecture by anchoring the capsule to the outer membrane leading to prevention of recognition and phagocytosis by host macrophages.^{181–184}

Among the acyl trehaloses, DAT has received by far the most attention, and various studies indicated that DAT exerts various immunomodulatory effects.^{185–187} DAT is able to inhibit monocyte production of pro-inflammatory cytokines and thus negatively regulates the immune response of the host.¹⁸⁸ Furthermore, it was demonstrated that DAT inhibits murine T-cell proliferation *in vitro*.¹⁸⁹

In the past, DAT (and to some extent TAT) has received attention for its antigenic properties and was regarded as a promising candidate for the development of antibody-based tests for Tb serodiagnosis.^{180,190–193} Due to difficulties in developing a reliable ELISA, little progress has been made in utilizing acyl trehaloses as diagnostic markers.¹⁹⁴ In recent years, DAT and TAT have been identified among other mycobacterial glycolipids as agonists of the immune receptor Mincle⁹⁰ suggesting that they have potential for application in the development of *Mtb* vaccine adjuvants. Thus far, natural DAT has been used in immunological assays, often as a mixture of structurally different DATs. Therefore, the biological effect of the individual DAT components, with well-defined chemical structure, was not ascertained.

In order to gain more insight into the effect of the individual DAT components on host immune responses, our group embarked on the total synthesis of three representatives of the DAT family (DAT_{1–3}).¹⁹⁵ By this, synthetic standards for immunological testing can be provided and the observed biological effects in functional assays can be without doubt attributed to the tested compounds rather than to minute

Scheme 39. Synthesis of Mycobacterial β -Gentiobiosyl Diglyceride Candidates β -gentiobiosyl diglyceride analogues

amounts of contaminants or isomers/related compounds resulting from isolation.

The three target DATs differ in the nature of the mycobacterial acyl residues. DAT₁ is esterified with mycosanoic acid on the 3-OH of trehalose, whereas DAT₂ and DAT₃ carry mycolipanic and mycolipenic acid esters on that position, respectively. For the synthesis of these methyl-branched lipids, a synthetic route was optimized, which was published by us previously.¹⁹⁶

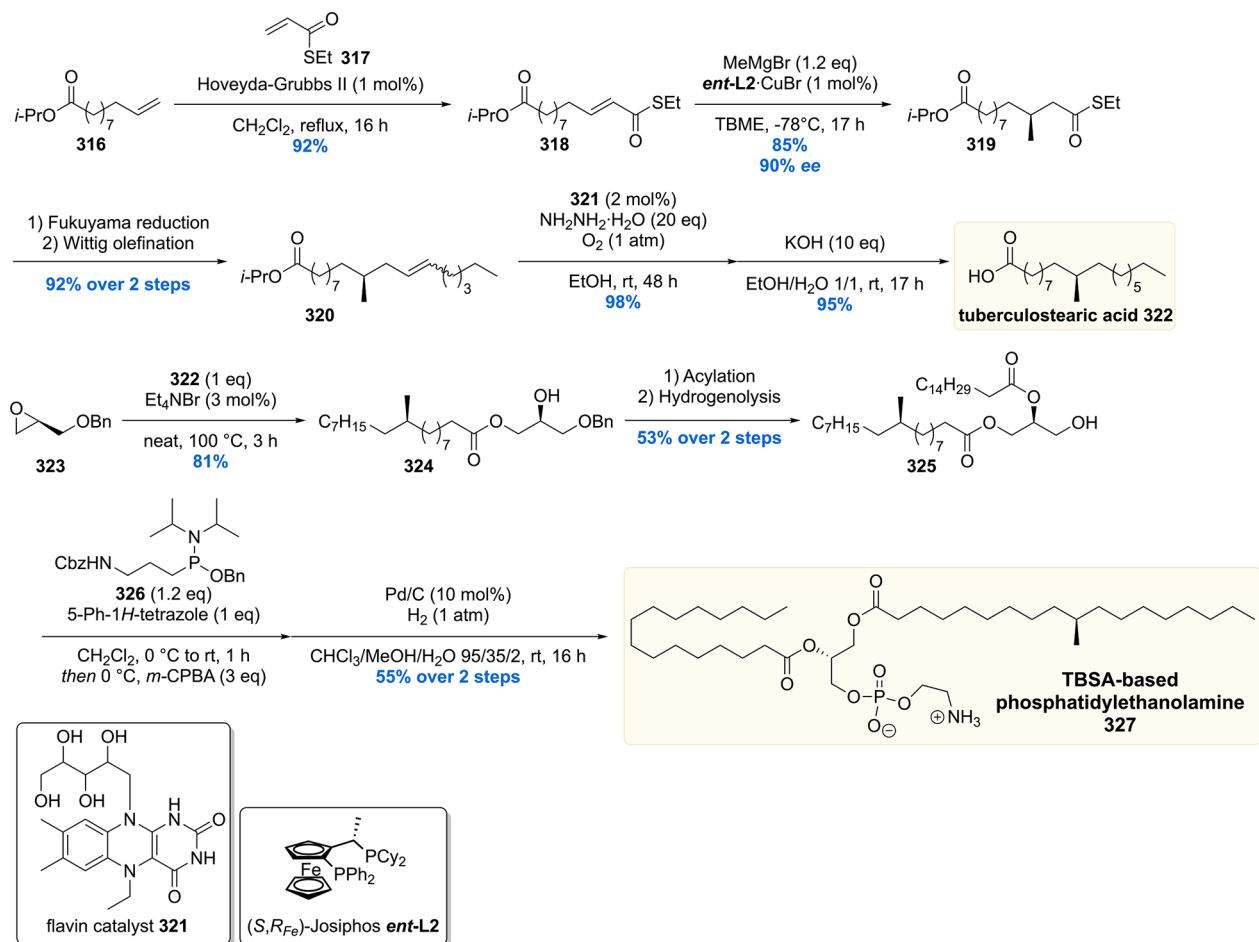
The synthesis of the mycobacterial lipids (Scheme 37) commenced with the previously discussed asymmetric Cu-cat ACA of methylmagnesium bromide to α,β -unsaturated thioester 135 providing 136 in 81% yield and 98% *ee*. DIBAL-H reduction of 136 followed by Horner–Wadsworth–Emmons olefination and a second asymmetric conjugate addition furnished 292 containing two methyl branches in 86% yield over three steps and *dr* > 20:1. The thioester moiety of 292 was then converted to the corresponding alcohol by two rounds of DIBAL-H reduction. After tosylation, the corresponding tosylate 293 was obtained in 88% yield over three steps. The C₁₆ alkyl tail of 294 was installed by copper-mediated Grignard alkylation of 293 in 96% yield. Desilylation of 294 followed by Dess–Martin periodinane oxidation then provided aldehyde 295 in 97% yield over two steps. From 295 the three target mycobacterial acids could be obtained in a few steps. Pinnick oxidation of 295 furnished mycosanoic acid 296 in 92% yield. The two remaining stereocenters of mycolipanic acid 299 were installed by diastereoselective Evans' aldol condensation of 295 with chiral auxiliary 297 and provided 298 in 82% yield and excellent diastereoselectivity exceeding 20:1. Cleavage of the chiral auxiliary of 298 then provided mycolipanic acid 299 in

quantitative yield. Lastly, mycolipenic acid 300 was accessed from aldehyde 295 by Wittig olefination and ester hydrolysis in 80% yield over two steps. Notably, by careful optimization of the reactions, the overall yield of the mycobacterial lipids was significantly improved, rendering the synthesis highly efficient. For mycosanoic acid an overall yield of 53% over 10 steps was achieved. Mycolipanic and mycolipenic acid were obtained in a total yield of 47% (previously 2%) and 46% (previously 5%)¹⁹⁶ over 11 steps.

With the three enantiopure lipids in hand, the synthesis of DAT_{1–3} was finalized by Yamaguchi esterification of protected trehalose 271 (Scheme 38). The diacylated trehaloses 301a–c were obtained in good yields ranging from 66% to 75%. In the case of mycolipanic acid 299, the procedure was optimized by lowering the equivalents of base and changing solvent to THF in order to suppress elimination of the unprotected β -hydroxyl moiety. After desilylation, under buffered conditions, and removal of the benzylidene protecting groups, the total synthesis of DAT₁ (303), DAT₂ (304), and DAT₃ (305) was completed.

In order to assess if the synthesized DATs indeed corresponded to the structures of the mycobacterial natural products, lipid extracts of *Mtb* strain H37Rv and three clinical isolates were analyzed by HPLC-MS. Comparison with the synthetic DATs showed coelution and identical mass spectra for DAT₁ and DAT₃, but for DAT₂ the retention times differed albeit with identical observed collisional mass-spectra. This confirms that synthetic DAT₁ and DAT₃ are identical to the natural glycolipids, whereas synthetic DAT₂ is likely an isomer of natural DAT₂, of which the exact structure remains to be elucidated. These results highlight the importance of chemical

Scheme 40. Total Synthesis of Mycobacterial TBSA-Based Phosphatidylethanolamine



synthesis of natural products to confirm and/or disprove proposed chemical structures of natural isolates.

In addition, the synthetic DATs were tested for activation of Mincle and compared to the known potent Mincle agonist trehalose dimycolate (TDM). Whereas DAT₁ and DAT₂ showed only weak binding to Mincle, DAT₃ was found to be a strong Mincle agonist (in the potency range of TDM), indicating that the nature of the chiral lipid strongly influences Mincle binding and activation.

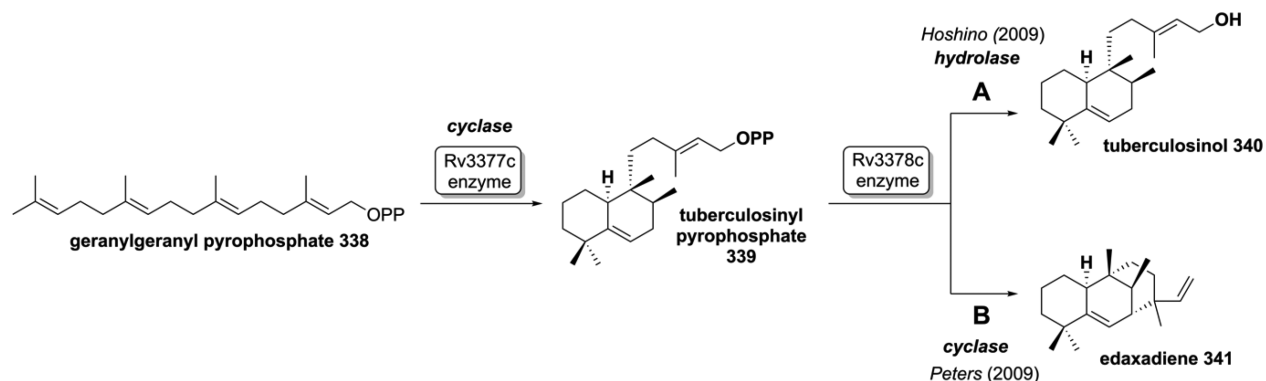
To further gain insight into their immunomodulatory properties, the synthetic DATs, with their well-defined structures, were investigated for their potential to be recognized by human T cells.¹⁹⁷ Tetramers of the lipid binding antigen presenting molecule CD1b were constructed and tested for their ability to present DAT molecules to human T cells. Interestingly, whereas DAT₃ was a potent agonist for Mincle, DAT₃ was not an antigen recognized by T cells. In contrast, DAT₁ and DAT₂, which were both weak binding Mincle ligands, were presented to T cells by CD1b and are thus lipid antigens. This intriguing result showed that the structure of the lipid in the C3 position is a determinant for the immunogenic properties of the DATs. More specifically, the α -stereocenter in the mycosanoic lipid of DAT₁ and mycolipanoic lipid of DAT₂ seems to be important for recognition by T cells, a structural feature missing from the myolipenic lipid in DAT₃. A broader conclusion from this work was that small structural differences determine recognition of mycobacterial lipids by different parts of the immune system and that DAT can be both an agonist for

the Mincle receptor and an antigen for T cells. It should be mentioned that such conclusions can only be reached with very well-defined chemical structures from synthesis rather than heterogeneous natural isolates, which is the case for the DATs, and thus highlight the importance of total synthesis in determining the immunomodulatory properties of *Mtb* lipids.

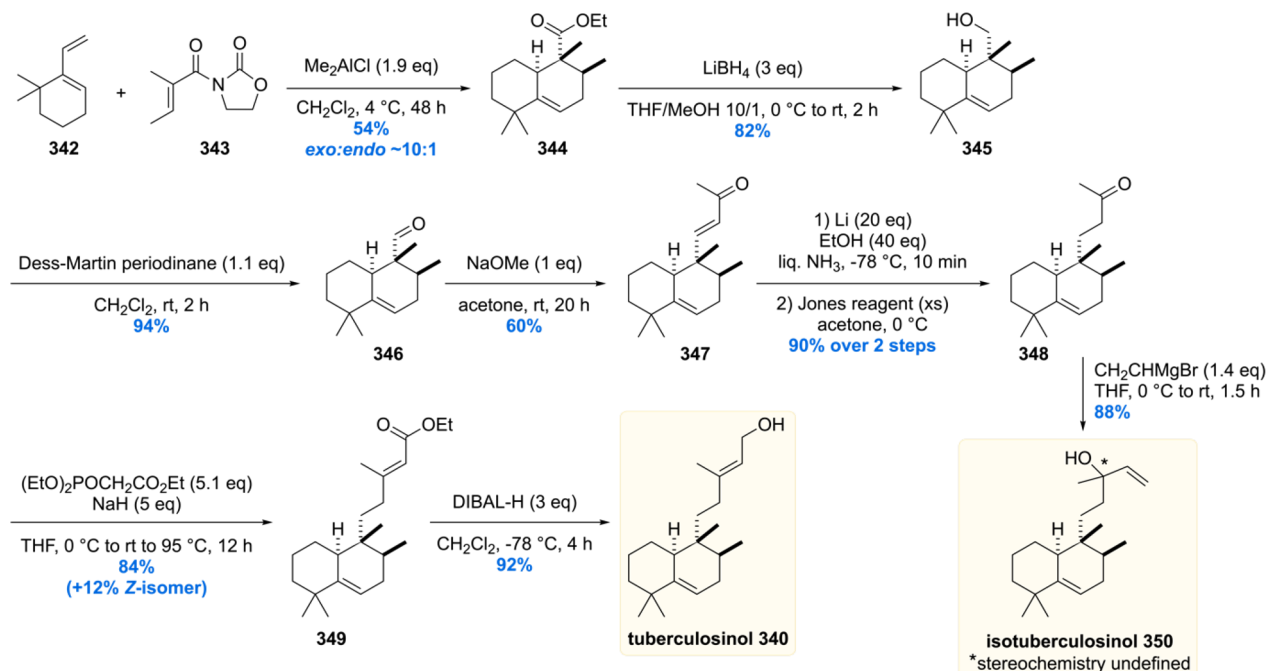
6. GLYCEROLIPIDS

6.1. β -Gentiobiosyl Diacylglycerides

The plethora of mycobacterial membrane lipids and glycolipids also includes the family of β -gentiobiosyl diacylglycerides. This series of glycerolipids was first described by Hunter et al. in 1986 and contains a common gentiobiosylglycerol motif.¹⁹⁸ The glycerol moiety carries long-chain *iso*- and *anteiso*-fatty acid ester homologues. The exact molecular structure of this class of glycolipids has not been elucidated or confirmed yet, but upon first isolation it was demonstrated that the mycobacterial β -gentiobiosyl diacylglycerides are serologically active. Yet, β -gentiobiosyl diacylglycerides are not limited to *Mtb* and are found to be of fungal origin (containing *anteiso*-fatty acyl groups) as well. The fungal β -gentiobiosyl diacylglycerides were found to be capable of activating the immune receptor Mincle, though only with moderate potency.¹⁹⁹ For decades the mycobacterial diglycosyl glycerolipids have not received much attention of researchers. It was only in 2015, when the Williams group embarked on the synthesis of a whole array of candidate structures and analogues to assess their Mincle signaling

Scheme 43. Original Proposed Biosynthetic Pathways of the Rv3377c-Rv3378c Locus of *Mtb*

Scheme 44. Snider's Total Synthesis of Tuberculosinol and Isotuberculosinol



order to install the phosphoglycerol moiety, **325** was converted into the phosphoramidite **335** mediated by diisopropylammonium tetrazolidine (DIPAT). The unstable phosphoramidite **335** was then reacted with dibenzylglycerol **336**, to form after hydrogenolysis the desired TBSA-based phosphatidylglycerol **337** in 53% over the last two steps.

7. TERPENE NUCLEOSIDES

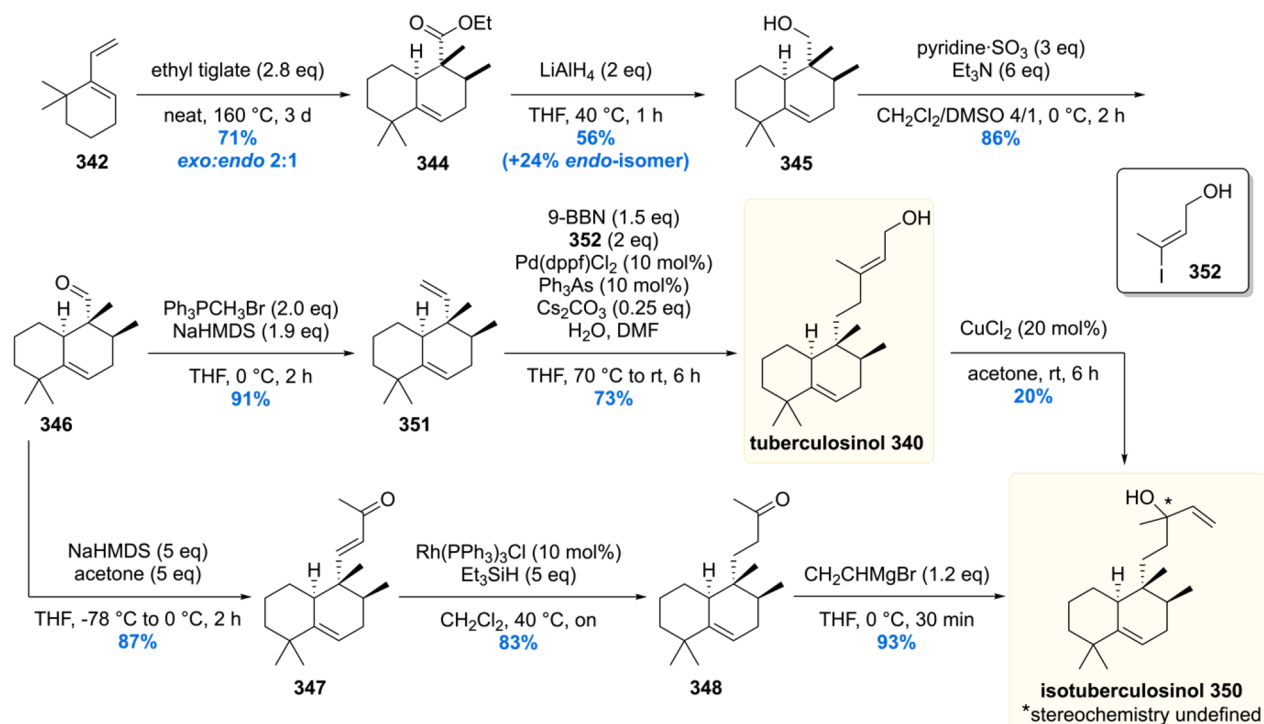
In 2004 the Russel laboratory disseminated a landmark publication reporting that transposon knockouts of the Rv3377c or Rv3378c gene led to reduced survival of *Mtb* in mice compared to wild-type *Mtb*.²¹⁴ More specifically, it was found that the phagosomal compartment, which forms after a macrophage internalizes a foreign invader, does not acidify (i.e., mature) to levels in which fusion with lysosomes, organelles containing acid and hydrolases, takes place. This means that pathogen digestion is inhibited, allowing the *Mtb* to escape the phagosomal compartment,¹⁶ enabling survival of *Mtb* within the harmless, yet nutritious, cytosol of immune cells. Although intracellular survival of *Mtb* cannot be pinpointed to one specific event, blockade of phagosomal maturation is paramount to the persistence of *Mtb* in its human host. Despite the fact that the

ability of *Mtb* to stop phagosome maturation has been recognized for decades,^{215,216} fundamental understanding of the molecular mechanism remained unknown.

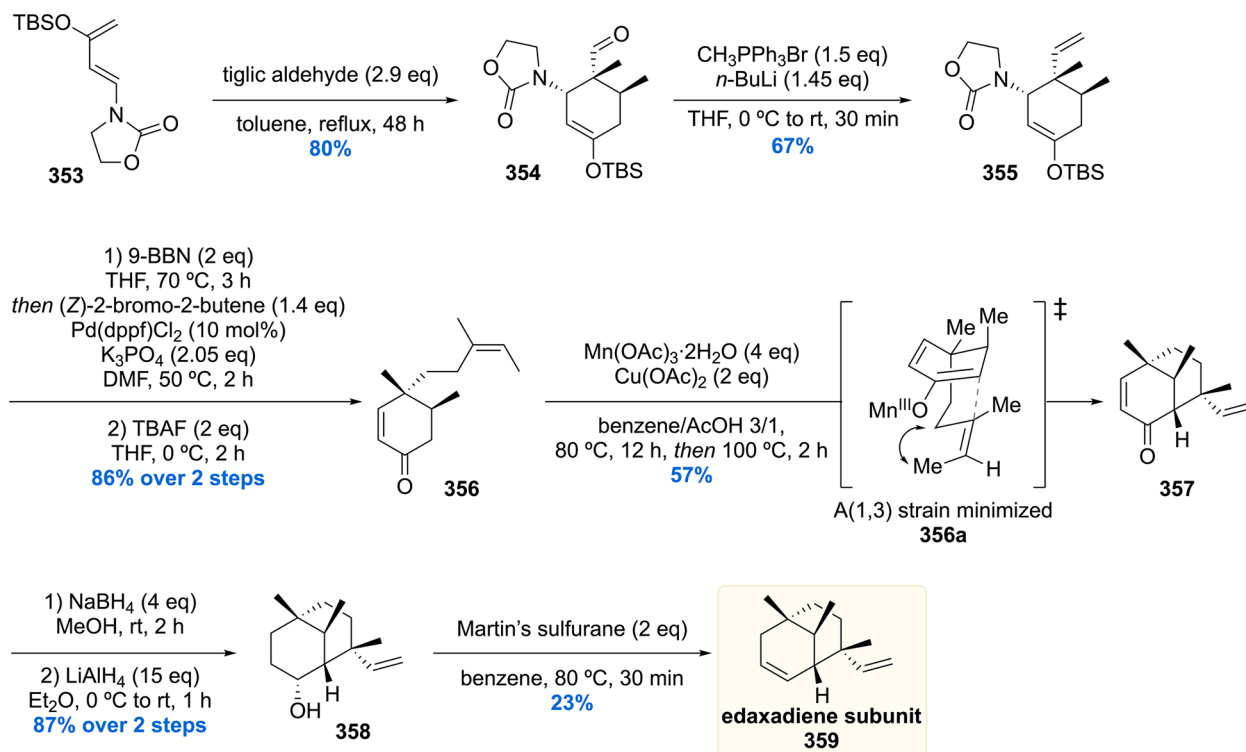
In 2005 the Hoshino group expressed the *Mtb* Rv3377c-gene in *E. coli*, establishing that geranylgeranyl pyrophosphate **338** was cyclized by Rv3377c to produce a halimane skeleton.^{217–219} The cyclized product was named tuberculosinyl pyrophosphate **339** and postulated to be hydrolyzed by Rv3378c to produce tuberculosinol **340** (Scheme 43).²¹⁸ In 2009, Peters reported that the enzyme Rv3378c does not act merely as a hydrolase but as a phosphatase that cyclizes tuberculosinylpyrophosphate **339** to form edaxadiene **341**.²²⁰ Importantly, these investigations, although contradictory, tied the Rv3377c-Rv3378c locus to a molecular structure which was accessible by total synthesis. Since the structure produced by the important Rv3377c-Rv3378c locus was uncertain at this stage, there was a driving force for synthetic chemists to solve this structural puzzle.

In 2010 the research groups of Snider²²¹ and Sorensen²²² reported the total synthesis of tuberculosinol **340**. Furthermore, both groups communicated the structural revision of the in 2009 proposed edaxadiene **341**. Both groups questioned the proposed structure upon careful inspection of the NMR spectra reported

Scheme 45. Sorensen's Total Synthesis of Tuberculosinol and Isotuberculosinol



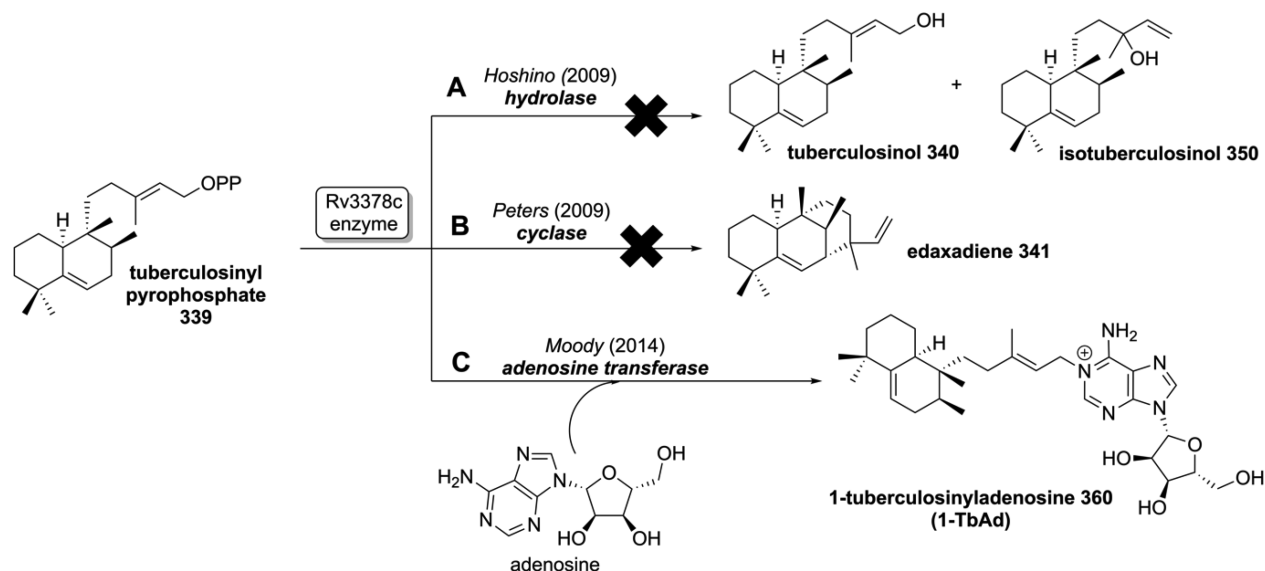
Scheme 46. Sorensen's Total Synthesis of Edaxadiene



for edaxadiene 341. It was concluded that the NMR spectra resembled that of isotuberculosinol 350, an isomer of tuberculosinol, corresponding to S_N2' hydrolysis of tuberculosinyl pyrophosphate 339.

The structure of (iso)tuberculosinol exhibits a cyclohexene ring which inevitably led to retrosynthetic disconnections, by both groups, involving a Diels–Alder cycloaddition. The target

Diels–Alder adduct however is unusual in the sense that it arises from *exo*-attack of the diene. This product is generally disfavored as a consequence of the inherent *endo*-preference (the *Alder endo* rule).²²³ The *endo*-preference could be overcome by the introduction of steric hindrance in the dienophile.²²⁴ The Snider laboratory performed the Diels–Alder cycloaddition of diene 342 with oxazolidinone tiglate 343 furnishing the

Scheme 47. Revised Biosynthetic Product of the Rv3378c Gene in *Mtb*

cyclization product **344** with an *exo:endo* ratio of 10:1 in 54% yield (Scheme 44).²²¹ Reduction of the oxazolidinone moiety and subsequent Dess–Martin oxidation gave the corresponding aldehyde **346**. The aldehyde was subjected to an aldol condensation with acetone, followed by a conjugate reduction/oxidation sequence to furnish ketone **348** in 54% yield over the three steps. A Grignard reaction on ketone **348**, with vinyl Grignard, provided isotuberculosinol **350**. By performing a Horner–Wadsworth–Emmons olefination on ketone **348**, followed by reduction of the freshly installed ester functionality, tuberculosinol **340** was obtained.

A similar, yet slightly different, approach to tuberculosinol was reported by Sorensen, who started with a Diels–Alder reaction between diene **342** and ethyl tiglate providing the desired *exo* product in a 2:1 ratio over the *endo* product (Scheme 45).²²² Enantiomeric separation by preparative supercritical fluid chromatography provided optically pure Diels–Alder adduct **344**. Reduction and oxidation gave aldehyde **346** which served as a common intermediate to construct both tuberculosinol **340** and isotuberculosinol **350**. A Wittig olefination provided alkene **351** which was subjected to a hydroboration with 9-BBN, to then be cross-coupled with vinyl iodide **352** in a Suzuki reaction, providing tuberculosinol **340**. CuCl₂-mediated isomerization converted tuberculosinol **340** directly into isotuberculosinol **350**, albeit in only 20% yield. An alternative route was performed, along the same lines as in the Snider synthesis, to give isotuberculosinol **350** in only three steps from aldehyde **346**.

The Sorensen lab also synthesized the edaxadiene substructure **359** proposed by Peters and co-workers (Scheme 46). This synthesis started with a Diels–Alder reaction between tiglic aldehyde and oxazolidinone-based modified Rawal's diene **353**, forming Diels–Alder adduct **354** in 80% yield. A Wittig homologation set the stage for a Suzuki coupling that was initiated by hydroboration of the terminal alkene functionality in **355** and subsequent cross-coupling with (*Z*)-2-bromo-2-butene. The silyl ether was cleaved with TBAF which initiated an E1cB elimination of the oxazolidinone, furnishing enone **356**. To create the *all*-carbon quaternary stereocenter, an intramolecular oxidative ketone allylation was performed using Mn^{III}(OAc)₃. The reaction proceeded via the intermediate conformer **356a** in

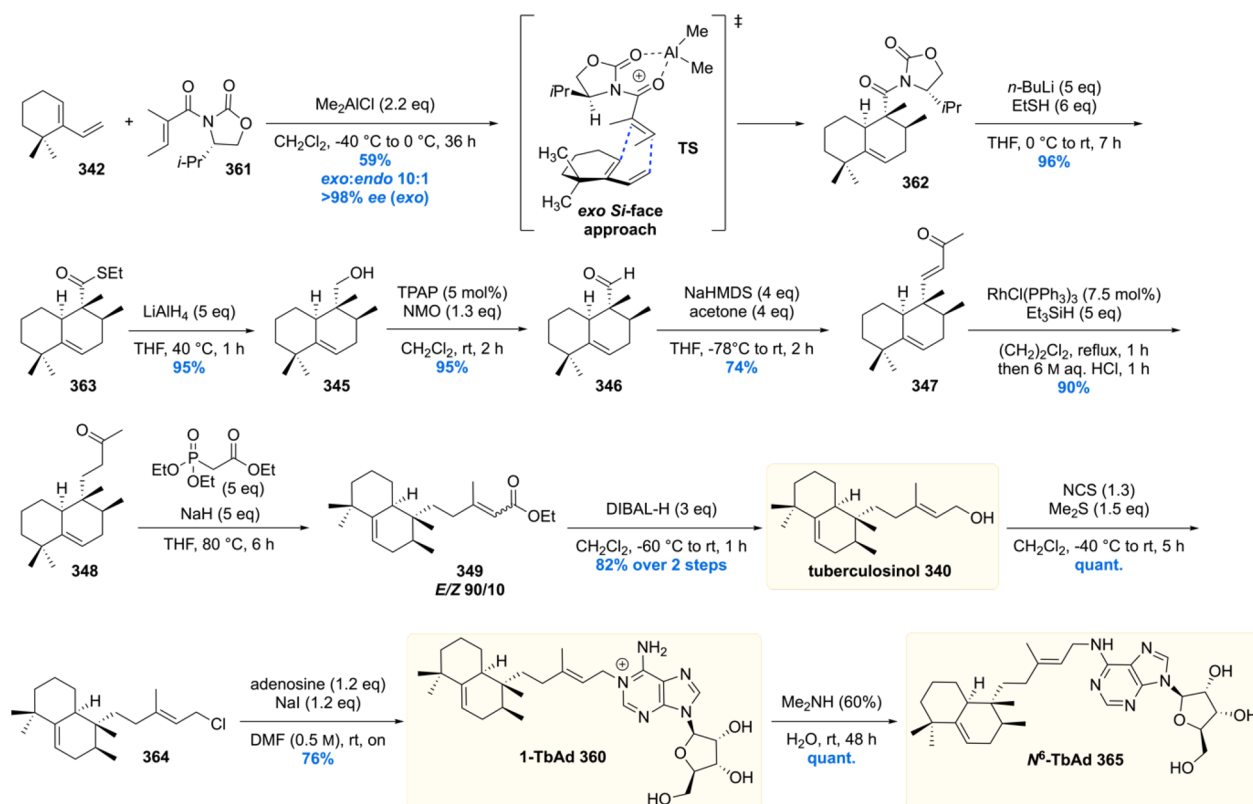
which the allylic 1,3-strain was minimized, leading to a single stereoisomer of [3.3.1] bicyclic compound **357** in 57% yield. Full reduction of the enone functionality, via a two-step protocol, provided alcohol **358** which was deoxygenated using Martin's sulfuran to provide edaxadiene subunit **359** after semipreparative gas chromatography.

NMR analysis of both isotuberculosinol **350** and edaxadiene subunit **359** undoubtedly showed that the natural isolate from Peters and co-workers corresponded with that of isotuberculosinol **350** and not edaxadiene **341** as proposed. Therefore, it was reasoned that Rv3378c acts as tuberculosinyl pyrophosphate hydrolase (Scheme 43, pathway A) rather than as cyclase (Scheme 43, pathway B).

In 2014 the Moody laboratory reported the isolation of an unknown compound from *Mtb*.²²⁵ The molecule was found during extensive lipidomics²²⁶ studies investigating the chemotaxonomy of the virulent *Mtb* versus the nonvirulent *M. bovis* BCG. It was found that this new molecule was abundant in *Mtb*, whereas it was completely absent in *M. bovis* BCG. This initial result prompted investigation into the nature of the molecule, its biosynthesis, and presence in other medically relevant bacteria.

Isolation and subsequent structure elucidation by NMR and collisional mass analysis resulted in the formulation of its structure being 1-tuberculosinyladenosine (1-TbAd), which is the tuberculosinyl lipid connected to the 1-position of adenosine, a structural feature rarely seen in nature. Since 1-TbAd contains the tuberculosinyl core, the cyclization product of geranylgeranyl pyrophosphate **339** by Rv3377c, it was hypothesized that Rv3378c is not a hydrolase as postulated earlier, but rather acts as an adenosine transferase (Scheme 47).

This biosynthesis proposal was put to the test by providing recombinant Rv3378c enzyme with synthetic racemic tuberculosinyl pyrophosphate **339** and adenosine. This experiment yielded 1-TbAd **360** (Scheme 47, pathway C) while the hydrolyzed products, (iso)tuberculosinols **340** and **350**, were not detected (Scheme 47, pathway A). Further evidence was provided by transformation of *Mycobacterium smegmatis* (*Msmeg*) with the Rv3377c-Rv3378c locus. Whereas *Msmeg* does not produce 1-TbAd, installation of the Rv3377c-Rv3378c genes did lead to 1-TbAd production. It was therefore concluded

Scheme 48. Asymmetric Total Synthesis of 1-TbAd and N⁶-TbAd

that the function of the Rv3778c enzyme is an adenosine transferase.²²⁷

1-TbAd was thus found to be abundantly produced (~1 w/w % of the total extractable lipids), and in a subsequent communication it was reported that 1-TbAd is specifically produced by *Mtb* and no other (myco)bacteria.²²⁷ Moreover, it was also discovered that 1-TbAd can rearrange into N⁶-TbAd via a nucleophile-promoted Dimroth rearrangement (*vide infra*).^{228,229} Both 1-TbAd and N⁶-TbAd were shown to be suitable biomarkers of *Mtb* infection in mice lung homogenates and prompt further investigation for its use in tuberculosis diagnostics.

The abundance, specificity, and association to Rv3377c and Rv3378c genes, involved in phagosome maturation arrest,²¹⁴ hinted that 1-TbAd might be a molecule that attributes to the intracellular survival (i.e., parasitic nature) of *Mtb*. To investigate its role, sufficient amounts of material had to be generated to aid the biological assays. Due to tedious isolation, which only provided microgram quantities of semipure 1-TbAd, chemical synthesis was the way to continue. The aforementioned reasons, and the potential of 1-TbAd and N⁶-TbAd as diagnostic molecules for tuberculosis infection, provided a strong rationale to embark on a stereoselective synthesis of 1-TbAd.

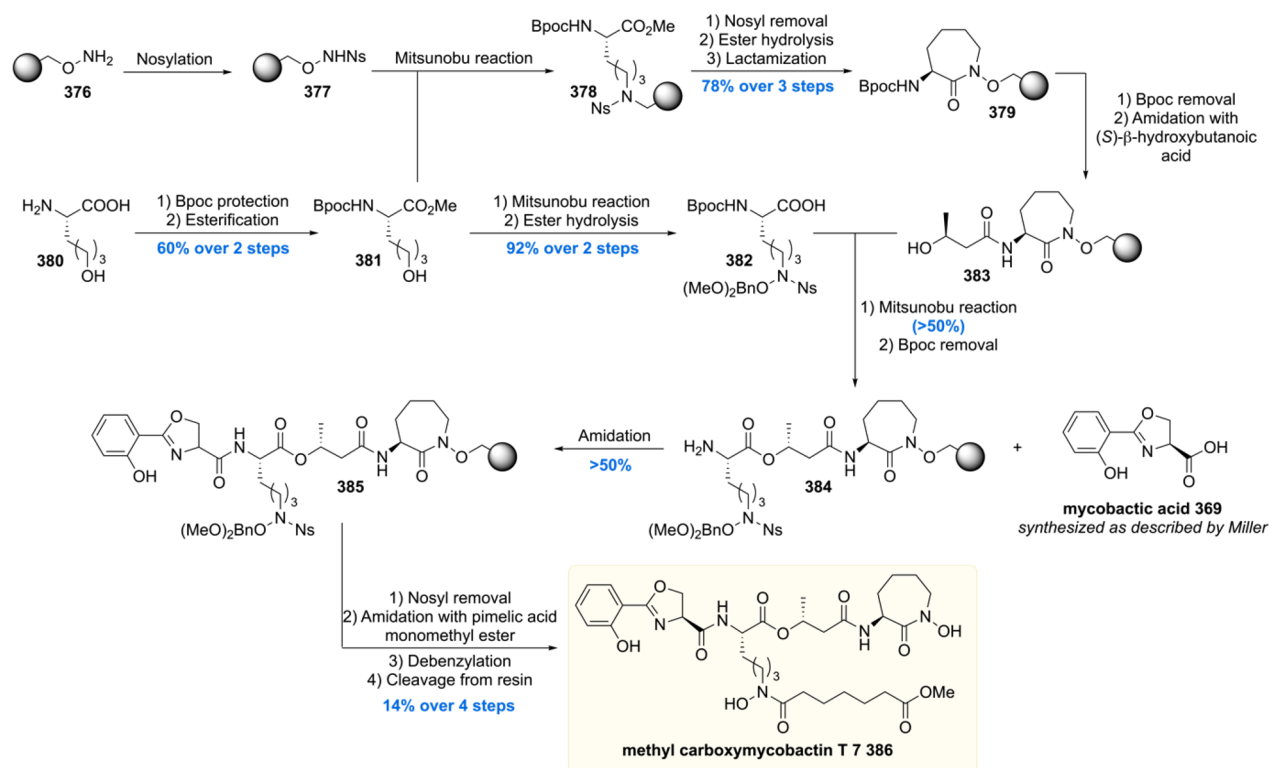
In 2016 we reported the first asymmetric total synthesis of 1-TbAd, providing 2.4 g of enantiopure compound.²³⁰ This multigram scale synthesis was initiated by an asymmetric Diels–Alder reaction (Scheme 48). Despite numerous attempts to construct the unsaturated decalin core employing an asymmetric copper-catalyzed *exo*-selective Diels–Alder reaction,²³¹ the successful approach proved to be the use of a chiral auxiliary. So, the reaction between diene **342** and chiral oxazolidinone tigloyl-based dienophile **361** was performed with excellent

stereoselection (>98% ee, 9:1 *exo:endo*). *In silico* studies showed that the Diels–Alder reaction proceeded stepwise from the *Si*-face (TS) according to the Curtin–Hammett principle via reaction from the thermodynamically less stable *s-cis* conformer. The chiral auxiliary of **362** was removed by the aid of ethanethiolate which smoothly produced thioester **363** in 96% yield. Reduction followed by oxidation provided aldehyde **346**, which was functionalized using an aldol reaction with acetone to provide enone **347**. Conjugate reduction by the aid of Wilkinson's catalyst with triethylsilane yielded ketone **348**. A Horner–Wadsworth–Emmons olefination was performed to install the alkene functionality, to produce, after reduction of the ester intermediate, tuberculosinol **340** in 82% over the two steps. Conversion of tuberculosinol **340** into allylic chloride **364** set the stage for the final coupling with adenosine. Alkylation under Finkelstein conditions in DMF smoothly provided the desired natural product, 1-TbAd **360**, in 76% yield. 1-TbAd **360** was also quantitatively converted into N⁶-TbAd **365** by a Dimroth rearrangement induced by aqueous dimethylamine.

Recently we reported biological investigations with synthetic 1-TbAd **360** to elucidate its biological function.²³² We discovered that 1-TbAd is cell wall associated and acts as a mycobacterial antacid which neutralizes acidic organelles. We showed 1-TbAd uses mechanisms independent of macrophage function since 1-TbAd producing *M. kansasii* can grow (= survive) in acidic culture media (pH 5.1), whereas wild-type *M. kansasii* (which does not produce 1-TbAd) cannot grow.

In the context of the macrophage, as alluded to earlier, phagosomal maturation is driven by acidification to induce fusion with the lysosome. This fusion leads to digestion of the bacterium by subjecting it to acid hydrolases. Due to the pK_a of 1-TbAd of ~8.5 (= acidic NH₂), it is in equilibrium with its neutral conjugate base, which can traverse biological membranes

Scheme 50. Solid Phase Synthesis of Methyl Carboxymycobactin T by Poreddy et al.



starvation and thus growth inhibition. Since minor changes in siderophore structure can significantly alter the iron binding affinities²⁵² or transport abilities,²⁵³ being able to make structurally very similar natural siderophores becomes even more important.

Another strong incentive for the synthesis of siderophores, and thus mycobactins, is its use as a “Trojan Horse” for carrying drugs into bacteria.^{254–258} Since mycobactins transfer iron through the mycobacterial cell wall, their access to the mycobacterial cytosol can be exploited by synthesis of mycobactin–drug conjugates. One particular example worth highlighting is the synthesis of a mycobactin T analogue conjugated with artemisinin reported by Miller and co-workers.²⁵⁹ Artemisinin is a potent antimalarial drug which by itself does not exhibit antituberculosis activity; however, conjugated to a mycobactin T analogue, the construct showed selective antituberculosis activity even against MDR and XDRT *Mtb*. Although for drug conjugation, analogues of the mycobactins are needed, which are not discussed in this review, the naturally occurring architectures serve as an indispensable template for such drug designs.

Mycobactin T is thus known for over 55 years but, surprisingly, no total synthesis of precisely this molecule has been undertaken. In 1997 the Miller laboratory, however, performed the total synthesis of mycobactin S.²⁶⁰ Although this molecule is formally from *M. smegmatis*, mycobactin S differs from mycobactin T in only one stereogenic center and thus resembles mycobactin T. Moreover, to further justify its inclusion in this review, mycobactin S was chosen as the target to test Francis’ hypothesis that alternative forms of my mycobactin might possess inhibitory activity against *Mtb*.

The Miller synthesis of mycobactin S (Scheme 49) started with construction of mycobactinic acid, the oxazoline containing fragment. Methyl salicylate 366 was amidated with *L*-serine benzyl

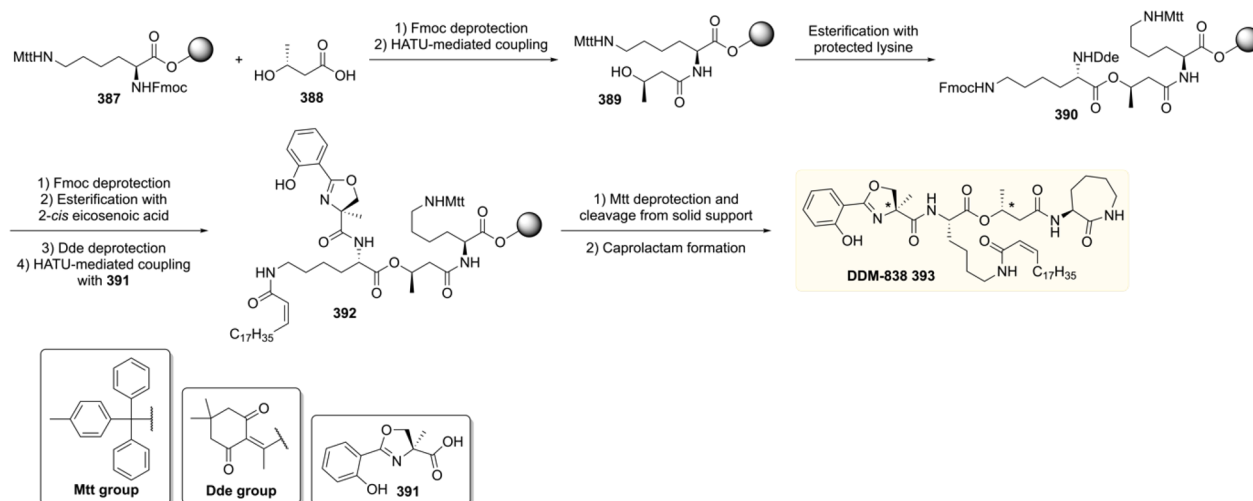
ester after a benzylation ester hydrolysis sequence. The oxazoline was installed by treatment of 367 with Burgess reagent 368, which rather than as a dehydrating agent functioned as a leaving group. Hydrogenolysis then provided mycobactinic acid 369 in 50% yield over the five steps.

The other two necessary fragments, cobactin T 372 and the SEM protected hydroxamic acid 373, were both constructed starting from amino acid derivative 370. The lactam was constructed in a six-step sequence via the intermediacy of a hydroxylamine (product from nitrene hydrolysis). The amine functionality in 371 was hydrogenolytically liberated after which it was reacted with β -hydroxybutanoic acid, to produce cobactin T 372 after removal of the silyl protecting group. Via a similar pathway SEM-protected hydroxamic acid 373 was produced. After removal of the Cbz-group, the fusion with mycobactinic acid 369 was executed. Hydrolysis of the methyl ester set the stage for the Mitsunobu reaction between 374 and cobactin T 372. The silyl groups were removed which provided mycobactin S 375 in a longest linear sequence of 10 steps.

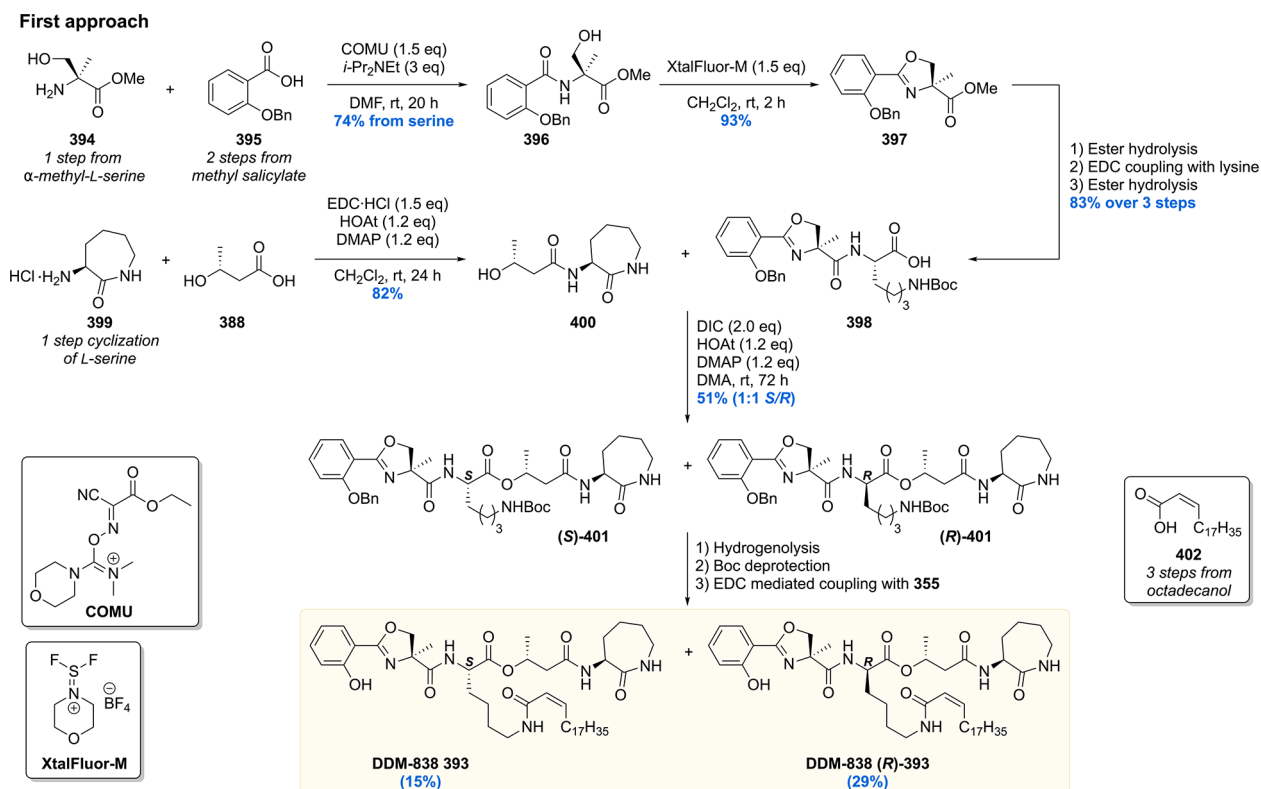
The obtained mycobactin S was subjected to biological tests and showed that at a concentration of 12.5 $\mu\text{g}/\text{mL}$ the growth of *Mtb* H37Rv was inhibited by 99% and that the minimum inhibitory concentration of mycobactin was 3.13 $\mu\text{g}/\text{mL}$. This result confirmed the 50-year-old hypothesis from Francis that alternative forms of my mycobactin might possess inhibitory activity against *Mtb*. It is remarkable that inversion of a single stereogenic center converts a growth factor for *Mtb*, mycobactin T, into a growth inhibitor.

In 2003, Poreddy et al. embarked on the solid-phase synthesis of methyl carboxymycobactin T 386 and several analogues (Scheme 50).²⁶¹ For their synthesis, hydroxyl amine *O*-functionalized with Wang resin was chosen as the solid-phase. The amine moiety was nosylated in order to be monofunctionalized with protected *L*-6-hydroxynorleucine 381 by means of a

Scheme 51. Solid-Phase Synthesis of Dideoxymycobactins



Scheme 52. Williams' Synthesis of Dideoxymycobactins



Mitsunobu reaction. The lactam was then introduced in three steps to, after removal of the Bpoc group, react with (*S*)- β -hydroxybutanoic acid to produce 383. 384 was then synthesized by first performing a Mitsunobu reaction between the carboxylic acid moiety in *L*-6-hydroxynorleucine 382 and the hydroxyl unit of 383, followed by removal of the 2-(*p*-biphenyl)-2-propyloxycarbonyl (Bpoc) protecting group. This set the stage

for introducing the mycobactinic acid 369 onto 384 using standard amidation chemistry. The desired methyl carboxymycobactin T 386 was then obtained in 14% over four steps.

The obtained carboxymycobactin catalogue was investigated for its iron binding properties, as well as their inhibitory activity of *M. avium*. While at different concentrations, growth was inhibited in the first week to about 10–15% of the control, the

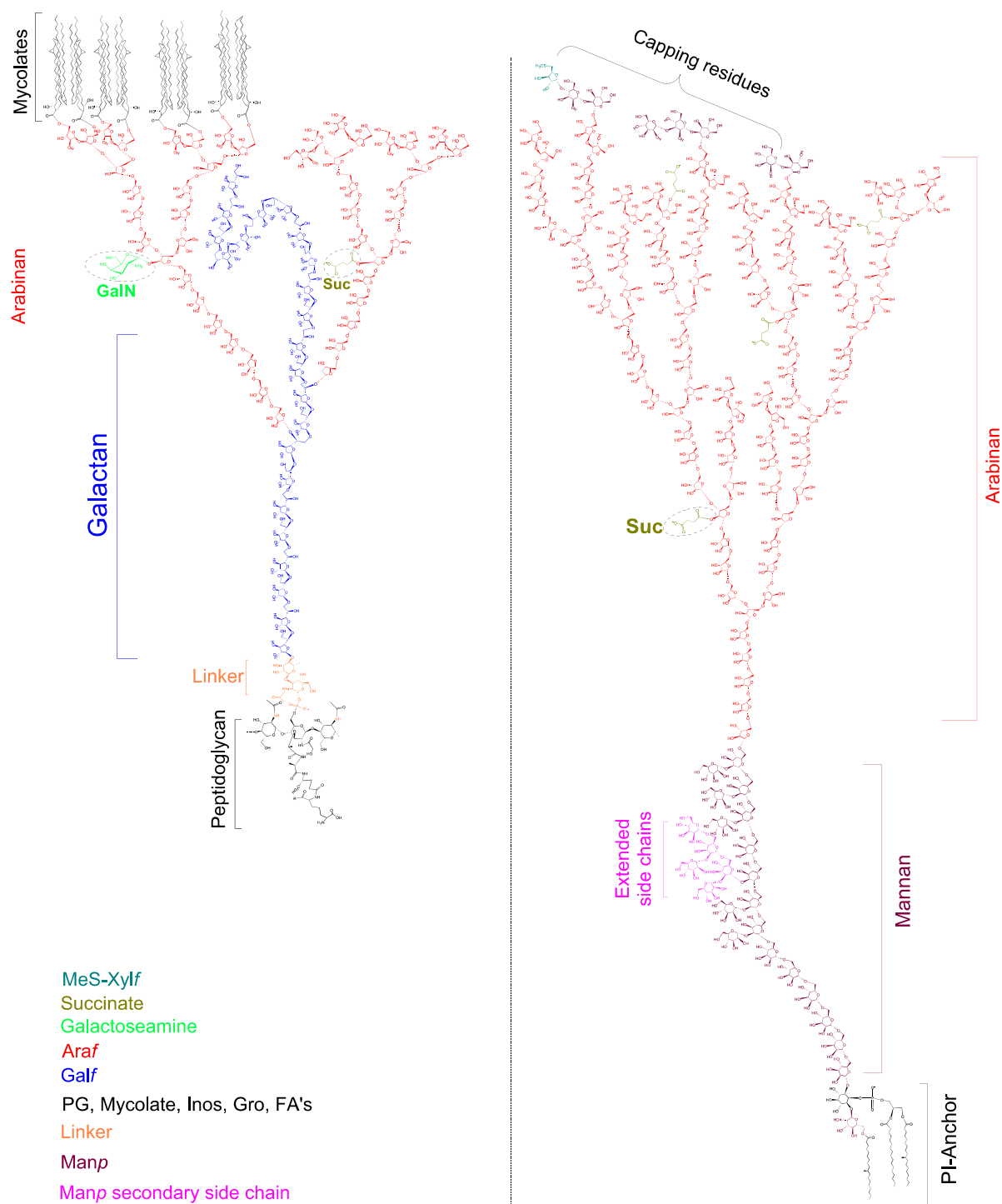
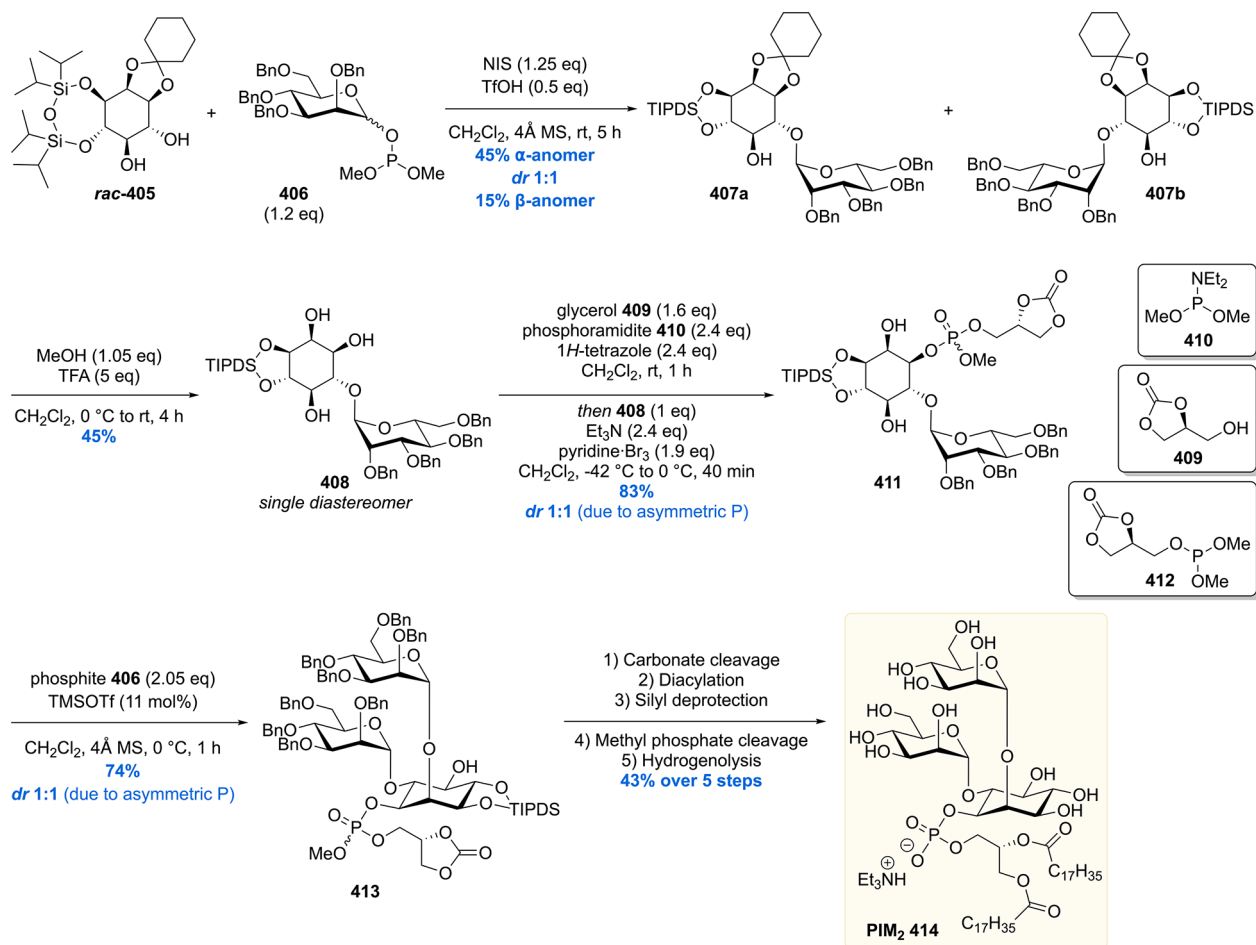


Figure 5. Chemical architecture of mycobacterial cell wall oligo- and polysaccharides.²⁶⁸ Reproduced with permission from ref 268. Copyright 2021 Springer Nature.

following weeks the inhibition diminished and was negligible compared to the control by week 3 and 4. These results were attributed to slow degradation of the carboxymycobactin by the bacteria.

In 2004 the Moody laboratory discovered a new member of the mycobactin family as part of a screening for candidate antigens of CD1a.²⁶² Subjecting chromatographic fractions of *Mtb* cell wall extracts to a CD1a-restricted T-cell line showed that these were activated by a molecule with a nominal mass of 838 Da. To gain more information about the molecular structure

that causes T-cell activation, collisional mass spectrometry and NMR analysis were performed revealing the structure to be congruent with the lipopeptide dideoxymycobactin (DDM). DDM is a depsipeptide with four stereogenic centers which are part of an unusual α -methyl serine that is cyclized to an oxazoline, a 3-hydroxy butyric acid unit, and two lysines of which one is cyclized as a caprolactam. The stereochemistry of the lysine amino acids was known, but the former two stereogenic residues were of unknown stereochemistry. Since NMR and mass spectrometry analyses were unable to address the question

Scheme 53. Watanabe's PIM₂ Total Synthesis

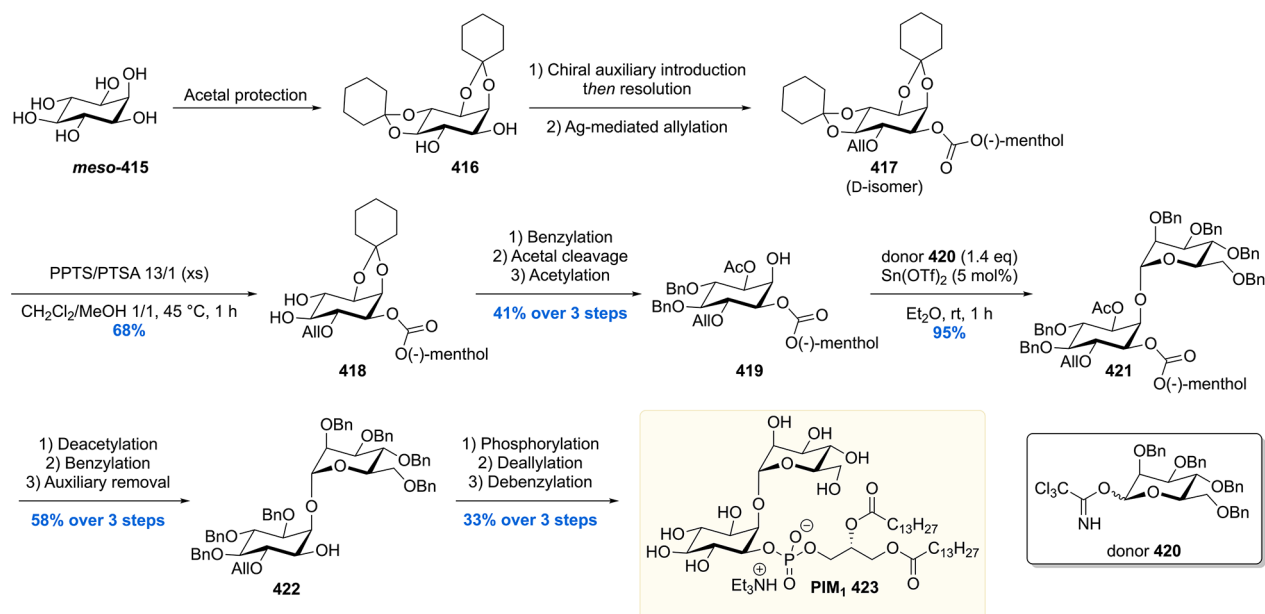
of the stereochemistry of DDM, together with insufficient quantities being isolated for studies of its role in iron acquisition and testing T-cell responses in human populations, there was sufficient incentive to embark on a total synthesis.

The first total synthesis of DDM-838 **393** was performed in the Moody laboratory and consisted of a solid-phase synthesis (Scheme 51).²⁶³ The synthesis was rather straightforward in the sense that standard solid-phase deprotection–coupling sequences were employed. The synthesis was built-up by first introducing the hydroxy butyramide functionality providing **389**, followed by a HATU-mediated esterification. The *cis*-eicosenonic amide moiety was constructed and then coupled with oxazolonic acid **391** to provide **392**. The 4-methyltrityl (Mtt) group in **392** was cleaved with simultaneous release from the solid support, after which the caprolactam was formed by intramolecular amide coupling. DDM-838 **393** was purified by preparative HPLC to provide submilligram quantities which were sufficient for further studies.

Using the solid-phase synthesis, all four diastereoisomers (varying the stereocenters designated as * in Scheme 51) were synthesized to elucidate the relative stereochemistry of DDM-838. The synthetic compounds were tested in a T-cell response assay using intact dendritic cells by subjecting CD1a-restricted T cells to the diastereomers. Interleukin-2 release was measured, and it was found that only DDM-838 with the (*S,R*)-stereochemistry on the α -methyl serine and 3-hydroxy butyric acid (as drawn in Scheme 51), respectively, exhibited the exact same bioactivity as the natural isolate. The diastereomeric

compounds, with alterations at either stereogenic center, exhibited a 1000-fold or greater loss of T-cell activation, showcasing the importance of enantiopure compounds in immunoassays.

A second total synthesis of DDM was reported in 2017 by the Williams group.²⁶⁴ Their synthesis was designed to optimize the synthesis by Young et al.²⁶³ in terms of overall yield and potentially, undetected, epimerization during esterification or peptide coupling. The Williams synthesis was initiated by construction of the two building blocks **398** and **400** (Scheme 52, first approach). Amine **394** was condensed with **395** using COMU as the peptide coupling agent to produce amide **396**. The α -methyl serine moiety was cyclized by the action of XtalFluor-M to introduce the oxazoline group in **397**. The ester of **397** was hydrolyzed, and the formed carboxylic acid was reacted with a protected lysine to form the peptide bond. The ester from the protected lysine was then hydrolyzed to give **398**, which was esterified with amide **400**, formed by reaction of caprolactam **399** with hydroxybutyric acid **388**. The esterification proceeded in a moderate 51% yield, and in addition, the stereocenter in **401** was fully epimerized under the coupling conditions providing a 1:1 mixture of *S* (desired) and *R* (undesired) isomers of **401**. A three-step sequence comprising benzyl hydrogenolysis, Boc deprotection, and EDC mediated coupling of **402** gave rise to DDM-838 **393** in 15% yield, together with its stereoisomer in 29% yield. An unexpected finding was that during the EDC-mediated coupling with pure (*Z*)-**402**, alkene isomerization took place as well, thereby also

Scheme 54. Total Synthesis of PIM₁ by the Schmidt Laboratory

providing two alkene isomers (*not shown*) of DDM-838 **393** and its stereoisomer.

To address the undesired epimerization in the esterification of **398** and **400**, and to circumvent the alkene isomerization in the last step of the DDM total synthesis, the Williams group designed a second synthetic strategy (Scheme 52, second approach). In this linear synthesis, the esterification reaction was performed with less complex reagents by employing a Mitsunobu reaction between **403** and Fmoc-L-lysine(Z)-OH. Despite a significant amount of elimination in this reaction, no epimerization was observed. Deprotection of the Fmoc moiety provided **404** in 26% over the two steps. The synthesis of DDM-838 **393** was finalized in a three-step sequence of which the last step was a DIC-mediated amide coupling with acid **402**. In this amidation reaction, no alkene isomerization took place. The overall yield for approach two was not higher than that of the first approach. However, despite the sacrifice of synthetic convergence in the second strategy, no unwanted isomerization reactions took place that hampered isolation procedures.

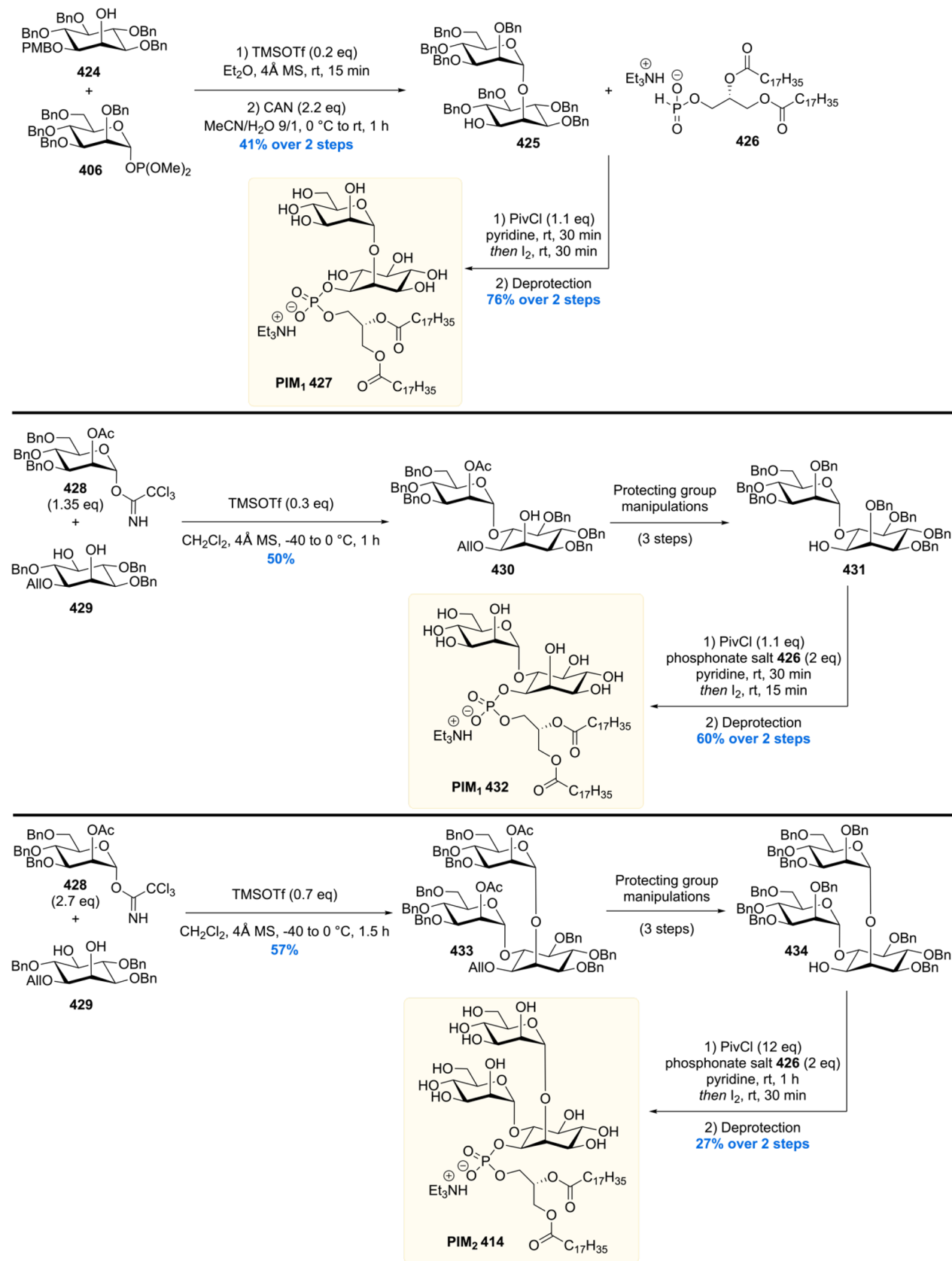
The synthetic compounds from this total synthesis were also used in biological assays to gain more insight into the structure–activity of DDM-838. Although not favored during synthesis, the stereoisomers with inverted stereochemistry at the lysine and the alkene geometrical isomer provided a unique opportunity to investigate the bioactivity of structurally related DDM-838 structures. In this immunoassay, CD1a restricted T-cells derived from unrelated human donors were subjected to the DDM-838 molecules. It was found that the molecules exhibited similar reactivity for each donor. Whereas in the study by Young et al. (*vide supra*)²⁶³ only DDM-838 showed bioactivity and other diastereomers not, the DDM-838 isomer with *E*-alkene geometry exhibited a significant but attenuated activity. Also, the DDM-838 isomer with opposite stereochemistry at the central lysine unit showed some activity. Bioactivity was not seen using DDM-838 having unnatural stereochemistry at the lysine and the acyl lipid. This structure–activity relationship, together with the results obtained by Young et al.,²⁶³ highlighted the eminent sensitivity of the CD1a restricted lipopeptide-reactive T-cells for naturally occurring DDM-838 stereochemistry.

9. CELL WALL OLIGO- AND POLYSACCHARIDES

Another major component of the mycobacterial cell wall is the mycolyl arabinogalactan peptidoglycan complex (mAGP), which is interspersed with the lipoglycans phosphatidylinositol mannosides (PIM), lipomannan (LM), lipoarabinomannan (LAM), and mannose-capped LAM (ManLAM) and anchored by non-covalent interactions with their phosphatidyl-*myo*-inositol (PI) moieties (Figure 5).^{265–267} LM, LAM, and ManLAM all contain a conserved PIM motif.

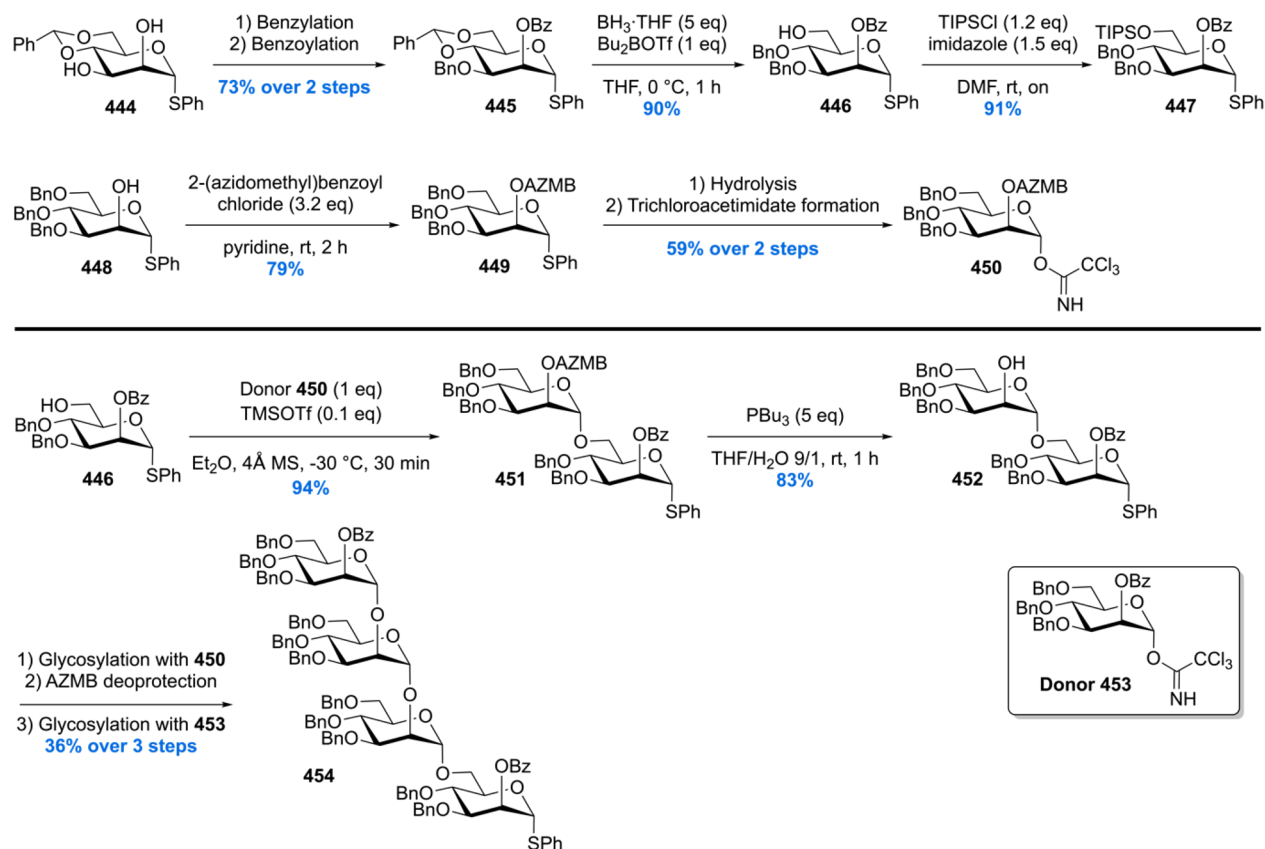
One can imagine that dissection and elucidation of this complex array of lipidated oligo- and polysaccharides has been a monumental task. Considering that even with modern analytical techniques deciphering these molecular architectures is challenging²⁶⁹ makes the pioneering work by Anderson, who identified the structural features of the PIMs, even more impressive.²⁷⁰ By saponification of phosphatide fractions from several mycobacteria, including *Mtb*, Anderson was able to identify all the structural elements belonging to the PIMs, namely fatty acids, an organophosphoric acid, phosphorylated glycan, and mannositolose which hydrolyzed to mannose and inositol. It was Ballou and co-workers who in a series of publications meticulously pieced together the fragments to arrive at the chemical structures we now know as the PIMs.^{271–274} There are multiple different PIMs with a varying number of mannose units (PIM_{1–6}) and acyl residues (up to four). In PIM₁, the inositol core of phosphatidylinositol is mannosylated at C-2 and PIM₂ contains an additional mannose at C-6. Further mannosylations give rise to PIM₃ to PIM₆. PIMs are known to carry different fatty acyl chains, with palmitic and tuberculostearic acids being the most abundant acyl residues. Thirty years after the impressive structure elucidation by Ballou, the position of the fatty acid moiety in the acetylated PIMs (Ac₁PIMs) was determined to be at the C6 position of the mannose linked to the C2-position of the inositol.²⁷⁵ Work by Gilleron et al. showed that another fatty acid, that in Ac₂PIMs, is present on the C3-position of the inositol core.²⁷⁶

The exact role of PIMs in *Mtb* pathogenesis remains unclear as studies describe various different biological effects of PIMs triggering divergent host responses, at times, also depending on

Scheme 55. Total Synthesis of Two Regioisomers of PIM₁ and Synthesis of PIM₂

the exact chemical identity of these lipoglycans.²⁷⁷ PIMs have been shown to induce early endosomal fusion within macrophages as such supplying nutrients to the pathogen.²⁷⁸

Furthermore, PIMs are involved in infection establishment by participation in receptor-mediated internalization in macrophages²⁷⁹ and inhibit macrophage activation and host

Scheme 57. Synthesis of PIM₆ Building Blocks

precursor for LM, LAM, and ManLAM. Further extension of position 6 of the PIM core by introduction of an α -1,6 linked mannoside backbone carrying varying amounts of single α -mannoside residues at the 2-position gives rise to LM. To this date, it is not established if LM is an end-product or merely a biosynthetic intermediate for the formation of LAM. Formation of LAM is achieved by further attachment of arabinans (repeating units of α -1,5 arabinose). The arabinan skeleton of LAM can be capped with one or two α -mannosides at position 5 producing ManLAM. LAM itself is a highly heterogeneous entity with varying degree and pattern of branching in the mannan and arabinan subunits.²⁶⁶ The elucidation of the exact structure of the cell wall oligo- and polysaccharides has still not been concluded as evident from a very recent report by Jackson and co-workers, who showed a structural refinement of the LAM structure.²⁶⁸ The structure elucidation of LAM has considerable history, and before this structural revision took place, other groups were dedicated to elucidating the structure. This started with the initial structure analysis of PIMs in 1965.²⁷⁴ A few years later, the attachment of arabinan to the α -1,6-mannan backbone was unraveled²⁸⁵ followed by the discovery that arabinomannan is linked to PIM.^{286,287} The position of the linkage was then unveiled to be at the 6-O of the mannosyl residue, which itself is attached at its 2-position to the 6-O of inositol.²⁸⁸ In 1999, the exact location of the acyl substituents in PIM and LAM of *M. bovis* was reported.²⁸⁹ Furthermore, structural research also shed light on the architecture of the six-linked mannan backbone, carrying terminal α -Manp residues at the 2-position.^{288,290,291} In addition, various structural studies on arabinan^{292,293} and its terminal caps^{290,294–296} have been communicated over the years. In a recent report, investigations of the LAM biosynthesis

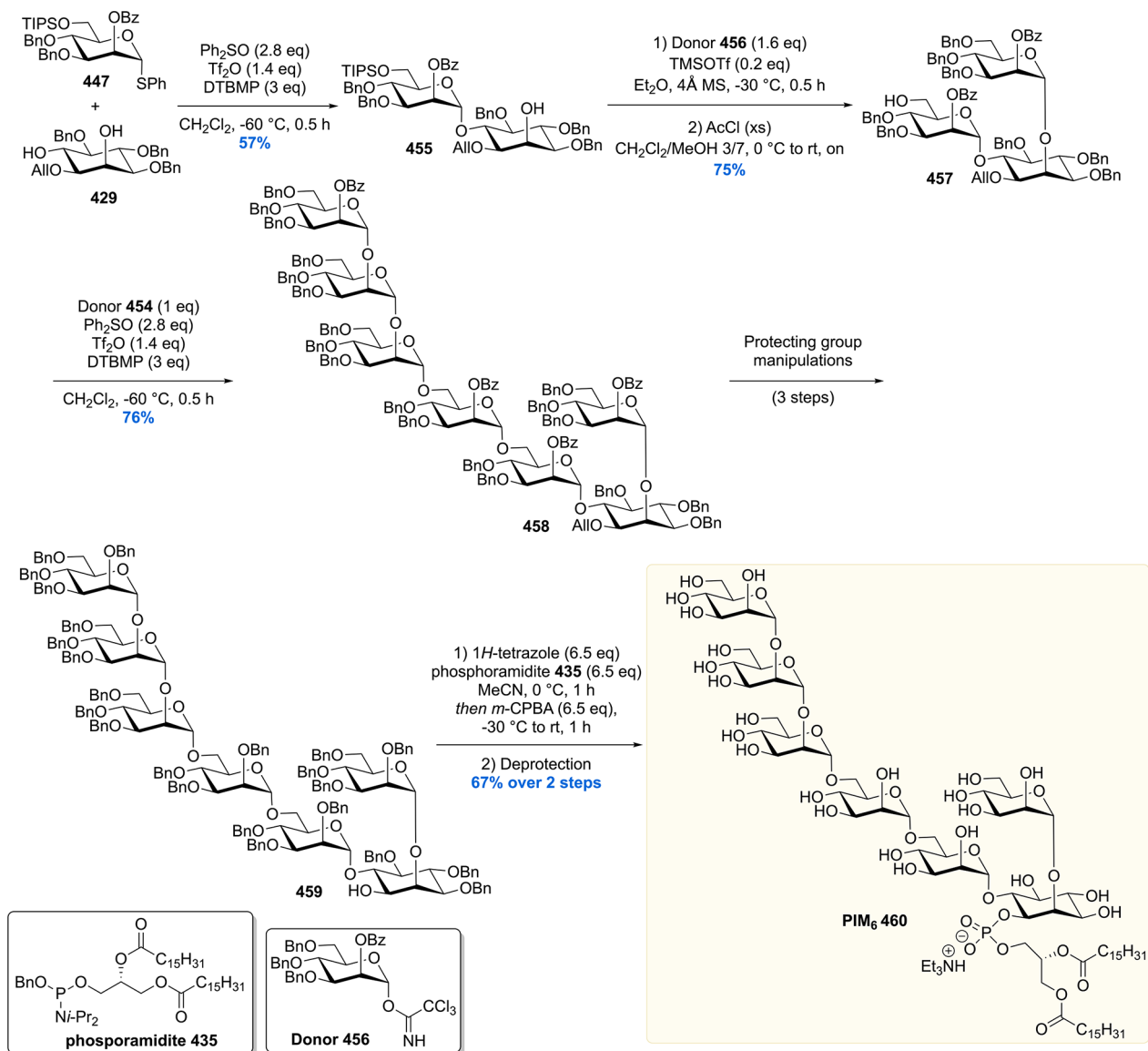
revealed that the first five to seven Manp units attached to inositol are present as a linear saccharide chain.²⁹⁷ Ultimately, a report from the Jackson laboratory then discovered the presence of extended secondary mannan side chains linked to the internal mannan chain, as well as that the attachment of the arabinan unit is at the nonreducing end of mannan and not at the internal regions as thought previously.²⁶⁸

The biological effects exerted by LM, LAM, and ManLAM have been reviewed extensively.^{32,267,298,299} In brief, ManLAM has been shown to engage the mannose receptor of macrophages thus inducing phagocytosis, whereas uncapped LAM (also referred to as AraLAM) did not produce this effect.³⁰⁰ This selectivity in biological effect was also observed in the activation of DC-SIGN on dendritic cells by ManLAM but not AraLAM, leading to the hypothesis that LAM capping evolved as the mechanism to attenuate host inflammatory responses.^{301,302} ManLAM also inhibits phagosome–lysosome fusion by engaging mannose receptors.^{303,304} Furthermore, LAM has been found to be an antigen and is presented in a mannose receptor mediated process to T-cells by loading on CD1b molecules.³⁰⁵ LAM is also a urine biomarker for active TB and utilized in point-of-care clinical tests.³⁰⁶

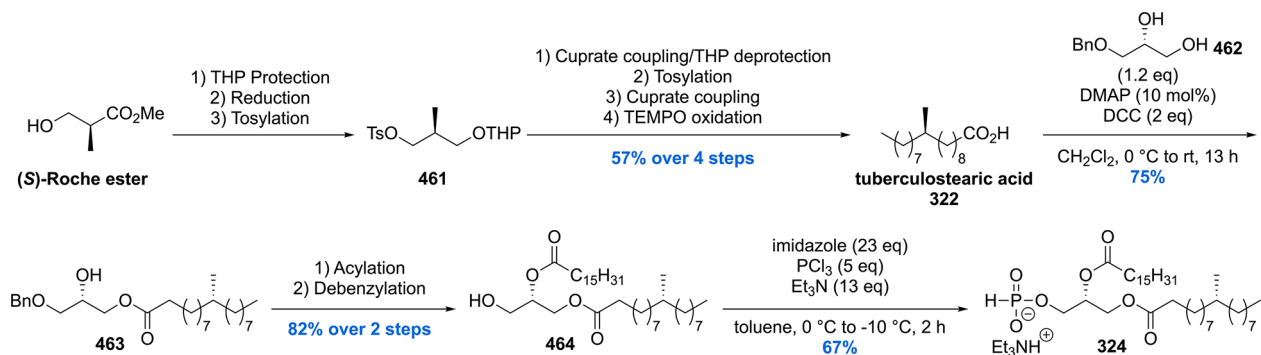
9.1. Phosphatidylinositol Mannosides

Several synthetic studies and total syntheses of PIMs have been reported up to 1995 but fall outside the scope of this review.^{307–309}

In 1996 Watanabe and co-workers reported a synthesis of a PIM₂ (Scheme 53).³¹⁰ Their synthetic approach relied heavily on in-house developed phosphite chemistry for both the glycosidations and the phosphorylation. Starting with such a phosphite glycosidation, *rac*-**405** was reacted with glycoside

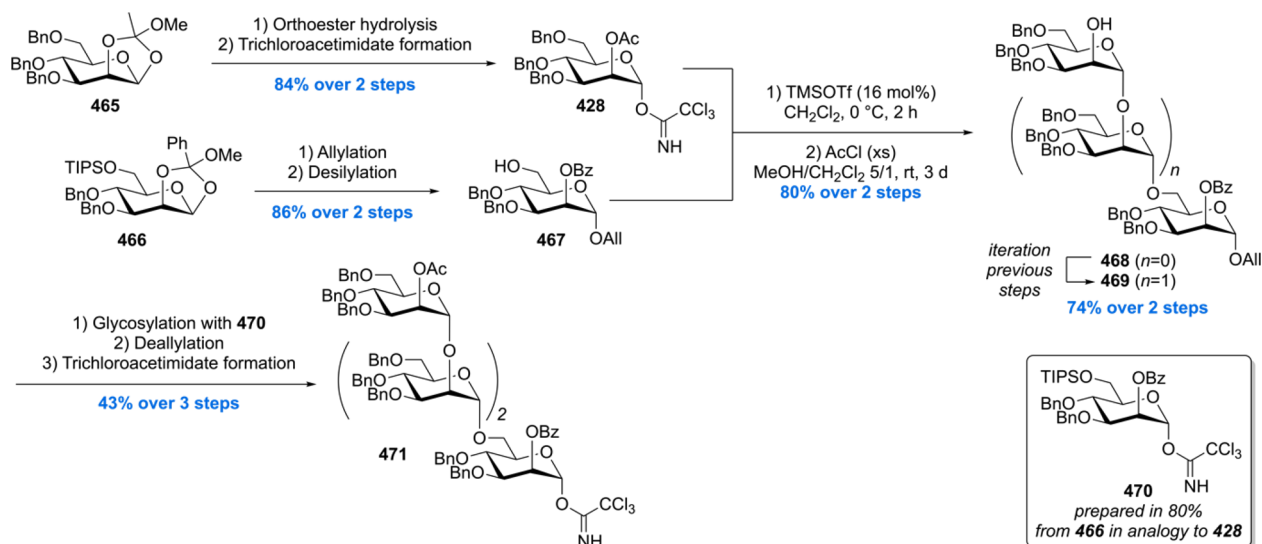
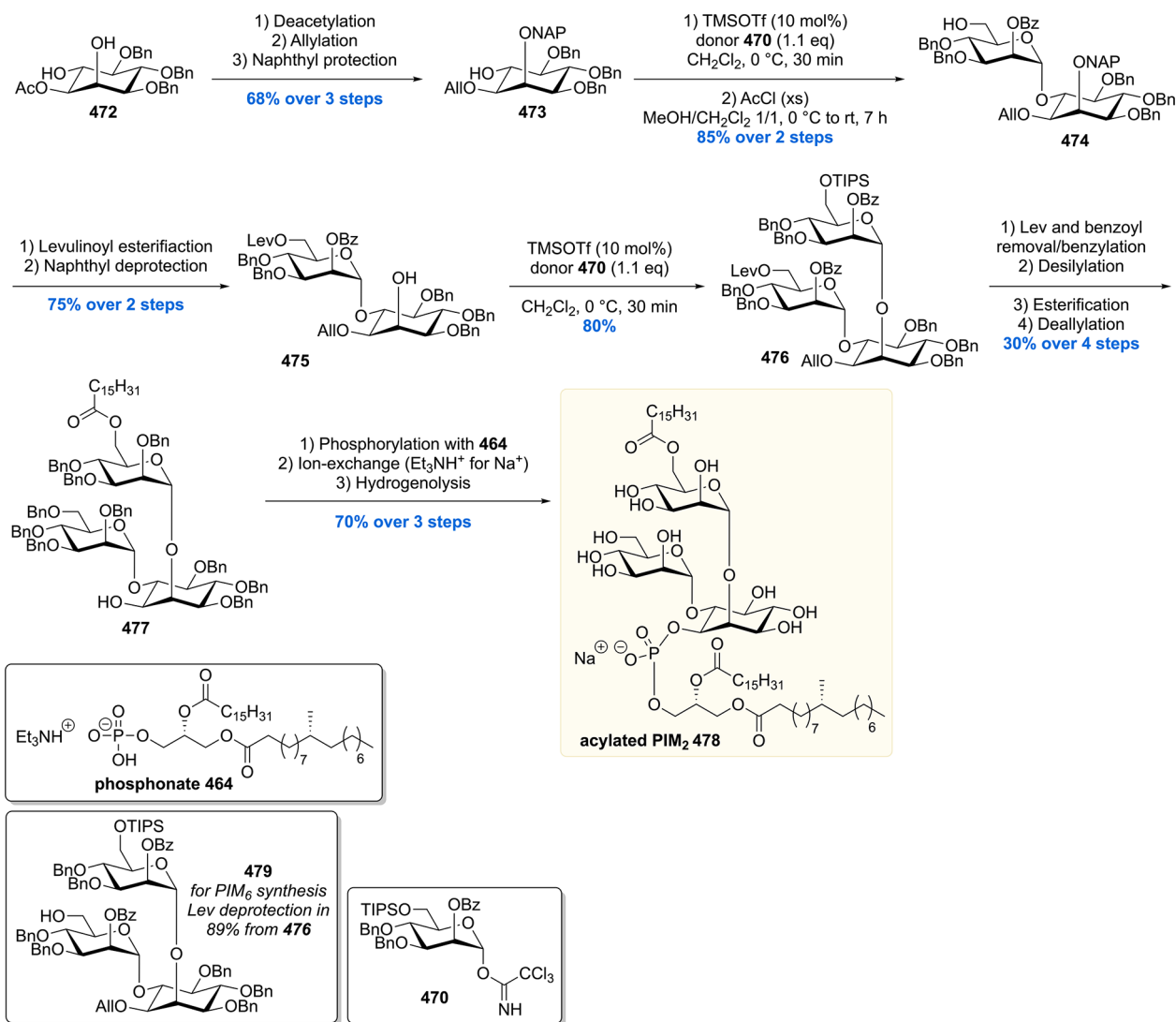
Scheme 58. PIM₆ Completion

Scheme 59. Tuberculostearic Acid Bearing Phospholipid Synthesis by Seeberger and co-workers



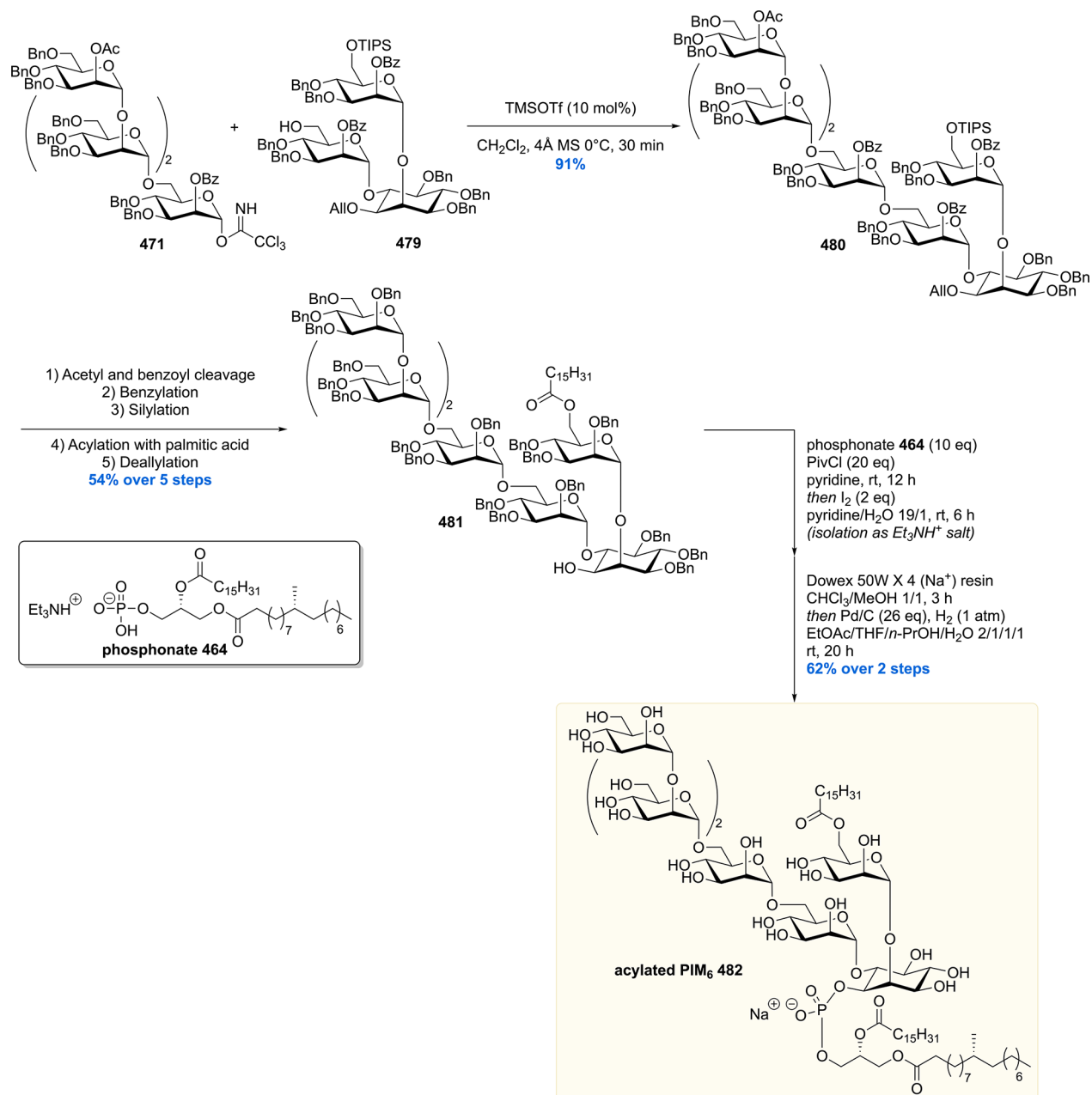
donor **406** yielding α -anomers **407a** and **407b** as an inseparable mixture (45%, 1:1) together with the easily removable β -anomer (15%). Acetal deprotection gave, after separation of the diastereomers, **408** in 45% yield. Triol **408** was subjected to a phosphorylation with glyceryl dimethyl phosphite **412**, derived from *sn*-glycerol 1,2-carbonate **409** and dimethyl *N,N*-

diisopropylphosphoramidite **410**. Treatment of **408** with phosphite **412** in the presence of pyridinium tribromide yielded phosphorylated glycoside **411** in 83% (*dr* = 1:1, due to the asymmetric P-atom) with excellent regioselectivity. The diastereomeric mixture of **411** was then stereo- and regioselectively glycosidated in 74% using **406** to furnish

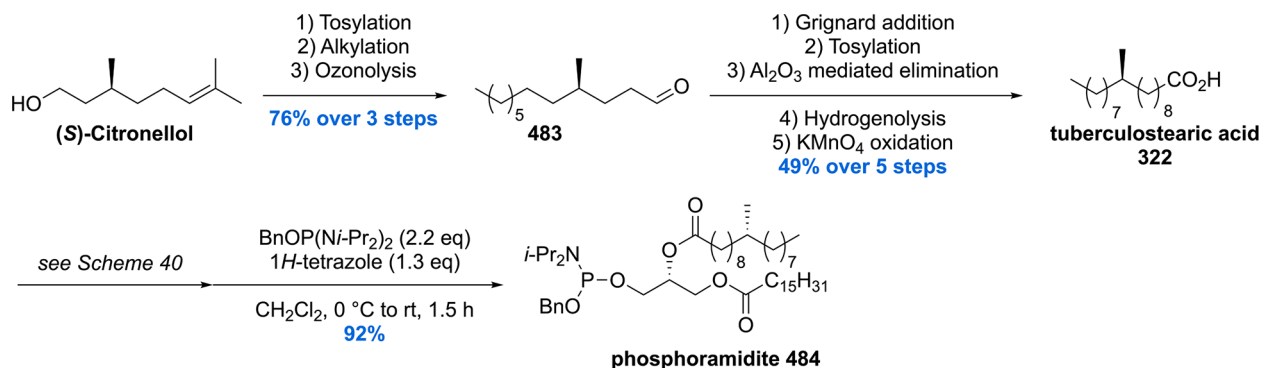
Scheme 60. Seeberger's Synthesis of AcPIM₂ and AcPIM₆ Building BlocksScheme 61. Seeberger's AcPIM₂ Synthesis

trisaccharide **413**. Carbonate cleavage by treatment with EtMgBr and regioselective diacylation were followed by a

three step deprotection sequence furnished PIM₂ **414** in 43% over the five steps.

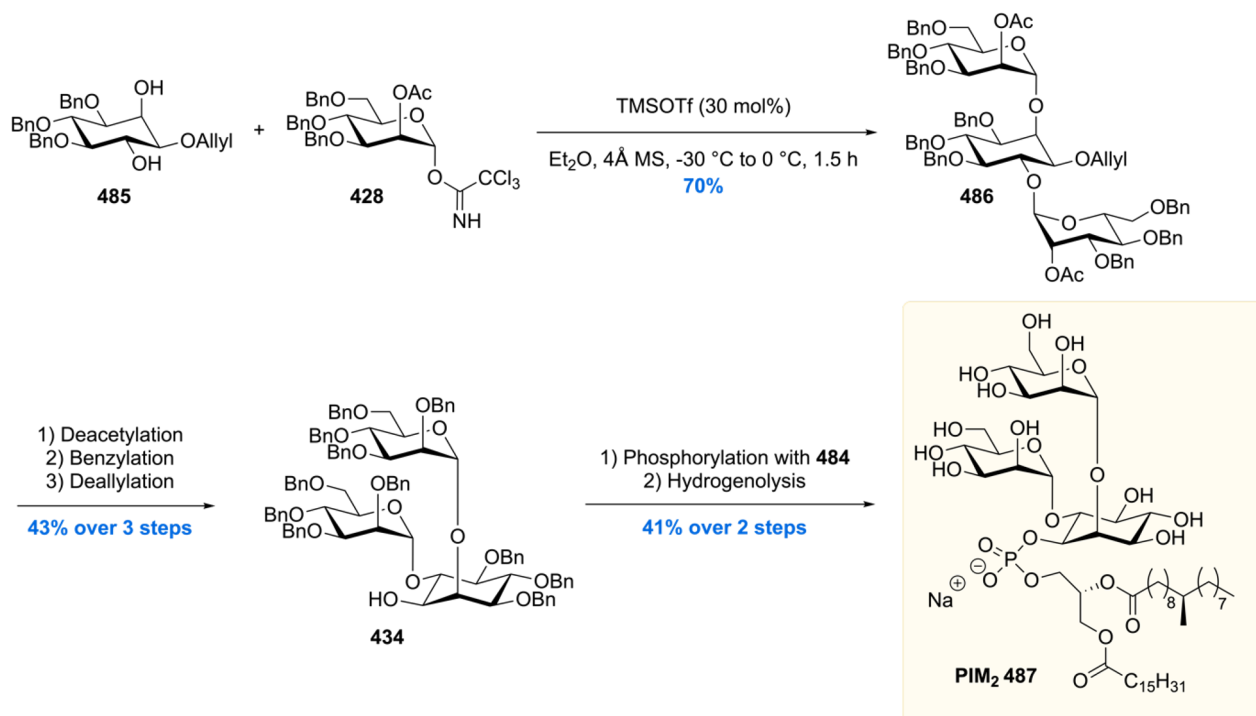
Scheme 62. Completion of the Total Synthesis of AcPIM₆

Scheme 63. Larsen's Tuberculostearic Acid and Phosphoramidite Synthesis

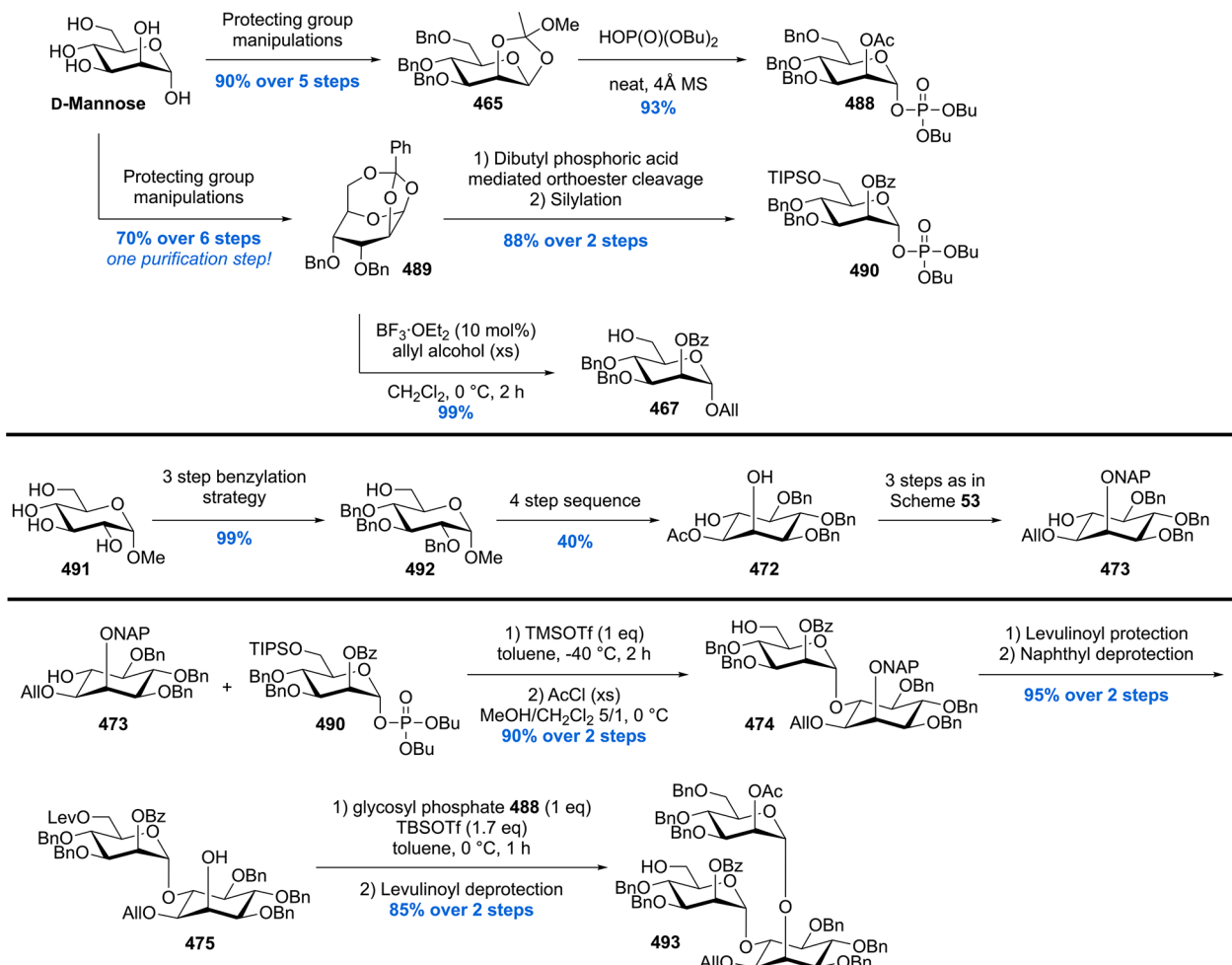


In 2003, Schmidt and co-workers communicated the total synthesis of PIM₁ (Scheme 54).³¹¹ Their endeavor started with

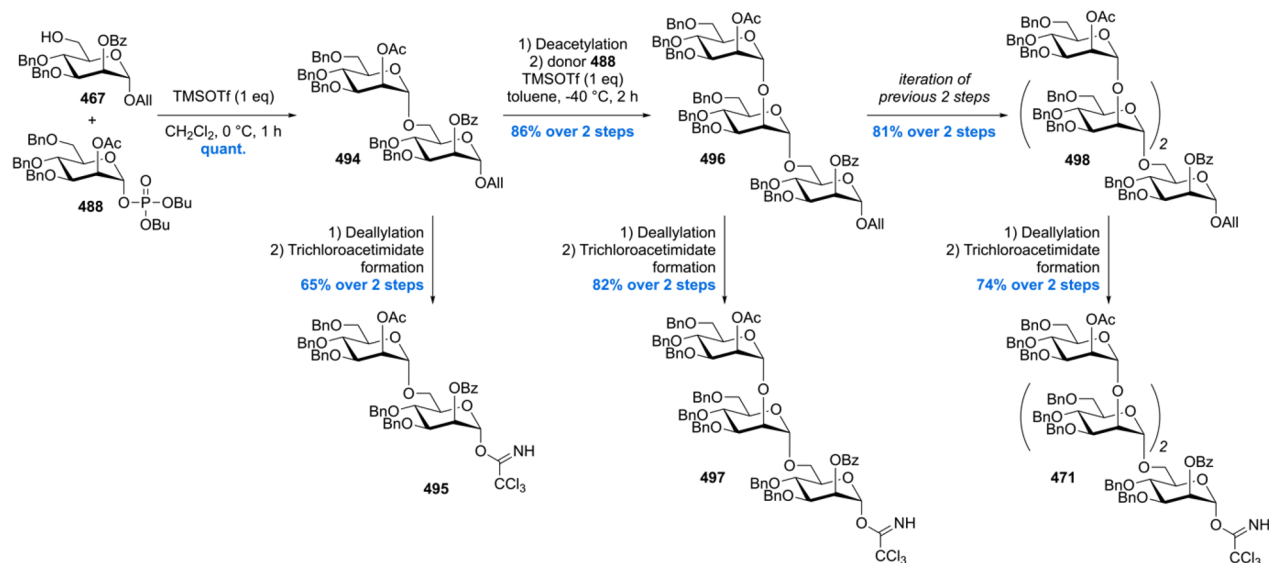
the acetal protection of *myo*-inositol **415** with cyclohexanone. This uncontrolled reaction provided, besides the desired

Scheme 64. Larsen's Total Synthesis of PIM₂

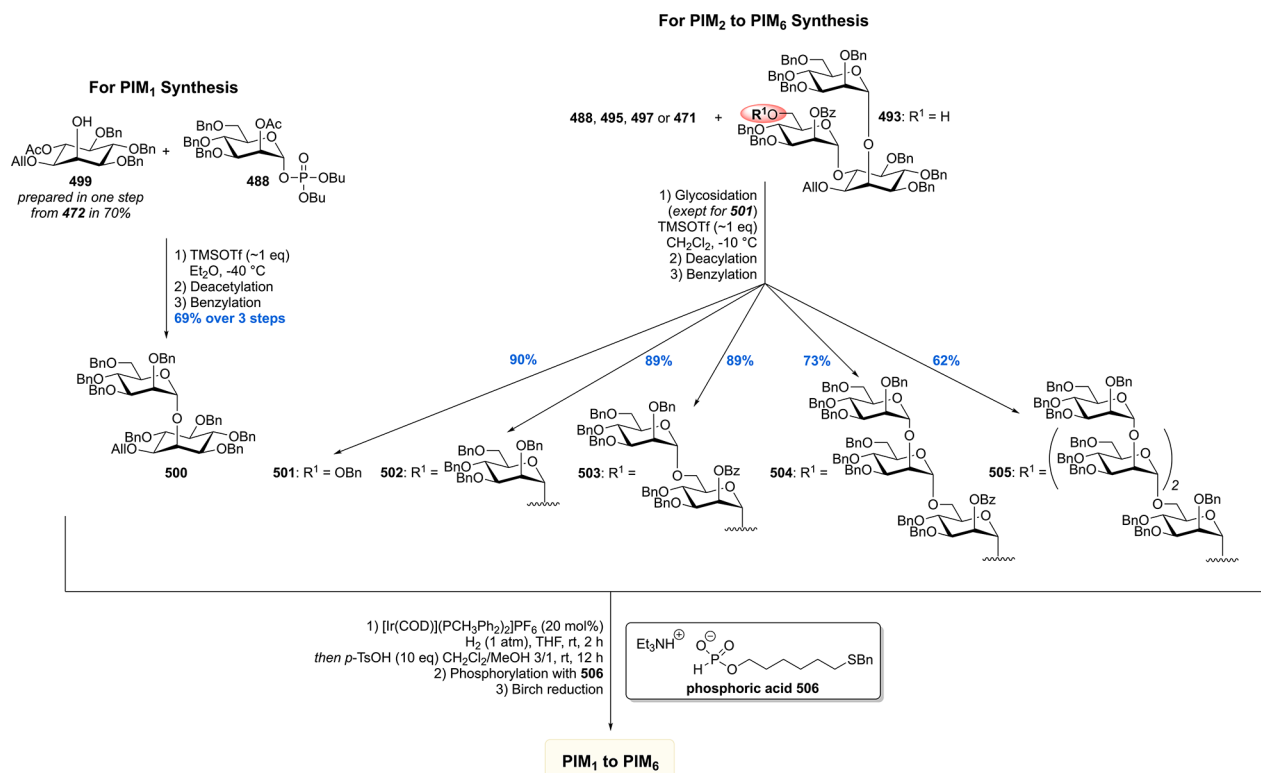
Scheme 65. Seeberger's Building Block Synthesis for the Entire PIM Catalogue



Scheme 66. Synthesis of the Oligomannosylating Agents for the Synthesis of the PIM Catalogue



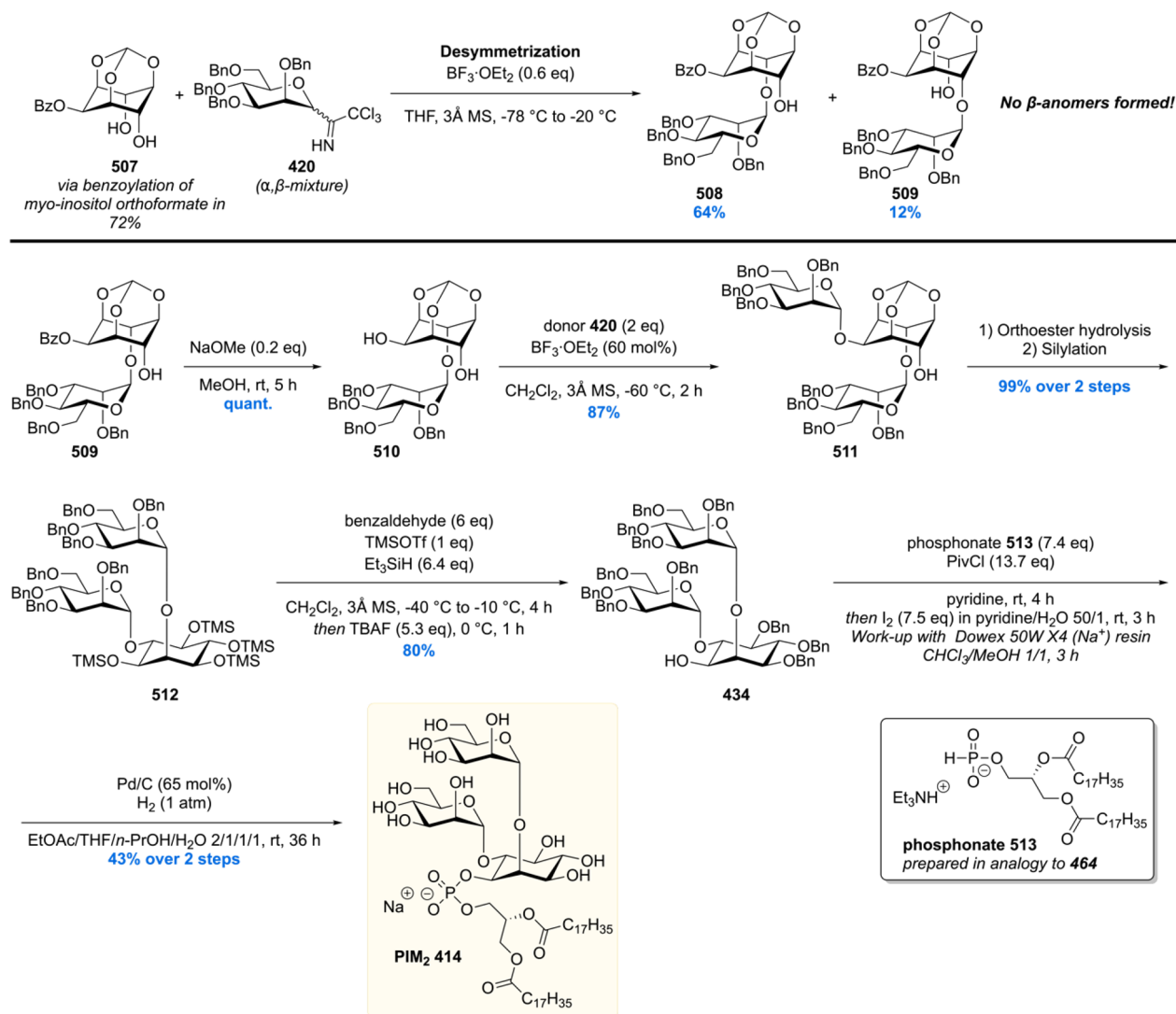
Scheme 67. Seeberger's Completion of the Synthesis of the Entire Catalogue of PIM Analogues



product **416**, also isomeric side-products. These were easily removed by crystallization and flash column chromatography affording clean **416**. In order to get the isomerically pure *D*-myo-inositol scaffold, a resolution was performed after selective installation of a menthol-derived chiral auxiliary. With the resolution performed, the allyl protecting group was installed affording **417**. Selective removal of the 4,5-*O*-cyclohexylidene acetal by treatment with a pyridinium *p*-toluenesulfonate (PPTS) *p*-toluenesulfonic acid (PTSA) mixture furnished diol **418** in 68% yield. A sequence of protecting group manipulations then set the stage for the glycosidation of *myo*-inositol **419** with trichloroacetimidate **420**. Using 5 mol% of Sn(OTf)₂ as the

catalyst, smooth glycosidation occurred providing pseudodisaccharide **421** with complete α -selectivity in 95% yield. With this key-step performed, a straightforward sequence of protecting group removal and phosphorylation provided the desired PIM₁ **423**.

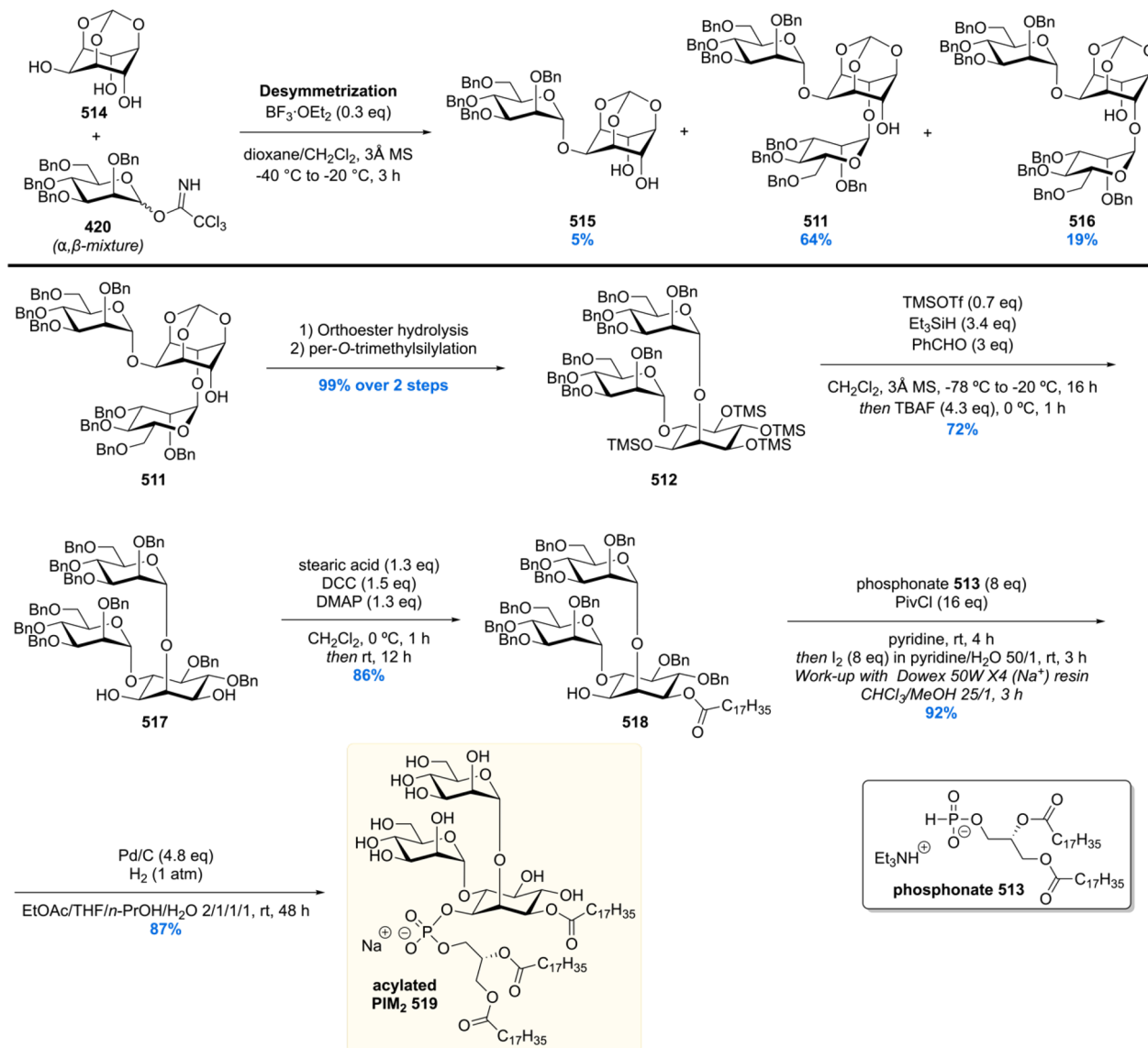
In 2006, the Larsen laboratory communicated their synthesis of two PIM₁ regioisomers **427** and **432** carrying a mannosyl group at the 2- and 6-positions of the inositol core, respectively, as well as PIM₂ **414** (Scheme 55).³¹² Contrary to previous syntheses, their prepared PIMs are equipped with stearyl esters at the phosphatidyl unit, as these have been identified to be present in biologically active PIM extracts. The synthesis of the

Scheme 68. Hung's Desymmetrization Strategy for the Synthesis of PIM₂

2-*O*-mannosylated PIM₁ **427** was initiated by the TMSOTf-promoted glycosylation of inositol acceptor **424** with mannosyl phosphite **406** providing an inseparable mixture of α - and β -configured pseudodisaccharides, which were separated after PMB removal, giving **425** in 41% yield. The phosphate group was then installed by coupling of **425** to phosphonate **426** in the presence of pivaloyl chloride, followed by iodine-mediated oxidation. The desired PIM₁ **427** was obtained as the triethylammonium salt in 76% yield over two steps. For the synthesis of 6-*O*-mannosyl PIM₁ **432**, diol **429** was selectively glycosylated with mannosyl imidate **428** to provide **430** in 50% yield. After a sequence of protecting group manipulations, pseudodisaccharide **431** was coupled to phosphonate **426** as done previously, giving 6-*O*-mannosyl-PIM₁ **432** in 60% yield over two steps. PIM₂ was also accessed starting from diol **429**. After double glycosylation with excess mannosyl imidate **428**, **433** was obtained in 57% yield. Again, a series of protecting group manipulations was performed arriving at **434**, which allowed access of PIM₂ by phosphonate-coupling and global deprotecting in 27% yield over two steps. The authors used the synthetic PIMs to assess their ability to suppress eosinophil (= type of white blood cell) recruitment in an asthma mouse model. After intranasal administration of the synthetic PIMs, a

significant decrease of the number of eosinophils were observed, with PIM₁ **432** generating the strongest immunosuppression. Furthermore, this effect was not only limited to eosinophils, but a decrease in the levels of both lymphocyte and macrophage was observed, demonstrating an immunosuppressive effect of mycobacterial PIMs that is not restricted to a single immune cell type. Following up on this synthesis, the crystal structure of murine CD1d bound to synthetic PIM₂ **414** was characterized. By gaining structural information on the binding mode of PIMs to CD1d, the authors anticipate that based on this, new agonists for NKT cells presented by CD1d could be designed in a rational fashion.³¹³

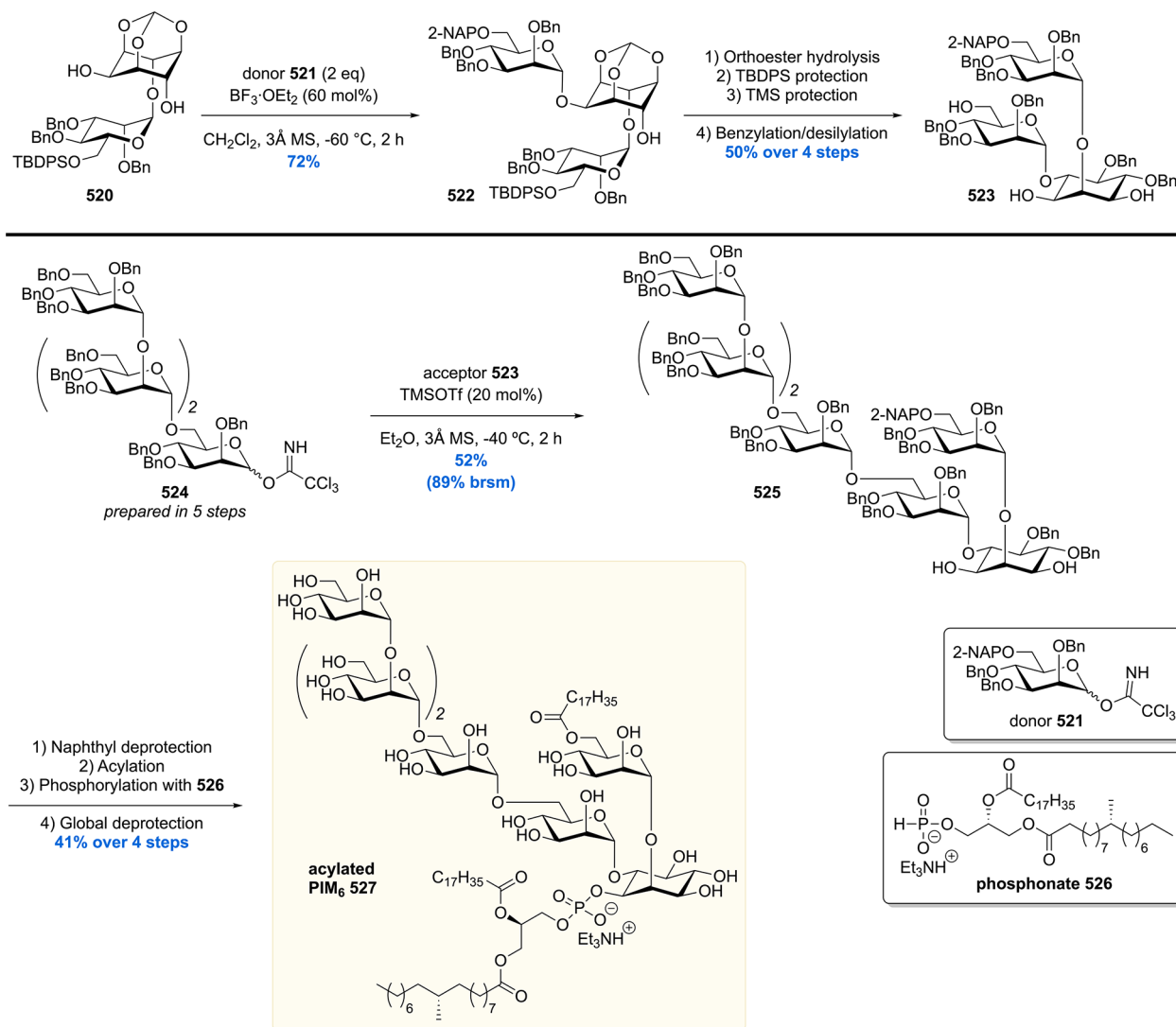
Shortly after their synthesis of PIM₁ **427** and **432**, and PIM₂ **414**, the same group reported the synthesis of PIM₄ **443** and an improved synthesis of PIM₂ **436** in order to investigate their immune adjuvant properties (Scheme 56).³¹⁴ The construction of the known pseudotrisaccharide **434** was performed in analogy to Scheme 55, yet the yield of the double glycosylation reaction could be improved to 70% by changing the solvent from dichloromethane to diethyl ether. The phosphate moiety was then installed by coupling of phosphoramidite **435** to **434** and *in situ* oxidation. After deprotection, the desired PIM₂ **436** was obtained in 66% yield. In the synthesis of PIM₄ **443**,

Scheme 69. Hung's Desymmetrization Strategy for the Synthesis of Triacylated PIM₂

disaccharide donor **439** was accessed in 58% over three steps by TMSOTf-promoted glycosylation of alcohol **437** with trichloroacetimidate **438**, followed by hydrolysis and imidate formation. Next, pseudotrisaccharide **433** was prepared by selective glycosylation of diol **429**, first with donor **438** followed by donor **440**. Subsequent desilylation provided then **433** in 27% yield over three steps. Building blocks **433** was then glycosylated with **439** were then coupled by glycosylation to give **441** in 80% yield, and subsequent routine protecting group manipulations delivered alcohol **442**. Pseudopentasaccharide **442** was then coupled, as done before, to phosphoramidite **435** and delivered after deprotection PIM₄ **443** in 46% yield over two steps. Synthetic PIM₂ **436** and PIM₄ **443** were then tested as potential adjuvants in an ovalbumin-specific mouse model. Injection of **436** and **443** with a model antigen resulted in a significant immune response as measured by INF- γ production compared to the negative control, with PIM₂ **436** causing a stronger response than PIM₄ **443**. Notably, both synthetic PIMs did not cause significant local lesions or edema compared to Complete Freund's Adjuvant (CFA), which was used as positive control,

indicating that PIMs possess adjuvant properties without the toxic effects of CFA.

Building on their synthesis of various PIMs, in 2011 Harper and Painter (collaborating with Larsen) reported the synthesis of PIM₆ **460**.³¹⁵ The synthesis was initiated with the preparation of tetramannosyl building block **454** (Scheme 57). Starting from benzylidene protected mannose thioglycoside **444**, the 2- and 3-OH groups were protected in 73% yield, followed by reductive opening of the benzylidene group providing alcohol **446** in 90% yield. The primary hydroxyl of **446** was then silylated giving thioglycoside **447**. Next, donor **450** was prepared by protection of the 2-OH of **448** as chemically orthogonal 2-(azidomethyl)-benzoyl (AZMB) ester and subsequent thioglycoside hydrolysis and trichloroacetimidate formation. With these monosaccharide units in hand, the desired tetrasaccharide building block **454** was assembled. For this, TMSOTf-promoted glycosidation of acceptor **446** with 2-OAZMB donor **450** provided disaccharide **451** in the excellent yield of 94%. The 2-OH was then liberated by removal of the AZMB ester with tributyl phosphine delivering acceptor **452** in 83% yield. Again, glycosylation of **452** with donor **450**, subsequent AZMB removal, and last

Scheme 70. Hung's Synthesis of Acylated PIM₆

glycosylation with donor **453** then provided the desired tetrasaccharide **454** in 36% yield over three steps.

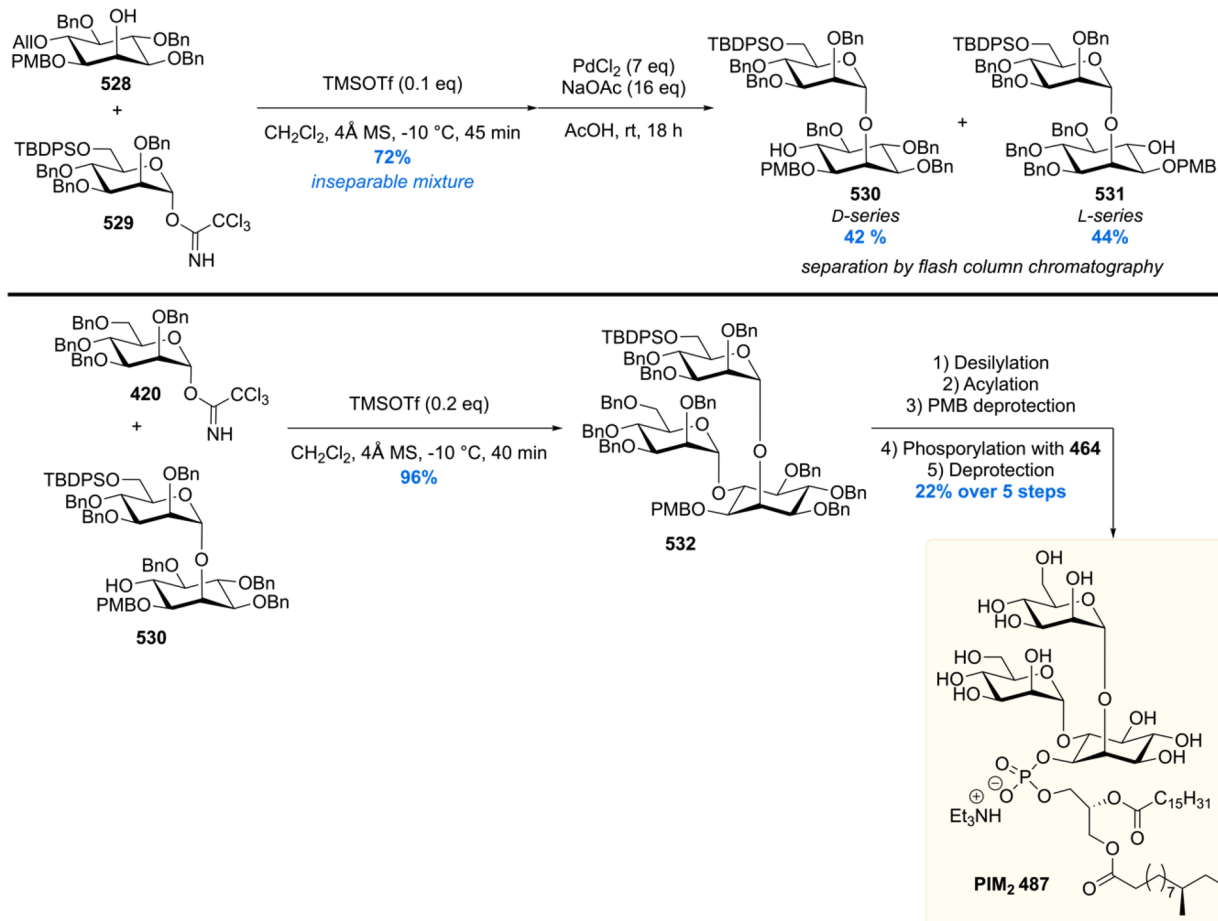
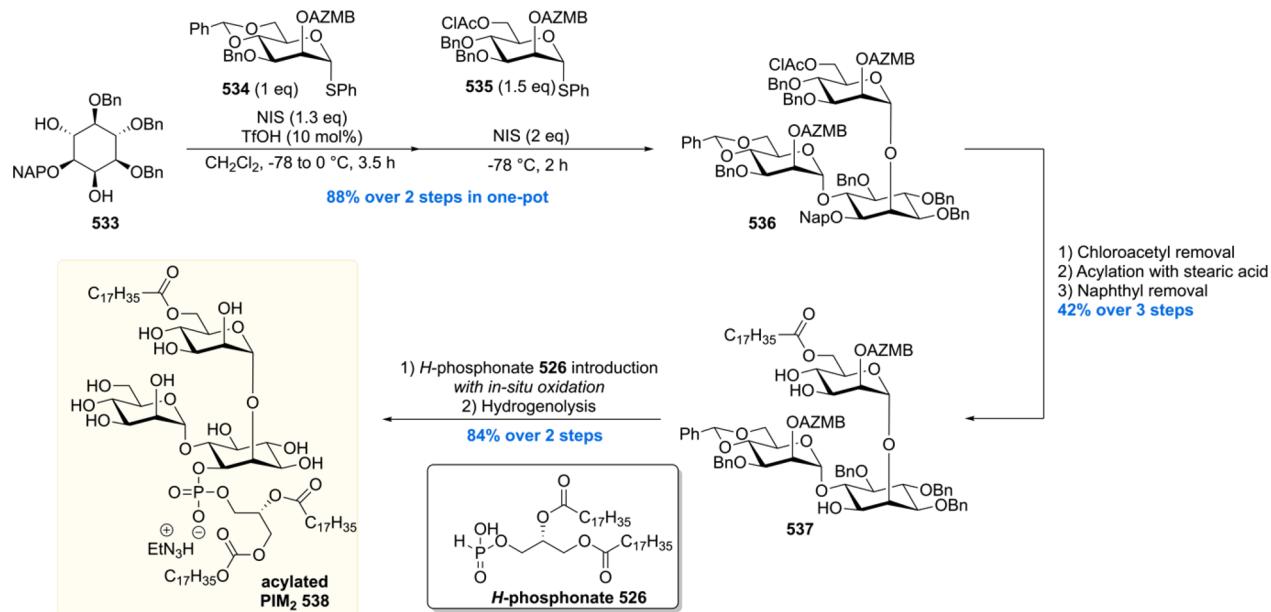
Next in the synthesis of PIM₆ **460**, the inositol core was prepared (Scheme 58). First, regioselective glycosylation of diol **429** with thioglycoside donor **447** provided **455** in 57%. Pseudodisaccharide **455** was then subjected to glycosylation with **456** followed by desilylation with acetyl chloride giving pseudotrisaccharide **457** in 75% yield over two steps. Coupling of **457** with tetrasaccharide **454** by glycosylation then delivered **458** in 76% yield which contained the complete carbohydrate skeleton of PIM₆ **460**. A sequence of protecting group manipulations then set the stage for the attachment of the phospholipid unit, which was brought about by coupling of **459** with phosphoramidite **435** and *in situ* oxidation. After global deprotection, the desired PIM₆ **460** was obtained as triethylammonium salt in 67% yield over two steps. The ¹H NMR spectra of natural and synthetic PIM₆ were compared and revealed that synthetic and natural material are in good agreement. With synthetic PIM₆, the authors sought to answer the question whether PIM₆ enhances or suppresses T-cell immune responses. In a human mixed lymphocyte reaction assay, synthetic PIM₆ caused dendritic cell dependent suppression of CD8⁺ T cell expansion in a dose dependent

manner. These results demonstrate the immunosuppressive effects of PIM₆ *in vitro*, an effect well-known for *Mtb* residing in human host cells.

After their efforts to access PIM₂, PIM₄, and PIM₆, the synthetic PIMs were tested as ligands for DC-SIGN, the major receptor for *Mtb* on dendritic cells. The study revealed that DC-SIGN has a higher affinity for PIM₆ compared to its lesser mannosylated counterparts PIM₂ and PIM₄. Yet, in experiments with *M. bovis* mutants lacking PIMs, DC-SIGN interactions were still intact, indicating that DC-SIGN interactions are far more complex and that mycobacteria express other DC-SIGN ligands beyond PIMs, potentially even mannosylated proteins.²⁸²

The group of Seeberger reported the combined synthesis of both natural acetylated PIM₂ and acetylated PIM₆.³¹⁶ Whereas previous syntheses focused merely on efficient introduction of the glycosidic bonds, in this study, the phospholipid moiety was installed mimicking the natural scenario. The nature of the phospholipid composition in antigenic glycosides can play a crucial role in immune response induction.³¹⁷

The lipid component of the phospholipid moiety is tuberculostearic acid **322**. Seeberger's synthesis of this lipid started with a THP protection of the (S)-Roche ester followed by reduction of the ester functionality and subsequent tosylation,

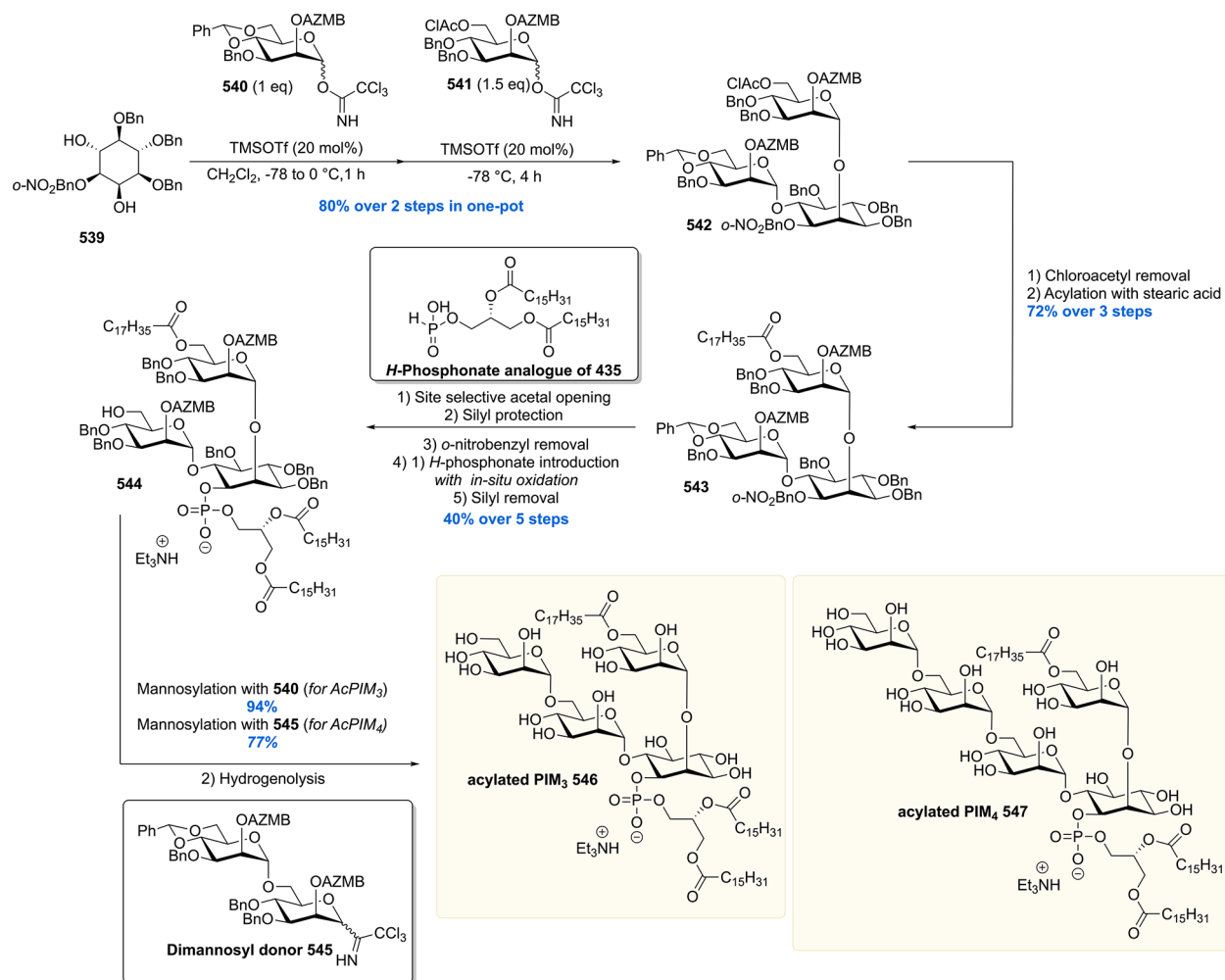
Scheme 71. Lear's PIM₂ Synthesis by ResolutionScheme 72. Acylated PIM₂ Synthesis by the Tanaka Laboratory

giving **461** (Scheme 59). A cuprate coupling/THP deprotection sequence, and again tosylation/cuprate coupling, gave after a TEMPO oxidation TBSA **322** in 57% over the four steps. A Steglich esterification of benzyl protected glycerol **462** provided **463** in 75% isolated yield, notably without acyl migration. A

second acylation and debenzoylation (with minor acyl 2 to 3 migration) giving **464** set the stage for the phosphorylation event yielding *H*-phosphonate **324**.

In order to maximize the synthetic convergence of the PIM₂ and PIM₆ syntheses, three mannose building blocks **428**, **467**,

Scheme 73. Total Synthesis of AcPIM3 and AcPIM4 by Tanaka and Co-workers



and 470, from two mannose orthoesters 465 and 466, were crafted (Scheme 60). Orthoester 465 was smoothly converted into trichloroacetimidate 428 using a hydrolysis/acetimidate formation sequence. Allylation and subsequent desilylation of 466 gave 467, a component in the synthesis of PIM₂.

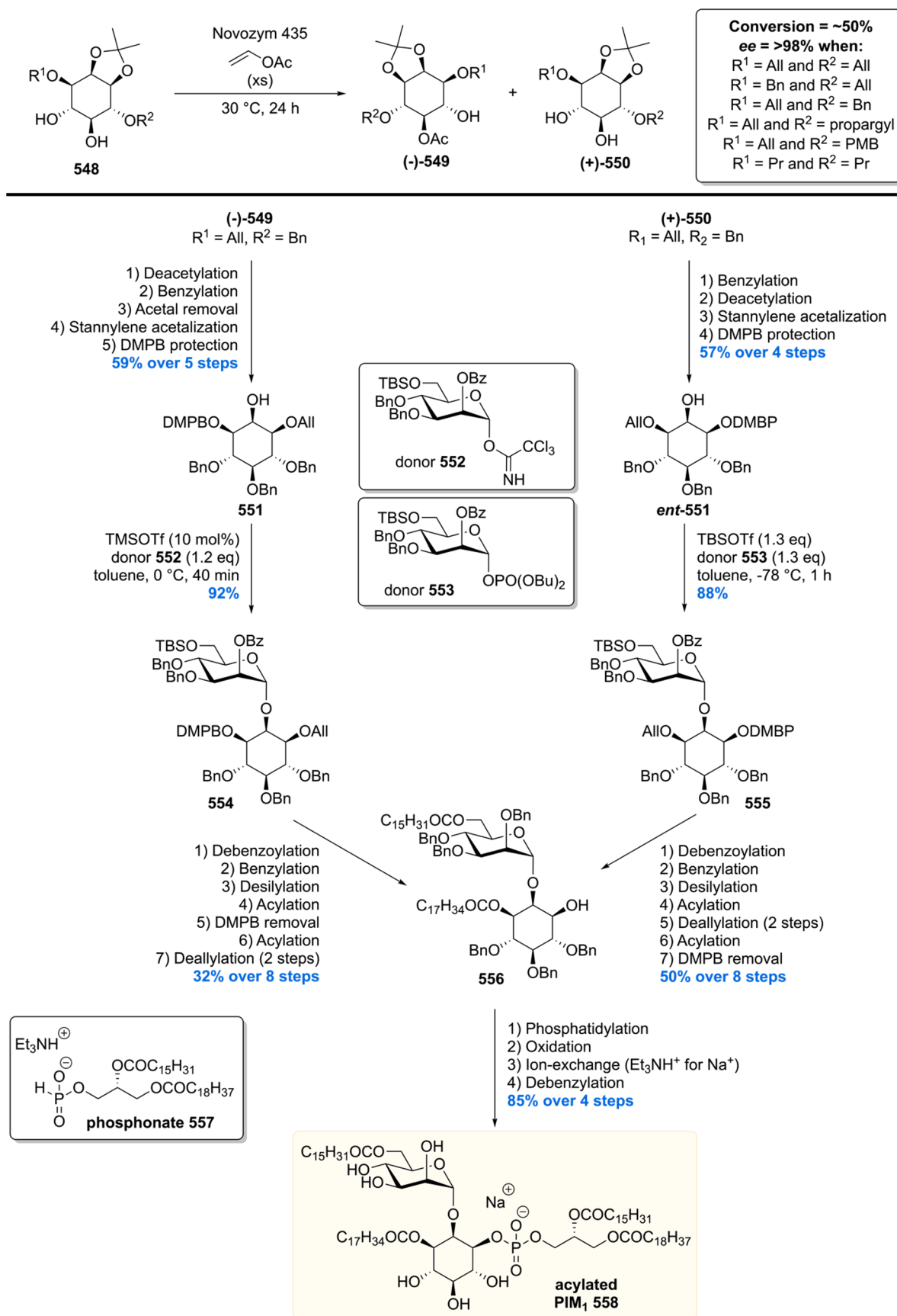
Glycoside donor 428 was reacted with glycoside acceptor 467 promoted by TMSOTf, followed by the cleavage of the acetate to furnish 468 in 80% over two steps. A second iteration of the glycosidation event using glycoside donor 428 furnished 469. This was followed by glycosylation, deallylation, and trichloroacetimidate formation to give tetramannoside 471, a key-component in the construction of PIM₆.

With all the building blocks in hand, the assembly of the components was performed by first constructing PIM₂ starting from enantiopure *myo*-inositol derivative 472 (Scheme 61).³¹⁸ A three-step sequence performed on 472 gave 473, which was glycosidated with trichloroacetimidate 470 and subsequently desilylated to furnish diglycoside 474. The free hydroxyl group of 474 was esterified with levulinic acid, and the naphthyl group was removed by treatment with DDQ yielding 475 in 75% over the two steps. Mannosylation of pseudodisaccharide 475 with 470 stereoselectively furnished 476. A protection/deprotection sequence, including palmitoylation, was executed with consecutive phosphorylation employing *H*-phosphonate 464 to obtain fully protected PIM₂. Deprotection, however, proved less than trivial since employing standard debenzoylation conditions with

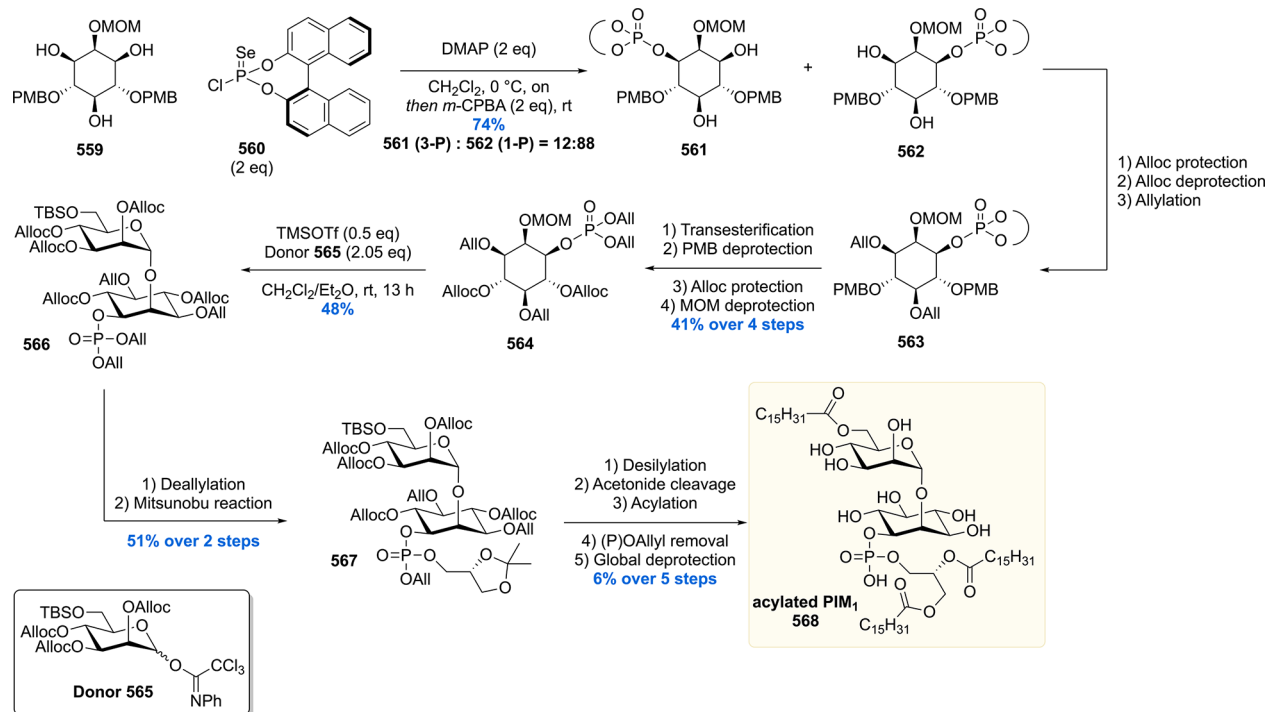
Pd(OH)₂/C in CHCl₃/MeOH/H₂O gave unexpected partial cleavage of the lipids from the carbohydrate backbone. Careful screening of the reaction conditions led to the debenzoylation employing Pd/C in EtOAc/THF/PrOH/H₂O, yielding AcPIM₂ 478 in 82%.

The syntheses outlined above provided the authors with tetrasaccharide 471 (Scheme 60) and trisaccharide 479 (obtained by delevulinoylation of 476, Scheme 61) needed for the construction of AcPIM₆ (Scheme 62). Thus, the union of saccharides 471 and 479 by treatment with catalytic TMSOTf gave 480 in 91% yield. A protection/deprotection strategy was employed comprising a palmitoylation to furnish heptasaccharide 481. The final deallylation, however, as in the PIM₂ synthesis (not discussed) using PdCl₂ as the catalyst, proved to be problematic. This deallylation reaction provided 481 in only 40% yield with an equal amount of Wacker oxidation byproduct (30% in the AcPIM₂ synthesis). The solution was found in the use of a cationic CpRu^{II} complex with quinaldic acid in MeOH³¹⁹ which cleanly afforded heptasaccharide 481 in 72% yield, albeit that a stoichiometric amount of catalyst was required. Phosphorylation and full debenzoylation of 481 as performed in the PIM₂ synthesis smoothly provide acetylated PIM₆ 482 in 62% over the two steps.

The second group to report on the synthesis of a tuberculostearic-based PIM₂ (and not shown PIM₁) was the Larsen laboratory.³²⁰ Their synthesis of the tuberculostearic acid

Scheme 74. Larsen's Enantioconvergent Synthesis of Triacylated PIM₁

Scheme 75. First Synthesis of AcPIM1 Reported by Fujimoto and Co-workers



322 was straightforwardly achieved in eight steps from commercially available (*S*)-citronellol (Scheme 63). The phospholipid 484 was accessed in four steps starting from (*R*)-benzylglycidol obtained by a catalytic kinetic resolution as described in Scheme 40.

The construction of the trisaccharide moiety was cleverly achieved by a double glycosidation of unsymmetrical *myo*-inositol building block 485 (Scheme 64) which was obtained via a Ferrier rearrangement of a glucose derivative.³¹⁸ The double glycosidation smoothly provided α,α -pseudotrisaccharide 486 with minor formation of the α,β -isomer (10%) when performed in ether as the solvent. Routine protecting group manipulations gave alcohol 434 in 43% over three steps. Treatment of 405 with phosphoramidite 484 in the presence of 1*H*-imidazole followed by *in situ* oxidation gave, after hydrogenolysis, the desired PIM₂ 487.

It should be noted that the synthesized PIM₂ has the TBSA lipid on the *sn*-2 position of the glycerol moiety, whereas in the previous described synthesis by Seeberger the TBSA lipid was on the *sn*-1 position. The reason was that both acylation patterns were reported to be present in the PIMs. In 2001 Gilleron et al. reported that PIM₂ comes in a 68:32 mixture of acylation patterns with the major species having the TBSA moiety on the *sn*-2 position (*synthesized by Larsen and co-workers*) and the minor species bearing two palmitoyl groups.³²¹ In 2003, however, it was reported by the same group that AcPIM₆ has the TBSA lipid on the *sn*-1 position³²² (*the PIM₂ isomer synthesized by Seeberger and co-workers*), thereby creating some structural ambiguity. Unfortunately for the Larsen lab this ambiguity was solved during the course of their synthetic efforts, as Gilleron and co-workers revised their previous structural characterization of the PIMs, concluding the TBSA lipid is located at the *sn*-1 position.²⁷⁶ Larsen and co-workers thus, unintentionally, synthesized an unnatural isomer.

Nevertheless, not putting their synthesized materials to waste, the natural PIM₁, unnatural PIM₂ (with TBSA on the *sn*-2

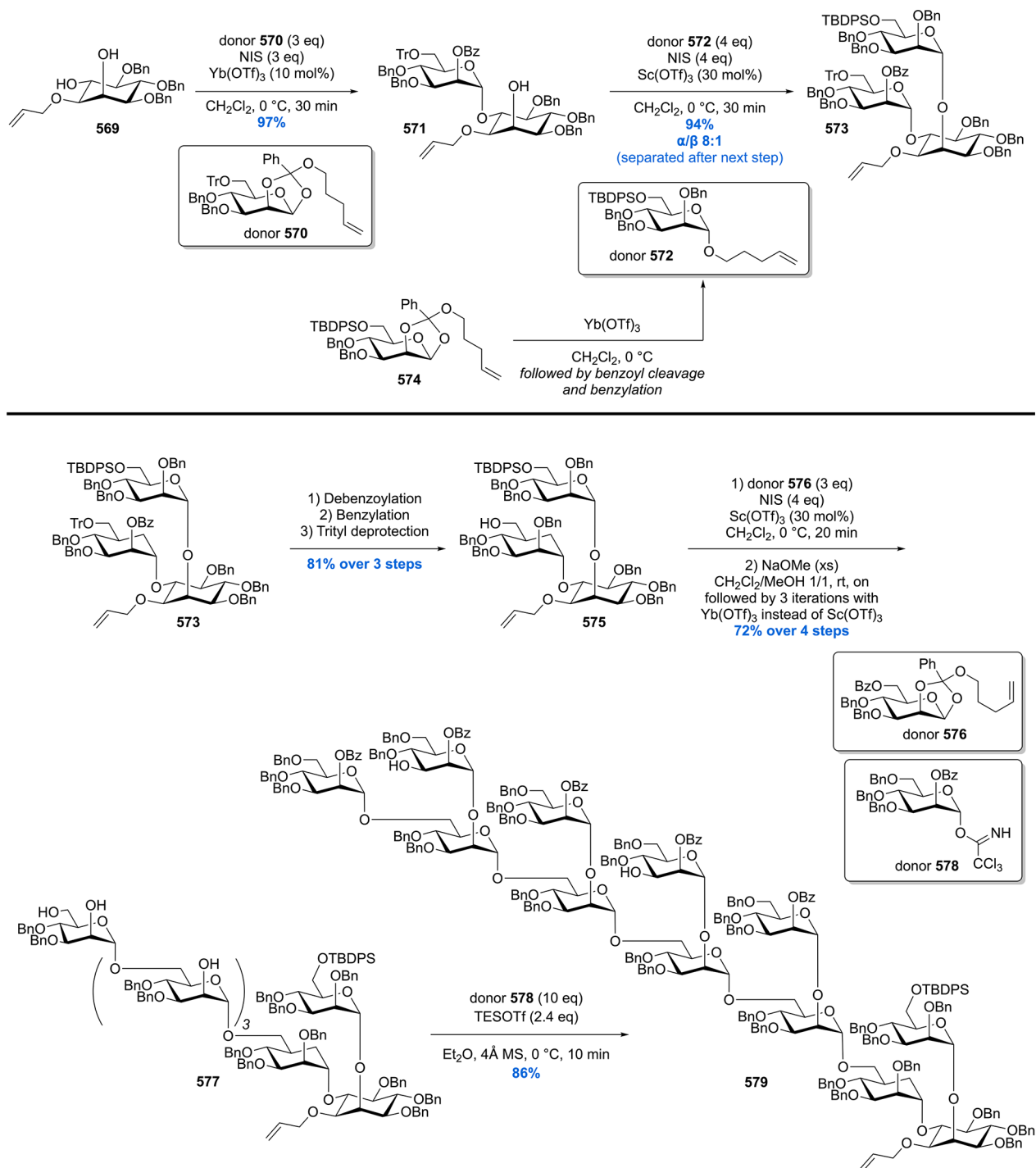
positions), and natural PIM₂ (containing two palmityl fatty acids) were subjected to a biological evolution. Due to their immunomodulatory properties, it was studied whether these PIMs modulate the release of the pro-inflammatory Th1 cytokine interleukin-12 (IL-12) by treatment of dendritic cells (DCs) from mice. Interestingly, in this *in vitro* experiment, the PIM₂ possessing two palmitoyl residues showed more IL-12 release than PIM₁ and the tuberculostearyl containing PIM₂ 487. This result shows that stimulation of the dendritic cell is very sensitive to minor structural changes in the fatty acid residue on the *sn*-2 position.

Merely two years after their first synthesis of PIM₂ and PIM₆, the Seeberger group communicated the synthesis of the complete catalogue of PIM analogues (PIM₁ to PIM₆).³²³ Importantly, in this synthesis the phosphate group was equipped with a thiol linker which allows immobilization to, for example, carrier proteins, beads, quantum dots, microarrays, or surface plasmon resonance (SPR) surfaces. In this way, the Seeberger group performed biochemical analysis of the complete PIM catalogue, something missing in previous synthetic studies.

In their first-generation PIM synthesis, the Seeberger laboratory used mannosyl trichloroacetimidates as glycosyl donors. This synthesis relied on the use of phosphate mannosyl donors 488 and 490 which were obtained from mannose (Scheme 65). Mannosides 490 and 467 were constructed via tricyclic orthoester 489, efficiently obtained in 70% overall yield, in six steps from mannose, notably with only one purification step. Phosphate 488 was obtained in six steps via orthoester intermediate 465.

The *myo*-inositol building block 473 was prepared from methyl glucopyranoside 491. The pyranoside functionality 492 was converted into the *myo*-inositol moiety via a Ferrier carbocyclization giving 472. Various protecting/deprotection reactions eventually furnished compound 473. Glycosidation of *myo*-inositol 473 with phosphate 490 provided the desired α -glycosidic bond in high yield. Protecting group manipulations

Scheme 76. Fraser-Reid's Total Synthesis of the Lipomannan Component



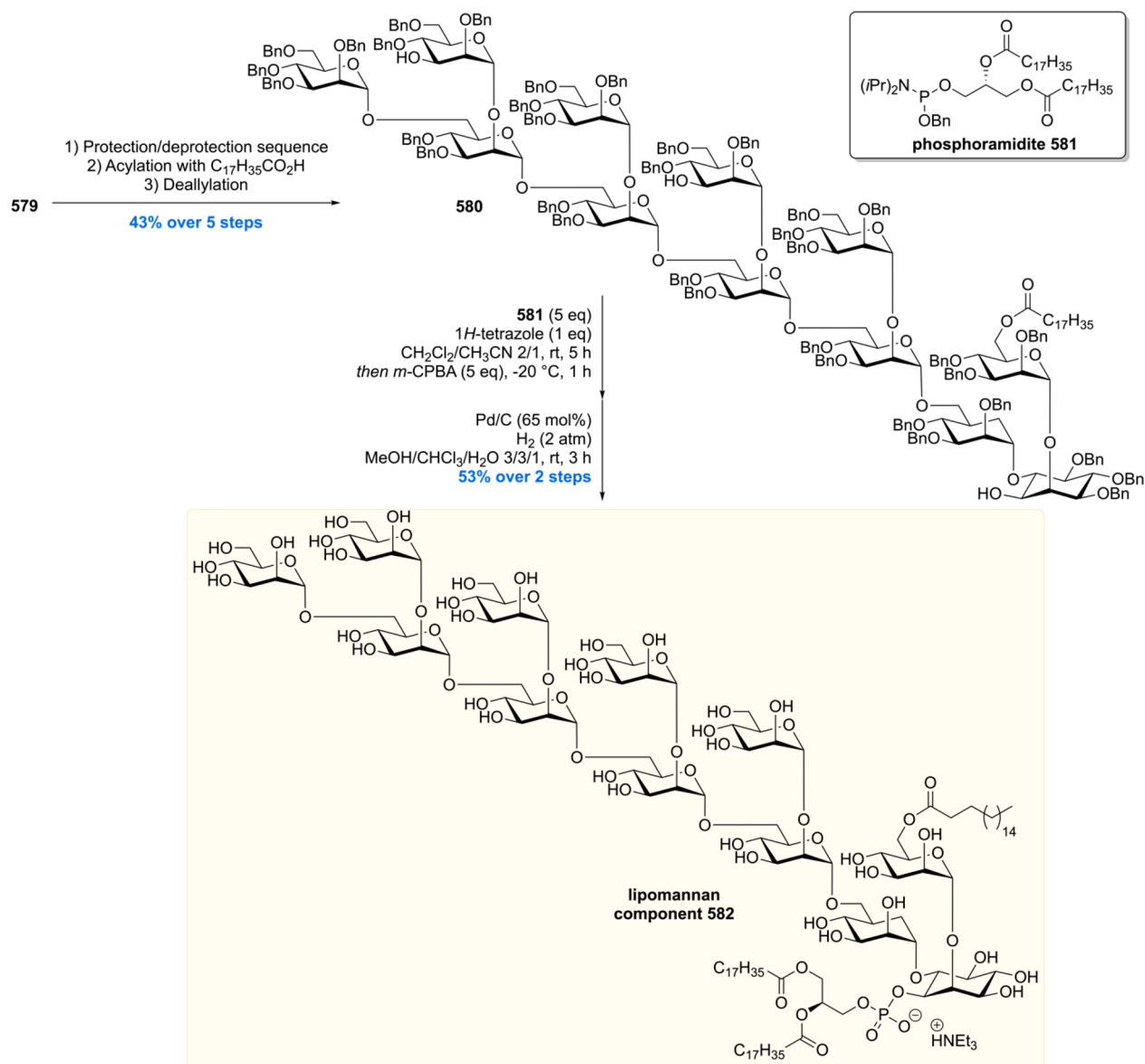
gave pseudodisaccharide 475 which was glycosidated, again, using mannosyl phosphate 488. This glycosidation was found to be nontrivial since reaction under the standard conditions (TMSOTf as promotor at $-40\text{ }^{\circ}\text{C}$) led to decomposition of 488 to form the corresponding anomeric alcohol. Changing the promotor TMSOTf to the milder activator TBSOTf had a significant effect, providing the glycoside in 27% yield. Changing the temperature to $0\text{ }^{\circ}\text{C}$ led to pseudotrisaccharide 493 in 85% yield after cleavage of the Lev protecting group. 493 served as the key component for the construction of PIM₂ to PIM₆.

The building blocks 467 and 488 were used to construct the three oligomannosylating agents 495, 497, and 471 for the

synthesis of PIM₄ to PIM₆ (Scheme 66). Glycosidation of 467 with 488 gave disaccharide 494. Deacylation of 494 followed by another glycosidation with 488 then gave trisaccharide 496. Repetition of this sequence on 496 also provided tetrasaccharide 498. All the oligosaccharides were deallylated and converted to the anomeric trichloroacetimidates to efficiently provide 495, 497, and 471.

The final stages of the PIM₂ to PIM₆ synthesis consisted of the unification of *myo*-inositol 499 with glycosyl donors 488, 495, 497, and 471 (Scheme 67). To construct PIM₁, phosphate 488 was reacted with *myo*-inositol 400 (synthesized from 472) to furnish 500 in 69% yield after deacetylation and benzoylation.

Scheme 77. Completion of the Total Synthesis of the Lipomannan Component by Fraser-Reid



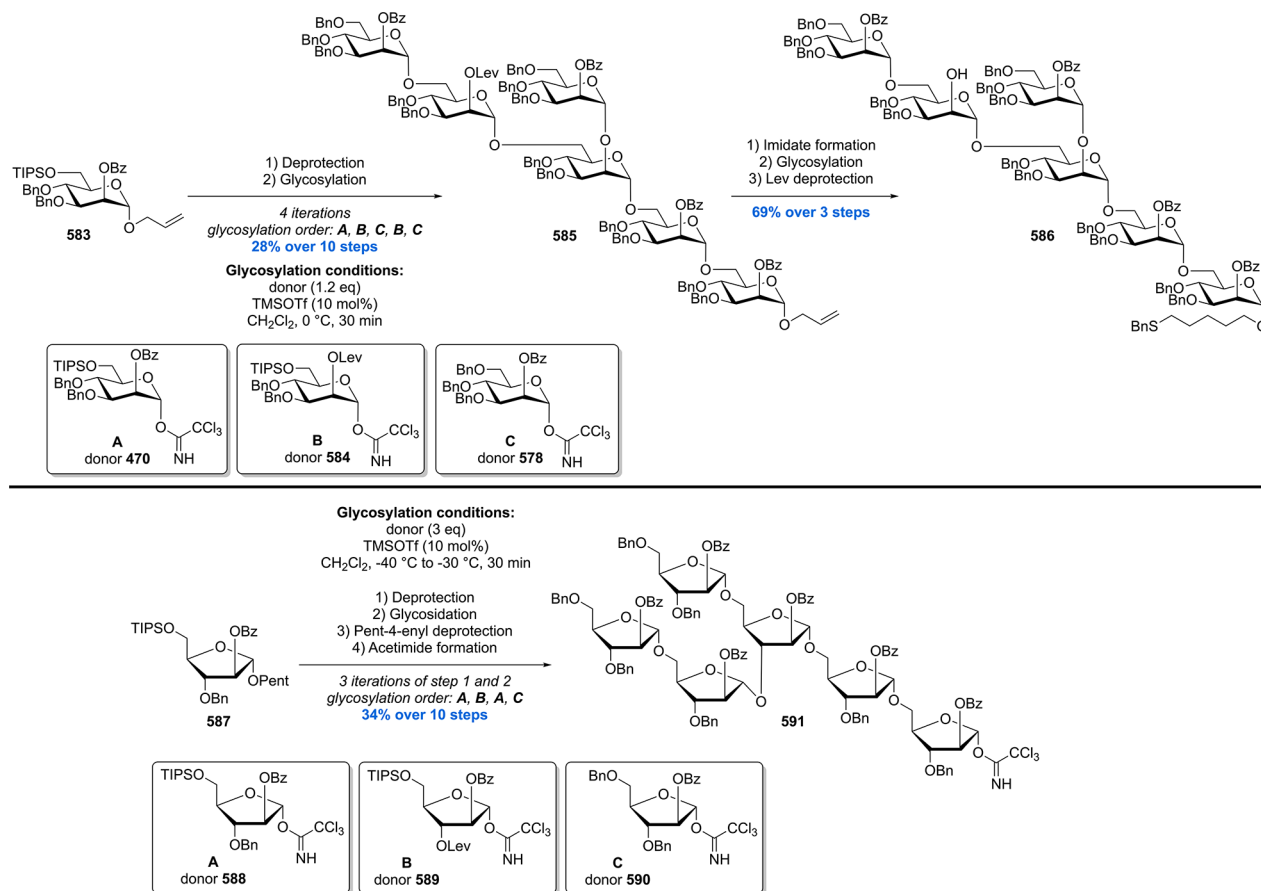
Pseudotrisaccharide **493** was glycosidated with donors **488**, **495**, **497**, and **471** followed by debenzoylation and benzylation to give the protected PIM₂ to PIM₆ backbones **501**–**505**. The protected PIMs **500**–**505** were deallylated using an [Ir(COD)-(PCH₃Ph₂)₂]₂PF₆-catalyzed isomerization to the corresponding enol ether which was subsequently hydrolyzed by treatment with *p*-TsoH. Installation of the phosphate moiety, with the thiohexyl linker, was followed by complete debenzoylation through Birch reduction to furnish the complete PIM catalogue. The PIMs were formed as a mixture of free thiols and disulfide dimers. Before immobilization of the PIMs on a maleimide activated glass slide, they were treated with tris(carboxyethyl) phosphine hydrochloride to reduce the dimeric product into the monomeric species.

Interestingly, after the synthetic efforts, the catalogue of PIM analogues was biologically evaluated for its activity in binding to DC-SIGN. This protein functions as a receptor on dendritic cells and is able to recognize evolutionary conserved pathogenic structures on the surface of either viruses or bacteria. Binding of the pathogen to the DC-SIGN protein sets into motion a

mechanism in which the antigens are internalized, processed, and presented, together with costimulatory molecules, on the surface of the dendritic cells. After binding of the DC-SIGN protein with the immobilized PIM molecules and incubation with fluorescein-conjugated anti-DC-SIGN antibody, the fluorescence intensity was monitored. It was found that the greatest binding was observed for PIM₅ and PIM₆, underlining the importance of the α -1,2-mannose motif in the PIMs and ManLAM structures. Furthermore, the adjuvant activity of the PIMs was also assessed, and it was shown that the PIMs act as immune stimulators during *in vivo* immunization experiments when coupled to the model antigen keyhole limpet hemocyanin (KHL). PIMs are thus potential candidates as adjuvants for vaccine development.

Three other recent synthetic endeavors into the synthesis of PIM₂ were reported by Hung and Lear in 2009 and 2010. Hung's synthesis was based on the deracemization of benzylated *meso-myo*-inositol 1,3,5-orthoformate **507** by reaction with D-mannose-derived donor **420** (Scheme 68).³²⁴ With four diastereomeric products possible, a series of experiments had

Scheme 78. Seeberger's Synthesis of Mannan Hexasaccharide and Hexa-Arabinose Building Blocks



to be conducted to find optimal conditions for the reaction. It was found that BF₃·OEt₂ was the best promoter when carrying out the reaction at an initial temperature of -78 °C and gradually warming to -20 °C. The reaction exclusively produced the α -anomers **508** and **509** in 64% and 12% yield, respectively, which were separable by flash chromatography. Debenzylation set the stage for a mannosylation of **510** with donor **420** to furnish pseudotrisaccharide **511** regioselectively as a single diastereomer in 87% yield. Cleavage of the orthoacetate in **511** produced a tetraol which had to be regioselectively benzylated at C3–5 to give alcohol **434**. Williamson ether synthesis with NaH and BnBr gave a complicated mixture of isomers, an outcome which was circumvented by first a complete silylation giving **512** and subsequent regioselective desilylation/benzylation by the aid of benzaldehyde, TMSOTf, and Et₃SiH. With alcohol **434** in hand, a phosphorylation with *H*-phosphonate **513** and removal of the benzyl protecting groups smoothly afforded PIM₂ **414**.

Just one year after their synthesis of PIM₂, the Hung laboratory communicated the synthesis of triacylated PIM₂ (Scheme 69).³²⁵ Here, their previously employed desymmetrization approach was evolved to a stereoselective one-pot double glycosylation of triol **514** with D-mannosyl trichloroacetimidate **420**. A mixture of three separable products was formed, and the desired pseudotrisaccharide **511** was isolated in 64% yield. With **511** in hand, the orthoester was hydrolyzed followed by per-*O*-trimethylsilylation providing **512** in excellent yield. Regioselective benzyl protection of two out of four available hydroxyl groups was achieved by utilizing their in-house developed two-step reductive benzylation giving diol **517** in 72% yield.

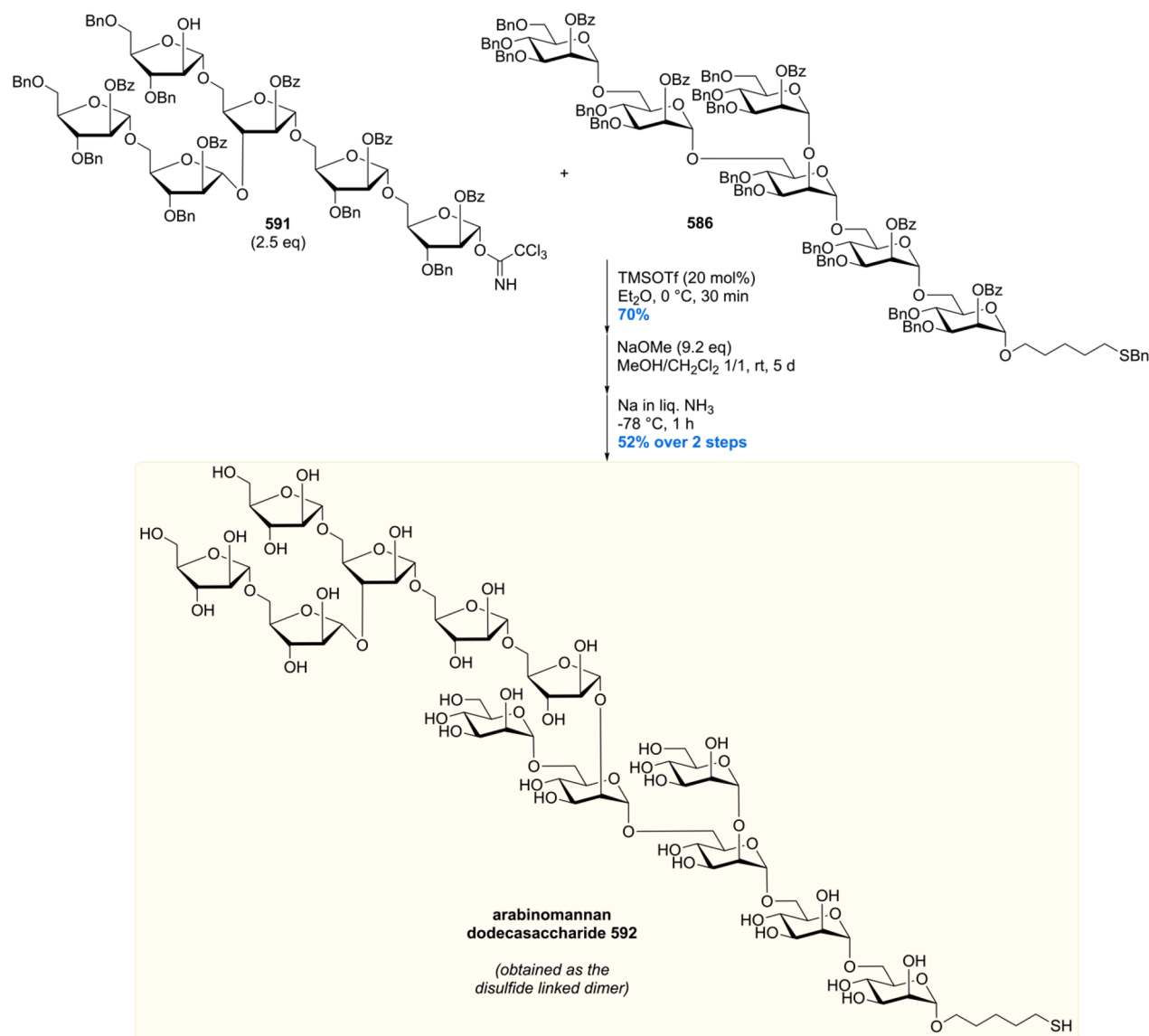
Regioselective Steglich esterification of **517** with stearic acid gave rise to **518** in 86% yield. The remaining free hydroxyl was coupled to *H*-phosphonate **513** mediated by pivaloyl chloride followed by ion exchange to provide, after benzyl hydrolysis, the sodium salt of the triacylated PIM₂ **519** in just seven steps.

In 2016, the Hung laboratory reported a follow-up study constructing Ac₂PIM₆, which was evaluated, together with PIM₁, PIM₂, and PIM₆ isolated from *Mtb* (H37Rv strain), for its immunomodulatory activity.³²⁶ As in their PIM₂ synthesis, the key building block was *meso*-*myo*-inositol 1,3,5-orthoformate **520** (Scheme 70). Glycosidation, as previously mentioned, provided pseudotrisaccharide **522** which, after a four-step sequence, led to diol **523**. The primary alcohol functionality in **523** was selectively glycosylated by reaction with tetrasaccharide **524** in 52% yield. The naphthyl protecting group of **525** was removed, and acylation was performed with stearic acid to install the linear fatty acid chain. Phosphonate **526** was then coupled, to give after a global deprotection triacylated PIM₆ **527**.

Assessment of the *in vivo* immunomodulatory activity was performed by coadministration of the PIMs (synthetic PIM₆ **527** and isolated PIM₁, PIM₂, and PIM₆) with ovalbumin or tetanus toxoid. The synthetic PIM was shown to exhibit comparable adjuvant activity, as evident from the induced production of interleukin-4 and interferon- γ , to that of the PIMs from the natural source. The acylated PIMs are thus considered to be candidate adjuvants for vaccine design.

Lear and co-workers reported a very efficient synthesis of PIM₂ based on a resolution strategy using D-mannoside **529** as a

Scheme 79. Seeberger's Completion of the Arabinomannan Dodecasaccharide



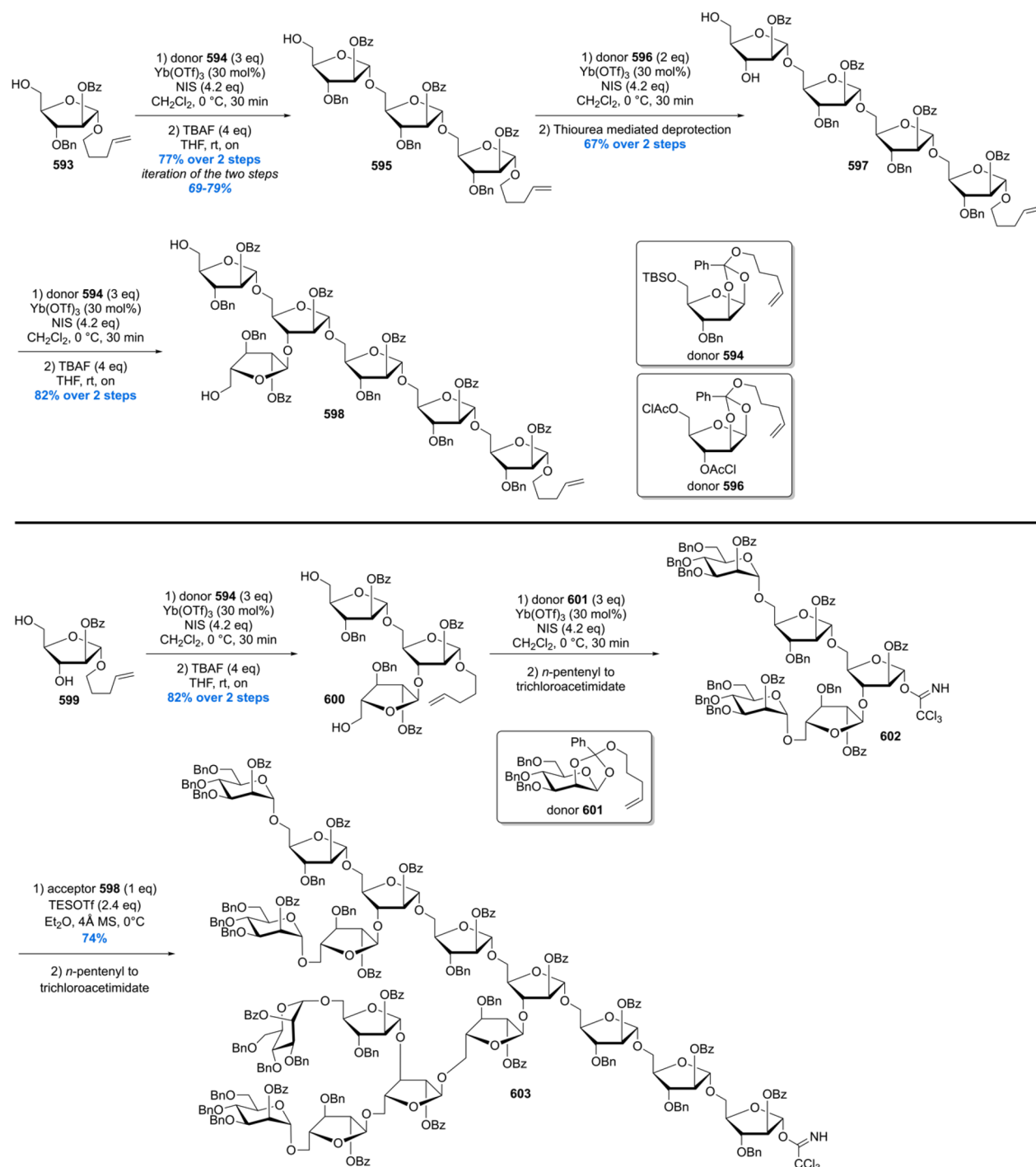
“permanent resolving agent” (Scheme 71).³²⁷ Mannosylation of racemic **528** with **529** under standard α -selective conditions, and subsequent deallylation, gave rise to a separable mixture of the diastereomers **530** and **531** formed in a 1:1 mixture. This direct resolution of C2-coupled *myo*-inositides **530** and **531** was speculated to be viable due to D-mannosyl donor **529** bearing the bulky TBDPS protecting group at C6. Further mannosylation of **530** gave pseudotrisaccharide **532** in 96% yield which was smoothly converted into PIM₂ **487** using established chemistry from previous synthetic endeavors of PIM₂.

Another group who set out to synthesize several PIMs was the Tanaka laboratory. Their first PIM synthesis was that of AcPIM₂ using 2-(azidomethyl)benzoyl (AZMB) mannosyl donors for formation of the glycosidic bonds (Scheme 72).³²⁸ This particular protecting group for the C2-position was chosen because glycosylation with benzoyl esters is known to proceed with complete α -selectivity due to anchimeric assistance. The problem with conventional benzoyl esters, however, is that selective removal without affecting the fatty acid-based acyl motifs is nearly impossible. In order to avoid this problem, generally, protecting group shuffling is performed after the

glycosylation. To circumvent such an undesired and nonideal sequence, the AZMB group was used. This group can be removed under hydrogenolytic conditions, which converts the azide into the corresponding amine which in turn will cyclize to form the lactam and liberate the sugar. Two AZMB C2-protected mannosyl donors **534** and **535** were used to mannosylate inositol **533**. The reaction was performed in a one-pot two-step procedure to afford the mannosylated inositol **536** in 88% yield with complete α -selectivity for both anomeric centers. The chloroacetyl group was removed using thiourea, and the now free C6-OH was acylated with stearic acid. After oxidative removal of the naphthyl unit, the phosphate group was installed, and final hydrogenolysis provided acylated PIM₂ **538**.

Importantly, the obtained synthetic material was used to confirm the binding of AcPIM₂ to a C-type lectin (like Mincle) named DCAR, which stands for dendritic cell immunostimulating receptor. Upon binding of a ligand, DCAR can trigger monocyte-derived inflammatory cell accumulation at the site of infection and promote a protective Th1 response. It was the Yamasaki laboratory which discovered that DCAR binds mycobacterial cell wall constituents, specifically AcPIM₂ and

Scheme 80. Fraser-Reid's Synthesis of the Branched Arabinan Unit Part 1

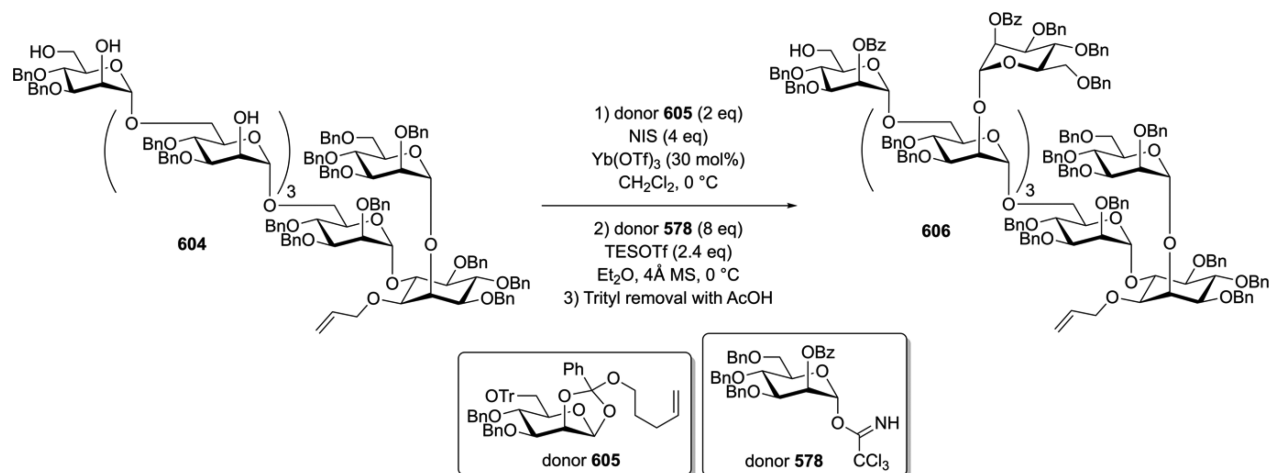


Ac₂PIM₂, and initiates the orchestration of host protective immunity.^{329,330} The PIMs used in the DCAR binding assay were isolated from *M. bovis* BCG, and it was recognized by the Yamasaki group that minute, unobservable, impurities might be responsible for the obtained result. To exclude such a false positive result in which potential impurities bind to DCAR, the synthetic AcPIM₂ from the Tanaka laboratory was used, which confirmed that AcPIM₂ is an active ligand for DCAR.

A year later, in 2015, the Tanaka group communicated yet another synthesis of several PIMs (Scheme 73). This time AcPIM₃ **546** and AcPIM₄ **547** were constructed via the intermediacy of a protected form of AcPIM₂ **544** synthesized

using a modified procedure.³³¹ The synthesis commenced with *o*-nitrobenzyl protected inositol **539** which was bis-mannosylated in a one-pot procedure to provide **542** in 80% yield. After introduction of the stearyl group, in 72% over two steps, the acetal in **543** was site-selectively opened to liberate the C6-OH. This hydroxyl function was silylated, followed by photodeprotection of the *o*-nitrobenzyl protecting group, which then set the stage for the phosphatidylation. The phosphorylation of the inositol in this stage of the synthesis is the highlight of the synthesis. In other syntheses of the PIMs, the phosphatidyl glycerol moiety was introduced in the final stage of the synthesis, right before the global deprotection. Tanaka

Scheme 81. Fraser-Reid's Synthesis of the Dodecasaccharide Acceptor



and co-workers introduced the phosphatidyl glycerol to then desilylate and subject this protected form of AcPIM₂ **544** to mannosylation with mannosyl donor **540** and **545** to produce, after hydrogenolysis, acylated PIM₃ **546** and acylated PIM₄ **547**.

In 2014 the Larsen group communicated the first synthesis of the acylated *myo*-inositol PIM₁ via an enantioconvergent route from *myo*-inositols (–)-**549** and (+)-**550** (Scheme 74).³³² The enantiopure *myo*-inositols were obtained by a desymmetrization employing the enzyme *Candida antarctica* lipase B (Novozym 435) as previously reported by Simas and co-workers.^{333,334} A wide variety of racemic *myo*-inositols were synthesized and subjected to the enzymatic desymmetrization reaction. In many cases the reaction was performed with near full conversion (~50%) leading to enantioselectivities, for both enantiomers, > 98% *ee*.

For the synthesis of Ac₃PIM₁, the authors chose to work further with *myo*-inositols (–)-**549** and (+)-**550**. It was realized that both enantiomers could be converted into the target inositol, thereby making optimal use of the racemic *myo*-inositol starting material. Thus, after acetate cleavage from (–)-**549**, both enantiomers were converted via standard protection and deprotection sequences into *myo*-inositols **551** and *ent*-**551**. Glycosidation with donors **552** or **553** then gave the PIM₁ core structures **554** and **555** which, via slightly different protecting group manipulations, afforded common pseudodisaccharide intermediate **556**. Phosphatidylation using *H*-phosphonate **557**, followed by oxidation, ion-exchange, and deprotection concluded the enantioconvergent total synthesis of acylated PIM₁ **558**.

The latest PIM synthesis was reported in 2020 by Fujimoto and co-workers (Scheme 75).³³⁵ They set out to be the first to synthesize AcPIM₁ **568** and employed a regioselective phosphorylation of protected *myo*-inositol **559** with BINOL-derived selenophosphoryl chlorides. Several selenophosphoryl chlorides with alternative BINOL structures were screened, but it was BINOL-derived selenophosphoryl chloride **560** that provided the best regioselectivity (88:12) while giving a satisfactory 74% yield as well. The obtained phosphorylated inositol regioisomers (as well as diastereomers) were then protected with an alloc group to enable separation. The alloc group was then swapped for an allyl group to form **563**. The BINOL moiety was removed by means of a transesterification with allyl alcohol, and three further steps provided inositol **564**. This compound was mannosylated by reaction with mannosyl

donor **565** bearing the *N*-phenyl-2,2,2-trifluoroacetimidate activating group to yield the α -anomer of mannosylated inositol **567** in 48% yield. One allyl group was removed from the phosphate diester which was subsequently esterified under Mitsunobu conditions with isopropylidenglycerol to furnish **568** in 51% over the two steps. The synthesis was finalized with a five-step sequence initiated by TBS and acetonide removal to be able to install the palmityl esters. The remaining phosphate allyl group was removed whereafter a global deprotecting gave rise to acylated PIM₁ **558**.

In collaboration with the Yamasaki laboratory, the synthesized AcPIM₁**568** was tested for its ability to bind to DCAR. Interestingly, AcPIM₁ proved to be a stronger agonist of DCAR compared to the previously known ligand AcPIM₂. This result implies that the AcPIM₁ moiety featured in AcPIM₂ was causing recognition by DCAR. Furthermore, it was shown that AcPIM₁ bound weakly to TLR2 (Toll-like receptor) and CD1d. The study of the immunomodulatory function of AcPIM₁ helps to understand host–pathogen interaction on a molecular level, as well as forming a basis for the design of novel vaccine adjuvants recognized by DCAR.

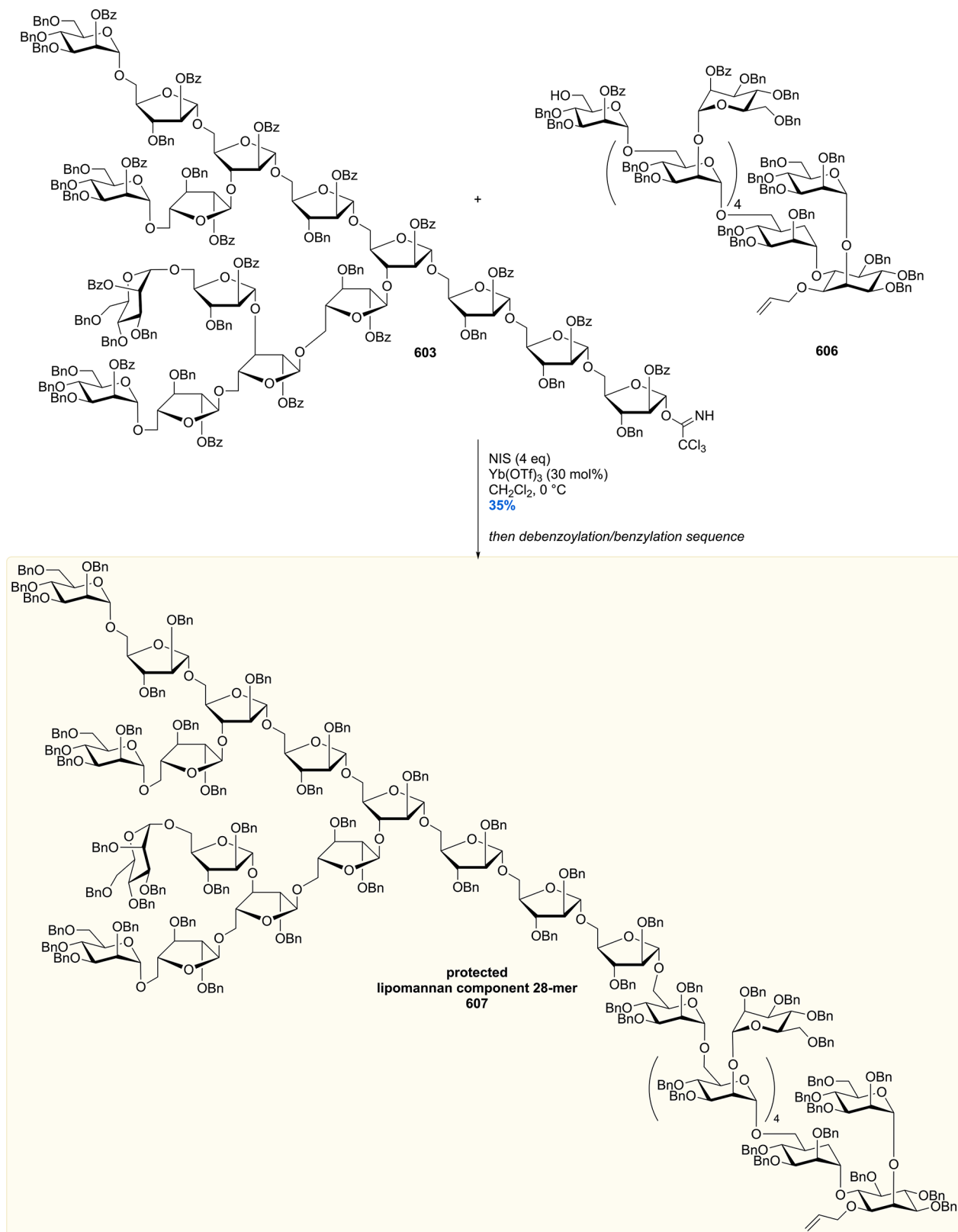
9.2. Higher Order Oligosaccharides

The Fraser-Reid laboratory was the first to report on the synthesis of the complex lipomannan (LM) domain **582**, part of the lipoarabinomannan capsule.³³⁶ Their overall strategy did not rely on skillful deployment of a wide variety of protecting groups but instead was based on Paulsen's concept of donor/acceptor "match".³³⁷ In its basic form this concept tells that a poor yield obtained from a given donor/acceptor pair could be enhanced by switching donors. The issue of regioselectivity was later addressed by Fraser-Reid to further elaborate Paulsen's concept of "match".

In their synthesis of the LM domain **582** (Scheme 76), known diol acceptor **569** was treated, under Lewis-acidic conditions, with *n*-pentenylorthoester donor **570**. Pseudodisaccharide **571** was formed with complete stereo- and regioselectivity in an almost quantitative yield of 97%. **571** was then converted with high selectivity ($\alpha/\beta = 8:1$, 94% yield) into pseudotrisaccharide **573** by reaction with armed³³⁸ glycosyl donor **572**.

A straightforward protection/deprotection sequence followed, providing glycoside acceptor **575**. Treatment of **575** with *n*-pentenyl orthoester **576** in the presence of NIS and Sc(OTf)₃, followed by benzylation, set the stage for further elaboration using an iterative strategy. The change of Sc(OTf)₃

Scheme 82. Completion of the Synthesis of the Protected 28-mer Lipoarabinomannan Component

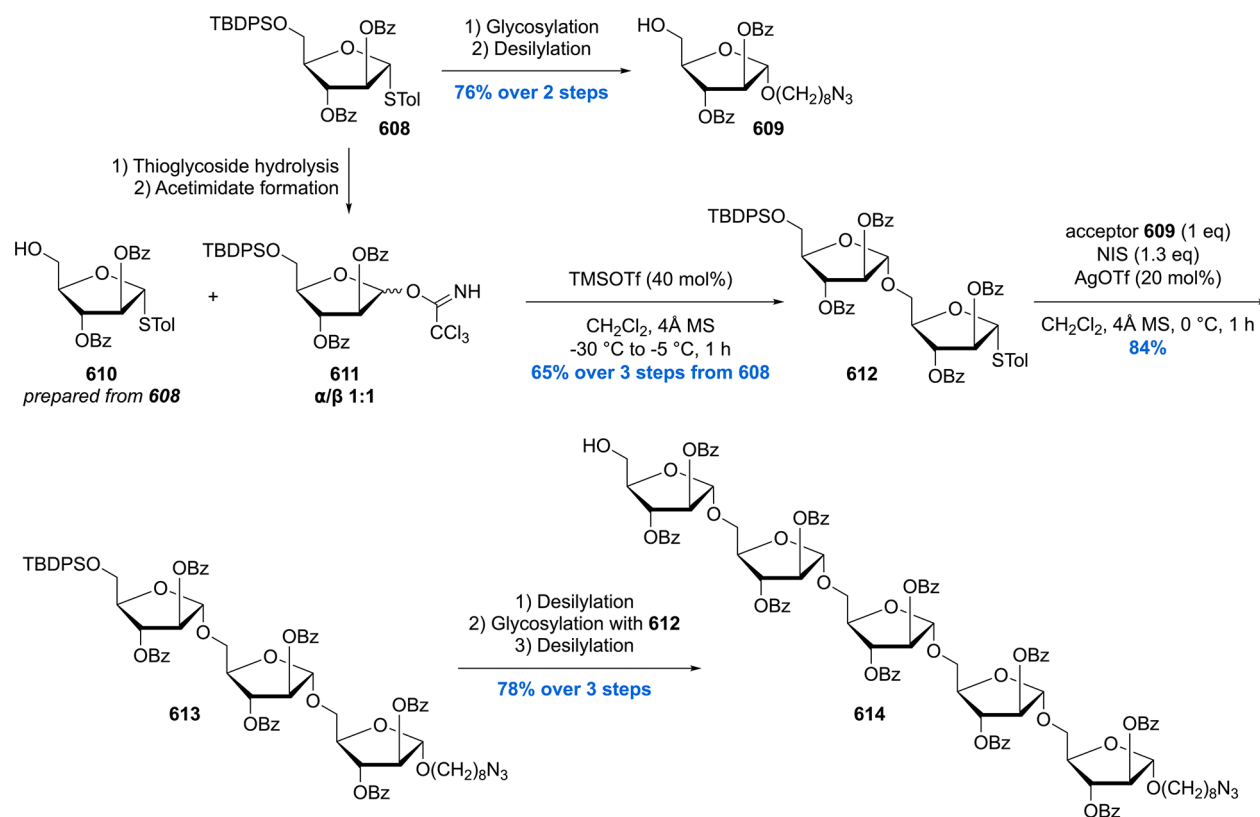


to Yb(OTf)₃ proved to be a necessity, since the generated diol (and later triol and tetraol) had to be regioselectively glycosidated at the primary hydroxyl group. After the iterative glycosidation/debenzoylation sequence, pentol **577** was glyco-

sidated with trichloroacetimidate **578** to give pseudododecasaccharide **579** in 86% yield.

The final stages of the LM domain synthesis were relatively straightforward (Scheme 77). A three-step protection/deprotection sequence on **579** gave after acylation and deallylation

Scheme 83. Lowary's Synthesis of the Pentasaccharide Building Block



alcohol **580**. Introduction of the phosphonate moiety using standard chemistry and subsequent debenzoylation then provided LM component **582**.

The synthesis of a LAM component was reported by the Seeberger laboratory in 2006.³³⁹ Whereas Frasier-Reid and co-workers reported the synthesis of the lipomannan (LM) backbone, Seeberger focused on the arabinomannan (AM) part. Key differences between the two LAM components are that the LM domain consists of a *myo*-inositol anchor with α -D-mannoside linkages, whereas the AM domain not only bears multiple α -D-mannoside linkages but also α -D-arabinofuranosyl linkages. Seeberger's strategy therefore relied on synthesis of the mannoside and arabinose fragments and subsequent coupling of the two oligosaccharides, maximizing synthetic convergence.

The endeavor started with the synthesis of multiple mannoside building blocks (**583**, **470**, **584**, and **578**) using known chemistry. With these building blocks in hand, the mannohexasaccharide **586** was quickly and efficiently assembled by multiple deprotections and subsequent glycosidations using catalytic amounts of TMSOTf (Scheme 78). The glycosidation sequence was initialized with mannoside donor **A** followed by four iterations using **B**, **C**, **B**, and once again **A**, providing mannohexasaccharide **585** in an impressive yield of 28% over 10 steps (!). A six-step protection/deprotection sequence (four steps to form the imidate) then furnished key intermediate **586**, for coupling with the arabinose component. For the purpose of utilizing the molecules in bioassays, the thio-functionality was installed for further coupling to a microarray or a protein carrier.

The arabinose motif was constructed in a similar approach as the mannan hexasaccharide **586**. First several arabinose building blocks (**587**, **588**, **589**, and **590**) were synthesized which were then coupled using an iterative approach (Scheme 78). Thus, four deprotection/glycosidation sequences (order: **A**, **B**, **A**, **C**)

were performed, after which pentenyl deprotection and subsequent acetimidate formation produced hexaarabinose **591**, in 34% over 10 steps (!).

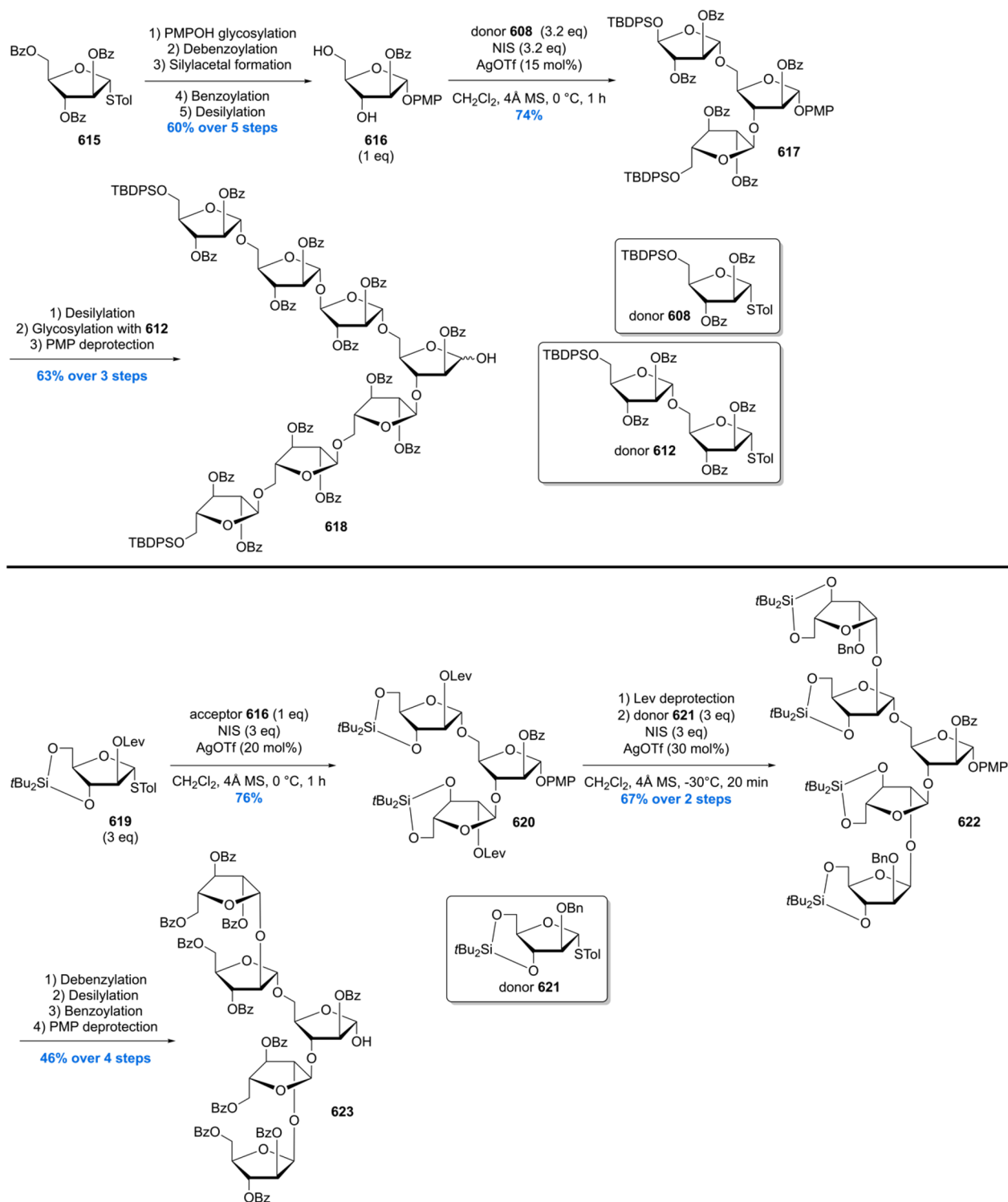
With the two hexasaccharide building blocks **586** and **591** in hand, unification could be achieved through a [6 + 6] glycosidation (Scheme 79). The glycosylation smoothly provided exclusively the α -anomer in 70% yield. Debzoylation was followed by debenzoylation under Birch conditions, affording AM domain **592** as a disulfide linked dimer.

Shortly after the disclosure of their LM domain synthesis, the Frasier-Reid laboratory reported the ambitious synthesis of the complete oligosaccharide core of the mycobacterial LAM domain.³⁴⁰ The synthesis of this 28-mer was regarded as a milestone in glycochemistry since at the time it was the largest hetero-oligosaccharide synthesized in a laboratory.

The synthesis started with the elaboration of the branched arabinan domain **603** which possesses furanoside units, linked α -1,5-linearly, with occasional C3 branches (Scheme 80). As in their synthesis of the complex LM domain **582** (Scheme 77), the strategy relied on the successful use of *n*-pentenyl orthoester chemistry. First *n*-pentenyl furanoside **593** was reacted under standard conditions with glycoside donor **594** followed by a deprotection of the silyl protecting group. Iteration of this sequence led to trisaccharide **595**, which was glycosidated under the same conditions with glycoside donor **596**. Tetrasaccharide **597** was obtained after deprotection of the acetyl chloride group using thiourea. The first branch of the arabinan motif was introduced by subjecting **597** to, once again, glycosylation with donor **594**, to give after desilylation hexasaccharide **598**.

Elaboration of the branches in hexasaccharide **598** came about by the construction of heteropentasaccharide **602** from a glycosidation/deprotection sequence employing donors **594** and **601**. Reaction of hexasaccharide **598** with pentasaccharide

Scheme 84. Lowary's Synthesis of Hepta- and Pentasaccharide Building Blocks



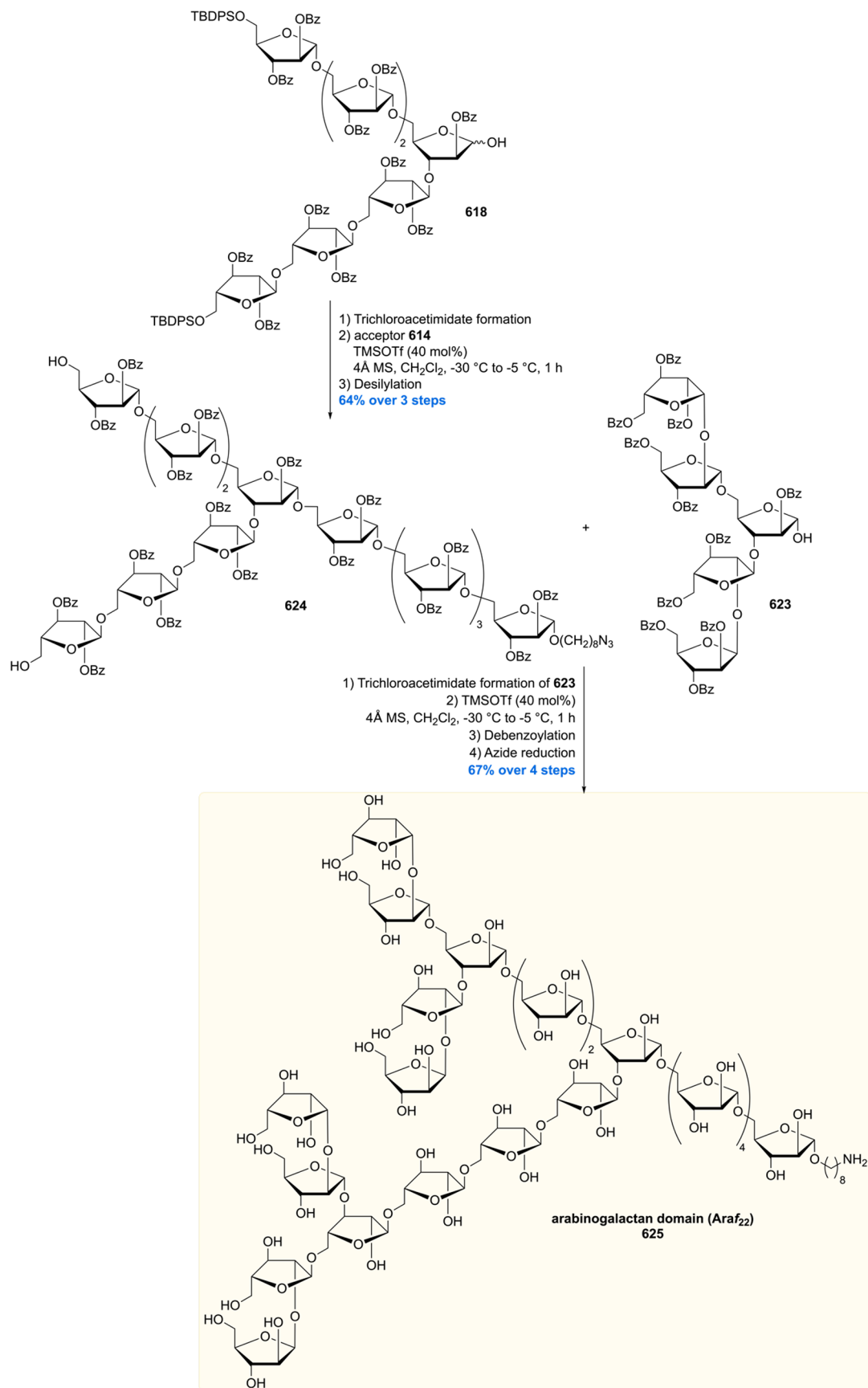
602 smoothly resulted in double glycosidation to furnish, after trichloroacetimidate installation, 16-mer donor **603**.

With the 16-mer arabinan motif **603** constructed, the remaining 12-mer mannan domain **606** was synthesized (Scheme 81). Heptasaccharide **604** (synthesis analogous to that of **577**; see Scheme 76) was first regioselectively glycosidated at C2 using orthoester **605** followed by glycosidation of the remaining free hydroxyl moieties with

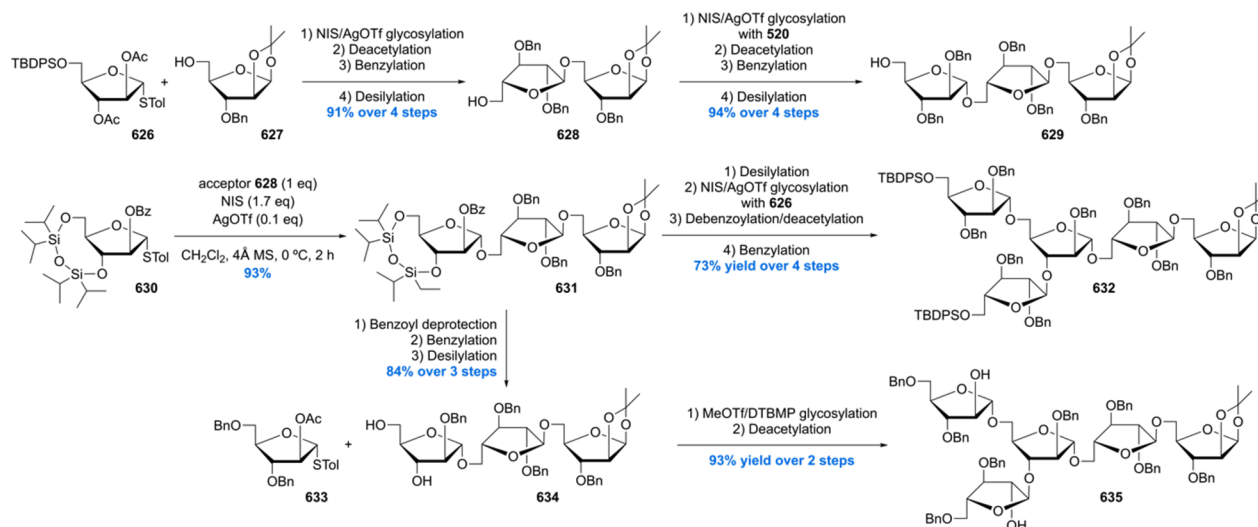
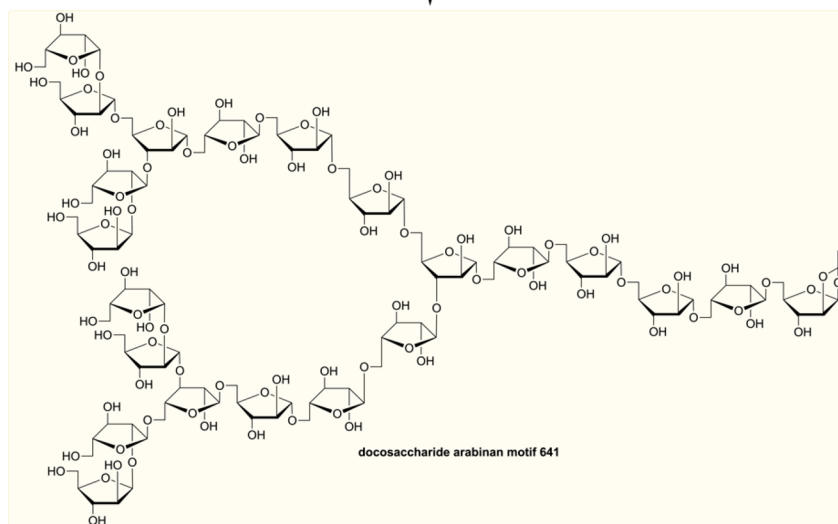
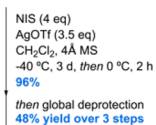
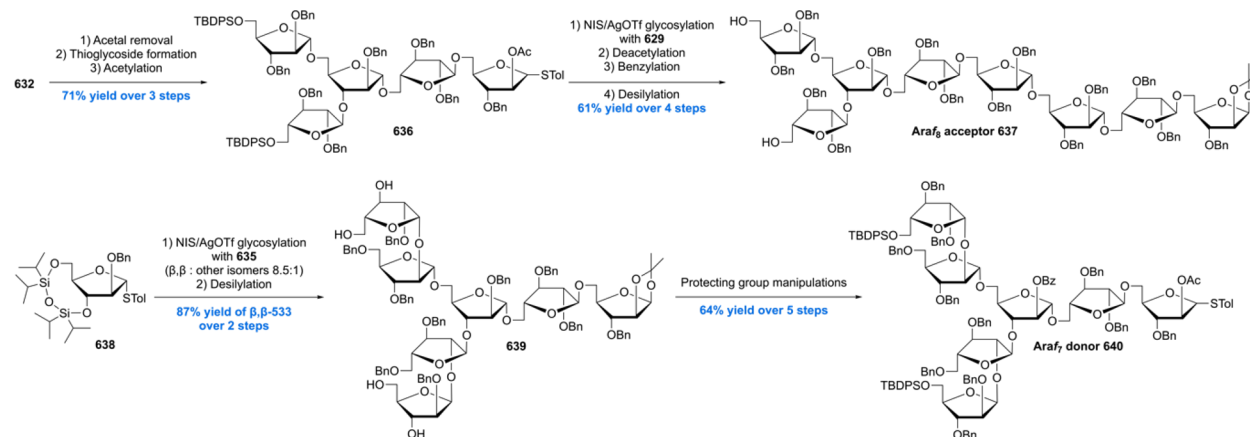
trichloroacetimidate donor **578**. Removal of the trityl protecting group gave rise to dodecasaccharide acceptor **606**.

With the synthesis of arabinan motif **603** and dodecasaccharide **606** realized, unification of both advanced building blocks was carried out in the presence of NIS and Yb(OTf)₃ to give the desired 28-mer in 35% yield (Scheme 82). To validate that the right product was obtained, a debenzoylation/benzoylation sequence was performed giving the desired protected lip-

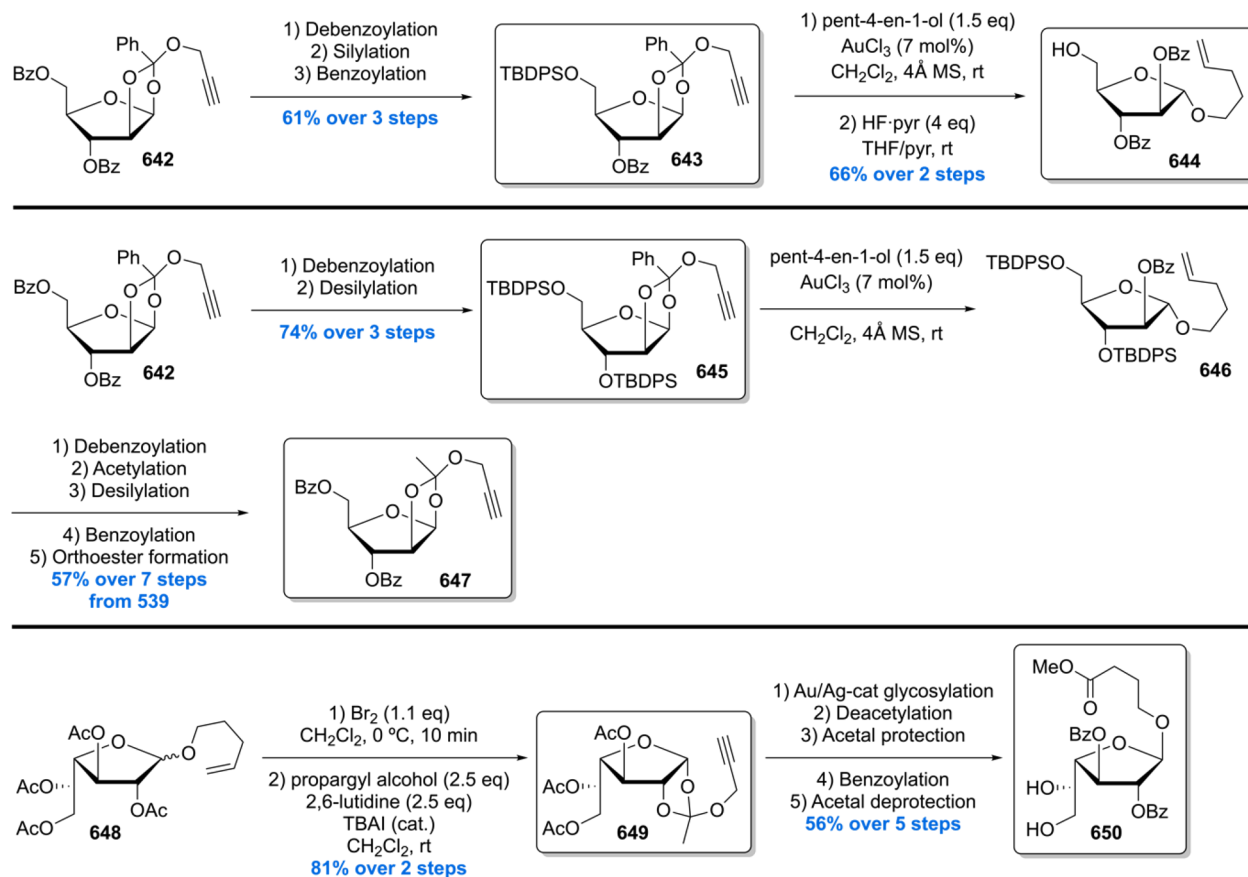
Scheme 85. Completion of the Total Synthesis of the Arabinogalactan 22-mer



Scheme 86. Ito's Synthesis of Tri- and Pentasaccharide Building Blocks

Scheme 87. Synthesis of Araf₇ Donor and Araf₈ Acceptor and Completion of the Docosaccharide Arabinan Motif

Scheme 88. Hotha's Furanoside Monomer Synthesis



oarabinomannan domain **607**, of which the mass-spectroscopic data clearly indicated the right decrease of mass (-224 u).

Another very important contribution to the synthesis of mycobacterial glycolipids, and to the field of glycochemistry in general, was communicated by Lowary and co-workers.³⁴¹ They reported the synthesis of an impressive 22-mer oligosaccharide from the arabinogalactan domain bearing the synthetically challenging 1,2-*cis* linked β -arabinofuranoside motif.

The synthesis of this molecule was tackled using a highly convergent approach, in which three main building blocks were united in a late stage of the synthesis. The first building block to be constructed was pentasaccharide **614** starting from thioglycoside **608** (Scheme 83), prepared from D-arabinose in six steps as previously reported.³⁴² Thioglycoside **608** also served as a precursor for multiple small building blocks such as azide **609**, which was crafted in only two straightforward steps. **608** was converted into trichloroacetimidate **611** which was reacted with thioglycoside **610** under standard conditions to furnish disaccharide **612**. Glycosidation of **612** with **609** smoothly provided trisaccharide **613** in 84% yield. Desilylation of the trisaccharide was followed by a glycosidation with disaccharide **612** followed by again a desilylation, furnishing pentasaccharide **614** in 78% over three steps.

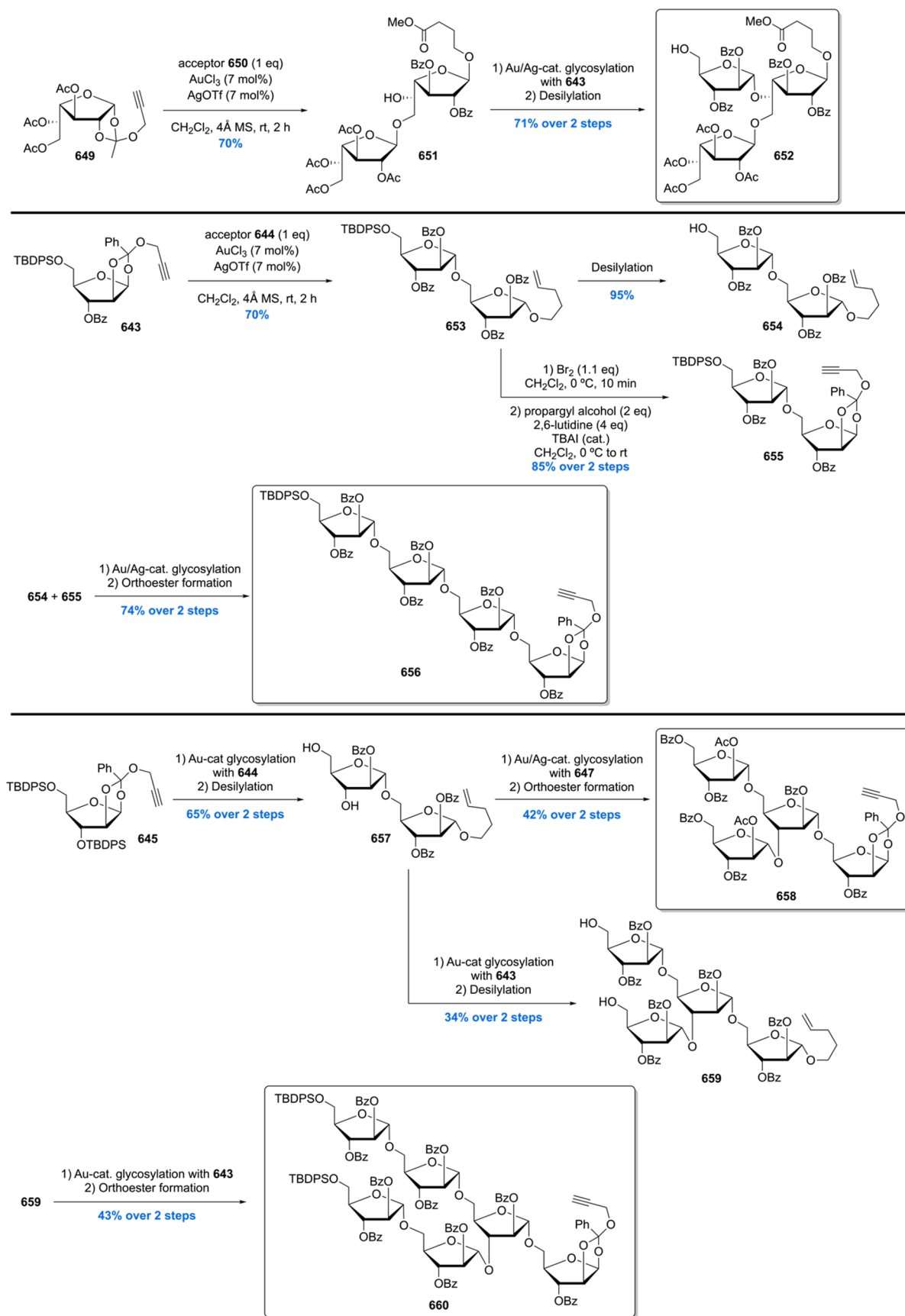
After construction of the first building block, the Lowary group focused on the construction of heptasaccharide **618** (Scheme 84). First, thioglycoside **615** was converted into diol **616** using a five-step protection/deprotection sequence in 60% yield. Diol **616** was then doubly glycosylated with thioglycoside **608**, giving trisaccharide **617** in 74% yield. Desilylation of **617** set the stage for another double glycosylation reaction but this

time with disaccharide **612** (see Scheme 83). Subsequent PMP deprotection then provided building block **618**.

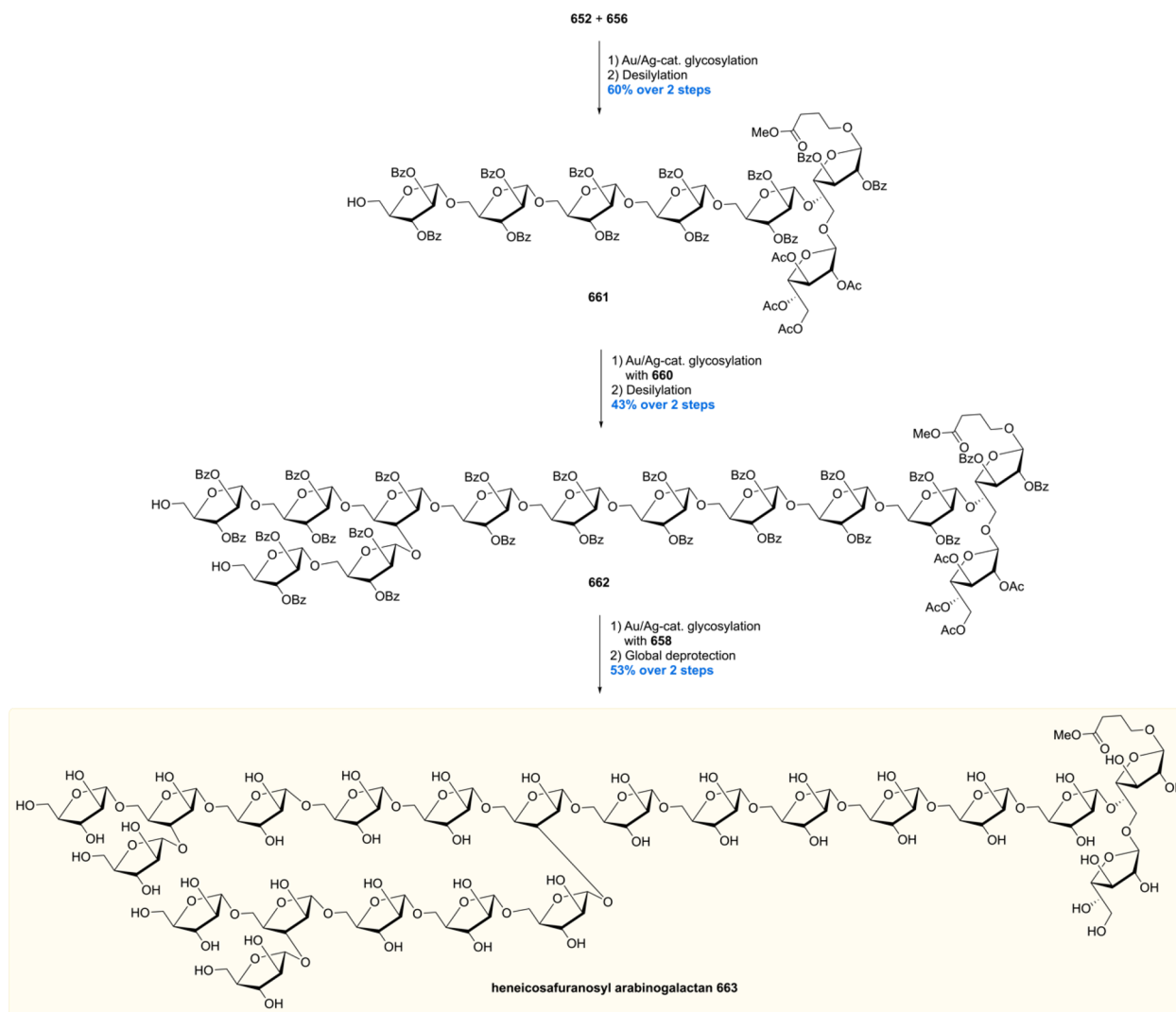
The third building block to be synthesized was pentasaccharide **623**, bearing the β -arabinofuranose (β -Araf) ramification (Scheme 84). This synthesis started by glycosylation of thioglycoside **619** with acceptor **616**. With trisaccharide **620** in hand the stage was set for the introduction of the β -Araf motif. It is the stereoselective introduction of this moiety which complicates the synthesis of the arabinogalactan domain. Several methods had been developed shortly before the synthesis of the arabinogalactan domain, and it was the strategy developed by the Boons laboratory which was ultimately utilized.³⁴³ It was shown that conformational constraints introduced by the silyl protecting group lock the intermediate oxocarbenium ion in such a way (*E*₃ conformer) that the β -face is more accessible. Having such protecting groups in trisaccharide **620**, after levulinoyl deprotection, the formation of the β -Araf functionality proceeded smoothly. The desired pentasaccharide **622** was obtained in 67% yield, together with a small amount (<8%) of inseparable isomers. A set of straightforward protecting group manipulations ultimately led to the completion of pentasaccharide **623**.

With the three building blocks **614**, **618**, and **623** in hand, the unification sequence was initiated by coupling of the first two building blocks, **618** and **614** (Scheme 85). Thus, after conversion of **618** into the corresponding trichloroacetimidate, glycosidation with **614** was performed promoted by TMSOTf, furnishing after desilylation, dodecasaccharide **624**. This molecule was coupled under the same conditions as before with the acetimidate of **623** to give, after debenzoylation and

Scheme 89. Hotha's Synthesis of Four Key Oligosaccharide Fragments



Scheme 90. Fragment Assembly and Completion of the Heneicosafuranosyl Arabinogalactan



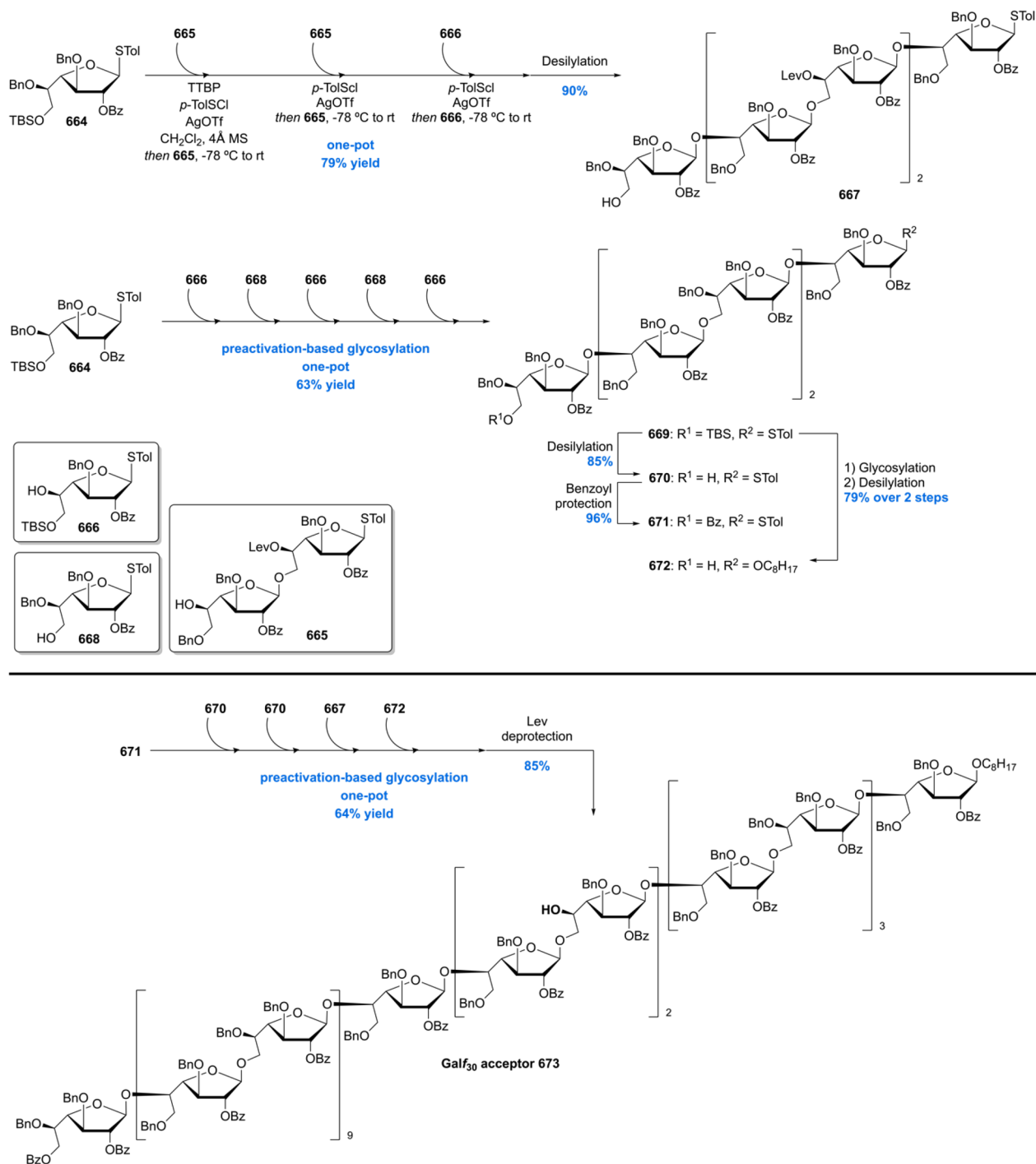
subsequent azide reduction, the desired arabinogalactan domain **625**. In addition to this synthesis, Lowary and co-workers also synthesized the proposed biosynthetic octadecasaccharide (Araf₂₂-β-Araf motif) precursor (synthesis not shown).

After Lowary's first report of the synthesis of the mycobacterial Araf₂₂ motif,³⁴¹ the Ito laboratory communicated their synthesis of this impressive oligosaccharide.³⁴⁴ Contrary to the Lowary synthesis, their strategy relied on fragment couplings in linear subunits rather than at the sites of branching. Their synthesis relied heavily on the use of thioglycoside donors built up by a convergent synthesis to access a series of tri- and pentasaccharide building blocks. These were coupled to arrive at two key fragments, Araf₇ donor **640** and Araf₈ acceptor **637** to ultimately construct the Araf₂₂ target structure. As part of their synthesis, various methods to stereoselectively access the β-Araf linkages were investigated.

The total synthesis of the Araf₂₂ motif was initiated by the synthesis of trisaccharide **629** and pentasaccharides **632** and **635** (Scheme 86). The NIS/AgOTf-promoted glycosylation of **626** and **627** followed by a series of protecting group manipulations gave disaccharide **628** in excellent yield of 91% over four steps. Disaccharide **628** was then subjected to the same series of glycosylation and protecting group changes giving trisaccharide **629**. Next, glycosylation of disaccharide **628** with donor **630**

gave trisaccharide **631** in very good yield. From **631**, pentasaccharide building block **632** was synthesized by a reaction sequence of desilylation, double glycosylation with **626**, and further protecting group manipulations, in 73% yield over four steps. To access pentasaccharide **635**, trisaccharide **631** was first subjected to debenzoylation, benzyl protection, and desilylation to give trisaccharide **634**. Double glycosylation promoted by methyl triflate and subsequent deacetylation cleanly provided pentasaccharide **635** in 93% yield over two steps.

Next, with the necessary building blocks in hand, the key fragments donor **640** and acceptor **637** were crafted (Scheme 87). Pentasaccharide **632** was subjected to a sequence of protecting group modifications giving **636**. NIS/AgOTf-promoted glycosylation of **636** with trisaccharide acceptor **629** followed by deacetylation, benzylation, and desilylation produced the desired Araf₈ acceptor **637** in 61% yield over four steps. For the synthesis of Araf₇ donor **640**, the β-Araf linkages were constructed by NIS/AgOTf-promoted double glycosylation of diol **635** with donor **638**, delivering heptasaccharide **639** in good stereoselectivity of 8.5:1 (β,β-639:other isomers). Desilylation then delivered the desired β,β-isomer **639** after purification in 87% yield over two steps. From

Scheme 91. Ye's Synthesis of Galf₃₀ Acceptor

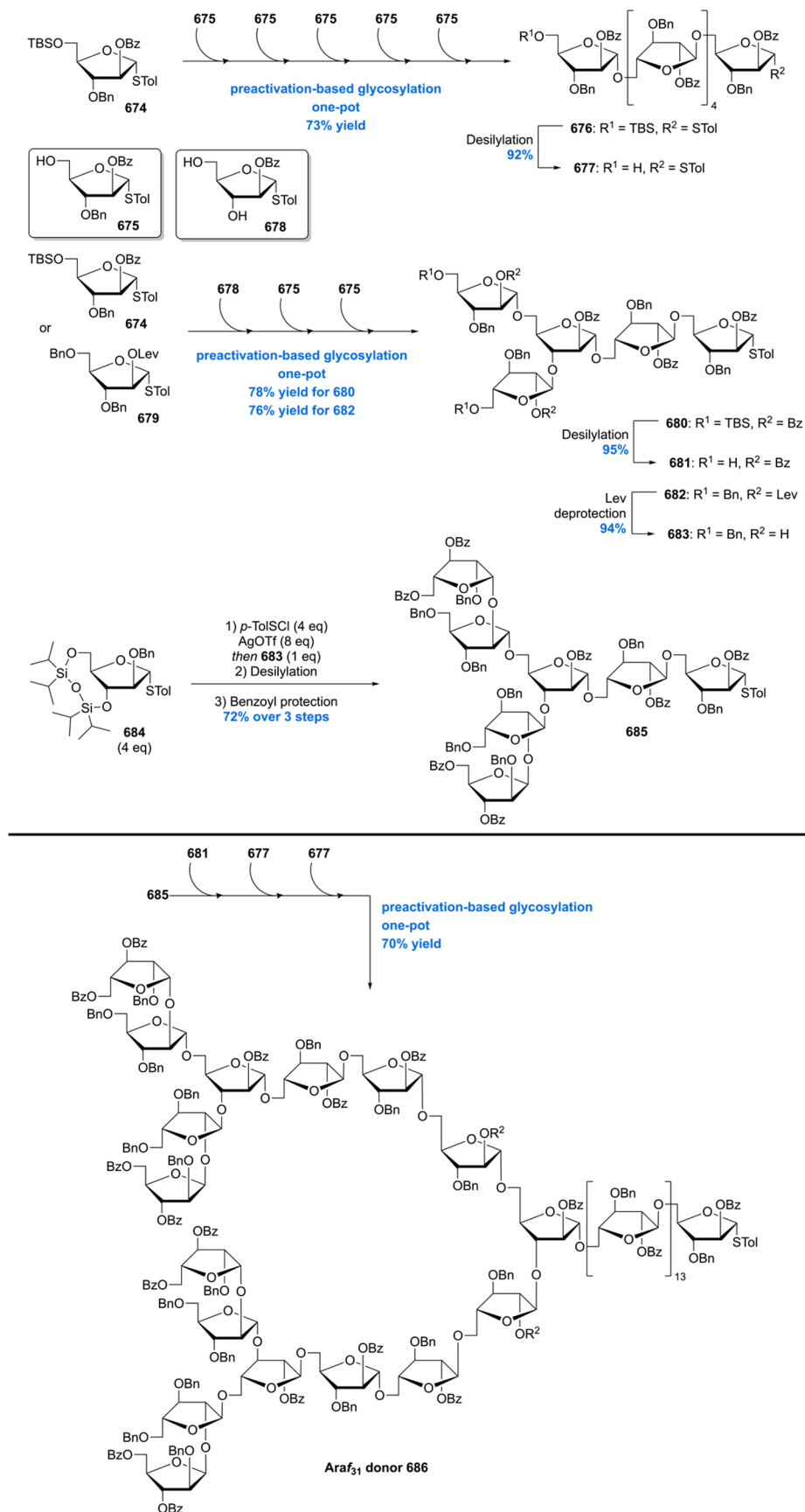
639, a series of protecting group manipulations finally delivered Araf₇ donor 640.

With the two key fragments 637 and 640 in hand, the target Araf₂₂ unit was constructed by glycosylation promoted by NIS/AgOTf in excellent yield of 96%. Global deprotection of the benzyl, acetyl, and silyl ether moieties then completed the synthesis of the docosaccharide arabinan motif 641.

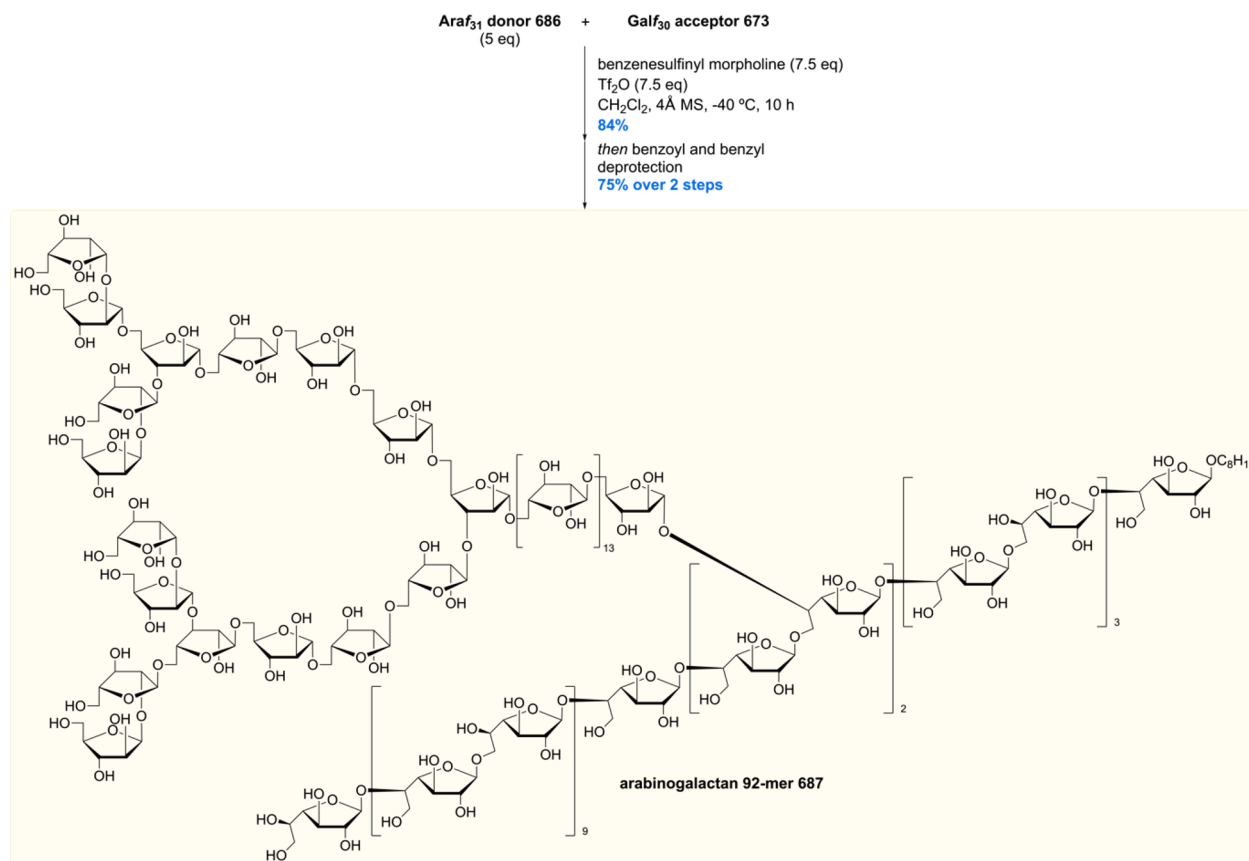
In 2017, the Hotha laboratory reported the synthesis of a mycobacterial heneicosafuranosyl arabinogalactan (HAG), consisting of 21 furanosyl monomers.³⁴⁵ Contrary to the oligosaccharides synthesized by the Lowary³⁴¹ and Ito³⁴⁴ groups, their target contains Araf as well as Galf units. For the

synthesis, a convergent strategy was developed, involving the synthesis of six monosaccharide building blocks (Scheme 88, in boxes), which were used to access four key oligosaccharide fragments (Scheme 89, in boxes). In order to construct these and unify them to arrive at the target HAG, their in-house developed gold-catalyzed glycosylation³⁴⁶ using alkynyl 1,2-orthoester donors was utilized.

The synthesis of HAG commenced with the synthesis of six furanosyl monomers (Scheme 88). Starting from 1,2-orthoester 642, a series of protecting group manipulations provided monomers 643 and 645 in 61% and 74% yield over three steps, respectively. Orthoester 643 was then converted to *n*-pentenyl

Scheme 92. Ye's Synthesis of the Araf₃₁ Donor

Scheme 93. Completion of the Total Synthesis of the Arabinogalactan 92-mer



furanoside monomer **644** by gold-catalyzed glycosylation followed by removal of the TBDPS ether in 66% yield over two steps. Furanosyl monomer **645** was subjected to gold-catalyzed glycosylation providing *n*-pentenyl furanoside **646**. Intermediate **646** was then subjected to a series of protecting group manipulations and ultimately was converted into 1,2-orthoester monomer **647** by preparation of the anomeric bromide and treatment with propargyl alcohol. The two Galf monomers were readily accessed from *n*-pentenyl furanoside **648**. 1,2-Orthoester monomer **649** was synthesized, again, by preparation of the anomeric bromide followed by treatment with propargyl alcohol in 81% yield over two steps. A series of synthetic steps then provided Galf monomer **650** in 56% yield over five steps.

With the furanosyl monomers in hand, the four key oligosaccharide fragments **652**, **656**, **658**, and **660** were synthesized (Scheme 89). Au/Ag-catalyzed glycosylation of Galf donor **649** with acceptor **650** provided disaccharide **651** in 70% yield. A second glycosylation of **651** with disaccharide acceptor **643** followed by TBDPS deprotection then delivered advanced building block **652** in 71% yield over two steps. Synthesis of building block **656** was initiated by Au/Ag-catalyzed glycosylation of 1,2-orthoester **643** with acceptor **644** giving *n*-pentenyl disaccharide **653** in 70% yield. From **653**, two intermediates were accessed. Desilylation of **653** gave primary alcohol **654**, and 1,2-orthoester formation from **653** via the anomeric bromide delivered disaccharide **655**. Coupling of disaccharides **654** and **655** by Au–Ag-catalyzed glycosylation and 1,2-orthoester synthesis concluded the synthesis of building block **656** in 74% over two steps. Next, gold-catalyzed glycosylation of 1,2-orthoester **645** with acceptor **644** furnished

disaccharide **657**. Another glycosylation of **657** with 1,2-orthoester **647** followed by installation of the 1,2-orthoester moiety delivered building block **658**. Disaccharide **657** was glycosylated with **643** under gold catalysis followed by desilylation to give diol **659**. The synthesis of hexasaccharide building block **660** was concluded by double gold-catalyzed glycosylation with **643** and introduction of the 1,2-orthoester unit in 43% yield over two steps.

In the end game of the synthesis (Scheme 90), building blocks **652** and **656** were unified by Au/Ag-catalyzed glycosylation followed by liberation of the primary alcohol, giving **661** in 60% yield over two steps. Another Au–Ag-catalyzed glycosylation of **661** with **660** and subsequent desilylation gave diol **662**. After coupling of **662** with **658** by Au/Ag-catalyzed glycosylation, and global deprotection, the stereoselective total synthesis of HAG **667** was completed in 0.09% overall yield. It is expected that this modular synthesis allows access of various synthetic analogues for further biological studies.

Shortly after the Hotha laboratory reported their synthesis of HAG,³⁴⁵ the group of Ye communicated the impressive first total synthesis of the mycobacterial arabinogalactan 92-mer(!).³⁴⁷ Contrary to the previous syntheses by Lowary³⁴¹ and Ito,³⁴⁴ this total synthesis features the complete construction of arabinogalactan rather than truncated oligosaccharide fragments. In order to achieve the preparation of the arabinogalactan 92-mer, a highly convergent synthesis route was designed. Their strategy was built on various preactivation-based one-pot glycosylation reactions to access various oligosaccharide building blocks, ultimately leading to two key fragments: a linear Galf₃₀ acceptor **673** and a branched Araf₃₁ donor **686**, to be unified giving the target polysaccharide.

The synthesis of *Galf*₃₀ acceptor **673** was initiated by the synthesis of linear hexasaccharide **667** (Scheme 91). Through a one-pot triple glycosylation of donor **664** with **665** (2×) and **666** in 79% yield followed by desilylation, **667** was obtained, carrying two orthogonal levulinoyl protecting groups for later coupling to the *Araf*₃₁ donor **686**. A series of additional hexasaccharide building blocks was synthesized by another one-pot glycosylation of **664** with monosaccharides **666** (3×) and **668** (2×) giving **669** in 63% yield. Desilylation of **669** then gave **670**, which was benzoylated providing **671**, whereas glycosylation of **669** with 1-octanol followed by desilylation gave building block **672**. The desired *Galf*₃₀ acceptor **673** was then constructed by a remarkable one-pot [6 + 6 + 6 + 6 + 6] glycosylation in 64% yield and subsequent liberation of the levulinoyl esters.

Next, for the synthesis of *Araf*₃₁ donor **686**, three oligosaccharide building blocks **677**, **681**, and **685** were prepared (Scheme 92). Starting from **674**, the linear hexasaccharide **676** was accessed in 73% yield by five consecutive glycosylations with monosaccharide **675** in one pot. The TBS ether of **676** was then removed providing intermediate **677**. The next two branched intermediates **680** and **682** were crafted by triple one-pot glycosylation of **674** or **679** with **678** and **675** (2×) in 78% and 76% yield, respectively. Desilylation of **680** provided pentasaccharide **681**, whereas **683** was synthesized by delevulinoylation of **682**. Glycosylation of diol **683** with donor **684** delivered the 1,2-*cis* linked heptasaccharide in excellent stereoselectivity. Next, removal of the silyl ether and benzoyl protection gave branched oligosaccharide building block **685**. With all necessary building blocks in hand, the desired *Araf*₃₁ donor **686** was assembled by one-pot triple preactivation glycosylation of **685** with **681** and **677** (2×) giving arabinofuranoside 31-mer **686** in 70% yield.

After complete synthesis of *Araf*₃₁ donor **686** and *Galf*₃₀ acceptor **673**, the two polysaccharide building blocks were coupled to arrive at the arabinogalactan 92-mer (Scheme 93). For this double glycosylation, a number of different reaction conditions were studied, eventually identifying the benzene-sulfinyl morpholine/*Tf*₂O promotor system as most successful. These conditions cleanly provided the coupled product in an impressive yield of 84%. Lastly, global deprotection involving debenzoylation and debenylation concluded the first total synthesis of the mycobacterial arabinogalactan 92-mer **687** in 75% yield over two steps.

10. CONCLUSION AND OUTLOOK

In this review we have compiled a quarter century of total syntheses of *Mtb* cell wall components ranging from lipids, glycolipids, terpenes, and lipopeptides to oligo- and even polysaccharides. It is evident from the variety and complexity of these molecular architectures, highlighted in this review, that *Mtb* can be considered a natural product “powerhouse”, showing these molecular entities to be of great interest and value to both synthetic chemists and immunologists. From an organic synthesis standpoint, these total syntheses have contributed significantly to the progress of the field of asymmetric synthesis and the development of synthesis methodology. A key example of this is the synthesis of (hydroxy)phthioceranic acid, which commenced with a robust linear synthesis and transitioned into remarkably convergent and efficient synthesis routes. This evolution of chemical methodology is also nicely illustrated by the synthetic efforts toward mycobacterial arabinogalactan, set in motion by the first reports of fragments to ultimately enable

total synthesis of the whole polysaccharide. Each of these reports is an example of pioneering work in organic synthesis.

Apart from pushing the boundaries of organic chemistry, total synthesis of mycobacterial natural products (as with any other natural product) allowed ultimate confirmation or elucidation of structure and stereochemistry. This has also very practical consequences. Research on the biosynthesis and immunology of *Mtb* components, either with molecular biology tools or using these components from cultured bacteria, can to a large extent take place successfully without knowledge of their precise molecular structure. Once such compounds are chemically synthesized, however, the structure including stereochemistry must be known. Indeed, any deviation from the structure of the natural compound leads to differences in biological activity. This was shown clearly in the synthesis of MPM and Ac₂SGL, where all attempts to change structure, stereochemistry, and even chain length of the lipid components led invariably to a diminished activity.

The syntheses of DAT and Ac₂SGL highlight the necessity for chemical synthesis for structure elucidation. The synthesis of three DAT structures ultimately revealed through direct comparison with natural material from cell wall extracts that synthetic DAT₂ does not correspond to the proposed structure of the natural material which needs to be revised. In the first synthesis of hydroxyphthioceranic acid as part of the synthesis of Ac₂SGL, the stereochemistry of its hydroxy group was unknown. Only by chemical synthesis and NMR comparison with natural material could the question of the stereochemistry be answered. Furthermore, the synthetic material obtained by total synthesis of elaborate mycobacterial natural products serves as an invaluable reference material for biological studies to answer fundamental questions on *Mtb* virulence and host immunology. A prime example is the asymmetric total synthesis of TbAd, which enabled detailed and extensive studies on the survival mechanisms of *Mtb* within macrophages. This total synthesis ultimately contributed to the elucidation of the role of TbAd as another virulence factor of *Mtb*.

The World Health Organization set the ambitious goal to eradicate Tb by 2035. Although certainly significant steps have been taken, judging the current yearly mortality and infection statistics, this target is not in sight yet. After all, despite the positive tone in the scientific literature, this review included, there is no effective vaccine against Tb, drug therapy is cumbersome and long, and there is an urgent need for low-cost diagnostics in developing countries. To reach the goals set by the WHO, the scientific community, e.g. academia, industry, and funding agencies, should make Tb eradication a top priority. Pertaining to this review, the authors believe that chemical synthesis endeavors greatly benefit from joint scientific projects in which compounds, knowledge, and inventions can be converted into actual point-of-care diagnosis, treatment and, ultimately, a vaccine. Such collaborations do require building bridges between seemingly distant fields of research, i.e. organic chemistry, bacteriology, immunology, and medicine. This is easier said than done, but with the common goal of ending Tb in mind, and the willingness to collaborate, a foundation can be laid from which exciting and eventually breakthrough discoveries can emerge.

After a large number of reported total syntheses, the field now approaches a turning point. Inherently it is not clear how many mycobacterial (cell wall) components are awaiting discovery. In order to drive the field further and to expand the knowledge on how *Mtb* utilizes cell wall constituents in virulence and host-

immunology, we need continuing efforts to discover new *Mtb*-specific molecules. Most known compounds have been accessed by synthesis. This by no means, however, makes them readily available. It is very important that many of the mycobacterial antigens become available to immunology as readily as antibodies and other “reagents”. This means that cutting-edge synthesis tools and creativity are required to develop the next generation syntheses of these antigens.

All in all, discoveries from interdisciplinary collaborations in this field can lead to the identification of new drug targets, vaccine adjuvants, or even new diagnostic platforms which would benefit millions of people.

AUTHOR INFORMATION

Corresponding Authors

Jeffrey Buter – *Stratingh Institute for Chemistry, University of Groningen, 9747 AG Groningen, The Netherlands*;
Phone: +31 (0)50 36 34235; Email: j.buter@rug.nl

Adriaan J. Minnaard – *Stratingh Institute for Chemistry, University of Groningen, 9747 AG Groningen, The Netherlands*; orcid.org/0000-0002-5966-1300;
Phone: +31 (0)50 36 34258; Email: a.j.minnaard@rug.nl;
<https://minnaardgroup.nl/>

Author

Mira Holzheimer – *Stratingh Institute for Chemistry, University of Groningen, 9747 AG Groningen, The Netherlands*; orcid.org/0000-0003-2157-0136

Complete contact information is available at:
<https://pubs.acs.org/10.1021/acs.chemrev.1c00043>

Notes

The authors declare no competing financial interest.

Biographies

Mira Holzheimer was born in Schweinfurt, Germany, in 1991. She completed her Bachelor in Pharmaceutical Sciences at the Ludwig-Maximilians University in Munich in 2013. After that, she moved to Leiden, The Netherlands, to pursue her Master studies in Bio-Pharmaceutical Sciences and obtained her Master's degree in 2016 with honors (*cum laude*). In the same year, she started her Ph.D. research in the group of Prof. Dr. Ir. Adriaan J. Minnaard which focuses on the asymmetric total synthesis of the complex archaeal membrane lipid crenarchaeol and on mycobacterial trehalose glycolipids (2016–2020). After receiving her Ph.D. degree in 2021 and a short postdoctoral stay in the Minnaard group, she is now a postdoctoral researcher with Prof. Alois Fürstner at the Max-Planck Institut für Kohlenforschung in Mülheim an der Ruhr, Germany, continuing in the field of total synthesis.

Jeffrey Buter studied molecular chemistry at the University of Groningen, The Netherlands. At the same university, he obtained his Ph.D. in the group of Prof. Adriaan J. Minnaard, working on the stereoselective total synthesis of terpenes containing quaternary stereocenters (2016). He then joined the laboratory of Prof. D. Branch Moody at Brigham and Women's Hospital/Harvard Medical School (United States of America) as a postdoctoral fellow (2016–2018). Here he investigated a survival mechanism of *Mycobacterium tuberculosis* (*Mtb*) and codiscovered a novel immunogenic lipid from *Salmonella* Typhi. In 2018 he joined the laboratory of Prof. Ben L. Feringa at the University of Groningen, where he is leading the catalysis group. Jeffrey secured his own research funding to unravel survival mechanisms of *Mtb* and for the development of a new therapeutic

strategy against tuberculosis disease (NWO-VENI and NWO-NWA idea generator grant). Together with Prof. Adriaan J. Minnaard, Prof. D. Branch Moody, and I. van Rhijn, he is the corecipient of the NWO Team Science Award (2020) for the collaborative effort involving discovery of novel tuberculosis lipids.

Adriaan J. Minnaard studied Molecular Sciences at Wageningen Agricultural University, The Netherlands. At the same university, he obtained his Ph.D. degree with Prof. Æ. De Groot in the field of natural product synthesis. He subsequently joined Royal DSM as a research scientist. In 1999 he joined the department of Prof. B. L. Feringa at the University of Groningen as an assistant professor. After a year as guest researcher at the Max Planck Institut für Molekulare Physiologie, Dortmund, Germany, in the department of Prof. H. Waldmann, he was appointed in 2009 professor in Bio-organic Chemistry at the University of Groningen. In 2016 he was appointed director of the Stratingh Institute for Chemistry. The main focus areas in his research are the chemistry of mycobacterial glycolipids, the synthesis of archaeal lipids, novel methods in homogeneous catalysis, and the selective modification of unprotected carbohydrates.

ACKNOWLEDGMENTS

The Dutch Research Council (NWO) is acknowledged for funding. J.B. specifically acknowledges NWO for funding through the NWO-VENI program (VI.Veni.192.122). The authors thank N. Marinus, N. R. M. Reintjens, N. Duindam, and C. H. M. van der Loo for proofreading the manuscript and B. L. H. Andringa for providing synthesis schemes of the mycoketide total synthesis.

REFERENCES

- (1) Hershkovitz, I.; Donoghue, H. D.; Minnikin, D. E.; Besra, G. S.; Lee, O. Y.-C.; Gernaey, A. M.; Galili, E.; Eshed, V.; Greenblatt, C. L.; Lemma, E.; Bar-Gal, G. K.; Spigelman, M. Detection and Molecular Characterization of 9000-Year-Old *Mycobacterium tuberculosis* from a Neolithic Settlement in the Eastern Mediterranean. *PLoS One* **2008**, *3*, No. e3426.
- (2) Barberis, I.; Bragazzi, N. L.; Galluzzo, L.; Martini, M. The History of Tuberculosis: From the First Historical Records to the Isolation of Koch's Bacillus. *J. Prev. Med. Hyg.* **2017**, *58*, E9–E12.
- (3) Cave, A. J. E. The Evidence for the Incidence of Tuberculosis in Ancient Egypt. *Br. J. Tuberc.* **1939**, *33*, 142–152.
- (4) Nerlich, A. G.; Haas, C. J.; Zink, A.; Szeimies, U.; Hagedorn, H. G. Molecular Evidence for Tuberculosis in an Ancient Egyptian Mummy. *Lancet* **1997**, *350*, 1404.
- (5) Zink, A. R.; Sola, C.; Reischl, U.; Grabner, W.; Rastogi, N.; Wolf, H.; Nerlich, A. G. Characterization of *Mycobacterium tuberculosis* Complex DNAs from Egyptian Mummies by Spoligotyping. *J. Clin. Microbiol.* **2003**, *41*, 359–367.
- (6) Kaufmann, S. H. E. Robert Koch, the Nobel Prize, and the Ongoing Threat of Tuberculosis. *N. Engl. J. Med.* **2005**, *353*, 2423–2426.
- (7) *Global tuberculosis report*; World Health Organization: Geneva, 2020.
- (8) Behr, M. A.; Edelstein, P. H.; Ramakrishnan, L. Is *Mycobacterium tuberculosis* Infection Life Long? *BMJ.* **2019**, *367*, l5770.
- (9) Cantres-Fonseca, O. J.; Rodriguez-Cintrón, W.; Del Olmo-Arroyo, F.; Baez-Corujó, S. In *Extra Pulmonary Tuberculosis: An Overview*; Chauhan, N. S., Ed.; 2018.
- (10) Bruchfeld, J.; Correia-Neves, M.; Källenius, G. Tuberculosis and HIV Coinfection. *Cold Spring Harbor Perspect. Med.* **2015**, *5*, No. a017871.
- (11) Floyd, K.; Glaziou, P.; Zumla, A.; Raviglione, M. The Global Tuberculosis Epidemic and Progress in Care, Prevention, and Research: An Overview in Year 3 of the End TB Era. *Lancet Respir. Med.* **2018**, *6*, 299–314.

- (12) Seung, K. J.; Keshavjee, S.; Rich, M. L. Multidrug-Resistant Tuberculosis and Extensively Drug-Resistant Tuberculosis. *Cold Spring Harbor Perspect. Med.* **2015**, *5*, No. a017863.
- (13) Pontali, E.; Raviglione, M. C.; Migliori, G. B.; Committee, w. g. m. o. t. G. T. N. C. T. Regimens to Treat Multidrug-Resistant Tuberculosis: Past, Present and Future Perspectives. *Eur. Respir. Rev.* **2019**, *28*, 190035.
- (14) Migliori, G. B.; Dara, M.; de Colombani, P.; Kluge, H.; Raviglione, M. C. Multidrug-Resistant Tuberculosis in Eastern Europe: Still on the Increase? *Eur. Respir. J.* **2012**, *39*, 1290–1291.
- (15) Acosta, C. D.; Dadu, A.; Ramsay, A.; Dara, M. Drug-Resistant Tuberculosis in Eastern Europe: Challenges and Ways Forward. *Public Health Action* **2014**, *4*, S3–S12.
- (16) van der Wel, N.; Hava, D.; Houben, D.; Fluitsma, D.; van Zon, M.; Pierson, J.; Brenner, M.; Peters, P. J. M. tuberculosis and M. leprae Translocate from the Phagolysosome to the Cytosol in Myeloid Cells. *Cell* **2007**, *129*, 1287–1298.
- (17) Pieters, J. Mycobacterium tuberculosis and the Macrophage: Maintaining a Balance. *Cell Host Microbe* **2008**, *3*, 399–407.
- (18) Vandal, O. H.; Nathan, C. F.; Ehrst, S. Acid Resistance in Mycobacterium tuberculosis. *J. Bacteriol.* **2009**, *191*, 4714–4721.
- (19) Meena, L. S.; Rajni. Survival Mechanisms of Pathogenic Mycobacterium tuberculosis H37Rv. *FEBS J.* **2010**, *277*, 2416–2427.
- (20) Jayachandran, R.; BoseDasgupta, S.; Pieters, J. Surviving the Macrophage: Tools and Tricks Employed by Mycobacterium tuberculosis. In *Curr. Top. Microbiol. Immunol.*; Pieters, J., McKinney, J. D., Eds.; Springer-Verlag: Berlin Heidelberg, 2013; Vol. 374, pp 189–209.
- (21) Cambier, C. J.; Falkow, S.; Ramakrishnan, L. Host Evasion and Exploitation Schemes of Mycobacterium tuberculosis. *Cell* **2014**, *159*, 1497–1509.
- (22) Zhai, W.; Wu, F.; Zhang, Y.; Fu, Y.; Liu, Z. The Immune Escape Mechanisms of Mycobacterium Tuberculosis. *Int. J. Mol. Sci.* **2019**, *20*, 340.
- (23) Batt, S. M.; Minnikin, D. E.; Besra, G. S. The Thick Waxy Coat of Mycobacteria, a Protective Layer Against Antibiotics and the Host's Immune System. *Biochem. J.* **2020**, *477*, 1983–2006.
- (24) Daffé, M.; Reyat, J.-M. *The Mycobacterial Cell Envelope*; ASM Press: Washington, D.C., 2008.
- (25) Kaur, D.; Guerin, M. E.; Škovicová, H.; Brennan, P. J.; Jackson, M. Biogenesis of the Cell Wall and Other Glycoconjugates of Mycobacterium tuberculosis. In *Advances in Applied Microbiology*; Elsevier: 2009; pp 23–78.
- (26) Jankute, M.; Cox, J. A. G.; Harrison, J.; Besra, G. S. Assembly of the Mycobacterial Cell Wall. *Annu. Rev. Microbiol.* **2015**, *69*, 405–423.
- (27) Ghazaei, C. Mycobacterium tuberculosis and Lipids: Insights into Molecular Mechanisms from Persistence to Virulence. *J. Res. Med. Sci.* **2018**, *23*, 63.
- (28) Sotgiu, G.; Centis, R.; D'ambrosio, L.; Migliori, G. B. Tuberculosis Treatment and Drug Regimens. *Cold Spring Harbor Perspect. Med.* **2015**, *5*, No. a017822.
- (29) Cao, B.; Williams, S. J. Chemical Approaches for the Study of the Mycobacterial Glycolipids Phosphatidylinositol Mannosides, Lipomannan and Lipoarabinomannan. *Nat. Prod. Rep.* **2010**, *27*, 919–947.
- (30) Shashidhar, M. S.; Patil, N. T. Recent Developments in the Synthesis of Biologically Relevant Inositol Derivatives. In *Carbohydrates in Drug Discovery and Development* **2020**, 283–329.
- (31) Daffé, M.; Lemassu, A. Glycobiology of the Mycobacterial Surface. In *Glycomicrobiology*; Doyle, R. J., Ed.; Kluwer Academic/Plenum Publishers: New York, 2002.
- (32) Chatterjee, D.; Khoo, K.-H. Mycobacterial Lipoarabinomannan: An Extraordinary Lipoheteroglycan with Profound Physiological Effects. *Glycobiology* **1998**, *8*, 113–120.
- (33) Alderwick, L. J.; Harrison, J.; Lloyd, G. S.; Birch, H. L. The Mycobacterial Cell Wall - Peptidoglycan and Arabinogalactan. *Cold Spring Harbor Perspect. Med.* **2015**, *5*, No. a021113.
- (34) Maitra, A.; Munshi, T.; Healy, J.; Martin, L. T.; Vollmer, W.; Keep, N. H.; Bhakta, S. Cell Wall Peptidoglycan in Mycobacterium tuberculosis: An Achilles' Heel for the TB-causing Pathogen. *FEMS Microbiol. Rev.* **2019**, *43*, 548–575.
- (35) Marrakchi, H.; Laneëlle, M. A.; Daffé, M. Mycolic Acids: Structures, Biosynthesis, and Beyond. *Chem. Biol.* **2014**, *21*, 67–85.
- (36) Kalscheuer, R.; Palacios, A.; Anso, I.; Cifuentes, J.; Anguita, J.; Jacobs, W. R., Jr.; Guerin, M. E.; Prados-Rosales, R. The Mycobacterium tuberculosis Capsule: A Cell Structure with Key Implications in Pathogenesis. *Biochem. J.* **2019**, *476*, 1995–2016.
- (37) Minnikin, D. E.; Brennan, P. J. Lipids of Clinically Significant Mycobacteria. In *Health Consequences of Microbial Interactions with Hydrocarbons, Oils, and Lipids*; Goldfine, H., Ed.; Springer International Publishing: Cham, 2020; pp 33–108.
- (38) Stanley, S. A.; Cox, J. S. Host-Pathogen Interactions During Mycobacterium tuberculosis infections. In *Curr. Top. Microbiol. Immunol.*; Pieters, J., McKinney, J. D., Eds.; Springer-Verlag: Berlin Heidelberg, 2013; Vol. 374, pp 211–241.
- (39) Ryll, R.; Kumazawa, Y.; Yano, I. Immunological Properties of Trehalose Dimycolate (Cord Factor) and Other Mycolic Acid-Containing Glycolipids-A Review. *Microbiol. Immunol.* **2001**, *45*, 801–811.
- (40) Guenin-Mace, L.; Simeone, R.; Demangel, C. Lipids of Pathogenic Mycobacteria: Contributions to Virulence and Host Immune Suppression. *Transboundary Emerging Dis.* **2009**, *56*, 255–268.
- (41) Astarie-Dequeker, C.; Nigou, J.; Passemar, C.; Guilhot, C. The Role of Mycobacterial Lipids in Host Pathogenesis. *Drug Discovery Today: Dis. Mech.* **2010**, *7*, e33–e41.
- (42) Jackson, M. The Mycobacterial Cell Envelope—Lipids. *Cold Spring Harbor Perspect. Med.* **2014**, *4*, No. a021105.
- (43) Queiroz, A.; Riley, L. W. Bacterial Immunostat: Mycobacterium tuberculosis Lipids and Their Role in the Host Immune Response. *Rev. Soc. Bras. Med. Trop.* **2017**, *50*, 9–18.
- (44) Singh, P.; Rameshwaram, N. R.; Ghosh, S.; Mukhopadhyay, S. Cell Envelope Lipids in the Pathophysiology of Mycobacterium tuberculosis. *Future Microbiol.* **2018**, *13*, 689–710.
- (45) Kinsella, R. L.; Zhu, D. X.; Harrison, G. A.; Mayer Bridwell, A. E.; Prusa, J.; Chavez, S. M.; Stallings, C. L. Perspectives and Advances in the Understanding of Tuberculosis. *Annu. Rev. Pathol.: Mech. Dis.* **2021**, *16*, 377–408.
- (46) Moreno-Mendieta, S. A.; Rocha-Zavaleta, L.; Rodriguez-Sanoja, R. Adjuvants in Tuberculosis Vaccine Development. *FEMS Immunol. Med. Microbiol.* **2010**, *58*, 75–84.
- (47) Wallis, R. S.; Kim, P.; Cole, S.; Hanna, D.; Andrade, B. B.; Maeurer, M.; Schito, M.; Zumla, A. Tuberculosis Biomarkers Discovery: Developments, Needs, and Challenges. *Lancet Infect. Dis.* **2013**, *13*, 362–372.
- (48) Tucci, P.; Gonzalez-Sapienza, G.; Marin, M. Pathogen-derived Biomarkers for Active Tuberculosis Diagnosis. *Front. Microbiol.* **2014**, *5*, 549.
- (49) Goletti, D.; Petruccioli, E.; Joosten, S. A.; Ottenhoff, T. H. Tuberculosis Biomarkers: From Diagnosis to Protection. *Infect. Dis. Rep.* **2016**, *8*, 6568.
- (50) Goletti, D.; Lee, M. R.; Wang, J. Y.; Walter, N.; Ottenhoff, T. H. M. Update on Tuberculosis Biomarkers: From Correlates of Risk, to Correlates of Active Disease and of Cure from Disease. *Respirology* **2018**, *23*, 455–466.
- (51) Murphy, K.; Weaver, C. *Janeway's Immunobiology*. 9th ed.; Garland Science: New York, 2016.
- (52) Sompayrac, L. *How the Immune System Works*, 5th ed.; John Wiley & Sons, Ltd.: Chichester, 2016.
- (53) Monie, T. P. Section 1 - A Snapshot of the Innate Immune System. In *The Innate Immune System*; Monie, T. P., Ed.; Academic Press, 2017; pp 1–40.
- (54) Monie, T. P. Section 5 - Connecting the Innate and Adaptive Immune Responses. In *The Innate Immune System*; Monie, T. P., Ed.; Academic Press, 2017; pp 171–187.
- (55) Barral, D. C.; Brenner, M. B. CD1 Antigen Presentation: How it Works. *Nat. Rev. Immunol.* **2007**, *7*, 929–941.
- (56) Siddiqui, S.; Visvabharathy, L.; Wang, C.-R. Role of Group 1 CD1-restricted T Cells in Infectious Disease. *Front. Immunol.* **2015**, *6*, 337.

- (57) Van Rhijn, I.; Moody, D. B. CD1 and Mycobacterial Lipids Activate Human T Cells. *Immunol. Rev.* **2015**, *264*, 138–153.
- (58) Ishikawa, E.; Ishikawa, T.; Morita, Y. S.; Toyonaga, K.; Yamada, H.; Takeuchi, O.; Kinoshita, T.; Akira, S.; Yoshikai, Y.; Yamasaki, S. Direct Recognition of the Mycobacterial Glycolipid, Trehalose Dimycolate, by C-type Lectin Mincle. *J. Exp. Med.* **2009**, *206*, 2879–2888.
- (59) Matsunaga, I.; Moody, D. B. Mincle is a Long Sought Receptor for Mycobacterial Cord Factor. *J. Exp. Med.* **2009**, *206*, 2865–2868.
- (60) Williams, S. J. Sensing Lipids with Mincle: Structure and Function. *Front. Immunol.* **2017**, *8*, 1662.
- (61) Lu, X.; Nagata, M.; Yamasaki, S. Mincle: 20 Years of a Versatile Sensor of Insults. *Int. Immunol.* **2018**, *30*, 233–239.
- (62) Patin, E. C.; Orr, S. J.; Schaible, U. E. Macrophage Inducible C-Type Lectin As a Multifunctional Player in Immunity. *Front. Immunol.* **2017**, *8*, 861.
- (63) Dockrell, H. M.; Smith, S. G. What Have We Learnt about BCG Vaccination in the Last 20 Years? *Front. Immunol.* **2017**, *8*, 1134.
- (64) Anderson, R. J. The Separation of Lipid Fractions from Tubercle Bacilli. *J. Biol. Chem.* **1927**, *74*, 525–535.
- (65) Minnikin, D. E.; Polgar, N. Studies on the Mycolid Acids from Human Tubercle Bacilli. *Tetrahedron Lett.* **1966**, *23*, 2643–2647.
- (66) Minnikin, D. E.; Polgar, N. The Methocymycolic and Ketomycolic Acids from Human Tubercle Bacilli. *Chem. Commun.* **1967**, 1172–1174.
- (67) Asselineau, J.; Tocanne, G.; Tocanne, J. F. Stéréochimie des Acides Mycoliques. *Bull. Soc. Chim. Fr.* **1970**, *4*, 1455–1459.
- (68) Watanabe, M.; Aoyagi, Y.; Ridell, M.; Minnikin, D. E. Separation and Characterization of Individual Mycolic Acids in Representative Mycobacteria. *Microbiology* **2001**, *147*, 1825–1837.
- (69) Moody, D. B.; Guy, M. R.; Grant, E.; Cheng, T.-Y.; Brenner, M. B.; Besra, G. S.; Porcelli, S. A. CD1b-mediated T Cell Recognition of a Glycolipid Antigen Generated from Mycobacterial Lipid and Host Carbohydrate during Infection. *J. Exp. Med.* **2000**, *192*, 965–976.
- (70) Lautenslager, G. T.; Simpson, L. L. Chimeric Molecules Constructed with Endogenous Substances. *Adv. Mol. Cell Biol.* **1994**, *9*, 233–262.
- (71) Watanabe, M.; Aoyagi, Y.; Mitome, H.; Fujita, T.; Naoki, H.; Ridell, M.; Minnikin, D. E. Location of Functional Groups in Mycobacterial Meromycolate Chains; The Recognition of new Structural Principles in Mycolic Acids. *Microbiology* **2002**, *148*, 1881–1902.
- (72) Al Dulayymi, J. R.; Baird, M. S.; Roberts, E.; Deysel, M.; Verschoor, J. The First Syntheses of Single Enantiomers of the Major Methoxymycolic Acid of Mycobacterium tuberculosis. *Tetrahedron* **2007**, *63*, 2571–2592.
- (73) Tahiri, N.; Fodran, P.; Jayaraman, D.; Buter, J.; Witte, M. D.; Ocampo, T. A.; Moody, D. B.; Van Rhijn, I.; Minnaard, A. J. Total Synthesis of a Mycolic Acid from Mycobacterium tuberculosis. *Angew. Chem., Int. Ed.* **2020**, *59*, 7555–7560.
- (74) Barry III, C. E.; Lee, R. E.; Khisimusi, M.; Sampson, A. E.; Schroeder, B. G.; Slayden, R. A.; Yuan, Y. Mycolic Acids: Structure, Biosynthesis and Physiological Functions. *Prog. Lipid Res.* **1998**, *37*, 143–179.
- (75) Nikaido, H. Prevention of Drug Access to Bacterial Targets: Permeability Barriers and Active Efflux. *Science* **1994**, *264*, 382–388.
- (76) Kremer, L. S.; Besra, G. S. Current Status and Future Development of Antitubercular Chemotherapy. *Expert Opin. Invest. Drugs* **2002**, *11*, 1033–1049.
- (77) Nataraj, V.; Varela, C.; Javid, A.; Singh, A.; Besra, G. S.; Bhatt, A. Mycolic Acids: Deciphering and Targeting the Achilles' Heel of the Tubercle Bacillus. *Mol. Microbiol.* **2015**, *98*, 7–16.
- (78) Winder, F. G.; Collins, P. B. Inhibition by Isoniazid of Synthesis of Mycolic Acids in Mycobacterium tuberculosis. *J. Gen. Microbiol.* **1970**, *63*, 41–48.
- (79) Takayama, K.; Wang, L.; David, H. L. Effect of Isoniazid on the In Vivo Mycolic Acid Synthesis, Cell Growth, and Viability of Mycobacterium tuberculosis. *Antimicrob. Agents Chemother.* **1972**, *2*, 29–35.
- (80) Vilcheze, C.; Jacobs, W. R., Jr. The Isoniazid Paradigm of Killing, Resistance, and Persistence in Mycobacterium tuberculosis. *J. Mol. Biol.* **2019**, *431*, 3450–3461.
- (81) Matsumoto, M.; Hashizume, H.; Tomishige, T.; Kawasaki, M.; Tsubouchi, H.; Sasaki, H.; Shimokawa, Y.; Komatsu, M. OPC-67683, a Nitro-Dihydro-Imidazooxazole Derivative with Promising Action against Tuberculosis In Vitro and In Mice. *PLoS Med.* **2006**, *3*, No. e466.
- (82) Stover, C. K.; Warrenner, P.; VanDevanter, D. R.; Sherman, D. R.; Arain, T. M.; Langhorne, M. H.; Anderson, S. W.; Towell, J. A.; Yuan, Y.; McMurray, D. N.; Kreiswirth, B. N.; Barry, C. E.; Baker, W. R. A Small-Molecule Nitroimidazopyran Drug Candidate for the Treatment of Tuberculosis. *Nature* **2000**, *405*, 962–966.
- (83) Dubnau, E.; Chan, J.; Raynaud, C.; Mohan, V. P.; Lanéelle, M.-A.; Keming, Y.; Quémard, A.; Smith, I.; Daffé, M. Oxygenated Mycolic Acids are Necessary for Virulence of Mycobacterium tuberculosis in Mice. *Mol. Microbiol.* **2000**, *36*, 630–637.
- (84) Korf, J.; Stoltz, A.; Verschoor, J.; De Baetselier, P.; Grooten, J. The Mycobacterium tuberculosis Cell Wall Component Mycolic Acid Elicits aathogen-Associated Host Innate Immune Responses. *Eur. J. Immunol.* **2005**, *35*, 890–900.
- (85) Russell, D. G.; Cardona, P.-J.; Kim, M.-J.; Allain, S.; Altare, F. Foamy Macrophages and the Progression of the Human Tuberculosis Granuloma. *Nat. Immunol.* **2009**, *10*, 943–948.
- (86) Beukes, M.; Lemmer, Y.; Deysel, M.; Al Dulayymi, J. R.; Baird, M. S.; Koza, G.; Iglesias, M. M.; Rowles, R. R.; Theunissen, C.; Grooten, J.; Toschi, G.; Roberts, V. V.; Pilcher, L.; Van Wyngaardt, S.; Mathebula, N.; Balogun, M.; Stoltz, A. C.; Verschoor, J. A. Structure-Function Relationships of the Antigenicity of Mycolic Acids in Tuberculosis Patients. *Chem. Phys. Lipids* **2010**, *163*, 800–808.
- (87) Moody, D. B.; Reinhold, B. B.; Guy, M. R.; Backman, E. M.; Frederique, D. E.; Furlong, S. T.; Ye, S.; Reinhold, V. N.; Sieling, P. A.; Modlin, R. L.; Besra, G. S.; Porcelli, S. A. Structural Requirements for Glycolipid Antigen Recognition by CD1b-Restricted T Cells. *Science* **1997**, *278*, 283–286.
- (88) Grant, E. P.; Beckman, E. M.; Behar, S. M.; Degano, M.; Frederique, D.; Besra, G. S.; Wilson, I. A.; Porcelli, S. A.; Furlong, S. T.; Brenner, M. B. Fine Specificity of TCR Complementarity-Determining Region Residues and Lipid Antigen Hydrophilic Moieties in the Recognition of a CD1-Lipid Complex. *J. Immunol.* **2002**, *168*, 3933–3940.
- (89) Van Rhijn, I.; Iwany, S. K.; Fodran, P.; Cheng, T.-Y.; Gapin, L.; Minnaard, A. J.; Moody, D. B. CD1b-Mycolic Acid Tetramers Demonstrate T-Cell Fine Specificity for Mycobacterial Lipid Tails. *Eur. J. Immunol.* **2017**, *47*, 1525–1534.
- (90) Decout, A.; Silva-Gomes, S.; Drocourt, D.; Barbe, S.; Andre, I.; Cueto, F. J.; Lioux, T.; Sancho, D.; Perouzel, E.; Vercellone, A.; Prandi, J.; Gilleron, M.; Tiraby, G.; Nigou, J. Rational Design of Adjuvants Targeting the C-type Lectin Mincle. *Proc. Natl. Acad. Sci. U. S. A.* **2017**, *114*, 2675–2680.
- (91) Layre, E.; Collmann, A.; Bastian, M.; Mariotti, S.; Czaplicki, J.; Prandi, J.; Mori, L.; Stenger, S.; De Libero, G.; Puzo, G.; Gilleron, M. Mycolic Acids Constitute a Scaffold for Mycobacterial Lipid Antigens Stimulating CD1-Restricted T Cells. *Chem. Biol.* **2009**, *16*, 82–92.
- (92) Prandi, J. A Convenient Synthesis of Glucose Monomycolate. *Carbohydr. Res.* **2012**, *347*, 151–154.
- (93) Al Dulayymi, J. R.; Baird, M. S.; Roberts, E. The Synthesis of a Single Enantiomer of a Major Alpha-Mycolic Acid of Mycobacterium tuberculosis. *Chem. Commun.* **2003**, 228–229.
- (94) Al Dulayymi, J. R.; Baird, M. S.; Roberts, E. The Synthesis of a Single enantiomer of a Major α -Mycolic Acid of M. tuberculosis. *Tetrahedron* **2005**, *61*, 11939–11951.
- (95) Grandjean, D.; Pale, P.; Chuche, J. Enzymatic Hydrolysis of Cyclopropanes. Total Synthesis of Optically Pure Dictyoterpenes A and C'. *Tetrahedron* **1991**, *47*, 1215–1230.
- (96) Koza, G.; Theunissen, C.; Al Dulayymi, J. R.; Baird, M. S. The Synthesis of Single Enantiomers of Mycobacterial Ketomycolic Acids Containing cis-Cyclopropanes. *Tetrahedron* **2009**, *65*, 10214–10229.

- (97) Koza, G.; Muzael, M.; Schubert-Rowles, R. R.; Theunissen, C.; Al Dulayymi, J. R.; Baird, M. S. The Synthesis of Methoxy and Keto Mycolic Acids Containing Methyl-trans-cyclopropanes. *Tetrahedron* **2013**, *69*, 6285–6296.
- (98) Vander Beken, S.; Al Dulayymi, J. R.; Naessens, T.; Koza, G.; Maza-Iglesias, M.; Rowles, R.; Theunissen, C.; De Medts, J.; Lanckacker, E.; Baird, M. S.; Grooten, J. Molecular Structure of the Mycobacterium tuberculosis Virulence Factor, Mycolic Acid, Determines the Elicited Inflammatory Pattern. *Eur. J. Immunol.* **2011**, *41*, 450–460.
- (99) Riley, L. W. Of Mice, Men and Elephants: Mycobacterium tuberculosis Cell Envelope Lipids and Pathogenesis. *J. Clin. Invest.* **2006**, *116*, 1475–1478.
- (100) Ali, O. T.; Sahb, M. M.; Al Dulayymi, J. R.; Baird, M. S. Glycerol Mycolates from Synthetic Mycolic Acids. *Carbohydr. Res.* **2017**, *448*, 67–73.
- (101) Chancellor, A.; Tocheva, A. S.; Cave-Ayland, C.; Tezera, L.; White, A.; Al Dulayymi, J. R.; Bridgeman, J. S.; Tews, I.; Wilson, S.; Lissin, N. M.; Tebruegge, M.; Marshall, B.; Sharpe, S.; Elliott, T.; Skylaris, C. K.; Essex, J. W.; Baird, M. S.; Gadola, S.; Elkington, P.; Mansour, S. CD1b-restricted GEM T Cell Responses are Modulated by Mycobacterium tuberculosis Mycolic Acid Meromycolate Chains. *Proc. Natl. Acad. Sci. U. S. A.* **2017**, *114*, E10956–E10964.
- (102) Moody, D. B.; Ulrichs, T.; Mühlecker, W.; Young, D. C.; Gurcha, S. S.; Grant, E.; Rosat, J.-P.; Brenner, M. B.; Costello, C. E.; Besra, G. S.; Porcelli, S. A. CD1c-mediated T-cell Recognition of Isoprenoid Glycolipids in Mycobacterium tuberculosis Infection. *Nature* **2000**, *404*, 884–888.
- (103) Crich, D.; Dudkin, V. Confirmation of the Connectivity of 4,8,12,16,20-Pentamethylpentacosylphosphoryl β -D-Mannopyranoside, an Unusual β -Mannosyl Phosphoisoprenoid from Mycobacterium avium, through Synthesis. *J. Am. Chem. Soc.* **2002**, *124*, 2263–2266.
- (104) van Summeren, R. P.; Reijmer, S. J.; Feringa, B. L.; Minnaard, A. J. Catalytic Asymmetric Synthesis of Enantiopure Isoprenoid Building Blocks: Application in the Synthesis of Apple Leafminer Pheromones. *Chem. Commun.* **2005**, 1387–1389.
- (105) van Summeren, R. P.; Moody, D. B.; Feringa, B. L.; Minnaard, A. J. Total Synthesis of Enantiopure β -D-Mannosyl Phosphomycoketides from Mycobacterium tuberculosis. *J. Am. Chem. Soc.* **2006**, *128*, 4546–4547.
- (106) Matsunaga, I.; Bhatt, A.; Young, D. C.; Cheng, T. Y.; Eyles, S. J.; Besra, G. S.; Briken, V.; Porcelli, S. A.; Costello, C. E.; Jacobs, W. R., Jr.; Moody, D. B. Mycobacterium tuberculosis pks12 Produces a Novel Polyketide Presented by CD1c to T Cells. *J. Exp. Med.* **2004**, *200*, 1559–1569.
- (107) Nicolaou, K. C.; Montagnon, T.; Baran, P. S.; Zhong, Y.-L. Iodine(V) Reagents in Organic Synthesis. Part 4. o-Iodoxybenzoic Acid as a Chemospecific Tool for Single Electron Transfer-Based Oxidation Processes. *J. Am. Chem. Soc.* **2002**, *124*, 2245–2258.
- (108) de Jong, A.; Arce, E. C.; Cheng, T.-Y.; van Summeren, R. P.; Feringa, B. L.; Dudkin, V.; Crich, D.; Matsunaga, I.; Minnaard, A. J.; Moody, D. B. CD1c Presentation of Synthetic Glycolipid Antigens with Foreign Alkyl Branching Motifs. *Chem. Biol.* **2007**, *14*, 1232–1242.
- (109) Ly, D.; Kasmar, A. G.; Cheng, T.-Y.; de Jong, A.; Huang, S.; Roy, S.; Bhatt, A.; van Summeren, R. P.; Altman, J. D.; Jacobs, W. R., Jr.; Adams, E. J.; Minnaard, A. J.; Porcelli, S. A.; Moody, D. B. CD1c Tetramers Detect ex vivo T Cell Responses to Processed Phosphomycoketide Antigens. *J. Exp. Med.* **2013**, *210*, 729–741.
- (110) Li, N.-S.; Scharf, L.; Adams, E. J.; Piccirilli, J. A. Highly Stereocontrolled Total Synthesis of β -D-Mannosyl Phosphomycoketide: A Natural Product from Mycobacterium tuberculosis. *J. Org. Chem.* **2013**, *78*, 5970–5986.
- (111) Roy, S.; Ly, D.; Li, N.-S.; Altman, J. D.; Piccirilli, J. A.; Moody, D. B.; Adams, E. J. Molecular Basis of Mycobacterial Lipid Antigen Presentation by CD1c and its Recognition by $\alpha\beta$ T Cells. *Proc. Natl. Acad. Sci. U. S. A.* **2014**, *111*, E4648–E4657.
- (112) Minnaard, A. J.; Andringa, R.; de Kok, N.; Driessen, A. A Unified Approach for the Total Synthesis of cyclo-Archaeol, iso-Caldarchaeol, Caldarchaeol, and Mycoketide. *Angew. Chem., Int. Ed.* **2021**, DOI: 10.1002/anie.202104759.
- (113) Minnikin, D. E.; Kremer, L.; Dover, L. G.; Besra, G. S. The Methyl-Branched Fortifications of Mycobacterium tuberculosis. *Chem. Biol.* **2002**, *9*, 545–553.
- (114) Jarlier, V.; Nikaido, H. Mycobacterial Cell Wall: Structure and Role in Natural Resistance to Antibiotics. *FEMS Microbiol. Lett.* **1994**, *123*, 11–18.
- (115) Dmitriev, B. A.; Ehlers, S.; Rietschel, E. T.; Brennan, P. J. Molecular Mechanics of the Mycobacterial Cell Wall: From Horizontal Layers to Vertical Scaffolds. *Int. J. Med. Microbiol.* **2000**, *290*, 251–258.
- (116) Jackson, M.; Stadthagen, G.; Gicquel, B. Long-chain Multiple Methyl-branched Fatty Acid-containing Lipids of Mycobacterium tuberculosis: Biosynthesis, Transport, Regulation and Biological Activities. *Tuberculosis* **2007**, *87*, 78–86.
- (117) Des Mazery, R.; Pullez, M.; López, F.; Harutyunyan, S. R.; Minnaard, A. J.; Feringa, B. L. An Iterative Catalytic Route to Enantiopure Deoxypropionate Subunits: Asymmetric Conjugate Addition of Grignard Reagents to α,β -Unsaturated Thioesters. *J. Am. Chem. Soc.* **2005**, *127*, 9966–9967.
- (118) Ter Horst, B.; Feringa, B. L.; Minnaard, A. J. Catalytic Asymmetric Synthesis of Phthioceranic Acid, a Heptamethyl-Branched Acid from Mycobacterium tuberculosis. *Org. Lett.* **2007**, *9*, 3013–3015.
- (119) Casas-Arce, E.; Ter Horst, B.; Feringa, B. L.; Minnaard, A. J. Asymmetric Total Synthesis of PDIM A: A Virulence Factor of Mycobacterium tuberculosis. *Chem. - Eur. J.* **2008**, *14*, 4157–4159.
- (120) Camacho, L. R.; Ensergueix, D.; Perez, E.; Gicquel, B.; Guilhot, C. Identification of a Virulence Gene Cluster of Mycobacterium tuberculosis by Signature-Tagged Transposon Mutagenesis. *Mol. Microbiol.* **1999**, *34*, 257–267.
- (121) Cox, J. S.; Chen, B.; McNeil, M.; Jacobs, W. R., Jr. Complex Lipid Determines Tissue-specific Replication of Mycobacterium tuberculosis in Mice. *Nature* **1999**, *402*, 79–83.
- (122) Rousseau, C.; Winter, N.; Pivert, E.; Bordat, Y.; Neyrolles, O.; Avé, P.; Huerre, M.; Gicquel, B.; Jackson, M. Production of Phthiocerol Dimycocerosates Protects Mycobacterium tuberculosis from the Cidal Activity of Reactive Nitrogen Intermediates Produced by Macrophages and Modulates the Early Immune Response to Infection. *Cell. Microbiol.* **2004**, *6*, 277–287.
- (123) Cambier, C. J.; Takaki, K. K.; Larson, R. P.; Hernandez, R. E.; Tobin, D. M.; Urdahl, K. B.; Cosma, C. L.; Ramakrishnan, L. Mycobacteria Manipulate Macrophage Recruitment Through Coordinated Use of Membrane Lipids. *Nature* **2014**, *505*, 218–222.
- (124) Camacho, L. R.; Constant, P.; Raynaud, C.; Laneelle, M. A.; Triccas, J. A.; Gicquel, B.; Daffe, M.; Guilhot, C. Analysis of the Phthiocerol Dimycocerosate Locus of Mycobacterium tuberculosis. *J. Biol. Chem.* **2001**, *276*, 19845–19854.
- (125) Astarie-Dequeker, C.; Le Guyader, L.; Malaga, W.; Seaphanh, F.-K.; Chalut, C.; Lopez, A.; Guilhot, C. Phthiocerol Dimycocerosates of M. tuberculosis Participate in Macrophage Invasion by Inducing Changes in the Organization of Plasma Membrane Lipids. *PLoS Pathog.* **2009**, *5*, No. e1000289.
- (126) Augenstreich, J.; Haanappel, E.; Ferré, G.; Czaplicki, G.; Jolibois, F.; Destainville, N.; Guilhot, C.; Milon, A.; Astarie-Dequeker, C.; Chavent, M. The Conical Shape of DIM Lipids Promotes Mycobacterium tuberculosis Infection of Macrophages. *Proc. Natl. Acad. Sci. U. S. A.* **2019**, *116*, 25649–25658.
- (127) Quigley, J.; Hughitt, V. K.; Velikovskiy, C. A.; Mariuzza, R. A.; El-Sayed, N. M.; Briken, V. The Cell Wall Lipid PDIM Contributes to Phagosomal Escape and Host Cell Exit of Mycobacterium tuberculosis. *mBio* **2017**, *8*, No. e00148-17.
- (128) Osman, M. M.; Pagán, A. J.; Shanahan, J. K.; Ramakrishnan, L. Mycobacterium marinum phthiocerol dimycocerosates enhance macrophage phagosomal permeabilization and membrane damage. *PLoS One* **2020**, *15* (7), No. e0233252.
- (129) Polgar, N. Constituents of the Lipids of Tubercle Bacilli. Part IV. Mycoceranic Acid. *J. Chem. Soc.* **1954**, 1011–1012.
- (130) Marks, G. S.; Polgar, N. Mycoceranic Acid. Part II. *J. Chem. Soc.* **1955**, 3851–3857.

- (131) Polgar, N.; Smith, W. Mycoceranic Acid. Part III. *J. Chem. Soc.* **1963**, 3081–3085.
- (132) Maskens, K.; Polgar, N. Stereochemistry of the Phthiocerols. *J. Chem. Soc. D* **1970**, 340.
- (133) Maskens, K.; Polgar, N. Absolute Configuration of the -CH(OMe)-CHMe- System in the Phthiocerols. *J. Chem. Soc., Perkin Trans. 1* **1973**, 1909–1912.
- (134) Ter Horst, B.; Feringa, B. L.; Minnaard, A. J. Catalytic Asymmetric Synthesis of Mycocerosic Acid. *Chem. Commun.* **2007**, 489–491.
- (135) Flentie, K. N.; Stallings, C. L.; Turk, J.; Minnaard, A. J.; Hsu, F.-F. Characterization of Phthiocerol and Phthiodiolone Dimycocerosate Esters of *M. tuberculosis* by Multiple-stage Linear Ion-trap MS. *J. Lipid Res.* **2016**, *57*, 142–155.
- (136) Nakamura, T.; Nakagome, H.; Sano, S.; Sadayuki, T.; Hosokawa, S. Total Synthesis of PDIM A. *Chem. Lett.* **2016**, *45*, 550–551.
- (137) Nakamura, T.; Kubota, K.; Ieki, T.; Hosokawa, S. Stereoselective Alkylation of the Vinylketene Silyl N,O-Acetal and Its Application to the Synthesis of Mycocerosic Acid. *Org. Lett.* **2016**, *18*, 132–135.
- (138) Hunter, S. W.; Brennan, P. J. A Novel Phenolic Glycolipid from *Mycobacterium leprae* Possibly Involved in Immunogenicity and Pathogenicity. *J. Bacteriol.* **1981**, *147*, 728–735.
- (139) Hunter, S. W.; Fujiwara, T.; Brennan, P. J. Structure and Antigenicity of the Major Specific Glycolipid Antigen of *Mycobacterium leprae*. *J. Biol. Chem.* **1982**, *257*, 15072–15078.
- (140) Tarelli, E.; Draper, P.; Payne, S. N. Structure of the Oligosaccharide Component of a Serologically Active Phenolic Glycolipid of *Mycobacterium leprae*. *Carbohydr. Res.* **1984**, *131*, 346–352.
- (141) Demartean-Ginsburg, H.; Lederer, E. Sur la Structure Chimique du Mycoside B. *Biochim. Biophys. Acta* **1963**, *70*, 442–451.
- (142) Villé, C.; Gastambide-Odier, M. Le 3-O-méthyl-l-rhamnose, sucre isolé du mycoside G de *Mycobacterium marinum*. *Carbohydr. Res.* **1970**, *12*, 97–107.
- (143) Gastambide-Odier, M.; Sarda, P. Contribution à l'étude de la structure et de la biosynthèse de glycolipides spécifiques isolés de mycobactéries: les mycosides A et B. *Lung* **1970**, *142*, 241–255.
- (144) Daffé, M.; Lacave, C.; Lanéeelle, M.-A.; Lanéeelle, G. Structure of the Major Triglycosyl Phenol-phthiocerol of *Mycobacterium tuberculosis* (Strain Canetti). *Eur. J. Biochem.* **1987**, *167*, 155–160.
- (145) Daffé, M.; Servin, P. Scalar, Dipolar-correlated and J-resolved 2D-NMR Spectroscopy of the Specific Phenolic Mycoside of *Mycobacterium tuberculosis*. *Eur. J. Biochem.* **1989**, *185*, 157–162.
- (146) Reed, M. B.; Domenech, P.; Manca, C.; Su, H.; Barczak, A. K.; Kreiswirth, B. N.; Kaplan, G.; Barry III, C. E. A Glycolipid of Hypervirulent Tuberculosis Strains that Inhibits the Innate Immune Response. *Nature* **2004**, *431*, 84–87.
- (147) Sinsimer, D.; Huet, G.; Manca, C.; Tsenova, L.; Koo, M. S.; Kurepina, N.; Kana, B.; Mathema, B.; Marras, S. A.; Kreiswirth, B. N.; Guilhot, C.; Kaplan, G. The Phenolic Glycolipid of *Mycobacterium tuberculosis* Differentially Modulates the Early Host Cytokine Response but Does Not in Itself Confer Hypervirulence. *Infect. Immun.* **2008**, *76*, 3027–3036.
- (148) Barnes, D. D.; Lundahl, M. L. E.; Lavelle, E. C.; Scanlan, E. M. The Emergence of Phenolic Glycans as Virulence Factors in *Mycobacterium tuberculosis*. *ACS Chem. Biol.* **2017**, *12*, 1969–1979.
- (149) Cambier, C. J.; O'Leary, S. M.; O'Sullivan, M. P.; Keane, J.; Ramakrishnan, L. Phenolic Glycolipid Facilitates Mycobacterial Escape from Microbicidal Tissue-Resident Macrophages. *Immunity* **2017**, *47*, 552–565.
- (150) Simonney, N.; Chavanet, P.; Perronne, C.; Lepotier, M.; Revol, F.; Herrmann, J. L.; Lagrange, P. H. B-cell Immune Responses in HIV Positive and HIV Negative Patients with Tuberculosis Evaluated with an ELISA Using a Glycolipid Antigen. *Tuberculosis* **2007**, *87*, 109–122.
- (151) Barroso, S.; Castelli, R.; Baggelaar, M. P.; Geerdink, D.; Ter Horst, B.; Casas-Arce, E.; Overkleef, H. S.; van der Marel, G. A.; Codee, J. D.; Minnaard, A. J. Total Synthesis of the Triglycosyl Phenolic Glycolipid PGL-tb1 from *Mycobacterium tuberculosis*. *Angew. Chem., Int. Ed.* **2012**, *51* (47), 11774–11777.
- (152) Geerdink, D.; Horst, B. t.; Lepore, M.; Mori, L.; Puzo, G.; Hirsch, A. K. H.; Gilleron, M.; de Libero, G.; Minnaard, A. J. Total Synthesis, Stereochemical Elucidation and Biological Evaluation of Ac2SGL; a 1,3-Methyl Branched Sulfoglycolipid from *Mycobacterium tuberculosis*. *Chem. Sci.* **2013**, *4*, 709–716.
- (153) Geerdink, D. *Total Synthesis of Enantiopure Lipids: On Mycobacterial Glycolipids and a Putative Sex Pheromone of Trichogramma turkestanica*. PhD Thesis, University of Groningen, Groningen, 2013.
- (154) Pischl, M. C.; Weise, C. F.; Muller, M. A.; Pfaltz, A.; Schneider, C. A Convergent and Stereoselective Synthesis of the Glycolipid Components Phthioceranic Acid and Hydroxyphthioceranic Acid. *Angew. Chem., Int. Ed.* **2013**, *52*, 8968–8972.
- (155) Rasappan, R.; Aggarwal, V. K. Synthesis of Hydroxyphthioceranic Acid Using a Traceless Lithiation-borylation-protodeboronation Strategy. *Nat. Chem.* **2014**, *6*, 810–814.
- (156) Balieu, S.; Hallett, G. E.; Burns, M.; Bootwicha, T.; Studley, J.; Aggarwal, V. K. Toward Ideality: The Synthesis of (+)-Kalkitoxin and (+)-Hydroxyphthioceranic Acid by Assembly-Line Synthesis. *J. Am. Chem. Soc.* **2015**, *137*, 4398–4403.
- (157) Xu, S.; Oda, A.; Bobinski, T.; Li, H.; Matsueda, Y.; Negishi, E. Highly Efficient, Convergent, and Enantioselective Synthesis of Phthioceranic Acid. *Angew. Chem., Int. Ed.* **2015**, *54*, 9319–9322.
- (158) Che, W.; Wen, D. C.; Zhu, S. F.; Zhou, Q. L. Iterative Synthesis of Polydeoxypropionates Based on Iridium-Catalyzed Asymmetric Hydrogenation of α -Substituted Acrylic Acids. *Org. Lett.* **2018**, *20*, 3305–3309.
- (159) Weise, C. F.; Pischl, M.; Pfaltz, A.; Schneider, C. A Non-Iterative, Flexible, and Highly Stereoselective Synthesis of Polydeoxypropionates-Synthesis of (+)-Vittatalactone. *Chem. Commun.* **2011**, *47*, 3248–3250.
- (160) Weise, C. F.; Pischl, M. C.; Pfaltz, A.; Schneider, C. A General, Asymmetric, and Noniterative Synthesis of Trideoxypropionates. Straightforward Syntheses of the Pheromones (+)-Vittatalactone and (+)-Norvittatalactone. *J. Org. Chem.* **2012**, *77*, 1477–1488.
- (161) Gilleron, M.; Stenger, S.; Mazorra, Z.; Wittke, F.; Mariotti, S.; Böhrer, G.; Prandi, J.; Mori, L.; Puzo, G.; De Libero, G. Diacylated Sulfoglycolipids Are Novel Mycobacterial Antigens Stimulating CD1-restricted T Cells during Infection with *Mycobacterium tuberculosis*. *J. Exp. Med.* **2004**, *199*, 649–659.
- (162) Guiard, J.; Collmann, A.; Gilleron, M.; Mori, L.; De Libero, G.; Prandi, J.; Puzo, G. Synthesis of Diacylated Trehalose Sulfates: Candidates for a Tuberculosis Vaccine. *Angew. Chem., Int. Ed.* **2008**, *47*, 9734–9738.
- (163) Guiard, J.; Collmann, A.; Garcia-Alles, L. F.; Mourey, L.; Brando, T.; Mori, L.; Gilleron, M.; Prandi, J.; De Libero, G.; Puzo, G. Fatty Acyl Structures of *Mycobacterium tuberculosis* Sulfoglycolipid Govern T Cell Response. *J. Immunol.* **2009**, *182*, 7030–7037.
- (164) James, C. A.; Yu, K. K. Q.; Gilleron, M.; Prandi, J.; Yedulla, V. R.; Moleda, Z. Z.; Diamanti, E.; Khan, M.; Aggarwal, V. K.; Reijneveld, J. F.; Reinink, P.; Lenz, S.; Emerson, R. O.; Scriba, T. J.; Souter, M. N. T.; Godfrey, D. I.; Pellicci, D. G.; Moody, D. B.; Minnaard, A. J.; Seshadri, C.; Van Rhijn, I. CD1b Tetramers Identify T Cells that Recognize Natural and Synthetic Diacylated Sulfoglycolipids from *Mycobacterium tuberculosis*. *Cell Chem. Biol.* **2018**, *25*, 392–402.
- (165) Madduri, A. V. R.; Minnaard, A. J. Formal Synthesis of the Anti-Angiogenic Polyketide (–)-Borrelidin under Asymmetric Catalytic Control. *Chem. - Eur. J.* **2010**, *16*, 11726–11731.
- (166) Geerdink, D.; Minnaard, A. J. Total Synthesis of Sulfolipid-I. *Chem. Commun.* **2014**, *50*, 2286–2288.
- (167) Goren, M. B. Sulfolipid I of *Mycobacterium tuberculosis*, Strain H37Rv II. Structural Studies. *Biochim. Biophys. Acta, Lipids Lipid Metab.* **1970**, *210*, 127–138.
- (168) Goren, M. B. Sulfolipid I of *Mycobacterium tuberculosis*, Strain H37Rv I. Purification and Properties. *Biochim. Biophys. Acta, Lipids Lipid Metab.* **1970**, *210*, 116–126.

- (169) Goren, M. B.; Brokl, O.; Das, B. C.; Lederer, E. Sulfolipid I of *Mycobacterium tuberculosis*, Strain H37Rv. Nature of the Acyl Substituents. *Biochemistry* **1971**, *10*, 72–81.
- (170) Gangadharam, P. R. J.; Cohn, M. L.; Middelrook, G. Infectivity, Pathogenicity and Sulfolipid Fraction of Some Indian and British Strains of Tubercle Bacilli. *Tubercle* **1963**, *44*, 452–455.
- (171) Pabst, M. J.; Gross, J. M.; Brozna, J. P.; Goren, M. B. Inhibition of Macrophage Priming by Sulfatide from *Mycobacterium tuberculosis*. *J. Immunol.* **1988**, *140*, 634–640.
- (172) Zhang, L.; Goren, M. B.; Holzer, T. J.; Andersen, B. R. Effect of *Mycobacterium tuberculosis*-Derived Sulfolipid I on Human Phagocytic Cells. *Infect. Immun.* **1988**, *56*, 2876–2883.
- (173) Brozna, J. P.; Horan, M.; Rademacher, J. M.; Pabst, K. M.; Pabst, M. J. Monocyte Responses to Sulfatide from *Mycobacterium tuberculosis*: Inhibition of Priming for Enhanced Release of Superoxide, Associated with Increased Secretion of Interleukin-1 and Tumor Necrosis Factor Alpha, and Altered Protein Phosphorylation. *Infect. Immun.* **1991**, *59*, 2542–2548.
- (174) Zhang, L.; English, D.; Andersen, B. R. Activation of Human Neutrophils by *Mycobacterium tuberculosis*-derived Sulfolipid-I. *J. Immunol.* **1991**, *146*, 2730–2736.
- (175) Gilmore, S. A.; Schelle, M. W.; Holsclaw, C. M.; Leigh, C. D.; Jain, M.; Cox, J. S.; Leary, J. A.; Bertozzi, C. R. Sulfolipid-1 Biosynthesis Restricts *Mycobacterium tuberculosis* Growth in Human Macrophages. *ACS Chem. Biol.* **2012**, *7*, 863–870.
- (176) Ruhl, C. R.; Pasko, B. L.; Khan, H. S.; Kindt, L. M.; Stamm, C. E.; Franco, L. H.; Hsia, C. C.; Zhou, M.; Davis, C. R.; Qin, T.; Gautron, L.; Burton, M. D.; Mejia, G. L.; Naik, D. K.; Dussor, G.; Price, T. J.; Shiloh, M. U. *Mycobacterium tuberculosis* Sulfolipid-1 Activates Nociceptive Neurons and Induces Cough. *Cell* **2020**, *181*, 293–305.
- (177) Minnikin, D. E.; Dobson, G.; Sesardic, D.; Ridell, M. Mycolipenates and Mycolipanolates of Trehalose from *Mycobacterium tuberculosis*. *Microbiology* **1985**, *131*, 1369–1374.
- (178) Daffé, M.; Lacave, C.; Lanéelle, M.-A.; Gillois, M.; Lanéelle, G. Polyphthienoyl Trehalose, Glycolipids for Virulent Strains of the Tubercle Bacillus. *Eur. J. Biochem.* **1988**, *172*, 579–584.
- (179) Daffé, M.; Papa, F.; Laszlo, A.; David, H. L. Glycolipids of Recent Clinical Isolates of *Mycobacterium tuberculosis*: Chemical Characterization and Immunoreactivity. *Microbiology* **1989**, *135*, 2759–2766.
- (180) Besra, G. S.; Bolton, R. C.; McNeil, M. R.; Ridell, M.; Simpson, K. E.; Glushka, J.; van Halbeek, H.; Brennan, P. J.; Minnikin, D. E. Structural Elucidation of a Novel Family of Acyltrehaloses from *Mycobacterium tuberculosis*. *Biochemistry* **1992**, *31*, 9832–9837.
- (181) Rousseau, C.; Neyrolles, O.; Bordat, Y.; Giroux, S.; Sirakova, T. D.; Prevost, M.-C.; Kolattukudy, P. E.; Gicquel, B.; Jackson, M. Deficiency in Mycolipenate- and Mycosanoate-Derived Acyltrehaloses Enhances Early Interactions of *Mycobacterium tuberculosis* with Host Cells. *Cell. Microbiol.* **2003**, *5*, 405–415.
- (182) Dubey, V. S.; Sirakova, P. E.; Kolattukude, P. E. Disruption of msl3 Abolishes the Synthesis of Mycolipanoic and Mycolipenic Acids Required for Polyacyltrehalose Synthesis in *Mycobacterium tuberculosis* H37Rv and Causes Cell Aggregation. *Mol. Microbiol.* **2002**, *45*, 1451–1459.
- (183) Gonzalo Asensio, J.; Maia, C.; Ferrer, N. L.; Barilone, N.; Laval, F.; Soto, C. Y.; Winter, N.; Daffe, M.; Gicquel, B.; Martin, C.; Jackson, M. The Virulence-associated Two-component PhoP-PhoR System Controls the Biosynthesis of Polyketide-derived Lipids in *Mycobacterium tuberculosis*. *J. Biol. Chem.* **2006**, *281*, 1313–1316.
- (184) Walters, S. B.; Dubnau, E.; Kolesnikova, I.; Laval, F.; Daffe, M.; Smith, I. The *Mycobacterium tuberculosis* PhoPR Two-Component System Regulates Genes Essential for Virulence and Complex Lipid Biosynthesis. *Mol. Microbiol.* **2006**, *60*, 312–330.
- (185) Gonzalo-Asensio, J.; Mostowy, S.; Harders-Westerveen, J.; Huygen, K.; Hernandez-Pando, R.; Thole, J.; Behr, M.; Gicquel, B.; Martin, C. PhoP: A Missing Piece in the Intricate Puzzle of *Mycobacterium tuberculosis* Virulence. *PLoS One* **2008**, *3*, No. e3496.
- (186) Hatzios, S. K.; Schelle, M. W.; Holsclaw, C. M.; Behrens, C. R.; Botyanszki, Z.; Lin, F. L.; Carlson, B. L.; Kumar, P.; Leary, J. A.; Bertozzi, C. R. PapA3 is an Acyltransferase Required for Polyacyltrehalose Biosynthesis in *Mycobacterium tuberculosis*. *J. Biol. Chem.* **2009**, *284*, 12745–12751.
- (187) Rodríguez, J. E.; Ramirez, A. S.; Salas, L. P.; Helguera-Repetto, C.; Gonzalez-Y-Merchand, J.; Soto, C. Y.; Hernandez-Pando, R. Transcription of Genes Involved in Sulfolipid and Polyacyltrehalose Biosynthesis of *Mycobacterium tuberculosis* in Experimental Latent Tuberculosis Infection. *PLoS One* **2013**, *8*, No. e58378.
- (188) Lee, K.-S.; Dubey, V. S.; Kolattukudy, P. E.; Song, C.-H.; Shin, A.-R.; Jung, S.-B.; Yang, C.-S.; Kim, S.-Y.; Jo, E.-K.; Park, J.-K.; Kim, H.-J. Diacyltrehalose of *Mycobacterium tuberculosis* Inhibits Lipopolysaccharide- and Mycobacteria-Induced Proinflammatory Cytokine Production in Human Monocytic Cells. *FEMS Microbiol. Lett.* **2007**, *267*, 121–128.
- (189) Saavedra, R.; Segura, E.; Leyva, R.; Esparza, L. A.; Lopez-Marín, L. M. Mycobacterial Di-O-Acyl-Trehalose Inhibits Mitogen- and Antigen-Induced Proliferation of Murine T Cells In Vitro. *Clin. Diagn. Lab. Immunol.* **2001**, *8*, 1081–1088.
- (190) Martín-Casabona, N.; Gonzales Fuente, T.; Papa, F.; Rosselló Urgell, J.; Vidal Plá, R.; Codina Gau, G.; Ruiz Camps, I. Time Course of Anti-SL-IV Immunoglobulin G Antibodies in Patients with Tuberculosis-Associated AIDS. *J. Clin. Microbiol.* **1992**, *30*, 1089–1093.
- (191) Papa, F.; Luquin, M.; David, H. L. DOT-ELISA for Detection of Phenolic Glycolipid PGL-Tb1 and Diacyl-Trehalose Antigens of *Mycobacterium tuberculosis*. *Res. Microbiol.* **1992**, *143*, 327–331.
- (192) Tórtola, M. T.; Lanéelle, M. A.; Martín-Casabona, N. Comparison of Two 2,3-Diacyl Trehalose Antigens from *Mycobacterium tuberculosis* and *Mycobacterium fortuitum* for Serology in Tuberculosis Patients. *Clin. Diagn. Lab. Immunol.* **1996**, *3*, S63–S66.
- (193) Muñoz, M.; Lanéelle, M.-A.; Luquin, M.; Torrelles, J.; Julián, E.; Ausina, V.; Daffé, M. Occurrence of an Antigenic Triacyl Trehalose in Clinical Isolated and Reference Strains of *Mycobacterium tuberculosis*. *FEMS Microbiol. Lett.* **1997**, *157*, 251–259.
- (194) Julián, E.; Cama, M.; Martínez, P.; Luquin, M. An ELISA for Five Glycolipids from the Cell Wall of *Mycobacterium tuberculosis*: Tween 20 Interference in the Assay. *J. Immunol. Methods* **2001**, *251*, 21–30.
- (195) Holzheimer, M.; Reijneveld, J. F.; Ramnarine, A. K.; Misiakos, G.; Young, D. C.; Ishikawa, E.; Cheng, T. Y.; Yamasaki, S.; Moody, D. B.; Van Rhijn, I.; Minnaard, A. J. Asymmetric Total Synthesis of Mycobacterial Diacyl Trehaloses Demonstrates a Role for Lipid Structure in Immunogenicity. *ACS Chem. Biol.* **2020**, *15*, 1835–1841.
- (196) Ter Horst, B.; van Wermeskerken, J.; Feringa, B. L.; Minnaard, A. J. Catalytic Asymmetric Synthesis of Mycolipenic and Mycolipanoic Acid. *Eur. J. Org. Chem.* **2010**, *2010*, 38–41.
- (197) Reijneveld, J. F.; Holzheimer, M.; Young, D. C.; Lopez, K.; Suliman, S.; Jimenez, J.; Calderon, R.; Lecca, L.; Murray, M. B.; Ishikawa, E.; Yamasaki, S.; Minnaard, A. J.; Moody, D. B.; Van Rhijn, I. Synthetic Mycobacterial Diacyl Trehaloses Reveal Differential Recognition by Human T Cell Receptors and the C-type Lectin Mincle. *Sci. Rep.* **2021**, *11*, 2010.
- (198) Hunter, S. W.; McNeil, M. R.; Brennan, P. J. Diglycosyl Diacylglycerol of *Mycobacterium tuberculosis*. *J. Bacteriol.* **1986**, *168*, 917–922.
- (199) Ishikawa, T.; Itoh, F.; Yoshida, S.; Saijo, S.; Matsuzawa, T.; Gono, T.; Saito, T.; Okawa, Y.; Shibata, N.; Miyamoto, T.; Yamasaki, S. Identification of Distinct Ligands for the C-type Lectin Receptors Mincle and Dectin-2 in the Pathogenic Fungus *Malassezia*. *Cell Host Microbe* **2013**, *13*, 477–488.
- (200) Richardson, M. B.; Torigoe, S.; Yamasaki, S.; Williams, S. J. *Mycobacterium tuberculosis* β -Gentiobiosyl Diacylglycerides Signal through the Pattern Recognition Receptor Mincle: Total Synthesis and Structure Activity Relationships. *Chem. Commun.* **2015**, *51*, 15027–15030.
- (201) Andrés, E.; Martínez, N.; Planas, A. Expression and Characterization of a *Mycoplasma genitalium* Glycosyltransferase in Membrane Glycolipid Biosynthesis. *J. Biol. Chem.* **2011**, *286*, 35367–35379.
- (202) Takato, K.; Kurita, M.; Yagami, N.; Tanaka, H.-N.; Ando, H.; Imamura, A.; Ishida, H. Chemical Synthesis of Diglycosyl Diacylglycer-

- ols Utilizing Glycosyl Donors with Stereodirecting Cyclic Silyl Protective Groups. *Carbohydr. Res.* **2019**, *483*, 107748.
- (203) Vance, J. E. Phosphatidylserine and Phosphatidylethanolamine in Mammalian Cells: Two Metabolically Related Aminophospholipids. *J. Lipid Res.* **2008**, *49*, 1377–1387.
- (204) Ter Horst, B.; Seshadri, C.; Sweet, L.; Young, D. C.; Feringa, B. L.; Moody, D. B.; Minnaard, A. J. Asymmetric Synthesis and Structure Elucidation of a Glycerophospholipid from *Mycobacterium tuberculosis*. *J. Lipid Res.* **2010**, *51*, 1017–1022.
- (205) Smit, C.; Fraaije, M. W.; Minnaard, A. J. Reduction of Carbon-Carbon Double Bonds Using Organocatalytically Generated Diimide. *J. Org. Chem.* **2008**, *73*, 9482–9485.
- (206) Fodran, P.; Minnaard, A. J. Catalytic Synthesis of Enantiopure Mixed Diacylglycerols - Synthesis of a Major *M. tuberculosis* Phospholipid and Platelet Activating Factor. *Org. Biomol. Chem.* **2013**, *11*, 6919–6928.
- (207) Furse, S. Is Phosphatidylglycerol Essential for Terrestrial Life? *J. Chem. Biol.* **2017**, *10*, 1–9.
- (208) Sarma, P. V. G. K.; Srikanth, L.; Venkatesh, K.; Murthy, P. S.; Sarma, P. U. Isolation, Purification and Characterization of Cardiolipin Synthase from *Mycobacterium phlei*. *Bioinformation* **2013**, *9*, 690–695.
- (209) Jackson, M.; Crick, D. C.; Brennan, P. J. Phosphatidylinositol is an Essential Phospholipid of *Mycobacteria*. *J. Biol. Chem.* **2000**, *275*, 30092–30099.
- (210) Van Rhijn, I.; van Berlo, T.; Hilmenyuk, T.; Cheng, T. Y.; Wolf, B. J.; Tatituri, R. V.; Uldrich, A. P.; Napolitani, G.; Cerundolo, V.; Altman, J. D.; Willemsen, P.; Huang, S.; Rossjohn, J.; Besra, G. S.; Brenner, M. B.; Godfrey, D. I.; Moody, D. B. Human Autoreactive T Cells Recognize CD1b and Phospholipids. *Proc. Natl. Acad. Sci. U. S. A.* **2016**, *113*, 380–385.
- (211) Tatituri, R. V.; Watts, G. F.; Bhowruth, V.; Barton, N.; Rothchild, A.; Hsu, F. F.; Almeida, C. F.; Cox, L. R.; Eggeling, L.; Cardell, S.; Rossjohn, J.; Godfrey, D. I.; Behar, S. M.; Besra, G. S.; Brenner, M. B.; Brigl, M. Recognition of Microbial and Mammalian Phospholipid Antigens by NKT Cells with Diverse TCRs. *Proc. Natl. Acad. Sci. U. S. A.* **2013**, *110*, 1827–1832.
- (212) Wolf, B. J.; Tatituri, R. V.; Almeida, C. F.; Le Nours, J.; Bhowruth, V.; Johnson, D.; Uldrich, A. P.; Hsu, F. F.; Brigl, M.; Besra, G. S.; Rossjohn, J.; Godfrey, D. I.; Brenner, M. B. Identification of a Potent Microbial Lipid Antigen for Diverse NKT Cells. *J. Immunol.* **2015**, *195*, 2540–2551.
- (213) Burugupalli, S.; Richardson, M. B.; Williams, S. J. Total Synthesis and Mass Spectrometric Analysis of a *Mycobacterium tuberculosis* Phosphatidylglycerol Featuring a Two-Step Synthesis of (R)-Tuberculostearic Acid. *Org. Biomol. Chem.* **2017**, *15*, 7422–7429.
- (214) Pethe, K.; Swenson, D. L.; Alonso, S.; Anderson, J.; Wang, C.; Russell, D. G. Isolation of *Mycobacterium tuberculosis* Mutants Defective in the Arrest of Phagosome Maturation. *Proc. Natl. Acad. Sci. U. S. A.* **2004**, *101*, 13642–13647.
- (215) Sturgill-Kszycki, S.; Schlesinger, P. H.; Chakraborty, P.; Haddix, P. L.; Collins, H. L.; Fok, A. K.; Allen, R. D.; Gluck, S. L.; Heuser, J.; Russel, D. G. Lack of Acidification in *Mycobacterium* Phagosomes Produced by Exclusion of the Vesicular Proton-ATPase. *Science* **1994**, *263*, 678–681.
- (216) Oh, Y.-K.; Straubinger, R. M. Intracellular Fate of *Mycobacterium avium*: Use of Dual-Label Spectrofluorometry To Investigate the Influence of Bacterial Viability and Oposonization on Phagosomal pH and Phagosome-Lysosome Interaction. *Infect. Immun.* **1996**, *64*, 319–325.
- (217) Nakano, C.; Okamura, T.; Sato, T.; Dairi, T.; Hoshino, T. *Mycobacterium tuberculosis* H37Rv3377c Encodes the Diterpene Cyclase for Producing the Halimane Skeleton. *Chem. Commun.* **2005**, 1016–1018.
- (218) Nakano, C.; Hoshino, T. Characterization of the Rv3377c Gene Product, a Type-B Diterpene Cyclase, from the *Mycobacterium tuberculosis* H37 Genome. *ChemBioChem* **2009**, *10*, 2060–2071.
- (219) Roncero, A. M.; Tobal, I. E.; Moro, R. F.; Diez, D.; Marcos, I. S. Halimane Diterpenoids: Sources, Structures, Nomenclature and Biological Activities. *Nat. Prod. Rep.* **2018**, *35*, 955–991.
- (220) Mann, F. M.; Xu, M.; Chen, X.; Fulton, D. B.; Russel, D. G.; Peters, R. J. Edaxadiene: A New Bioactive Diterpene from *Mycobacterium tuberculosis*. *J. Am. Chem. Soc.* **2009**, *131*, 17526–17527.
- (221) Mangel, N.; Mann, F. M.; Hillwig, M. L.; Peters, R. J.; Snider, B. B. Synthesis of (±)-Nosyberkol (Isotuberculosin, Revised Structure of Edaxadiene) and (±)-Tuberculosin. *Org. Lett.* **2010**, *12*, 2626–2629.
- (222) Spangler, J. E.; Carson, C. A.; Sorensen, E. J. Synthesis Enables a Structural Revision of the *Mycobacterium tuberculosis*-produced Diterpene, Edaxadiene. *Chem. Sci.* **2010**, *1*, 202–205.
- (223) Alder, K.; Stein, G. Untersuchungen über den Verlauf der Diensynthese. *Angew. Chem.* **1937**, *50*, 510–519.
- (224) Yoon, T.; Danishefsky, S. J.; de Gala, S. A Concise Total Synthesis of (±)-Mamanuthaquinone by Using an exo-Diels-Alder Reaction. *Angew. Chem., Int. Ed. Engl.* **1994**, *33*, 853–855.
- (225) Layre, E.; Lee, H. J.; Young, D. C.; Martinot, A. J.; Buter, J.; Minnaard, A. J.; Annand, J. W.; Fortune, S. M.; Snider, B. B.; Matsunaga, I.; Rubin, E. J.; Alber, T.; Moody, D. B. Molecular Profiling of *Mycobacterium tuberculosis* Identifies Tuberculosinyl Nucleoside Products of the Virulence-associated Enzyme Rv3378c. *Proc. Natl. Acad. Sci. U. S. A.* **2014**, *111*, 2978–2983.
- (226) Layre, E.; Sweet, L.; Hong, S.; Madigan, C. A.; Desjardins, D.; Young, D. C.; Cheng, T. Y.; Annand, J. W.; Kim, K.; Shamputa, I. C.; McConnell, M. J.; Debono, C. A.; Behar, S. M.; Minnaard, A. J.; Murray, M.; Barry, C. E., 3rd; Matsunaga, I.; Moody, D. B. A Comparative Lipidomics Platform for Chemotaxonomic Analysis of *Mycobacterium tuberculosis*. *Chem. Biol.* **2011**, *18*, 1537–1549.
- (227) Young, D. C.; Layre, E.; Pan, S. J.; Tapley, A.; Adamson, J.; Seshadri, C.; Wu, Z.; Buter, J.; Minnaard, A. J.; Coscolla, M.; Gagneux, S.; Copin, R.; Ernst, J. D.; Bishai, W. R.; Snider, B. B.; Moody, D. B. In Vivo Biosynthesis of Terpene Nucleosides Provides Unique Chemical Markers of *Mycobacterium tuberculosis* Infection. *Chem. Biol.* **2015**, *22*, 516–526.
- (228) El Ashry, E. S. H.; Nadeem, S.; Shah, M. R.; El Kilany, Y. Chapter 5 - Recent Advances in the Dimroth Rearrangement: A Valuable Tool for the Synthesis of Heterocycles. In *Advances in Heterocyclic Chemistry*; Katritzky, A. R., Ed.; Elsevier Inc.: 2010; Vol. 101, pp 161–228.
- (229) Krajczyk, A.; Boryski, J. Dimroth Rearrangement-Old but not Outdated. *Curr. Org. Chem.* **2017**, *21*, 2515–2529.
- (230) Buter, J.; Heijnen, D.; Wan, I. C.; Bickelhaupt, F. M.; Young, D. C.; Otten, E.; Moody, D. B.; Minnaard, A. J. Stereoselective Synthesis of 1-Tuberculosinyl Adenosine; a Virulence Factor of *Mycobacterium tuberculosis*. *J. Org. Chem.* **2016**, *81*, 6686–6696.
- (231) Buter, J. *On the Total Synthesis of Terpenes Containing Quaternary Stereocenters: Stereoselective Synthesis of the Taiwaniaquinoids, Mastigophorene A, and Tuberculosinyl Adenosine*. PhD Thesis, University of Groningen, Groningen, 2016.
- (232) Buter, J.; Cheng, T.-Y.; Ghanem, M.; Grootemaat, A. E.; Raman, S.; Feng, X.; Plantijn, A. R.; Ennis, T.; Wang, J.; Cotton, R. N.; Layre, E.; Rammarine, A. K.; Mayfield, J. A.; Young, D. C.; Jezek Martinot, A.; Siddiqi, N.; Wakabayashi, S.; Botella, H.; Calderon, R.; Murray, M.; Ehrst, S.; Snider, B. B.; Reed, M. B.; Oldfield, E.; Tan, S.; Rubin, E. J.; Behr, M. A.; van der Wel, N. N.; Minnaard, A. J.; Moody, D. B. *Mycobacterium tuberculosis* Releases an Anticid that Remodels Phagosomes. *Nat. Chem. Biol.* **2019**, *15*, 889–899.
- (233) de Duve, C.; de Barsy, T.; Poole, B.; Trouet, A.; Tulkens, P.; Van Hoof, F. Lysosomotropic Agents. *Biochem. Pharmacol.* **1974**, *23*, 2495–2531.
- (234) Ghanem, M.; Dubé, J.-Y.; Wang, J.; McIntosh, F.; Houle, D.; Domenech, P.; Reed, M. B.; Raman, S.; Buter, J.; Minnaard, A. J.; Moody, D. B.; Behr, M. A. Heterologous Production of 1-Tuberculosinyladenosine in *Mycobacterium kansasii* Models Pathoevolution towards the Transcellular Lifestyle of *Mycobacterium tuberculosis*. *mBio* **2020**, *11*, No. e02654-20.
- (235) Ratledge, C. Iron, *Mycobacteria* and Tuberculosis. *Tuberculosis* **2004**, *84*, 110–130.

- (236) Schaible, U. E.; Kaufmann, S. H. Iron and Microbial Infection. *Nat. Rev. Microbiol.* **2004**, *2*, 946–953.
- (237) Fang, Z.; Sampson, S. L.; Warren, R. M.; Gey van Pittius, N. C.; Newton-Foot, M. Iron Acquisition Strategies in Mycobacteria. *Tuberculosis* **2015**, *95*, 123–130.
- (238) Snow, G. A. Mycobactins: Iron-Chelating Growth Factors from Mycobacteria. *Bacteriol. Rev.* **1970**, *34*, 99–125.
- (239) Neilands, J. B. Siderophores: Structure and Function of Microbial Iron Transport Compounds. *J. Biol. Chem.* **1995**, *270*, 26723–26726.
- (240) Saha, R.; Saha, N.; Donofrio, R. S.; Bestervelt, L. L. Microbial Siderophores: A Mini Review. *J. Basic Microbiol.* **2013**, *53*, 303–317.
- (241) Wilson, B. R.; Bogdan, A. R.; Miyazawa, M.; Hashimoto, K.; Tsuji, Y. Siderophores in Iron Metabolism: From Mechanism to Therapy Potential. *Trends Mol. Med.* **2016**, *22*, 1077–1090.
- (242) Khan, A.; Singh, P.; Srivastava, A. Synthesis, Nature and Utility of Universal Iron Chelator - Siderophore: A Review. *Microbiol. Res.* **2018**, *212–213*, 103–111.
- (243) Patel, K.; Butala, S.; Khan, T.; Suvarna, V.; Sherje, A.; Dravyakar, B. Mycobacterial Siderophore: A Review on Chemistry and Biology of Siderophore and its Potential as a Target for Tuberculosis. *Eur. J. Med. Chem.* **2018**, *157*, 783–790.
- (244) Francis, J.; Macturk, H. M.; Madinavetta, J.; Snow, G. A. Mycobactin, a Growth Factor for Mycobacterium johnei. *Biochem. J.* **1953**, *55*, 596–607.
- (245) Twort, F. W.; Ingram, G. L. Y. *A monograph on Johne's disease (enteritis chronica pseudotuberculosis bovis)*; Baillièere, Tindall and Cox: London, 1913.
- (246) Snow, G. A.; Mycobactin. A Growth Factor for Mycobacterium johnei. Part II. Degradation, and Identification of Fragments. *J. Chem. Soc.* **1954**, 2588–2596.
- (247) Snow, G. A.; Mycobactin. A Growth Factor for Mycobacterium johnei. Part III. Degradation and Tentative Structure. *J. Chem. Soc.* **1954**, 4080–4093.
- (248) Snow, G. A. The Structure of Mycobactin P, a Growth Factor for Mycobacterium johnei, and the Significance of its Iron Complex. *Biochem. J.* **1965**, *94*, 160–165.
- (249) Snow, G. A. Isolation and Structure of Mycobactin T, a Growth Factor from Mycobacterium tuberculosis. *Biochem. J.* **1965**, *97*, 166–175.
- (250) Gobin, J.; Moore, C. H.; Reeve Jr, J. R.; Wong, D. K.; Gibson, B. W.; Horwitz, M. A. Iron Acquisition by Mycobacterium tuberculosis: Isolation and Characterization of a Family of Iron-Binding Exochelins. *Proc. Natl. Acad. Sci. U. S. A.* **1995**, *92*, 5189–5193.
- (251) Gobin, J.; Horwitz, M. A. Exochelins of Mycobacterium tuberculosis Remove Iron from Human Iron-binding Proteins and Donate Iron to Mycobactins in the M. tuberculosis Cell Wall. *J. Exp. Med.* **1996**, *183*, 1527–1532.
- (252) Carpenter, J. G. D.; Moore, J. W. Synthesis of an Analogue of Mycobactin. *J. Chem. Soc. C* **1969**, *12*, 1610–1611.
- (253) Maurer, P. J.; Miller, M. J. Total Synthesis of a Mycobactin: Mycobactin S2. *J. Am. Chem. Soc.* **1983**, *105*, 240–245.
- (254) Roosenberg, J. M.; Lin, Y.-M.; Lu, Y.; Miller, M. J. Studies and Syntheses of Siderophores, Microbial Iron Chelators, and Analogs as Potential Drug Delivery Agents. *Curr. Med. Chem.* **2000**, *7*, 159–197.
- (255) He, J.-L.; Xie, J.-O. Advances in Mycobacterium Siderophore-Based Drug Discovery. *Acta Pharm. Sin.* **2011**, *1*, 8–13.
- (256) Ji, C.; Juárez-Hernández, R. E.; Miller, M. J. Exploiting Bacterial Iron Acquisition: Siderophore Conjugates. *Future Med. Chem.* **2012**, *4*, 297–313.
- (257) Górska, A.; Sloderbach, A.; Marszall, M. P. Siderophore-Drug Complexes: Potential Medicinal Applications of the ‘Trojan Horse’ Strategy. *Trends Pharmacol. Sci.* **2014**, *35*, 442–449.
- (258) Negash, K. H.; Norris, J. K. S.; Hodgkinson, J. T. Siderophore-Antibiotic Conjugate Design: New Drugs for Bad Bugs? *Molecules* **2019**, *24*, 3314.
- (259) Miller, M. J.; Walz, A. J.; Zhu, H.; Wu, C.; Moraski, G.; Möllmann, U.; Tristani, E. M.; Crumbliss, A. L.; Ferdig, M. T.; Checkley, L.; Edwards, R. L.; Boshoff, H. I. Design, Synthesis, and Study of a Mycobactin-Artemisinin Conjugate That Has Selective and Potent Activity against Tuberculosis and Malaria. *J. Am. Chem. Soc.* **2011**, *133*, 2076–2079.
- (260) Hu, J.; Miller, M. J. Total Synthesis of a Mycobactin S, a Siderophore and Growth Promoter of Mycobacterium Smegmatis, and Determination of its Growth Inhibitory Activity against Mycobacterium tuberculosis. *J. Am. Chem. Soc.* **1997**, *119*, 3462–3468.
- (261) Poreddy, A. R.; Schall, O. F.; Marshall, G. R.; Ratledge, C.; Slomczynska, U. Solid-Phase Synthesis of Methyl Carboxymycobactin T 7 and Analogues as Potential Antimycobacterial Agents. *Bioorg. Med. Chem. Lett.* **2003**, *13*, 2553–2556.
- (262) Moody, D. B.; Young, D. C.; Cheng, T.-Y.; Rosat, J.-P.; Rouramir, C.; O'Connor, P. B.; Zajonc, D. M.; Walz, A.; Miller, M. J.; Levery, S. B.; Wilson, I. A.; Costello, C. E.; Brenner, M. B. T Cell Activation by Lipopeptide Antigens. *Science* **2004**, *303*, 527–531.
- (263) Young, D. C.; Kasmar, A.; Moraski, G.; Cheng, T.-Y.; Walz, A. J.; Hu, J.; Xu, Y.; Endres, G. W.; Uzieblo, A.; Zajonc, D.; Costello, C. E.; Miller, M. J.; Moody, D. B. Synthesis of Dideoxymycobactin Antigens Presented by CD1a Reveals T Cell Fine Specificity for Natural Lipopeptide Structures. *J. Biol. Chem.* **2009**, *284*, 25087–25096.
- (264) Cheng, J. M. H.; Liu, L.; Pellicci, D. G.; Reddiex, S. J. J.; Cotton, R. N.; Cheng, T.-Y.; Young, D. C.; Van Rhijn, I.; Moody, D. B.; Rossjohn, J.; Fairlie, D. P.; Godfrey, D. I.; Williams, S. J. Total Synthesis of Mycobacterium tuberculosis Dideoxymycobactin-838 and Stereoisomers: Diverse CD1a-Restricted T Cells Display a Common Hierarchy of Lipopeptide Recognition. *Chem. - Eur. J.* **2017**, *23*, 1694–1701.
- (265) Jankute, M.; Grover, S.; Rana, A. K.; Besra, G. S. Arabinogalactan and Lipoarabinomannan Biosynthesis: Structure, Biogenesis and Their Potential as Drug Targets. *Future Microbiol.* **2012**, *7*, 129–147.
- (266) Angala, S. K.; Belardinelli, J. M.; Huc-Claustre, E.; Wheat, W. H.; Jackson, M. The Cell Envelope Glycoconjugates of Mycobacterium tuberculosis. *Crit. Rev. Biochem. Mol. Biol.* **2014**, *49*, 361–399.
- (267) Zhou, K.-L.; Li, X.; Zhang, X.-L.; Pan, Q. Mycobacterial Mannose-Capped Lipoarabinomannan: A Modulator Bridging Innate and Adaptive Immunity. *Emerging Microbes Infect.* **2019**, *8*, 1168–1177.
- (268) Angala, S. K.; Li, W.; Boot, C. M.; Jackson, M.; McNeil, M. R. Secondary Extended Mannan Side Chains and Attachment of the Arabinan in Mycobacterial Lipoarabinomannan. *Commun. Chem.* **2020**, *3*, 3.
- (269) Nigou, J.; Gilleron, M.; Brando, T.; Puzo, G. Structural Analysis of Mycobacterial Lipoglycans. *Appl. Biochem. Biotechnol.* **2004**, *118*, 253–267.
- (270) Anderson, R. J. The Chemistry of the Lipids of the Tubercle Bacillus and Certain Other Microorganisms. *Prog. Chem. Org. Nat. Prod.* **1939**, *3*, 145–202.
- (271) Ballou, C. E.; Vilkas, E.; Lederer, E. Structural Studies on the Myo-inositol Phospholipids of Mycobacterium tuberculosis (var. bovis, strain BCG). *J. Biol. Chem.* **1963**, *238*, 69–76.
- (272) Ballou, C. E.; Lee, Y. C. The Structure of a Myo-inositol Mannoside from Mycobacterium tuberculosis Glycolipid. *Biochemistry* **1964**, *3*, 682–685.
- (273) Lee, Y. C.; Ballou, C. E. Structural Studies on the Myo-inositol Mannosides from the Glycolipids of Mycobacterium tuberculosis and Mycobacterium phlei. *J. Biol. Chem.* **1964**, *239*, 1316–1327.
- (274) Lee, Y. C.; Ballou, C. E. Complete Structures of the Glycophospholipids of Mycobacteria. *Biochemistry* **1965**, *4*, 1395–1404.
- (275) Khoo, K.-H.; Dell, A.; Morris, H. R.; Brennan, P. J.; Chatterjee, D. Structural Definition of Acylated Phosphatidylinositol Mannosides from Mycobacterium tuberculosis: Definition of a Common Anchor for Lipomannan and Lipoarabinomannan. *Glycobiology* **1995**, *5*, 117–127.
- (276) Gilleron, M.; Lindner, B.; Puzo, G. MS/MS Approach for Characterization of the Fatty Acid Distribution on Mycobacterial Phosphatidyl-myoinositol Mannosides. *Anal. Chem.* **2006**, *78*, 8543–8548.
- (277) Garcia-Vilanova, A.; Chan, J.; Torrelles, J. B. Underestimated Manipulative Roles of Mycobacterium tuberculosis Cell Envelope Glycolipids During Infection. *Front. Immunol.* **2019**, *10*, 2909.

- (278) Vergne, I.; Fratti, R. A.; Hill, P. J.; Chua, J.; Belisle, J.; Deretic, V. Mycobacterium tuberculosis Phagosome Maturation Arrest: Mycobacterial Phosphatidylinositol Analog Phosphatidylinositol Mannoside Stimulates Early Endosomal Fusion. *Mol. Biol. Cell* **2004**, *15*, 751–760.
- (279) Villeneuve, C.; Gilleron, M.; Maridonneau-Parini, I.; Daffé, M.; Astarie-Dequeker, C.; Etienne, G. Mycobacteria Use Their Surface-Exposed Glycolipids to Infect Human Macrophages Through a Receptor-Dependent Process. *J. Lipid Res.* **2005**, *46*, 475–483.
- (280) Court, N.; Rose, S.; Bourigault, M.-L.; Front, S.; Martin, O. R.; Dowling, J. K.; Kenny, E. F.; O'Neill, L.; Erard, F.; Quesniaux, V. F. J. Mycobacterial PIMs Inhibit Host Inflammatory Responses through CD14-Dependent and CD14-Independent Mechanisms. *PLoS One* **2011**, *6*, No. e24631.
- (281) Torrelles, J. B.; Azad, A. K.; Schlesinger, L. S. Fine Discrimination in the Recognition of Individual Species of Phosphatidyl-myoinositol Mannosides from Mycobacterium tuberculosis by C-Type Lectin Pattern Recognition Receptors. *J. Immunol.* **2006**, *177*, 1805–1816.
- (282) Driessen, N. N.; Ummels, R.; Maaskant, J. J.; Gurucha, S. S.; Besra, G. S.; Ainge, G. D.; Larsen, D. S.; Painter, G. F.; Vandenbroucke-Grauls, C. M. J. E.; Geurtsen, J.; Appelmelk, B. J. Role of Phosphatidylinositol Mannosides in the Interaction between Mycobacteria and DC-SIGN. *Infect. Immun.* **2009**, *77*, 4538–4547.
- (283) de la Salle, H.; Mariotti, S.; Angenieux, C.; Gilleron, M.; Garcia-Alles, L.-F.; Malm, D.; Berg, T.; Paoletti, S.; Maitre, B.; Mourey, L.; Salamero, J.; Cazenave, J. P.; Hanau, D.; Mori, L.; Puzo, G.; De Libero, G. Assistance of Microbial Glycolipid Antigen Processing by CD1e. *Science* **2005**, *310*, 1321–1324.
- (284) Rojas, R. E.; Thomas, J. J.; Gehring, A. J.; Hill, P. J.; Belisle, J. T.; Harding, C. V.; Boom, W. H. Phosphatidylinositol Mannoside from Mycobacterium tuberculosis Binds $\alpha 5\beta 1$ Integrin (VLA-5) on CD4+ T Cells and Induces Adhesion to Fibronectin. *J. Immunol.* **2006**, *177*, 2959–2968.
- (285) Misaki, A.; Azuma, I.; Yamamura, Y. Structural and Immunochemical Studies on D-Arabinomannans and D-Mannans of Mycobacterium tuberculosis and Other Mycobacterium Species. *J. Biochem.* **1977**, *82*, 1759–1770.
- (286) Hunter, S. W.; Gaylord, H.; Brennan, P. J. Structure and Antigenicity of the Phosphorylated Lipopolysaccharide Antigens from the Leprosy and Tubercle Bacilli. *J. Biol. Chem.* **1986**, *261*, 12345–12351.
- (287) Hunter, S. W.; Brennan, P. J. Evidence for the Presence of a Phosphatidylinositol Anchor on the Lipoarabinomannan and Lipomannan of Mycobacterium tuberculosis. *J. Biol. Chem.* **1990**, *265*, 9272–9279.
- (288) Chatterjee, D.; Hunter, S. W.; McNeil, M.; Brennan, P. J.; Lipoarabinomannan. Multiglycosylated Form of the Mycobacterial Mannosylphosphatidylinositols. *J. Biol. Chem.* **1992**, *267*, 6228–6233.
- (289) Gilleron, M.; Nigou, J.; Cahuzac, B.; Puzo, G. Structural Study of the LipoMannans from Mycobacterium bovis BCG: Characterisation of Multiacylated Forms of the Phosphatidyl-myoinositol Anchor. *J. Mol. Biol.* **1999**, *285*, 2147–2160.
- (290) Chatterjee, D.; Khoo, K.-H.; McNeil, M.; Dell, A.; Morris, H. R.; Brennan, P. J. Structural Definition of the Non-Reducing Termini of Mannose-Capped LAM from Mycobacterium tuberculosis Through Selective Enzymatic Degradation and Fast Atom Bombardment-Mass Spectrometry. *Glycobiology* **1993**, *3*, 497–506.
- (291) Nigou, J.; Vercellone, A.; Puzo, G. New Structural Insights into the Molecular Deciphering of Mycobacterial Lipoglycan Binding to C-type Lectins: Lipoarabinomannan Glycoform Characterization and Quantification by Capillary Electrophoresis at the Subnanomole Level. *J. Mol. Biol.* **2000**, *299*, 1353–1362.
- (292) Chatterjee, D.; Bozic, C. M.; McNeil, M.; Brennan, P. J. Structural Features of the Arabinan Component of the Lipoarabinomannan of Mycobacterium tuberculosis. *J. Biol. Chem.* **1991**, *266*, 9652–9660.
- (293) Shi, L.; Berg, S.; Lee, A.; Spencer, J. S.; Zhang, J.; Vissa, V.; McNeil, M. R.; Khoo, K. H.; Chatterjee, D. The Carboxy Terminus of EmbC from Mycobacterium smegmatis Mediates Chain Length Extension of the Arabinan in Lipoarabinomannan. *J. Biol. Chem.* **2006**, *281*, 19512–19526.
- (294) Monsarrat, B.; Brando, T.; Condouret, P.; Nigou, J.; Puzo, G. Characterization of Mannooligosaccharide Caps in Mycobacterial Lipoarabinomannan by Capillary Electrophoresis/Electrospray Mass Spectrometry. *Glycobiology* **1999**, *9*, 335–342.
- (295) Treumann, A.; Xidong, F.; McDonnell, L.; Derrick, P. J.; Ashcroft, A. E.; Chatterjee, D.; Homans, S. W. 5-Methylthiopentose: A New Substituent on Lipoarabinomannan in Mycobacterium tuberculosis. *J. Mol. Biol.* **2002**, *316*, 89–100.
- (296) Turnbull, W. B.; Shimizu, K. H.; Chatterjee, D.; Homans, S. W.; Treumann, A. Identification of the 5-Methylthiopentose Substituent in Mycobacterium tuberculosis Lipoarabinomannan. *Angew. Chem., Int. Ed.* **2004**, *43*, 3918–3922.
- (297) Kaur, D.; Angala, S. K.; Wu, S. W.; Khoo, K. H.; Chatterjee, D.; Brennan, P. J.; Jackson, M.; McNeil, M. R. A Single Arabinan Chain Is Attached to the Phosphatidylinositol Mannosyl Core of the Major Immunomodulatory Mycobacterial Cell Envelope Glycoconjugate, Lipoarabinomannan. *J. Biol. Chem.* **2014**, *289*, 30249–30256.
- (298) Strohmeier, G. R.; Fenton, M. J. Roles of Lipoarabinomannan in the Pathogenesis of Tuberculosis. *Microbes Infect.* **1999**, *1*, 709–717.
- (299) Nigou, J.; Gilleron, M.; Rojas, M.; García, L. F.; Thurnher, M.; Puzo, G. Mycobacterial Lipoarabinomannans: Modulators of Dendritic Cell Function and the Apoptotic Response. *Microbes Infect.* **2002**, *4*, 945–953.
- (300) Schlesinger, L. S.; Hull, S. R.; Kaufmann, T. M. Binding of the Terminal Mannosyl Units of Lipoarabinomannan From a Virulent Strain of Mycobacterium tuberculosis to Human Macrophages. *J. Immunol.* **1994**, *152*, 4070–4079.
- (301) Geijtenbeek, T. B.; Van Vliet, S. J.; Koppel, E. A.; Sanchez-Hernandez, M.; Vandenbroucke-Grauls, C. M. J. E.; Appelmelk, B.; Van Kooyk, Y. Mycobacteria Target DC-SIGN to Suppress Dendritic Cell Function. *J. Exp. Med.* **2003**, *197*, 7–17.
- (302) Maeda, N.; Nigou, J.; Herrmann, J.-L.; Jackson, M.; Amara, A.; Lagrange, P. H.; Puzo, G.; Gicquel, B.; Neyrolles, O. The Cell Surface Receptor DC-SIGN Discriminates between Mycobacterium Species through Selective Recognition of the Mannose Caps on Lipoarabinomannan. *J. Biol. Chem.* **2003**, *278*, 5513–5516.
- (303) Vergne, I.; Chua, J.; Deretic, V. Tuberculosis Toxin Blocking Phagosome Maturation Inhibits a Novel Ca²⁺/Calmodulin-PI3K hVSP34 Cascade. *J. Exp. Med.* **2003**, *198*, 653–659.
- (304) Kang, P. B.; Azad, A. K.; Torrelles, J. B.; Kaufman, T. M.; Beharka, A.; Tibesar, E.; DesJardin, L. E.; Schlesinger, L. S. The Human Macrophage Mannose Receptor Directs Mycobacterium tuberculosis Lipoarabinomannan-Mediated Phagosome Biogenesis. *J. Exp. Med.* **2005**, *202*, 987–999.
- (305) Prigozy, T. I.; Sieling, P. A.; Clemens, D.; Stewart, P. L.; Behar, S. M.; Porcelli, S. A.; Brenner, M. B.; Modlin, R. L.; Kronenberg, M. The Mannose Receptor Delivers Lipoglycan Antigens to Endosomes for Presentation to T Cells by CD1b Molecules. *Immunity* **1997**, *6*, 187–197.
- (306) Bulterys, M. A.; Wagner, B.; Redard-Jacot, M.; Suresh, A.; Pollock, N. R.; Moreau, E.; Denking, C. M.; Drain, P. K.; Broger, T. Point-Of-Care Urine LAM Tests for Tuberculosis Diagnosis: A Status Update. *J. Clin. Med.* **2020**, *9*, 111.
- (307) Elie, C. J. J.; Dreef, C. E.; Verduyn, R.; Van der Marel, G. A.; Van Boom, J. H. Synthesis of 1-O-(1,2-Di-O-Palmitoyl-sn-glycero-3-phosphoryl)-2-O- α -D-mannopyranosyl-D-myoinositol: A Fragment of Mycobacterial Phospholipids. *Tetrahedron* **1989**, *45*, 3477–3486.
- (308) Elie, C. J. J.; Verduyn, R.; Dreef, C. E.; Van der Marel, G. A.; Van Boom, J. H. Iodinium Ion-Mediated Mannosylations of Myo-Inositol: Synthesis of a Mycobacteria Phospholipid Fragment. *J. Carbohydr. Chem.* **1992**, *11*, 715–739.
- (309) Zamyatina, A. Y.; Shvets, V. I. The Synthesis of 1-O-(2-N-Stearoyl-D-erythro-sphinganine-1-phosphoryl)-2-O-(α -D-mannopyranosyl)-D-myoinositol: A Fragment of the Naturally Occurring Inositol-Containing Glycophosphosphingolipids. *Chem. Phys. Lipids* **1995**, *76*, 225–240.

- (310) Watanabe, Y.; Yamamoto, T.; Ozaki, S. Regiospecific Synthesis of 2,6-Di-O- (α -D-mannopyranosyl)phosphatidyl-d-myo-inositol. *J. Org. Chem.* **1996**, *61*, 14–15.
- (311) Stadelmaier, A.; Schmidt, R. R. Synthesis of Phosphatidylinositol Mannosides (PIMs). *Carbohydr. Res.* **2003**, *338*, 2557–2569.
- (312) Ainge, G. D.; Hudson, J.; Larsen, D. S.; Painter, G. F.; Gill, G. S.; Harper, J. L. Phosphatidylinositol Mannosides: Synthesis and Suppression of Allergic Airway Disease. *Bioorg. Med. Chem.* **2006**, *14*, 5632–5642.
- (313) Zajonc, D. M.; Ainge, G. D.; Painter, G. F.; Severn, W. B.; Wilson, I. A. Structural Characterization of Mycobacterial Phosphatidylinositol Mannoside Binding to Mouse CD1d. *J. Immunol.* **2006**, *177*, 4577–4583.
- (314) Ainge, G. D.; Parlane, N. A.; Denis, M.; Hayman, C. M.; Larsen, D. S.; Painter, G. F. Phosphatidylinositol Mannosides: Synthesis and Adjuvant Properties of Phosphatidylinositol Di- and Tetramannosides. *Bioorg. Med. Chem.* **2006**, *14*, 7615–7624.
- (315) Ainge, G. D.; Compton, B. J.; Hayman, C. M.; Martin, W. J.; Toms, S. M.; Larsen, D. S.; Harper, J. L.; Painter, G. F. Chemical Synthesis and Immunosuppressive Activity of Dipalmitoyl Phosphatidylinositol Hexamannoside. *J. Org. Chem.* **2011**, *76*, 4941–4951.
- (316) Liu, X.; Stocker, B. L.; Seeberger, P. H. Total Synthesis of Phosphatidylinositol Mannosides of Mycobacterium tuberculosis. *J. Am. Chem. Soc.* **2006**, *128*, 3638–3648.
- (317) Wu, D.; Xing, G.-W.; Poles, M. A.; Horowitz, A.; Kinjo, Y.; Sullivan, B.; Bodmer-Narkevitch, V.; Plettenburg, O.; Kronenberg, M.; Tsuji, M.; Ho, D. D.; Wong, C.-H. Bacterial Glycolipids and Analogs as Antigens for CD1d-Restricted NKT Cells. *Proc. Natl. Acad. Sci. U. S. A.* **2005**, *102*, 1351–1356.
- (318) Jia, Z. J.; Olsson, L.; Fraser-Reid, B. Ready Routes to Key myo-Inositol Component of GPIs Employing Microbial Arene Oxidation or Ferrier Reaction. *J. Chem. Soc., Perkin Trans. 1* **1998**, 631–632.
- (319) Tanaka, S.; Saburi, H.; Ishibashi, Y.; Kitamura, M. CpRuIPPF₆/Quinaldic Acid-Catalyzed Chemoselective Allyl Ether Cleavage. A Simple and Practical Method for Hydroxyl Deprotection. *Org. Lett.* **2004**, *6*, 1873–1875.
- (320) Dyer, B. S.; Jones, J. D.; Ainge, G. D.; Denis, M.; Larsen, D. S.; Painter, G. F. Synthesis and Structure of Phosphatidylinositol Dimannoside. *J. Org. Chem.* **2007**, *72*, 3282–3288.
- (321) Gilleron, M.; Ronet, C.; Mempel, M.; Monsarrat, B.; Gachelin, G.; Puzo, G. Acylation State of the Phosphatidylinositol Mannosides from Mycobacterium bovis Bacillus Calmette Guérin and Ability to Induce Granuloma and Recruit Natural Killer T Cells. *J. Biol. Chem.* **2001**, *276*, 34896–34904.
- (322) Gilleron, M.; Quesniaux, V. F.; Puzo, G. Acylation State of the Phosphatidylinositol Hexamannosides from Mycobacterium bovis Bacillus Calmette Guérin and Mycobacterium tuberculosis H37Rv and Its Implication in Toll-like Receptor Response. *J. Biol. Chem.* **2003**, *278*, 29880–29889.
- (323) Boonyarattanakalin, S.; Liu, X.; Michieletti, M.; Lepenies, B.; Seeberger, P. H. Chemical Synthesis of All Phosphatidylinositol Mannoside (PIM) Glycans from Mycobacterium tuberculosis. *J. Am. Chem. Soc.* **2008**, *130*, 16791–16799.
- (324) Patil, P. S.; Hung, S.-C. Total Synthesis of Phosphatidylinositol Dimannoside: A Cell-Envelope Component of Mycobacterium tuberculosis. *Chem. - Eur. J.* **2009**, *15*, 1091–1094.
- (325) Patil, P. S.; Hung, S.-C. Synthesis of Mycobacterial Triacylated Phosphatidylinositol Dimannoside Containing an Acyl Lipid Chain at 3-O of Inositol. *Org. Lett.* **2010**, *12*, 2618–2621.
- (326) Patil, P. S.; Cheng, T.-J. R.; Zulueta, M. M. L.; Yang, S.-T.; Lico, L. S.; Hung, S.-C. Total Synthesis of Tetraacylated Phosphatidylinositol Hexamannoside and Evaluation of its Immunomodulatory Activity. *Nat. Commun.* **2015**, *6*, 7239.
- (327) Ali, A.; Wenk, M. R.; Lear, M. J. Total Synthesis of a Fully Lipidated Form of Phosphatidyl-myo-Inositol Dimannoside (PIM-2) of Mycobacterium tuberculosis. *Tetrahedron Lett.* **2009**, *50*, 5664–5666.
- (328) Ohira, S.; Yamaguchi, Y.; T, T.; H, T. Synthesis of a Phosphatidylinositol Dimannoside Using 2-(Azidomethyl)benzoate Mannosyl Donors. *Heterocycles* **2014**, *89*, 763–774.
- (329) Toyonaga, K.; Torigoe, S.; Motomura, Y.; Kamichi, T.; Hayashi, J. M.; Morita, Y. S.; Noguchi, N.; Chuma, Y.; Kiyohara, H.; Matsuo, K.; Tanaka, H.; Nakagawa, Y.; Sakuma, T.; Ohmuraya, M.; Yamamoto, T.; Umemura, M.; Matsuzaki, G.; Yoshikai, Y.; Yano, I.; Miyamoto, T.; Yamasaki, S. C-Type Lectin Receptor DCAR Recognizes Mycobacterial Phosphatidyl-Inositol Mannosides to Promote a Th1 Response during Infection. *Immunity* **2016**, *45*, 1245–1257.
- (330) Omahdi, Z.; Horikawa, Y.; Nagae, M.; Toyonaga, K.; Imamura, A.; Takato, K.; Teramoto, T.; Ishida, H.; Kakuta, Y.; Yamasaki, S. Structural Insight Into the Recognition of Pathogen-Derived Phosphoglycolipids by C-type Lectin Receptor DCAR. *J. Biol. Chem.* **2020**, *295*, 5807–5817.
- (331) Ohira, S.; Yamaguchi, Y.; Takahashi, T.; Tanaka, H. The Chemoselective O-glycosylation of Alcohols in the Presence of a Phosphate Diester and its Application to the Synthesis of Oligomannosylated Phosphatidyl Inositols. *Tetrahedron* **2015**, *71*, 6602–6611.
- (332) Lee, A. M. M.; Painter, G. F.; Compton, B. J.; Larsen, D. S. Resolution of Orthogonally Protected myo-Inositols with Novozym 435 Providing an Enantioconvergent Pathway to Ac2PIM1. *J. Org. Chem.* **2014**, *79*, 10916–10931.
- (333) Cunha, A. G.; da Silva, A. A. T.; da Silva, A. J. R.; Tinoco, L. W.; Almeida, R. V.; de Alencastro, R. B.; Simas, A. B. C.; Freire, D. M. G. Efficient Kinetic Resolution of (\pm)-1,2-O-isopropylidene-3,6-di-O-benzyl-myo-inositol with the Lipase B of Candida antarctica. *Tetrahedron: Asymmetry* **2010**, *21*, 2899–2903.
- (334) Simas, A. B. C.; da Silva, A. A. T.; Cunha, A. G.; Assumpção, R. S.; Hoelz, L. V. B.; Neves, B. C.; Galvão, T. C.; Almeida, R. V.; Albuquerque, M. G.; Freire, D. M. G.; de Alencastro, R. B. Kinetic Resolution of (\pm)-1,2-O-isopropylidene-3,6-di-O-benzyl-myo-inositol by Lipases: An Experimental and Theoretical Study on the Reaction of a Key Precursor of Chiral Inositols. *J. Mol. Catal. B: Enzym.* **2011**, *70*, 32–40.
- (335) Arai, Y.; Torigoe, S.; Matsumaru, T.; Yamasaki, S.; Fujimoto, Y. The Key Entity of a DCAR Agonist, Phosphatidylinositol Mannoside Ac1PIM1: Its Synthesis and Immunomodulatory Function. *Org. Biomol. Chem.* **2020**, *18*, 3659–3663.
- (336) Jayaprakash, K. N.; Lu, J.; Fraser-Reid, B. Synthesis of a Lipomannan Component of the Cell-Wall Complex of Mycobacterium tuberculosis Is Based on Paulsen's Concept of Donor/Acceptor "Match. *Angew. Chem., Int. Ed.* **2005**, *44*, 5894–5898.
- (337) Paulsen, H. *Selectivity: A goal for synthetic efficiency*; Verlag Chemie: Basel, 1985.
- (338) Fraser-Reid, B.; Wu, Z.; Udodong, U. E.; Ottosson, H. Armed/Disarmed Effects in Glycosyl Donors: Rationalization and Sidetracking. *J. Org. Chem.* **1990**, *55*, 6068–6070.
- (339) Hölemann, A.; Stocker, B. L.; Seeberger, P. H. Synthesis of a Core Arabinomannan Oligosaccharide of Mycobacterium tuberculosis. *J. Org. Chem.* **2006**, *71*, 8071–8088.
- (340) Fraser-Reid, B.; Lu, J.; Jayaprakash, K. N.; López, J. C. Synthesis of a 28-mer Oligosaccharide Core of Mycobacterial Lipoarabinomannan (LAM) Requires only Two n-Pentenyl Orthoester Progenitors. *Tetrahedron: Asymmetry* **2006**, *17*, 2449–2463.
- (341) Joe, M.; Bai, Y.; Nacario, R. C.; Lowary, T. L. Synthesis of the Docosanasaccharide Arabinan Domain of Mycobacterial Arabinogalactan and a Proposed Octadecasaccharide Biosynthetic Precursor. *J. Am. Chem. Soc.* **2007**, *129*, 9885–9901.
- (342) Callam, C. S.; Gadikota, R. R.; Lowary, T. L. Sensitivity of 1JC1-H1Magnitudes to Anomeric Stereochemistry in 2,3-Anhydro-O-furanosides. *J. Org. Chem.* **2001**, *66*, 4549–4558.
- (343) Zhu, X.; Kawatkar, S.; Rao, Y.; Boons, G.-J. Practical Approach for the Stereoselective Introduction of β -Arabinofuranosides. *J. Am. Chem. Soc.* **2006**, *128*, 11948–11957.
- (344) Ishiwata, A.; Ito, Y. Synthesis of Docosanasaccharide Arabinan Motif of Mycobacterial Cell Wall. *J. Am. Chem. Soc.* **2011**, *133* (7), 2275–22791.

(345) Thadke, S. A.; Mishra, B.; Islam, M.; Pasari, S.; Manmode, S.; Rao, B. V.; Neralkar, M.; Shinde, G. P.; Walke, G.; Hotha, S. [Au]/[Ag]-Catalysed Expedient Synthesis of Branched Heneicosafuranosyl Arabinogalactan Motif of *Mycobacterium tuberculosis* Cell Wall. *Nat. Commun.* **2017**, *8*, 14019.

(346) Thadke, S. A.; Mishra, B.; Hotha, S. Gold(III)-Catalyzed Glycosidations for 1,2-trans and 1,2-cis Furanosides. *J. Org. Chem.* **2014**, *79*, 7358–7371.

(347) Wu, Y.; Xiong, D. C.; Chen, S. C.; Wang, Y. S.; Ye, X. S. Total Synthesis of Mycobacterial Arabinogalactan Containing 92 Monosaccharide Units. *Nat. Commun.* **2017**, *8*, 14851.